EEG-fMRI signatures of spontaneous brain activity in healthy volunteers and epilepsy patients

Helmut Laufs, M.D.

DEPARTMENT OF CLINICAL AND EXPERIMENTAL EPILEPSY

INSTITUTE OF NEUROLOGY

UNIVERSITY COLLEGE LONDON (UCL)

UNITED KINGDOM

THESIS SUBMITTED TO THE UNIVERSITY OF LONDON FOR THE DEGREE OF DOCTOR OF PHILOSOPHY, 2013

LEFT BLANK INTENTIONALLY

Personal contribution

I, Helmut Laufs, confirm that the work presented in this thesis is my own. Where information has been derived from other sources, I confirm that this has been indicated in the thesis. The work reflects the contributions of a team of researchers, and my individual contributions to each study are outlined below w.r.t. the responsibility for and contribution to recruitment, data acquisition and archiving, (statistical) data analysis, preparation of graphical data presentation (figures), and data interpretation following discussions with colleague researchers and at regular supervision meetings.

Preface and Acknowledgements

It has been a pleasure to work as part of the Department of Clinical and Experimental Epilepsy during my period of research, to learn from the scientific community at Queen Square and to have been exposed to the British culture of life in Chalfont St. Peter. First of all, I would like to thank Professors Louis Lemieux, my principal supervisor and John S. Duncan, my subsidiary supervisor for their warm welcoming in the research team, guidance, support and also acceptance of my own ideas throughout the course of this thesis. I appreciate many lessons taught.

Equally, I am grateful to many more people who have helped make this such an enjoyable and rewarding experience: Rachel Thornton, Roman Rodionov, Khalid Hamandi, David Carmichael, Anna Vaudano, Matthew Walker, Matthias Koepp, Mark Richardson, Max Guye, Torben Lund, Afraim Salek-Haddadi, Dominique Flügel, Mark Symms, Shelagh Smith, Catherine Scott, Jean Daunizeau, Rob Powell, Peeler's, Graham, Ley Sander, Elaine Williams, Philippa Bartlett, Jane Burdett, Joan Blisset, Xavier de Tiège, Sajitha Cannadathu , Andrew McEvoy, Silvia Bonelli, Sofia Eriksson, Peter Gilford, Adam Liston, Karsten Krakow, Andreas Kleinschmidt, Anne-Lise Giraud, Phil Boulby, Oliver Josephs, Peter Brown, Philip Patsalos, Her Royal Highness The Countess of Wessex, and Karl Friston. I remember especially Tuuli Salmenpera, her husband and their three children.

Thanks to all the patients who volunteered enthusiastically to give up their time in order to contribute to (this) research - and their referrers. Thanks to the Deutsche Forschungsgemeinschaft who funded my stay (LA 1452/3).

My family – which started in Chalfont – I thank for their presence and support. Finally I think of my father for whom academia always was an important purpose in life.

1 Abstract

Background

Functional magnetic resonance imaging (fMRI) provides maps of neuronal activity with uniform resolution across the brain. Simultaneous recording of electroencephalography (EEG) during fMRI (EEG-fMRI) was developed to localize spontaneously occurring epileptiform discharges. In focal epilepsy, it can identify candidate brain regions for surgical removal as a treatment option in medically refractory epilepsy; and in generalized epilepsy syndromes reveals those involved during the EEG changes. In healthy subjects, EEG-fMRI has linked spontaneous ongoing EEG activity with fMRI resting state networks.

Methods

After method refinements, patients with medically refractory focal epilepsy and those with generalized epilepsy were studied with EEG-fMRI and group analyses performed to identify typical sets of brain regions involved in the epileptic process.

Findings

In individual patients with refractory focal epilepsy, EEG-fMRI can produce activity maps including the seizure onset zone and propagated epileptic activity. Clinically, these can be confirmatory of results from alternative diagnostic techniques, or alternatively serve to generate a hypothesis on the potential epileptic focus, but under certain conditions may also be of negative predictive value w.r.t. to surgical treatment success. At the group level in patients with temporal lobe epilepsy and complex partial seizures as well as in patients with generalized epilepsy and absence seizures, altered resting state network activity during EEG changes were found in default mode brain regions fitting well the ictal semiology, because these are known to reduce their activity during states of reduced consciousness. In lateralized temporal lobe; in an unselected mix of focal epilepsies; and in generalized epilepsies, activity increases occurred in typical brain regions suggesting an associated hub function, namely ipsilateral to the presumed cortical focus in the hippocampus; in an area near the frontal piriform cortex; and bilaterally in the thalamus, respectively. These findings argue for a network rather than a zone concept of epilepsy.

2 Table of contents

3 Publications resulting from the work described in this thesis

Original Articles

Hamandi, K., Salek-Haddadi, A., Laufs, H., Liston, A., Friston, K., Fish, D.R., Duncan, J.S., Lemieux, L., 2006. EEG-fMRI of idiopathic and secondarily generalized epilepsies. Neuroimage 31, 1700-1710. See chapter 9.3.2.

Laufs, H., Hamandi, K., Salek-Haddadi, A., Kleinschmidt, A.K., Duncan, J.S., Lemieux, L., 2007. Temporal lobe interictal epileptic discharges affect cerebral activity in "default mode" brain regions. Human Brain Mapping 28, 1023-1032. See chapter 9.3.3.

Laufs, H., Hamandi, K., Walker, M.C., Scott, C., Smith, S., Duncan, J.S., Lemieux, L., 2006. EEG-fMRI mapping of asymmetrical delta activity in a patient with refractory epilepsy is concordant with the epileptogenic region determined by intracranial EEG. Magn Reson Imaging 24, 367-371. See chapter 9.2.1.

Laufs, H., Holt, J.L., Elfont, R., Krams, M., Paul, J.S., Krakow, K., Kleinschmidt, A., 2006. Where the BOLD signal goes when alpha EEG leaves. Neuroimage 31, 1408-1418. See chapter 9.1.1.

Laufs, H., Lengler, U., Hamandi, K., Kleinschmidt, A., Krakow, K., 2006. Linking generalized spike-and-wave discharges and resting state brain activity by using EEG/fMRI in a patient with absence seizures. Epilepsia 47, 444-448. See chapter 9.3.1.

Laufs, H., Richardson, M.P., Salek-Haddadi, A., Vollmar, C., Duncan, J.S., Gale, K., Lemieux, L., Loscher, W., Koepp, M.J., 2011. Converging PET and fMRI evidence for a common area involved in human focal epilepsies. Neurology 77, 904-910. See chapter 9.5.1.

Review Articles

Laufs, H., 2008. Endogenous brain oscillations and related networks detected by surface EEG-combined fMRI. Hum Brain Mapp 29, 762-769. See chapter 6.

Laufs, H., 2010. Multimodal analysis of resting state cortical activity: what does EEG add to our knowledge of resting state BOLD networks? Neuroimage 52, 1171-1172. See chapter 8.

Laufs, H., 2012. Functional imaging of seizures and epilepsy: evolution from zones to networks. Curr Opin Neurol 25, 194-200. See chapter 10.

Laufs, H., 2012. A personalized history of EEG-fMRI integration. Neuroimage 62, 1056-1067. See chapter 8.

Laufs, H., Daunizeau, J., Carmichael, D.W., Kleinschmidt, A., 2008. Recent advances in recording electrophysiological data simultaneously with magnetic resonance imaging. Neuroimage 40, 515-528. See chapter 8.

Laufs, H., Duncan, J.S., 2007. Electroencephalography/functional MRI in human epilepsy: what it currently can and cannot do. Curr Opin Neurol 20, 417-423. See chapter 8.1.4.1.

4 Thesis structure

The core work presented in this thesis was performed at the Epilepsy Society in Chalfont St. Peter and the Institute of Neurology of the University College London. The inspiration of the thesis is intimately linked to my scientific work carried out in Frankfurt, Germany prior to (Laufs, Kleinschmidt et al. 2003; Laufs, Krakow et al. 2003) and stimulated my current research work concerned with the characterisation of brain states associated with varying degrees of consciousness (Brodbeck, Kuhn et al. 2012; Jahnke, von Wegner et al. 2012; Laufs 2012; Laufs 2012; Nöth, Laufs et al. 2012; Tagliazucchi, von Wegner et al. 2012). During the past 10 years working with EEG-fMRI, a relatively comprehensive picture of the presented research has formed in my mind which has been published and peer-reviewed and which I believe relates the different pieces of work to one another in a meaningful manner (Laufs and Duncan 2007; Laufs 2008; Laufs, Daunizeau et al. 2008; Laufs 2012; Laufs 2012).

The work performed in London will form the core chapters of this thesis while the prior studies and subsequent work and interpretation are reflected in the Introduction and the Discussion sections, respectively. Not described in detail in this thesis are the fruitful (Thornton, Laufs et al. 2007; Thornton, Laufs et al. 2010; Thornton, Rodionov et al. 2010; Thornton, Vulliemoz et al. 2011) efforts which were directed at launching an international multi centre study with the main aim of validating EEG-fMRI as a clinical tool in epilepsy.

Briefly, the work leading up to the research project at UCL consisted in establishing electroencephalography (EEG) recordings simultaneously with functional magnetic resonance imaging (fMRI) and the discovery that with this technique, brain states can be characterised. Then, the application of EEG-fMRI to cohorts of epilepsy patients led to the insight that interictal epileptic discharge (IED)-correlated signal changes reflect brain state changes associated with IED and that imaging supports the appreciation of epilepsy as a network disorder impacting on ongoing brain function also remote to the traditional epileptogenic regions (Rosenow and Lüders 2001). In the Conclusion, I point to a recent Current Opinion in Neurology article which might be considered a main result of my thesis work (Laufs 2012).

5 Introduction and Objective

Epilepsy is a common condition affecting around 50 million people globally. Each year, 40–190 per 100 000 people are newly affected. Appropriate pharmacological management can result in seizure freedom for 60–70% of patients, however, around 30% of this population never achieve optimal seizure control (Stephen and Brodie 2012). Drug resistant (Kwan, Arzimanoglou et al. 2010) patients with focal epilepsy might benefit from epilepsy surgery requiring presurgical evaluation encompassing careful history and physical examination, interictal EEG including sleep, video EEG monitoring, structural MRI with specific sequences, and neuropsychological and neuropsychiatric assessment (Duncan 2011; Wiebe and Jette 2012). In individuals in whom a confident solution cannot be arrived at with these non-invasive data, functional data need to be used to inform the placement of intracranial EEG electrodes to try to localize the area of seizure onset derived from fluorodeoxyglucose Positron Emission Tomography (PET), ictal Single Photon Emission Computed Tomography (SPECT), magnetoencephalography (MEG), or - developed more recently - simultaneous EEG–fMRI (Duncan 2011).

The development of EEG-fMRI was motivated by this goal, i.e. the identification of epileptogenic brain regions (Laufs and Duncan 2007). The investigations of healthy volunteers with EEG-fMRI suggested that fMRI correlates of EEG activity can identify entire sets of brain regions reflecting the brain state for which the respective EEG phenomenon of interest is characteristic (Laufs 2008). With this insight, previously difficult to interpret fMRI activation patterns in response to interictal epileptic activity appeared in a new light, and group level analyses were performed in order to reveal general principles underlying different epileptic syndromes and explaining associated conditions (Laufs 2012).

This thesis retraces the evolution of this new conceptualization based on (own) previous resting state research, the observations of which nourished the question of how knowledge of physiological brain function can be used in the interpretation of epilepsy EEG-fMRI data, especially in temporal lobe and generalized epilepsies with their common and characteristic semiological features of reduced consciousness. Given recently developed treatment options such as deep brain stimulation and targeted drug delivery, the identification of syndrome-specific networks and crucial “hubs” might pave the way for new disease management strategies.

6 Spontaneous brain activity

The following section will give an introduction to spontaneous, specifically resting state, brain activity as observable by means of EEG, fMRI and their combination. This is necessary for the appreciation of the input of investigations made in healthy subjects into the study of epilepsy patients.

6.1 Spontaneous brain activity in healthy volunteers

Spontaneous brain activity during wakeful rest is the summary of a dynamic mixture of brain states compatible with responsiveness, action planning and execution, the ability to (re-)direct attention and the processing of information in higher-order cortices. This contrasts more homogeneous brain activity induced by a specific task set. In the wakeful state, the brain generates a large number of neural processes that interact as a complex regulatory network and which can be grouped into functional modules characterized by anatomical connectivity and co-varying levels of neural activity. The scope here is to briefly introduce work on spontaneous brain activity during wakeful rest, i.e. a task-free condition, rather than to present an exhaustive enumeration of the wealth of processes occurring spontaneously, such as sensory processing and homeostatic regulation. Given that the experimental setting underlying the resting state actually represents a non-condition, i.e. is defined by the absence of a specific task, the resting state concept at first sight remains cloudy. Methodologically, findings are discussed which were obtained with electroencephalography (EEG) and functional magnetic resonance imaging (fMRI), either acquired separately or simultaneously. While the EEG signal reflects the electrical activity of cortical neuronal populations in the kHz range, the blood oxygen level-dependent (BOLD) fMRI signal reflects hemodynamic changes associated with neural activity covering the whole brain at a low temporal sampling rate (usually < 1 Hz).

6.1.1 Resting state brain activity: EEG

Long before spontaneous brain activity moved into the focus of (imaging) neuroscience (Biswal, Yetkin et al. 1995) it already represented a common condition during which patients were examined: the clinical “Routine EEG”. In this context, spontaneous ongoing EEG activity is sufficiently informative for the identification of focal pathology, epileptic activity, encephalopathy, or the degree of wakefulness; and hence a task is not required and potentially not feasible to be performed universally by any patient.

The EEG hallmark of spontaneous brain activity during wakefulness is the alpha rhythm, an amplitude-modulated 8-12 per second oscillation with the largest amplitudes during a relaxed eyes-closed condition and at occipital electrodes. This rhythm was already described in the publication of the first EEG recordings in 1929 (Berger 1929). The amplitude of the alpha rhythm diminishes almost immediately upon eye-opening or with the onset of a cognitive task (Berger 1929). This reduction in amplitude is interpreted as a desynchronization of the oscillatory generators, in other words, the generators oscillate synchronously during rest and desynchronize with the onset of processing. The alpha rhythm was considered an 'idling rhythm' (Pfurtscheller, Stancak et al. 1996), indicating a default pattern of cortical activity when the corresponding area is task-free, but ready to react. A contrasting interpretation states that the negative correlation of alpha band amplitude and task engagement reflects an active inhibitory process (Jensen and Mazaheri 2010). During wakeful rest, the main oscillations besides the alpha rhythm are the beta and gamma rhythms, related to a spectral peak in the 13-30 Hz range (beta frequency band) and a broadband activity in the 30-80 Hz range (gamma frequency band) of resting state EEG spectra (Freeman 2004). Beta-gamma band activity is generally associated with attention and active cortical processing (Freeman 2004). In order to describe the brain state of wakeful rest, it is necessary to characterize related states such as drowsiness and sleep. Similar to eye opening or cognitive processing, the EEG correlate of transitions to states of reduced vigilance is the desynchronization of the occipital alpha rhythm and, to a lesser extent, the appearance of slower oscillations (Loomis, Harvey et al. 1935; Davis, Davis et al. 1937; Rechtschaffen and Kales 1968; AASM 2007). During this transition to sleep, the EEG shows low amplitude activity without distinct peaks in the frequency

distribution. The similarity of low alpha amplitude patterns associated with reduced vigilance and those observed regularly in certain neuropsychiatric disorders was also discussed by Roth (Roth 1961). He noted that vigilance fluctuations are common during EEG recordings of healthy subjects and that the EEG of wakefulness is markedly non-stationary. The preceding discussion shows that alpha band amplitude cannot be interpreted as a vigilance marker on its own, since drowsiness on the one side, and engagement in a cognitive task or in sensory processing on the other, are likewise reflected by a marked decrease in occipital alpha activity. These results were summarized and quantified as a bell-shaped relationship between the vigilance level and alpha band amplitude by Ota (Ota, Toyoshima et al. 1996).

6.1.2 Resting state brain activity: fMRI

In the context of fMRI, the term “resting state” was coined. It describes spontaneous brain activity during wakefulness, which occurs in a task-free condition when minimal systematic confounds arise from task-related activations.

Resting state-specific activation patterns can be analyzed in different ways: a) Statistically contrasting the between-task (resting state) condition against the task condition ('reverse subtraction') yields a set of regions termed task-specific deactivations (Raichle and Snyder 2007), b) It can be studied using data driven methods, mainly independent component analysis (ICA), to identify coherent and mutually independent activity patterns (Beckmann, DeLuca et al. 2005), c) using non-fMRI modalities such as EEG derived measures (Laufs 2008), surface EMG (van Rootselaar, Renken et al. 2007) or other physiological measurements (de Munck, Goncalves et al. 2008) as regressors in a generalized linear model of the BOLD signal.

In the early years of resting state research, the search for task-specific deactivations yielded a set of brain regions termed the default mode network (DMN) (Raichle, MacLeod et al. 2001), including the medial prefrontal cortex, the posterior cingulate cortex, the precuneus and parts of the parietal cortex. This set of regions has been accredited special importance as it appears to be independent of the task against

which the resting state condition is contrasted (Buckner, Andrews-Hanna et al. 2008). Complementary to the default mode network, another, regionally non-overlapping network positively correlated to tasks was found and termed the anti-correlated network (Fox and Raichle 2007; Raichle and Snyder 2007). Functionally, activity in the DMN has been related to the processing of internal or self-related information while the anticorrelated network has been associated with attention and working memory (Buckner, Andrews-Hanna et al. 2008). Closer inspection of DMN dynamics showed that DMN activity is reorganized, rather than deactivated during task initiation and performance (Fransson 2006) and that brain activity during relaxed wakefulness spontaneously switches between modes that were interpreted as an introspective (default) mode and an alert mode with the readiness to process changes in the internal or external environment (Fransson 2005).

Because of its link to self-related information processing, the role of the DMN during wakefulness was investigated in a number of studies. The results of these studies show that DMN activity at least partially reflects intrinsic patterns of brain activity unrelated to consciousness, as shown by intact DMN activity in states of reduced or absent consciousness (sleep, coma, anaesthesia) (Boly, Phillips et al. 2008). Likewise, the combination of fMRI and fibre tract visualization using diffusion tensor imaging showed that the DMN as well as other resting state networks are reflected in the intrinsic white matter connectivity of the brain, i.e. that functional networks are at least partially determined by anatomy (van den Heuvel and Hulshoff Pol 2010).

When extracting resting state networks from fMRI time series using ICA, it is generally observed that different subsystems of the brain spontaneously activate and deactivate without apparent external stimuli conditioning these systems to engage or disengage (Beckmann, DeLuca et al. 2005). The identified subsystems were found to match networks characteristically involved in task processing, among them visual cortices, the auditory and sensorimotor systems, and the executive control network (Beckmann, DeLuca et al. 2005). Using voxel-wise functional connectivity analysis, the set of networks representing functional brain modules could be reproduced, and further networks of still unknown functional relevance were described (Power, Cohen et al. 2011).

7 Epilepsy

In the following section, I will give a brief general introduction to epilepsy and its clinical investigation and two epilepsy syndromes in particular to which the primary studies presented in this thesis will relate. Unless citations indicate otherwise, material is taken from http://www.e-epilepsy.org.uk/pages/articles/ as available in 2012.

7.1 Definition and Epidemiology

The definition of epilepsy is constantly in flux trying to do justice to clinical usefulness and current scientific insights. The International League Against Epilepsy (ILAE) and the International Bureau for Epilepsy (IBE) in 2005 have come to consensus definitions for the terms epileptic seizure and epilepsy. An epileptic seizure is a transient occurrence of signs and/or symptoms due to abnormal excessive or synchronous neuronal activity in the brain. Epilepsy is a disorder of the brain characterized by an enduring predisposition to generate epileptic seizures and by the neurobiological, cognitive, psychological, and social consequences of this condition. The definition of epilepsy requires the occurrence of at least one epileptic seizure (Fisher, van Emde Boas et al. 2005).

The formerly and in many cultures still widely held belief is that a person with epilepsy is seized by a supernatural force or power. This ancient belief is reflected in the name of the disorder - the word "epilepsy" being derived from the Greek word "epilambanein" which means "to seize or attack". It is now known, however, that seizures are the result of sudden, usually brief, excessive electrical discharges in a group of neurons and that these discharges can manifest in different parts of the brain. Manifestations of seizures will therefore vary and depend on where in the brain the disturbance first starts and how far it spreads. Transient symptoms can occur, such as loss of awareness or consciousness and disturbances of movement, sensation (including vision, hearing and taste), mood or mental function.

Up to 5% of the world's population may have a single seizure at some time in their lives, but a diagnosis of epilepsy is reserved for those who have recurring seizures, or other indicators such as EEG or structural imaging pathology indicative of a significant risk of seizure occurrence.

From many studies around the world it has been estimated that the mean prevalence of active epilepsy (i.e. continuing seizures or the need for treatment) is approximately 8.2 per 1,000 of the general population. However, this may be an underestimate as some studies in developing countries suggest a prevalence of more than 10 per 1,000.

Studies in developed countries suggest an annual incidence of epilepsy of approximately 50 per 100,000 of the general population. However, studies in developing countries suggest that this figure is nearly double that at 100 per 100,000 due to a higher risk of experiencing a condition which can lead to permanent brain damage (neurocysticercosis, meningitis, malaria, pre- and perinatal complications, malnutrition and alcohol consumption) (Forsgren, Beghi et al. 2005).

7.1.1 Morbidity

Epilepsy is complicated by psychiatric, cognitive, and social comorbidities which should never be neglected in view of their adverse effect on the course and quality of life (Lin, Mula et al. 2012). Scientifically, the persistence of cognitive impairment motivates studies investigating altered (resting state) network activity in the interictal state.

Cognitive and psychiatric impairment affect half of all epilepsy patients and represent the main clinical manifestations of pathological interictal behaviour (Bonelli, Powell et al. 2010; Duncan 2011; Jensen 2011). Factors contributing to cognitive dysfunction are the type and frequency of seizures, the location of underlying brain lesions (epilepsy syndrome) and anticonvulsive drugs (Vijayaraghavan, Natarajan et al. 2011). Effects can be “indirect” in that they alter sleep physiology and via this mechanism induce pathology, e.g. memory deficits (Chan, Baldeweg et al. 2011). Altered sleep is another example of disturbed network function caused by epilepsy. The interaction of sleep and epilepsy can easily be observed: many grand mal or frontal lobe seizures occur

upon awakening or from sleep, respectively; interictal discharges can occur exclusively during sleep, or their frequency is sleep stage-dependent (Siniatchkin, Groening et al. 2010; De Tiege, Goldman et al. 2011). Research has progressed in identifying mechanisms common to epilepsy and sleep (Halasz 2010; Halasz 2010; Eriksson 2011; Sinha 2011). In particular, the (reticular) thalamo-cortical network also involved in the generation of sleep spindles and K complexes (Steriade and Contreras 1998; Caporro, Haneef et al. 2011; Jahnke, von Wegner et al. 2011) was repeatedly found to be active during generalized spike and wave discharges.

It is conceivable that interictal morbidity is reflected in altered activity in resting state brain regions extending into their task functioning. For example, in epilepsy syndromes with impaired consciousness, the default mode network thought to be crucially involved in processes requiring consciousness will be of special interest in this respect.

7.1.2 Epilepsy syndromes

Focal epilepsies are thought to arise in the neocortex and limbic structures, especially the hippocampus and amygdala. Experimental models produced detailed theories on the generation of brief (~100-500 ms) epileptic events analogous to the 'inter-ictal spikes' often found in the EEGs of humans with focal epilepsies. It is important to realize that the site of interictal spiking can be separate from the zone of seizure onset (Duncan, Sander et al. 2006), which has implications for the interpretation of interictal spike-correlated EEG-fMRI studies.

In the context of this thesis, I will briefly introduce temporal lobe and idiopathic generalized epilepsy syndromes which are both characterized semiologically by an ictal impairment of consciousness.

7.1.2.1 Temporal Lobe Epilepsy

The commonest cause of refractory localisation related epilepsy is temporal lobe epilepsy (TLE). TLE can be divided on clinico-anatomical grounds to mesiobasal TLE,

affecting part of the limbic system, and TLE originating in the neocortical part of the temporal lobe.

TLE accounts for approximately 60-70% of focal epilepsies. It is characterised by a combination of simple and complex partial ("dyscognitive") seizures and less frequent secondarily generalised seizures. The characteristic semiology of simple partial seizures including auras consists of an epigastric rising, or visceral sensation. Dyscognitive seizures manifest with impairment of consciousness, oro-alimentary automatisms, and in the limbs, ipsilateral automatisms and contralateral dystonic posturing. Partial seizures are often refractory to medical therapy, but there can be a good outcome with surgical treatment (anterior temporal lobectomy or amygdalohippocampectomy) (Wiebe, Blume et al. 2001).

Common pathological substrates for mesial TLE include hippocampal sclerosis (HS), malignant and benign tumours (astrocytomas, gangliogliomas, dysembryoplastic neurospithelial tumours (DNET)), vascular (cavernous and venous angiomas, arteriovenous malformations (AVM)) and malformations of cortical development (MCDs) or traumatic and other injuries (infective agents, most commonly viral, and cerbrovascular disease) other developmental abnormalities (Diehl and Duncan 2011).

Neocortical or lateral TLE is less common than mesial TLE, making up around 10% of TLE cases. Simple partial, complex partial and rarer secondary generalised seizures are characteristic. Clinical manifestations of simple partial seizures include auditory and mental hallucinations or illusions, vestibular phenomena, dreamy states and misconceptions. Language is disturbed if the focus is in the dominant hemisphere. Anterior lateral TLE is associated with olfactory and gustatory sensations. Motor manifestations include clonic movement of facial muscles, facial grimacing, limb automatisms and dystonic posturing. Lateral TLE can be due to the same structural causes as mesial TLE, except hippocampal sclerosis.

7.1.2.2 Generalized epilepsy

The idiopathic generalised epilepsies (IGE) are characterised by "typical absences" (states of behavioural arrest and impaired responsiveness) and/or myoclonic jerks and

generalised tonic-clonic seizures; EEG features such as generalised spike and wave or polyspike and wave activity of frequencies around 3 per second, and the absence of other neurological signs or symptoms in the neurological examination.

IGE constitutes nearly one third of all epilepsies. Many have a hereditary predisposition and are benign and age related. Further sub-classification is made depending on the combination of the features mentioned above in addition to age of onset and diurnal seizure pattern, giving the main subgroups of Childhood asence epilepsy (CAE), Juvenile myoclonic epilepsy (JME), Juvenile absence epilepsy (JAE), Epilepsy with Generalised tonic clonic seizures on awakening (IGE-GTCS).

In all IGE syndromes, seizures are characteristically exacerbated by sleep deprivation and alcohol. The response to appropriate antiepileptic drug treatment is generally good but often needs to be lifelong.

Long standing models exist on the basic mechanisms of IGE (Vaudano, Laufs et al. 2009). It arises from the thalamocortical system, and appears to depend on the properties of both cortex and thalamus. The classic three per second spike-wave activity is thought to depend on synchronisation of the thalamus by rhythmic activity of networks of inhibitory neurons with the 3/s rhythm arising from the interaction of inhibitory postsynaptic potentials (IPSPs) with low threshold calcium channels in thalamic cells. Evidence, especially from the Generalised Absence Epilepsy Rats from Strasbourg (GAERS) model, suggests that the thalamic T current may not be critical and that the frontal cortex may play a key role, a point that contributes to blurring the distinction between localisation-related and primary generalised epilepsies (Timofeev and Steriade 2004).

7.2 The clinical investigation of epilepsy

The three corner stones of epilepsy diagnosis are 1. clinical history and examination, 2. Again clinical history, and 3. structural MRI and EEG. In focal epilepsies, another line of work up relates to the identification of the most likely seizure origin. While seizure semiology alone often is helpful to narrow down the potential focus, when treatment

with anticonvulsive medication is unsatisfactory, further diagnostic tests are required in view of potential surgical intervention.

7.2.1 Neurophysiology

7.2.1.1 Electroencephalography

EEG is a neurophysiologic technique that measures bioelectric neural currents arising in the pyramidal neurons of the cerebral cortex. These currents produce excitatory postsynaptic potentials (EPSP) and inhibitory postsynaptic potentials (IPSP) along the dendritic tree of the pyramidal neurons. Current flow within the pyramidal neurons is called the primary current. The intracellular currents produce compensatory extracellular currents called secondary currents, also known as volume currents. These propagate throughout the body in a manner determined by the conductivity of each tissue. EEG records potential differences arising from secondary currents when electrodes are attached to the scalp or implanted into the brain (Barkley and Baumgartner 2003).

EEG is important for the investigation of epilepsy. It is used to support the clinical diagnosis by the identification of localized – or general – paroxysmal discharges or patterns. The inter-ictal EEG does not provide a reliable index of the severity, control or prognosis of epilepsy. A reduction in the amount of epileptiform activity shows only a weak association with reduced seizure frequency. But a correlation between the number of interictal discharges and cognitive function has been proposed (Binnie 2003).

7.2.1.2 Magnetencephalography

Over the recent years, magnetoencephalography (MEG) has emerged as another clinical neurophysiological tool providing unique data not obtainable by other neuroimaging techniques – reflected by the number of new devices being set up. While it is mainly being used in the area of cognitive research (event-related potential

studies), MEG can also be used clinically. Unlike in EEG, where usually ongoing brain activity is monitored and reported, MEG serves to model the sources of interictal epileptic discharges (Barkley and Baumgartner 2003). Given the heterogeneity of patients and a lack of standardization for MEG in a clinical setting, its value is difficult to assess systematically. Accordingly, MEG's largest possible role was seen to increase the number of patients who can undergo epilepsy surgery but that it should not be used to deny surgery to any patient (Stefan, Rampp et al. 2011).

7.2.2 Imaging

While neurophysiological investigations can reveal pathological function of the brain, structural imaging will highlight morphological abnormalities. One aim of the different functional imaging techniques is to bridge the gap between the former approaches by identifying pathological function in the spatial structural domain.

7.2.2.1 Structural Magnetic Resonance Imaging

Visualisation of lesions that give rise to focal epilepsy and identification of patients who are suitable for surgical treatment are important goals in the imaging of epilepsy. In patients with newly diagnosed epilepsy, MRI is clearly superior to X-ray computed tomography (CT) and may identify an epileptogenic lesion in 12–14%, but up to 80% of the patients with recurrent seizures have structural abnormalities evident on MRI. The most common abnormalities identified are hippocampal sclerosis (HS), malformations of cortical development (MCD), vascular malformations, tumours, and acquired cortical damage (Salmenpera and Duncan 2005).

7.2.2.2 Magnetic resonance spectroscopy

Over the last decade single voxel Magnetic Resonance Spectroscopy (MRS) and MRS imaging have advanced as non-invasive tools for the investigation of cerebral metabolism (McLean and Cross 2009). Depending on the imaging coil used, metabolites such as N-Acetyl-Aspartate, cholin, myoinositol, creatinine, glutamate

(proton MRS), phospho-esters, phosphor-creatinine, adenosine-triphosphate and others (phosphor MRS) can be quantified regionally and point to (lateralized) pathological brain tissue (Kuzniecky 1999). Currently, MRS is still compromised by its limited spatial sampling and long acquisition times and so far has struggled to find entry into routine epilepsy-specific use (Kuzniecky 2004).

7.2.2.3 Positron Emission Tomography

Maps can be derived from ^{18}F-deoxyglucose (FDG) and 15O-water ($H_2{}^{15}O$) Positron Emission Tomography reflecting cerebral glucose metabolism and cerebral blood flow respectively.

Studies with FDG-PET have defined the major cerebral metabolic associations and consequences of epilepsy but the data are unspecific with regard to aetiology, and abnormalities are often more widespread than the pathological lesions. The place of the investigation is in the presurgical work up of patients with refractory focal epilepsy and normal or non-definitive MRI scans. In these instances, or if data are discordant the goal is to generate a hypothesis that may then be tested with intracranial EEG recordings (Salmenpera and Duncan 2005).

PET studies of specific ligands may be used to demonstrate the binding of specific ligands—for example, ^{11}C-flumazenil (FMZ) to the central benzodiazepine-$GABA_A$ receptor complex, ^{11}C-diprenorphine and ^{11}C-carfentanil to opiate receptors, and ^{11}C-deprenyl to MAO-B. The technique is costly and scarce, but gives quantitative data with superior spatial resolution to SPECT (see below) (Hammers 2004).

$GABA_A$–benzodiazepine receptors: flumazenil ^{11}C-flumazenil (FMZ) is a useful marker of the $GABA_A$– central benzodiazepine receptor (cBZR) complex.

FMZ PET detects abnormalities in the medial temporal lobe of TLE patients with normal MRI. Potentially surgically useful reductions in hippocampal or extrahippocampal FMZ binding have been found in 47% of MRI negative TLE patients.

Studies of extratemporal epilepsy patients including those with normal MRI have indicated that surgically useful abnormalities of ^{11}C-FMZ binding can be found in half of the cases (Duncan and Koepp 2000).

In summary, PET offers a tool for investigating neurochemical abnormalities associated with epilepsies. The method is an important research tool and can be useful in selected clinical situations, especially when there is not good concordance between MRI, EEG, and other data (Theodore 2002). Further ligands, particularly tracers for excitatory amino acid receptors, subtypes of the opioid receptors and the $GABA_B$ receptor, will improve the characterisation of different epileptic syndromes (Salmenpera and Duncan 2005).

7.2.2.4 Single Photon Emission Computed Tomography

Single photon emission computed tomography (SPECT) is a nuclear medicine imaging method that allows measurements of regional cerebral blood flow changes in the areas affected by epileptic activity. A comparison of the ictal (tracer injection as early as possible during a seizure) with the interictal perfusion pattern is considered to indicate brain tissue involved in seizure generation - or propagation (Van Paesschen, Dupont et al. 2007).

7.2.2.5 Functional Magnetic Resonance Imaging

Functional magnetic resonance imaging (fMRI) is a non-invasive neuroimaging technique commonly applied clinically in psychology, cognitive and basic neuroscience research. In specialized centers, it is being used routinely as a tool for clinical decision-making in epilepsy. It has proven useful to determine language location and laterality in patients eliminating the need for invasive tests (Powell and Duncan 2005). fMRI can been used pre-surgically to guide resection margins, preserving eloquent cortex (e.g. motor mapping). Other fMRI paradigms assessing memory, visual and somatosensory systems show great promise. Simultaneous recording of electroencephalogram (EEG) and fMRI has also provided insights into the networks underlying seizure generation

and is increasingly being used in epilepsy centres (Beers and Federico 2012) - as becomes evident throughout this thesis.

8 General Methods

8.1 Acquisition

8.1.1 Why and how was EEG-fMRI developed?

The content of the following section has been published in the Neuroimage Special Issue: "Twenty Years of Functional MRI: The Science and the Stories" (Laufs 2012) (**Fehler! Verweisquelle konnte nicht gefunden werden.**) and gives my personal account on the history of EEG-fMRI, which is biased towards the European history of EEG-fMRI integration, specifically a "London perspective" (Hamandi, Salek-Haddadi et al. 2004), the one which I was most closely involved with.

A more balanced view can be obtained by studying review articles on the topic which will show that many more groups contributed greatly to the field, such as those around John Archer, David Abbott and Graeme Jackson in Melbourne/Australia (Archer, Briellman et al. 2003; Archer, Briellmann et al. 2003), Margitta Seeck, Christoph Michel and Theodor Landis in Geneva/Switzerland (Seeck, Lazeyras et al. 1998), Jean Gotman and colleagues in Montréal/Canada (Benar, Gross et al. 2002; Al-Asmi, Benar et al. 2003; Bénar, Aghakhani et al. 2003), Alexander Hoffmann, Lorenz Jäger and Maximilian Reiser in Munich/Germany (Hoffmann, Jager et al. 2000; Jäger, Werhahn et al. 2002), and Steven Warach, John Ives and Donald Schomer in Boston/U.S.A. (Ives, Warach et al. 1993; Warach, Ives et al. 1996) - just to name a few.

On March 2nd, 2002, Louis Lemieux and Robert Turner held the 'First Workshop on EEG-fMRI' at Queen Square in London with David Fish (Institute of Neurology, UCL, UK), Georgio Bonmassar (Hardvard, U.S.A.), John Stern (UCLA, USA), Afraim Salek-Haddadi (Institute of Neurology, UK), Walter Freeman (Berkeley, USA), Arno Villringer (Charité, Germany), Jean Gotman (Montreal Neurological Institute, Canada) and Fabio Babiloni (Roma 1, Italy) as the speakers. I had the opportunity to attend this in retrospect historical meeting as the companion of Karsten Krakow. He had completed his PhD at UCL as the first medical fellow (under David Fish) acquiring EEG-fMRI at the

National Society for Epilepsy (now called The Epilepsy Society, Chalfont St. Peter, UK) from Queen Square (The National Hospital for Neurology and Neurosurgery, UCL, UK) epilepsy patients (Krakow, Woermann et al. 1999) with Philip Allen's MR-compatible EEG system (Krakow, Woermann et al. 1999; Hamandi, Salek-Haddadi et al. 2004). Karsten Krakow after his PhD had moved to the Department of Neurology at the Goethe University in Frankfurt (Germany), where I met him starting my fellowship in neurology. It was at that symposium that apart from the speakers I had the opportunity to meet in person some of the EEG-fMRI pioneers including Phil Allen, Oliver Josephs and Mark Symms.

At the inception of EEG-fMRI, advances on the technical as well as the analysis side were tremendous and went hand in hand with one another, while later on, when the first major technical hurdles had been taken and good hard- and software were available commercially, scientific applications and analysis strategies could advance independently of the engineering side of matters.

The idea of EEG-fMRI integration was clinically motivated and its development driven by the desire of epileptologists to localize electrical sources of epileptic discharges (Ives et al., 1993). Of course, it was the engineers – usually having been working in close contact with medics already - who made things factually happen (Ives, Warach et al. 1993; Goldman, Stern et al. 2000; Krakow, Allen et al. 2000). Particularly boosted by working in a clinical environment, engineers from the start were not only facing the technical side of things (magnetic field, radio frequency, image quality, EEG quality) but also quite rightly very concerned about patient safety (Ives, Warach et al. 1993; Lemieux, Allen et al. 1997).

At first glance, using EEG-fMRI may appear an indirect approach to the clinical question where high density EEG electrical source localization should provide a more straightforward solution. Yet, w.r.t. localizing sources to deeper brain structures the precision of fMRI in localizing with confidence the spatial topography of neural processes was and still is considered superior to that of scalp EEG (Ives et al., 1993; Grova et al., 2008).

Spike triggered, interleaved, event-related simultaneous and continuous EEG-fMRI

The great potential of EEG-fMRI seen by epilepsy researchers lead to methodological milestones including both acquisition hardware and artifact reduction algorithms (Lemieux et al., 1997; Allen et al., 1998).

That was before the application of EEG-fMRI was extended to physiological human brain function, predominantly the study of event-related potentials (Bonmassar et al., 1999; Kruggel et al., 2000) and oscillations (Goldman, Stern et al. 2002; Laufs, Kleinschmidt et al. 2003; Moosmann, Ritter et al. 2003). Until decent artefact reduction methods were available, EEG-fMRI had to be performed in an 'interleaved' fashion such that readable EEG epochs were obtained inside the MRI scanner: image volume acquisition blurring the EEG was only 'triggered' following the online detection of an epileptiform discharge by a trained observer. The EEG was recorded continuously inside the MR scanner with MRI compatible equipment such that the traces could be monitored on a screen while the fMRI acquisition did not obscure them. When the occurrence of an event triggered the manual start of echo planar image (EPI) acquisition, the relative delay in the hemodynamic response to the event was exploited. For comparison, baseline images were acquired in an analogous fashion when it was thought that the EEG was 'event-free'. A subsequent t-test served to identify BOLD signal changes in response to the triggering events (Warach et al., 1996; Seeck et al., 1998; Krakow et al., 1999; Patel et al., 1999; Krakow et al., 2000; Lazeyras et al., 2000; Jager et al., 2002). A significant drawback of this technique was that the EEG recorded during MR gradient switching could not be evaluated, and an absence of interictal epileptic discharges (IED) could not be guaranteed. An approach was taken to try and acquire pharmacologically induced IED-free EEG by means of benzodiazepines (Seeck et al., 1998) – but this does not leave hemodynamic coupling and basic neuronal functioning unaffected (Yoshizawa et al., 1997). The next step was the periodic acquisition of individual EPI volumes with *a priori* gaps between subsequent image volumes facilitating EEG inspection during the interleaved scanner pause. Still, this lead to a relevant loss of potentially interpretable (EEG) data. Eventually, Phil Allen hand in hand with building his EEG hardware developed algorithms which allowed recovery of the remaining EEG epochs obscured by pulse (cardio-ballistic) and imaging artefact. Eventually, continuous image acquisition during EEG recording became available facilitating true event-related, IED-based fMRI analysis approaches (Lemieux

et al., 2001). An excellent and detailed review of the early studies from spike-triggered to event-related studies was written by Salek-Haddadi, Karsten Krakow's successor and another pioneer in the EEG-fMRI world (Salek-Haddadi, Friston et al. 2003), whom I personally owe very much as he solidly introduced me to the field of EEG-fMRI and associated methodologies.

A key issue for high quality EEG signals after artefact reduction via the subtraction of a template of the MRI-induced artefact was the synchronization of the artefact correction algorithm with the MRI slice acquisition making possible online artefact subtraction (Allen, Polizzi et al. 1998; Allen, Josephs et al. 2000; Goldman, Stern et al. 2000). The first step to synchronizing the EEG hardware with the MR scanner was made by Mark Cohen, who patented the triggering of EEG digitization at the onset of every MRI volume acquisition. Years later, the value of this was re-appreciated and elaborated (Mandelkow, Halder et al. 2006): the EEG digitization (hardware) was continuously synchronized with the MR scanner clock, i.e. the image acquisition and associated gradient switching. In the ideal case, if EEG digitization is fully driven by the MR clock, there is no drift between the running sequence and the EEG digitization making possible the creation of an accurate template of the gradient artefact and good EEG quality after its subtraction.

Before commercial online artefact subtraction tools were marketed, Oliver Josephs from the Functional Imaging Laboratory (Wellcome Trust Centre for Neuroimaging, UCL, UK) had meanwhile created both a device on a circuit board synchronizing EEG digitization with the MR scanner clock and MATLAB code facilitating *online* artefact correction suitable for seamless combination with a commercially available MR compatible EEG recording system. Gareth Bahlke, a colleague of Phil Allen's at the 'Neurophyisology Workshop' of the National Hospital for Neurology and Neurosurgery at Queen Square (London, UK) later redesigned the circuit such that it would fit into a battery driven device no larger than the size of a cigarette box. A commercial 'clock divider' adjustable to any scanner clock's frequency had meanwhile become available. In the early days of EEG-fMRI, like in London (Krakow, Allen et al. 2000), other centres such as those in Melbourne (Archer, Briellmann et al. 2003), Rome (Iannetti, Di Bonaventura et al. 2002) or Los Angeles (Goldman, Stern et al. 2000) worked with

custom-built equipment. Other groups used early commercial equipment sometimes originating from the mentioned devices, e.g. the “Opti-Link” system from Neuro Scan Labs (Charlotte, NC, U.S.A.) developed by John Ives in the early 1990s, or the “EMR10” (EMR16/21/32 gitial, respectively) from Schwarzer (Munich, Germany) developed around Alexander Hoffmann in the later 1990s. The Opti-Link (MagLink) system transmitted the multiplexed analogue EEG signals to the control room outside the MR scanner room, where the data was de-multiplexed and fed into a conventional analogue EEG amplifier (modified SynAmps). In contrast to this ‘transfer system’, the EMR could be placed near the MR scanner and the digitized EEG was guided via fibre optics to a computer outside the scanner room providing good signal quality at least during times in between gradient switching. Phil Allen’s system could ‘live’ near the scanner, too, using a bipolar montage at the recording level reducing artefacts before amplification and digitization which - in addition to low pass filtering – facilitated EEG recording during gradient switching. Similar to Phil Allen’s approach, Brain Products GmbH (Gilching, Germany) developed an amplifier *de novo*, especially designed for use with MRI scanning as opposed to e.g. shielding an existing device or simply adding a ‘transfer system’. This was one important clue to their continued success: their BrainAmp MR provided the first system operating from within the scanner bore with 32 channels. Our centre gained experience with it in the early 2000s, and due to their close collaboration with us and other researchers, the company finally provided us with an additional (initially external) 250 Hz low pass filter, with which we finally managed to record high quality EEG continuously during EPI acquisition (Laufs, Kleinschmidt et al. 2003).

Most of the mentioned systems persist until today in the form of ‘next generation’ models characterised by better signal characteristics, more channels and improved overall usability. Likewise, correction algorithms for the reduction of MR gradient and ECG (ballistocardiogram) artefact reduction methods have been refined. Not infrequently, when a group first engaged in EEG-fMRI research they explored different artefact correction methods and (fortunately) tried to make advances by developing their own by modifying and for their individual purposes improving mostly existing algorithms (Sijbersa, Van Audekerke et al. 2000; Ellingson, Liebenthal et al. 2004; Ford, Sands et al. 2004; Huiskamp 2005; Srivastava, Crottaz-Herbette et al. 2005; Wan, Iwata et al. 2006; Wan, Iwata et al. 2006; Debener, Strobel et al. 2007; Goncalves, Pouwels et

al. 2007; Masterton, Abbott et al. 2007; Negishi, Pinus et al. 2007; Otzenberger, Gounot et al. 2007; Ritter, Becker et al. 2007; Vincent, Larson-Prior et al. 2007; Laufs, Daunizeau et al. 2008; Mahadevan, Mugler et al. 2008; Koskinen and Vartiainen 2009; Ryali, Glover et al. 2009; Mandelkow, Brandeis et al. 2010; Mullinger, Yan et al. 2011). Some of these methods are freely available, e.g. in the form of user-friendly toolboxes (Kim, Yoon et al. 2004; Niazy, Beckmann et al. 2005; Moosmann, Schonfelder et al. 2009; Leclercq, Schrouff et al. 2011).

8.1.2 How is EEG-fMRI (to be) performed?

Simultaneous recording of brain activity by different neurophysiological modalities can yield insights that reach beyond those obtained by each technique individually, even when compared to those from the post-hoc integration of results from each technique recorded sequentially. Success in the endeavour of real-time multimodal experiments requires special hardware and software as well as purpose-tailored experimental design and analysis strategies.

In the following I will review the key methodological issues in recording electrophysiological data in humans simultaneously with magnetic resonance imaging (MRI), focusing on technical and analytical advances in the field. Parts of the following section were published in Neuroimage (Laufs, Daunizeau et al. 2008). This publication additionally contains examples derived from simultaneous electroencephalography (EEG) and electromyography (EMG) during functional MRI in cognitive and systems neuroscience as well as in clinical neurology, in particular in epilepsy and movement disorders and concludes with an outlook on current and future efforts to achieve true integration of electrical and haemodynamic measures of neuronal activity using data fusion models. Of course, other reviews exist (Salek-Haddadi, Friston et al. 2003; Gotman, Kobayashi et al. 2006; Ritter and Villringer 2006; Herrmann and Debener 2007).

Hardware

The signal transduction chain of the electrophysiological signal of interest (e.g. EEG, EMG, skin impedance) starts at the subject's surface where electrodes make skin contact with the aid of a conductive gel or paste. The currents generated by synchronously active and parallel oriented pyramidal neurons will cause a potential between EEG electrodes which then generate current flow detected by the amplifier which is digitised and recorded. The signal is relayed between the electrode and amplifier through wires. Either, these [metallic] wires reach from inside the scanner bore to the outside of the electro-magnetically shielded scanner room, in which case, conventional EEG amplification and digitization hardware can be used (provided a sufficient amplitude recording range and sampling rate can be obtained). Or, preferably, the signal is amplified and digitized within or near the scanner bore before leaving the scanner room through optical fibres (Allen, Josephs et al. 2000). This has the advantages of both increased signal fidelity and patient safety. An interesting alternative is the use of the MR receiver hardware to transmit the EEG signals via the MR scanner receiver coil encoded alongside the MR signals (Van Audekerkea, Peeters et al. 2000; Hanson, Skimminge et al. 2006).

The induced artifact in the EEG is due to a complex combination of factors including the field strength (and so frequency), orientation, positioning of the recording equipment relative to the RF coil, and the geometric relationship between the magnetic field gradients relative to the electrophysiological equipment. When measuring limb EMG, for example, increasing distance between the recording locations and the magnet isocentre does not necessarily translate into reduced artifact (despite decreasing field strength) because the field homogeneity decreases and hence motion will cause greater artifact than in the homogenous field. Generally, artifact will increase with the distance relative to the gradient direction and within the linear part of the gradients be determined significantly by the distance between measurement and reference electrode.

Subject safety issues pertain to current flow and heating within the body that is normally greatest close to the electrodes. The time-varying (switching) magnetic field gradients can induce voltages in electrodes and leads. Where the subject provides

significant impedance within this circuit, current will flow within tissue which in turn could potentially cause stimulation, electric shock and tissue damage. Similarly, movement of an electric circuit (loop) in the static magnetic field will cause current flow and could cause injury via the same mechanisms (Lemieux, Allen et al. 1997). Especially at higher field strengths, the MR sequence (and coil) used in the presence of the multimodal recording equipment should not lead to excess energy deposition (e.g. specific absorption rate, (Angelone, Potthast et al. 2004; Angelone, Vasios et al. 2006)).

The primary safety risk is due to heating arising from the interaction of the radio frequency (RF) fields used for MRI signal excitation with the electrophysiology recording equipment. It should be noted that no direct connections need to be present at RF frequencies for low impedance loops to be formed that will have current induced within them due to the RF fields. Maximum heating will occur when a conductor is resonant at the frequency of the RF field. It is important to realise that a single wire can be resonant (effectively acting as an RF antenna) and cause dangerous heating in nearby tissue, particularly at the ends of the wire where the electric field is normally concentrated (Achenbach, Moshage et al. 1997; Dempsey, Condon et al. 2001; Pictet, Meuli et al. 2002). Resonant lengths can vary between tens of centimetres and several metres depending on a number of factors including scanner frequency (i.e. field strength), wire environment, shape and position. From this it follows that careful choice and testing of leads and electrodes used within an MRI scanner is necessary and inductance should be reduced by minimising the length of wires and avoiding loops (Ives, Warach et al. 1993; Lemieux, Allen et al. 1997; Goldman, Stern et al. 2000; Dempsey, Condon et al. 2001; Lazeyras, Zimine et al. 2001). Empirical evidence (Baumann and Noll 1999) and theoretical considerations suggest that it is best to guide wires in close proximity to the axis around which the gradient switching occurs, i.e. the z-axis of the scanner. Such a geometry minimises the angle between the changing magnetic field and the electrical conductor - and at the same time avoids loop formation (Lazeyras, Zimine et al. 2001). These advantages outweigh the effect of the electrical field parallel to the z-axis as long as the field decays quickly outside the (head) coil. In addition, current limiting resistance will be of protective benefit and can be implemented either by putting resistors close to the electrodes or distributed

within the leads (Lemieux, Allen et al. 1997; Dempsey, Condon et al. 2001; Vasios, Angelone et al. 2006).

Both reduced (non-optical) lead length and increased lead impedance limit the induced amplitude of the artifact in the recorded EEG. While these procedures reduce the required input range of the amplifier, they also correspondingly reduce the signal. Electrode caps help to keep wires in an optimized predefined position (Baumann and Noll 1999), without loops and direct electrical contact yet bundled together. Twisting of all wires together has been proposed with the idea that induced fields cancel each other out (Goldman, Stern et al. 2000), but to work this assumes very similar resistances of the conductors. Even if achieved in practice, any remaining voltage difference would still be amplified. Generally, cables should be fixed to protect them against motion, such as gradient switching-generated vibrations (Thees, Blankenburg et al. 2003), by means of sandbags (dampening effect), tape or bandage (Bénar, Aghakhani et al. 2003).

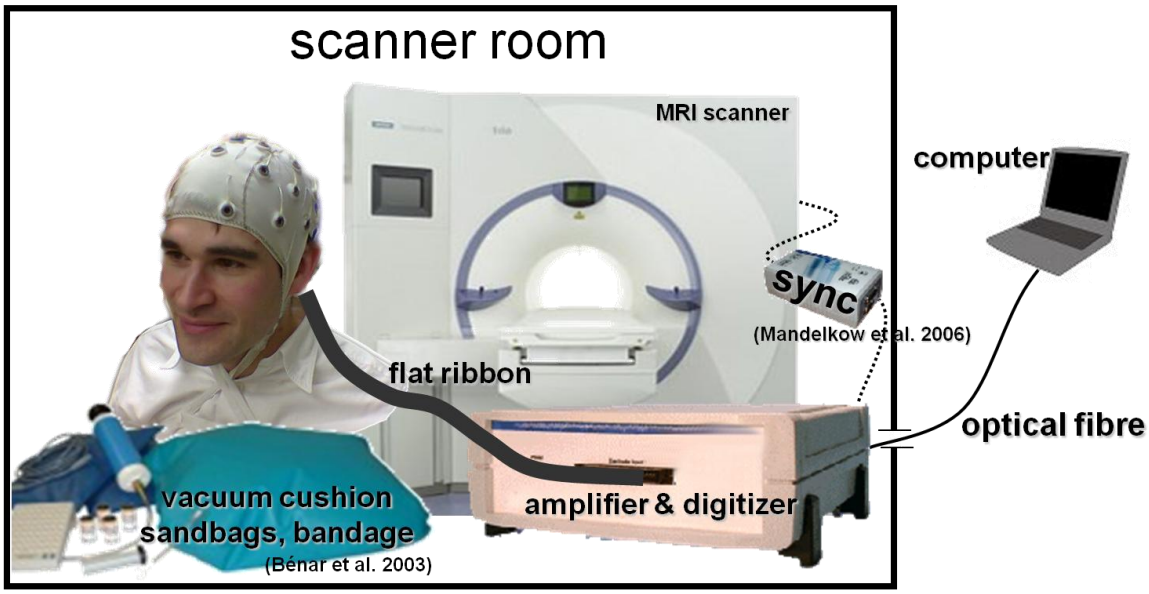

Figure 8.1-1: Schematic EEG-fMRI experimental set-up.

Materials should be non-ferrous (wires are mostly copper or carbon), and all equipment introduced into the shielded MRI room must not emit RF in the scanner frequency band (Ives, Warach et al. 1993) such that scanner functionality, image quality and subject safety are not compromised (Angelone, Potthast et al. 2004; Angelone, Vasios et al. 2006). Obviously, the electrophysiology recording equipment needs to remain operational within the MR scanner environment and during scanner

operation (Ives, Warach et al. 1993). A balance must be struck between tolerable artifact on the images and practicality of the materials used. In that respect, for example, gold electrodes have been preferred over carbon electrodes (Krakow, Allen et al. 2000). Sintered Ag/AgCl ring "floating" electrodes are also widely used and include a surface mounted safety resistor. These electrodes i) do not directly touch the skin, ii) have good artifact characteristics, and iii) provide ease of use.

The amount of conductive agent used should be minimised, and it should be tested for related image artifacts, especially within the brain (Krakow, Allen et al. 2000; Bonmassar, Hadjikhani et al. 2001). Conversely, signal alterations confined to the electrode positions themselves may in fact be used for their localization. Finally, the entire ensemble should be tested together, as the MRI 'signal to noise ratio' (SNR) will be a function of 'radio frequency (RF) coil loading' that is increased with the amount of conductive material introduced into the RF scanner coil: in materials of high electrical conductivity RF (involved in excitation and detection of the MR signal) generates large surface current densities which act to screen the RF field from the interior of the material and hence compromise image quality. These currents also disturb the B1-field within regions in close proximity to the conductor, and finally, due to RF field-conductor interaction, the RF coil resistance increases further reducing SNR. Specifically, shielding-effects of multi electrode set-ups (Scarff, Reynolds et al. 2004) and altered B_0 and/or B_1 field homogeneity including that caused by EOG and ECG leads can manifest in the human head (via flip angle reduction) and thus may reduce the SNR of the images in areas of interest (Mullinger, Debener et al. 2007).

Directing special effort at subject comfort is warranted for increasing tolerance of the subject and thus also limiting head motion. Using a vacuum head cushion (Bénar, Aghakhani et al. 2003) has been found to minimise both motion-induced artifacts on the images as well as motion-induced currents contaminating the electrophysiological signal. This is especially important for patient studies in general and when recording EMG which is highly motion sensitive (Salek-Haddadi, Friston et al. 2003; Hamandi, Salek-Haddadi et al. 2004). The use of sedative agents to suppress motion needs careful consideration as 'neuroactive' substances can alter net synaptic activity in a region-specific manner and thus fMRI signal intensity (Bloom, Hoffmann et al. 1999;

Kleinschmidt, Bruhn et al. 1999; Iannetti and Wise 2007). Depending on the study design, the administration of such substances may confound the results such that observations can be falsely attributed to the effect of interest while they may in fact be to major parts caused by the pharmacologic agent (Ricci, De Carli et al. 2004; Iannetti and Wise 2007). Under certain circumstances sedation cannot always be avoided, e.g. when studying very young children with fMRI (Jacobs, Kobayashi et al. 2007), but valuable patient data sets acquired without sedation can often be recovered if motion effects are modelled sufficiently at the analysis stage (Lemieux, Salek-Haddadi et al. 2007).

EMG recordings during fMRI are particularly affected by artifact induced by motion in the static field because even during isometric contractions (i.e. muscle contraction without gross limb movement) some degree of electrode movement in the field is inevitable. Moreover, this artifact will tend to be grossly task-correlated while still irregular and thus difficult to model (van Duinen, Zijdewind et al. 2005; Richardson, Grosse et al. 2006; Post, van Duinen et al. 2007). In these cases, true bipolar recordings are advantageous as artifact common to closely positioned electrodes is already reduced prior to correction (Goldman, Stern et al. 2000; Richardson, Grosse et al. 2006). If required for polygraphic measurements, other physiological data can be recorded such as respiration and pulse oximetry in addition to the various electrophysiological measurements (Laufs, Walker et al. 2007; Jahnke, von Wegner et al. 2012). Respective pneumatic and optic devices are provided by most scanner manufacturers and thus do not require special consideration of MR-compatibility.

Raw data quality remains essential despite sophisticated gradient and pulse artifact reduction algorithms. The generic set-up outlined above thus needs to be adapted to and optimized for every scanner, electrophysiological recording equipment and site. One should also consider switching off the scanner cooling pump and AC power sockets in the room to avoid these additional artifact sources. Finally, synchronization of EEG sampling with the MR sequence vastly improves the effectiveness of MRI artifact reduction methods (Mandelkow, Halder et al. 2006). For their correction to work gradient artifacts must not exceed the amplitude range of the amplifier, the latter additionally requiring suitable signal-to-noise recording characteristics (see

below). Special care should be taken during electrode preparation since relatively high skin-electrode impedances, which can still yield good data quality when the MR scanner is not running, will become detrimental to signal quality once scanning is underway.

MR-compatible EEG amplifiers should allow sampling of the electrophysiological signal including the gradient artifact at a high temporal rate and within a large amplitude range. The temporal resolution – unless perfect synchronization is warranted between the scanner and the recording equipment (Anami, Mori et al. 2003; Mandelkow, Halder et al. 2006) – is required because of the high slew rates of MRI sequences, and a large amplitude input range in order to avoid clipping of the signal and allow artifact reduction (see below). Widely used amplifiers permit MR-synchronized recording of 128 or more data channels at 5000 Hz with a dynamic amplitude range of +/- 3.2 mV to +/- 325 mV and respective resolution (16-bit sampling); noise characteristics <1 uVpp, 125 dB common mode rejection, switchable 10 Mega/10 Giga Ohm input impedance. With such an amplifier, conventional echo planar imaging sequences for blood oxygen level-dependent (BOLD) contrast and arterial spin labelling (ASL) have been successfully applied at up to 3 T (Hamandi, Laufs et al. 2007). No human EEG-fMRI studies have yet been published for higher field strengths, but safety evaluation and experiments carried out in non-human primates suggest that respective studies in humans may follow in due course (Angelone, Potthast et al. 2004; Angelone, Vasios et al. 2006; Schmid, Oeltermann et al. 2006; Vasios, Angelone et al. 2006).

Post processing: artifact reduction algorithms

Understanding how artifacts arise is the key to designing artifact reduction algorithms. Three types of artifacts in electrophysiological recordings originate specifically from the MR scanner. All these unavoidable artifacts manifest themselves as induced voltages that add linearly to the EEG signal and thus threaten to obscure the biological signal of interest. The three artifact types arise from: 1) MRI scanning ('imaging artifact'): This is usually the largest in amplitude (in the order of mV) but the most stable over time (Allen, Josephs et al. 2000). Its origin has already been discussed above: the time varying electromagnetic fields induce currents resulting in artificial voltages in the recorded electrophysiological data; 2) cardiac pulsation ('pulse artifact')

(Allen, Polizzi et al. 1998): This is thought to be due to heart beat-related movements (systolic pulsation) of the head or of electrodes adjacent to blood vessels, or of the blood itself caused by systolic acceleration and abrupt diastolic directional change of blood flow in large body vessels and – arguably (Nakamura, Anami et al. 2006) – due to fluctuations of the Hall-voltage due to the pulsatile arterial blood flow (Ellingson, Liebenthal et al. 2004); 3) the amplitude and topography of the previous artifact types are affected, and the constant nature – which is the crucial basis for most artifact subtraction strategies - of 1) is compromised by subject motion, any change in position of the metallic recording components in the static field (Hill, Chiappa et al. 1995), drift of the electrode impedances and of the MR scanner magnetic field gradients that change by a small amount over time predominantly due to gradient heating.

The scanner-generated imaging artifact is theoretically the easiest one to remove owing to its periodicity. All currently available artifact subtraction methods exploit this regularity to varying degrees. However, since the regularity is not perfect, neither are the correction algorithms. Due to the scanner artifact's huge amplitude compared to the biological EEG signal (about a factor of 1000 for a standard set-up), even slight imperfections of the artifact correction leave EEG activity hard to visualise. In the absence of the perfect algorithm, depending on the purpose of the study, different approaches may be more or less suitable than others.

The principle of the first MRI scanner artifact reduction method was based on determining a template artifact waveform by time-locked averaging time-locked to the periodic MR-acquisition (Sijbers, Michiels et al. 1999; Allen, Josephs et al. 2000). This procedure is based on the rationale that those components of the recorded signal, which are not time-locked to image acquisition, should average to zero. Because of the additive property of the theoretically constant imaging artifact, averaging results in a template which can be subtracted from the data and thus recover the biological signal (and noise). Artifact drifts can be partly addressed by sliding average formation and subsequent linear filtering and, theoretically, adaptive noise cancellation (Allen, Josephs et al. 2000; Wan, Iwata et al. 2006).

These methods cannot entirely make up for asynchrony between the MR sequence and electrophysiology data sampling: despite EEG sampling rates of several kHz, MR slew rates at the order of several hundred T/m/s and gradient strengths of several dozen mT/m will result in very subtle temporal jitter and in turn compromise template accuracy. Digital up-sampling by interpolation of the recorded data and subsequent re-alignment of the segments before averaging (Allen, Josephs et al. 2000), or grouping of segments to form several average 'families' based on correlation criteria (BrainVision Analyzer, Brainproducts, Munich, Germany) further improve correction quality – and can be performed online. But ideally EEG sampling should be *a priori* time-locked to the MR scanner and the TR an exact multiple of the sampling interval (Mandelkow, Halder et al. 2006).

A fixed temporal relation between EEG and MRI sampling is also a prerequisite for the 'stepping stone' technique, the idea of which is to avoid sampling EEG during periods of magnetic field gradient switching in the MRI pulse sequence but constrain sampling to periods without gradient switching where no related artifact is induced (Anami, Mori et al. 2003). However, this criterion imposes a constraint on the MRI sequences that can be used. Nonetheless further subsequent artifact correction is required, and continuous EEG is not obtained (Anami, Mori et al. 2003). Other approaches to imaging artifact correction have been suggested that also rely on the (*a priori* knowledge of the) specific sequence-related artifact shape (Hoffmann, Jager et al. 2000; Garreffa, Carni et al. 2003; Wan, Iwata et al. 2006), its determination using principle component analysis (Negishi, Abildgaard et al. 2004; Niazy, Beckmann et al. 2005) and subsequent respective artifact fitting and filtering steps. Combining different methods can prove very efficient (Niazy, Beckmann et al. 2005) however the correction of artifacts in EMG signals currently remains challenging (van Duinen, Zijdewind et al. 2005; Richardson, Grosse et al. 2006; Post, van Duinen et al. 2007), and algorithms will have to be developed accounting for artifact as a function of both electromagnetic field changes and simultaneous relative subject (electrode) movement therein.

The pulse artifact often requires more attention than the imaging artifact: it can be very subtle with an amplitude in the range of the biological signals (Allen, Polizzi et al. 1998). Non-invasive manipulation of this artifact for its exploration is difficult, but

studying it at different field strengths demonstrated that the pulse artifact adds a spatio-temporally complex, non-stationary signal to the EEG (Debener, Mullinger et al. 2007). Depending on the planned analysis, reducing the pulse artifact may not be required at all – despite its contribution to a broad frequency range -, for example, where discrete features such as IEA need to – and can readily - be identified on the EEG standing out clearly from the background (Bénar, Aghakhani et al. 2003). However, automated IEA detection algorithms may be compromised (Siniatchkin, Möller et al. 2007), and frequency analysis can be impaired by pulse artifact (Laufs, Kleinschmidt et al. 2003).

Methods for pulse artifact subtraction very much resemble those discussed above for the imaging artifact: due to its periodic nature, the average subtraction approach can be applied (Allen, Polizzi et al. 1998). However, the periodicity of this biological artifact is subject to heart rate variability and drift artifacts, leading to greater instability of the pulse artifact compared to the imaging artifact. This is the reason why a sliding average approach with or without additional weighting is beneficial (Allen, Polizzi et al. 1998; Sijbers, Michiels et al. 1999; Goldman, Stern et al. 2000; Ellingson, Liebenthal et al. 2004) or the use of several artifact templates per channel (Niazy, Beckmann et al. 2005). Again, similar approaches to the average artifact subtraction have been suggested, for example measuring pulsatile motion (and not the ECG itself) directly with a piezoelectric transducer before regressing it out (Bonmassar, Purdon et al. 2002; Ellingson, Liebenthal et al. 2004) or adding an additional, wavelet-based de-noising step after the average template subtraction (Kim, Yoon et al. 2004).

All averaging methods critically rely on the exact detection of corresponding instances of the cardiac cycle, such that averaging results in an accurate template (Negishi, Abildgaard et al. 2004). Here, sophisticated QRS or “R-peak” detection methods (Meyer, Fernandez Gavela et al. 2006) developed for automatic ECG processing are of use, but those relying on the typical morphology of the ECG waveform may fail because of the distorted ECG shape inside a strong magnetic field. Due to physiologically (Snisarenko 1978) and psychologically induced (Michal, Roder et al. 2007) changes in heart rate, the length of the template to subtract will vary and should fit the shortest beat-to-beat period of the correction epoch. The amplitude of the

artifact reflects the strength of the pulse wave, and the template should thus be centred such that it encompasses the part of the cardiac cycle most strongly affecting the electrophysiological data. The delay between the detected ECG feature and the amplitude 'centre of mass' obviously varies and can be determined empirically, e.g. ~ 0.2 s average delay when the QRS complex has been marked in healthy young adults (Allen, Polizzi et al. 1998). However, if a different part of the ECG is marked, the delay needs to be defined individually and ideally automatically. One practical way to achieve this is to calculate the smoothed global field power (Skrandies 1990) only for those channels containing above average artifact power and to determine the temporal midpoint between the local minima bordering the global field power maximum (documented within and implemented as "CBC Parameters" [2006] in BrainVision Analyzer, Brain Products, Munich, Germany).

Other methods use channel-wise ECG-locked temporal PCA (Negishi, Abildgaard et al. 2004; Niazy, Beckmann et al. 2005), or PCA of representative epochs of data building a spatial filter to remove pulse-artifact related components (Bénar, Aghakhani et al. 2003). The question of the selection and refinement of the components to remove is a problem inherent to data driven approaches. Similarly for ICA, that can be used to further process the averaged pulse-contributed signal (Nakamura, Anami et al. 2006) or to determine and remove related components (Bénar, Aghakhani et al. 2003; Niazy, Beckmann et al. 2005; Srivastava, Crottaz-Herbette et al. 2005; Nakamura, Anami et al. 2006; Mantini, Perrucci et al. 2007). Again, combining different approaches can be advantageous (Debener, Strobel et al. 2007), but because of the non-stationarity of the signal, the use of statistical procedures such as ICA and PCA is limited (Debener, Mullinger et al. 2007).

In principle, the quality of different pulse and imaging artifact correction methods can be evaluated by looking at signal to noise measures, or, in the context of a specific application, by seeing whether a signal property is preserved, such as the known topography of an event related potential component (Debener, Strobel et al. 2007). Nevertheless, it would be very difficult to prove superiority of one artifact subtraction method over another, as the outcome depends not only on the quality criteria applied but also on whether all methods in question have been optimally applied. For example,

methods not requiring exact triggers (e.g. scan onset markers or ECG feature markers) may seemingly outperform those which are dependent on accurate timing signals, when reliable synchronisation has not been achieved. It is thus reasonable to select or further develop one of the existing methods for artifact subtraction based on the individual needs and data (Grouiller, Vercueil et al. 2007). Because of the additive nature of all artifacts to the biologically generated electrical field, average artifact subtraction techniques are *a priori* valid; in addition, they are unbiased, computationally efficient and can be performed online (Allen, Josephs et al. 2000). The latter feature is for instance relevant in the context of electrophysiological biofeedback fMRI investigations extending existing work in this area (Nagai, Critchley et al. 2004; Nagai, Critchley et al. 2004).

On June 17th, 2003 in his introduction of the HBM (9th Annual Meeting of the Organization for Human Brain Mapping in New York) satellite symposium 'EEG-fMRI', Louis Lemieux thought-provokingly suggested to the 99 attendees that every MRI scanner in the future should be shipped with a compatible EEG system. Many of the audience were already well-known in the EEG or fMRI world, and most others have meanwhile become so, all acting as multipliers within the growing EEG-fMRI community: today, eight years later, it is probably fair to say that if not every scanner is equipped with, then at least every brain imaging centre is in possession of an MRI-compatible EEG system (and possibly even using it).

While epilepsy was from the start and still is the most important clinical application for the method, cognitive neurosciences equally have become aware of the over-additive benefit when combining EEG with fMRI. The multi-modal experimental set-up, study design, analysis strategy and result interpretation are unique and benefit from the roughly 20 years of experience in the field since the idea of EEG-fMRI was born. Because of its user-friendliness and accessibility, more and more researchers consider it an equal method among other neuroscience tools when looking for the means with which to best address their research question. Although requiring some extra thought, EEG-fMRI no longer will have to become itself the subject of every user's research.

8.1.3 Which are some remaining challenges of EEG-fMRI?

Technical challenges

Naturally, the future of simultaneous EEG-fMRI is dependent on technical advances of each modality in isolation as well as the progress in the understanding of the signals and their combined analysis. Like at the inception of EEG-fMRI, safety issues will again be crucial when taking the next steps.

On the EEG side, there is a clear trend towards high-density recordings, i.e. recordings with 128 channels or more benefitting source localization. Bringing this into an MRI set up, user- and subject-friendliness of the MR-compatible kit need to be improved to limit preparation time and guarantee subject comfort. The challenge of an increased number of channels can be met by e.g. having multiple amplifiers work in parallel. But the increased amount of material brought into the magnetic field, i.e. electrodes and wires, lead to shielding requiring stronger radio frequency pulses leading to an increased specific absorption rate (SAR) and associated heating. This poses a safety problem (e.g. burns) (Lemieux, Allen et al. 1997), and the shielding image quality issues (Krakow, Allen et al. 2000). Hence, potentially, other materials will need to be explored, like ink as proposed by the group around Bonmassar (Vasios, Angelone et al. 2006). On the (f)MRI side, field strength increases and faster sequences are designed challenging both gradient and cardioballistogram artefact reduction algorithms. Since the relationship between the electrical field induced by the MR gradients and that originating from the neurons of the brain is additive and current EEG sampling rates and ranges are not yet pushed to their limits, no immediate development appears necessary from this perspective (Neuner, Warbrick et al. 2011). But when MRI sequences run at increasing field strengths this is associated with an increasingly high SAR leading to safety problems because of associated heating of the EEG equipment attached to the subjects (Nöth, Laufs et al. 2010). Such sequences cannot be used in combination with simultaneous EEG, unless the hardware and safety set up are further optimized and tested carefully. These issues are currently being addressed.

Again it is at The Epilepsy Society (Chalfont St. Peter, UK) and Queen Square (University College London, UK) that limits are being pushed: David Carmichael and colleagues successfully have gone a long way to assess the feasibility and safety of the next generation of EEG-fMRI integration, the combination of intracranial EEG (icEEG) with

MRI (Carmichael, Thornton et al. 2008; Carmichael, Thornton et al. 2010; Vulliemoz, Carmichael et al. 2011). This will benefit epilepsy patients because – among other aspects - the fMRI-correlates of icEEG will reveal activity changes remote to the implantation site(s) and foster the understanding of what is imaged with surface EEG-fMRI. Of course, irrespective of the pathological condition, the fundamentals of the relationship between electrical and neuronal BOLD activity can be studied in humans (Carmichael, Vulliemoz et al. 2011). Linked to this, with the growing success of therapeutic brain stimulation in clinical neurology (Rasche, Rinaldi et al. 2006; Salanova and Worth 2007; Bronstein, Tagliati et al. 2011; Holtzheimer and Mayberg 2011), the vision of imaging safely with fMRI the entire brain circuitry in response to *in vivo* stimulation appears a fascinating goal to work for (Gupte, Shrivastava et al. 2011).

Analytical

Nourished by their farsightedness in combination with the spatial and scientific familiarity among the neuroscience research teams at Queen Square in London, Karl Friston and his colleagues early on initiated the development of concepts and analysis tools (e.g. biophysical modelling) for EEG-fMRI (Rosa, Daunizeau et al. 2010). Despite some scepticism I share with Rosa and colleagues about whether symmetrical analysis approaches represent a final wisdom especially for non-invasive, i.e. scalp EEG-fMRI (see brief discussion above), more experience with them is required which can only be gained by their more intense application (it took my colleagues and me looking at hundreds of empty or speckled EEG-correlated statistical result maps – in addition to a few meaningful ones - to develop a vague appreciation of what EEG-correlated fMRI maps might or might not mean. Similarly, the creativity of the growing community of researchers applying EEG-fMRI in their fields of interest and their augmented experience over time will bring about further advances in the field of EEG-fMRI integration.

8.1.4 Analysis

8.1.4.1 Why are epilepsy patients studied with EEG-fMRI at rest?

As highlighted in the previous sections, the development of EEG recording during fMRI had its clinical motivation in the wish to localize electrical sources of neuronal activity, in particular epileptic discharges (Ives, Warach et al. 1993). EEG-fMRI provides a unique opportunity to investigate spontaneously occurring synaptic activity and map haemodynamic correlates of changes in neuronal activity by means of imaging of the BOLD signal. Interictal (and ictal) activity occur spontaneously, and initially each event triggered fMRI image acquisition. This means that historically the condition under which the patient was examined was “at rest” since any additional task or activity could have interfered or even obscured the EEG. But even with the advent of simultaneous and continuous EEG-fMRI acquisition it appeared wise to study the patients at rest for the same reason: when aiming to identify the irritative zone, it was assumed that haemodynamic changes induced by interictal activity was best contrasted against a resting state background both conceptually and practically w.r.t. to the analysis (see below). The “resting background” in fact is very variable and it strongly interacts with interictal activity (Laufs, Hamandi et al. 2006; Laufs, Lengler et al. 2006; De Tiege, Harrison et al. 2007; Laufs and Duncan 2007; Rodionov, De Martino et al. 2007; Laufs 2008; Laufs, Daunizeau et al. 2008; Vaudano, Laufs et al. 2009; Thornton, Rodionov et al. 2010).

Provocation manoeuvres such as hyperventilation will induce subject motion detrimental to the data (Lemieux, Salek-Haddadi et al. 2007) and alter haemodynamics making valid modelling of the data complicated if not impossible (Jack, Kemp et al. 2010; Vogt, Ibinson et al. 2011). Photic stimulation has been performed in patients with photosensitivity (Moeller, Siebner et al. 2009). Provocation manoeuvres naturally bare the risk – or potential – to induce seizures (Moeller, Siebner et al. 2009). Apart from ethical considerations (a medically supervised MRI scanner bore is not necessarily an unsafe place to have a seizure), depending on the type of seizure, the experiment will need to be aborted, or the data may be affected by motion. In any case, any stimulation procedure acts like a task and will require special consideration at the data modelling and analysis stage (Thornton, Rodionov et al. 2010; Chaudhary, Duncan et al. 2011).

If identification of the irritative or seizure onset zone (Rosenow and Lüders 2001; Laufs 2012) is not the primary goal of the fMRI study, task-related fMRI in epilepsy patients is commonly performed, e.g. to map language or memory function (Powell and Duncan 2005; Bonelli, Powell et al. 2010). Taking matters a step further, the combination of EEG-fMRI and cognitive paradigms will shed light on the interaction of interictal activity and cognitive performance (Berman, Negishi et al. 2010; Laufs 2012).

8.1.4.2 How is spontaneous brain activity analysed?

The concept:

Generally, it is difficult to study the brain 'at rest' with the approach generally pursued in science when external manipulation (independent variable) is used to obtain informative measurements (dependent variable) about the object of interest, because it may suspend the resting state. A related detailed review can be found in a Special Issue of Human Brain Mapping (Laufs 2008) (see **Fehler! Verweisquelle konnte nicht gefunden werden.**). Concurrent electroencephalography (EEG) and functional magnetic resonance imaging (fMRI) allow the simultaneous measurement of brain activity from two angles. One modality can be chosen to be interpreted as the independent variable and the other one as the dependent variable. Spontaneous activity can be studied without external manipulation. Particularly, the EEG data can describe spontaneously occurring epileptic discharges and can be treated as the independent variable, forming a regressor to interrogate the fMRI data (dependent variable). The inverse is equally possible (Laufs, Krakow et al. 2003; Morillon, Lehongre et al. 2010), and fusion analyses (Rosa, Daunizeau et al. 2010) attempt to treat EEG and fMRI data equally (Daunizeau, Grova et al. 2007; Laufs, Daunizeau et al. 2008; Valdes-Sosa, Sanchez-Bornot et al. 2009; Daunizeau, Vaudano et al. 2010; Luessi, Babacan et al. 2011).

The physiology of the signals and their conceptual link

Blood oxygen level-dependent (BOLD) functional magnetic resonance imaging (fMRI) measures the haemodynamic correlate of neuronal activity, probably local field potentials (LFP) and – to a lesser degree – multi unit activity (Logothetis, Pauls et al. 2001). Accordingly, BOLD signal decreases are related to neuronal activity decreases

(Shmuel, Augath et al. 2006). The BOLD signal may reflect also sub-threshold activity, simultaneous inhibition with excitation and the result of modulating afferent input of remote neurons (Nunez and Silberstein 2000).

Scalp electroencephalogram (EEG) measures neuronal activity in the form of postsynaptic excitatory and inhibitory potentials (EPSP and IPSP) of pyramidal cells perpendicular to the cortical surface. The overlap between EPSP and LFP remains unknown, and fMRI and EEG are measurements not of identical neuronal processes, providing valuable complementary information. Because of this, the relationship between simultaneously acquired EEG and fMRI data needs further consideration.

In practice: Still, as a best guess it is generally assumed in EEG-fMRI studies that interictal paroxysmal EEG discharges are associated with a haemodynamic response analogous to that commonly used for modelling in event-related studies in cognitive neuroscience, commonly called the canonical event-related haemodynamic response function (canonical HRF). Analyses based on that assumption have produced significant response patterns that are generally concordant with prior electroclinical data. Assessing this formally, we used a more flexible model of the event-related response, a Fourier basis set, to investigate the presence of other responses in relation to individual IED in 30 experiments in patients with focal epilepsy. We found significant responses that had a noncanonical time course in 37% of cases, compared with 40% for the conventional, canonical HRF-based approach. In two cases, the Fourier analysis suggested activations where the conventional model did not. The noncanonical activations were almost always remote from the presumed generator of epileptiform activity. In the majority of cases with noncanonical responses, the noncanonical responses in single-voxel clusters were suggestive of artifacts. We did not find evidence for IED-related noncanonical HRFs arising from areas of pathology, suggesting that the BOLD response to IED is primarily canonical. Noncanonical responses may represent a number of phenomena, including artefacts and propagated epileptiform activity (Lemieux, Laufs et al. 2008) .

When contrasting spontaneously occurring events against rest, the risk of false-positive activation is potentially higher than in studies with block or optimized event-related designs. False positives – or negatives – due to image degradation can for

example arise from subject motion which is usually worse in patients than in healthy subjects. Because discarding patient data is usually not an option, strategies need to be pursued optimising the yield of each experiment while minimizing the risk of false-positive activation. Afraim Salek-Haddadi developed a method, “scan nulling” (Salek-Haddadi, Diehl et al. 2006) which models “jerky” head motion in addition to the established regression of scan-to-scan subject movement (Friston, Williams et al. 1996). We evaluated the efficacy of this approach by mapping the proportion of the brain for which F-tests across the additional regressors were significant. In 95% of cases, there was a significant effect of motion in 50% of the brain or greater; for the scan nulling effect, the proportion was 36%; this effect was predominantly in the neocortex. We concluded that the proposed approach is effective (Lemieux, Salek-Haddadi et al. 2007).

Another source of noise in resting state data is of physiological origin and due to cardiac pulsation and respiration and several methods have been proposed for their reduction (Glover, Li et al. 2000; Birn, Diamond et al. 2006; Laufs, Walker et al. 2007; Birn, Smith et al. 2008). We also developed a method to reduce cardiac noise modelling it as an effect of no interest. Our model is based on an over-complete basis set covering a linear relationship between cardiac-related MR signal and the phase of the cardiac cycle or time after pulse (TAP). This method showed that, on average, 24.6 +/- 10.9% of grey matter voxels contained significant cardiac effects. 22.3 +/- 24.1% of those voxels exhibiting significantly interictal epileptic discharge-correlated BOLD signal also contained significant cardiac effects. We quantified the improvement of the TAP model over the original model without cardiac effects, by evaluating changes in efficiency. Over voxels containing significant cardiac-related signal efficiency was improved by 18.5 +/- 4.8%. Over the remaining voxels, no improvement was demonstrated (Liston, Lund et al. 2006).

8.1.4.3 Do we need spikes?

Ideally, patients who undergo an EEG-fMRI study show clearly identifiable and classifiable interictal epileptic activity occurring with a temporal spacing that will give optimal statistical power in an event-related general linear model. In reality, spiking

patterns are different. In 63 patients with focal epilepsy, Afraim Salek-Haddadi found a tendency for more spikes, less motion, more runs of IEDs and less EEG background abnormality in cases showing any IED-correlated BOLD signal changes compared to those not showing any (Salek-Haddadi, Diehl et al. 2006). In his series, 42% of the patients analysed and which were pre-selected based on spiking on a recent routine EEG did not have any interictal activity in 35 min. In our series of patients with focal cortical dysplasia (FCD), only about half of the subjects considered for epilepsy surgery exhibited interictal epileptic discharges during two or three twenty minute sessions of EEG-fMRI acquisition (Thornton, Vulliemoz et al. 2011). This raises the question whether "spike-less" EEG-fMRI data can be analysed such that useful clinical information can be obtained. One solution can be to build a GLM based on information extracted from the ongoing "background" EEG. A proof of principle case report was published in MRI (Laufs, Hamandi et al. 2006) (see 9.2.1): We studied a patient with refractory focal epilepsy using continuous EEG-correlated fMRI. Seizures were characterized by head turning to the left and clonic jerking of the left arm, suggesting a right frontal epileptogenic region. Interictal EEG showed occasional runs of independent nonlateralized slow activity in the delta band with right frontocentral dominance and had no lateralizing value. Ictal scalp EEG had no lateralizing value. Ictal scalp EEG suggested right-sided central slow activity preceding some seizures. Structural 3-T MRI showed no abnormality. There was no clear epileptiform abnormality during simultaneous EEG–fMRI. I modelled asymmetrical EEG delta activity at 1–3 Hz near frontocentral electrode positions. Significant blood oxygen level-dependent (BOLD) signal changes in the right superior frontal gyrus correlated with right frontal oscillations at 1–3 Hz but not at 4–7 Hz and with neither of the two frequency bands when derived from contralateral or posterior electrode positions, which served as controls. Motor fMRI activations with a finger-tapping paradigm were asymmetrical: they were more anterior for the left hand compared with the right and were near the aforementioned EEG-correlated signal changes. A right frontocentral perirolandic seizure onset was identified with a subdural grid recording, and electric stimulation of the adjacent contact produced motor responses in the left arm and after discharges. The fMRI localization of the left hand motor and the detected BOLD activation associated with modeled slow activity suggest a role for localization of the epileptogenic region with EEG–fMRI even in the absence of clear interictal discharges.

An alternative approach to “spike-less”, or data with too few events are data driven, hypothesis-free methods. Being based on the fMRI data with homogeneous resolution across the entire brain, these methods might be sensitive to epileptic activity in brain regions to which scalp EEG is insensitive, e.g. subcortical and other areas far from the surface of the brain. After evaluation of a temporal clustering method showing false positive results most likely due to subject motion (Hamandi, Salek Haddadi et al. 2005), in our group, we decided not to pursue the approach originally suggested by (Morgan, Price et al. 2004). The clustering method is based on the temporal profile of BOLD signal intensity values which are thresholded based on observer-defined criteria defined yielding “activation” maps. An alternative method is independent component analysis, which separates a multivariate signal into additive subcomponents supposing the mutual statistical independence of the source signals. The main advantage of this method is that it represents the original functional time series as a set of independent components (IC), which may separate meaningful neurophysiological sources and artefacts. However, the lack of a prior hypothesis and the potentially large number of IC generated render interpretation of the results difficult (Beckmann and Smith 2004). An automated characterization technique has been introduced and implemented to reduce the number of meaningful IC requiring interpretation (De Martino, Gentile et al. 2007). In this method, the classification of patterns as BOLD-like relies on a set of spatial and temporal characteristics derived from data acquired in normal healthy subjects. Given our findings of mainly canonical haemodynamic responses also in the context of epilepsy, we consider this classifier suitable for our data. For evaluation of the technique, we applied ICA to EEG-fMRI data sets of patients in whom interictal spikes were present on the EEG and GLM-based BOLD signal localized the epileptic foci to regions also identified with other techniques (EEG, structural MRI, or surgical outcome) (Rodionov, De Martino et al. 2007). Concordance between the ICA and GLM-derived results was assessed based on spatio-temporal criteria. In each patient, one of the IC satisfied corresponded to the IED-based GLM result. The remaining IC were consistent with BOLD patterns of spontaneous brain activity and may include epileptic activity that was not evident on the scalp EEG. We found that ICA of fMRI is capable of revealing areas of epileptic activity in patients with focal epilepsy and may be useful

for the analysis of EEG–fMRI data in which abnormalities are not apparent on scalp EEG.

Another situation when surface EEG may not sufficiently reflect epileptic activity is during seizures. We evaluated the technique in this context and compared it to a GLM-based approach and the gold standard of intracranial EEG recordings (Thornton, Rodionov et al. 2010). Nine of 83 patients with focal epilepsy undergoing pre-surgical evaluation had seizures during EEG-fMRI and were analysed using three approaches, two based on the general linear model (GLM) and one using independent component analysis (ICA). The canonical GLM analysis revealed significant BOLD signal changes associated with seizures on EEG in 7/9 patients, concordant with the seizure onset zone in 4/7. The GLM analysis revealed changes in BOLD signal corresponding with the results of the canonical analysis in two patients. ICA revealed components spatially concordant with the seizure onset zone in all patients (8/9 confirmed by intracranial EEG). In conclusion, ictal EEG-fMRI visualises plausible seizure related haemodynamic changes. The GLM approach to analysing EEG-fMRI data reveals localised BOLD signal changes concordant with the ictal onset zone when scalp EEG reflects seizure onset. ICA provides additional information when scalp EEG does not accurately reflect seizures and may give insight into ictal haemodynamics.

If interictal epileptic discharges are present on the scalp EEG, their accurate classification, or grouping, into distinct and reproducible event classes is vital for the successful creation of regressors in a GLM-based analysis. If paroxysms of different spatial origins are erroneously modelled as a single event type, this will be detrimental to the sensitivity of the analysis. We assessed whether an automated spike classification procedure can increase the model's sensitivity and additionally, automated detection procedures can serve to increase IED identification on the EEG in the first place (Liston, De Munck et al. 2006): For patients with multiple IED generators, sensitivity to IED-correlated BOLD signal changes can be improved when the fMRI analysis model distinguishes between IEDs of differing morphology and field. In an attempt to reduce the subjectivity of visual IED classification, we implemented a semi-automated system, based on the spatio-temporal clustering of EEG events. We illustrated the technique's usefulness using EEG-fMRI data from a subject with focal epilepsy in whom 202 IEDs were visually identified and then clustered semi-

automatically into four clusters. Each cluster of IEDs was modelled separately for the purpose of fMRI analysis. This revealed IED-correlated BOLD activations in distinct regions corresponding to three different IED categories. In a second step, Signal Space Projection (SSP) was used to project the scalp EEG onto the dipoles corresponding to each IED cluster. This resulted in 123 previously unrecognised IEDs, the inclusion of which into the GLM increased the experimental efficiency as reflected by significant BOLD activations. We also showed that the detection of extra IEDs is robust in the face of fluctuations in the set of visually detected IEDs. We concluded that automated IED classification can result in more objective fMRI models of IEDs and significantly increased sensitivity.

9 Results of original work

9.1 Mapping of ongoing physiological EEG information identifies different brain states in healthy volunteers

9.1.1 Where the BOLD signal goes when alpha EEG leaves[1]

Abstract

Previous studies using simultaneous EEG and fMRI recordings have yielded discrepant results regarding the topography of brain activity in relation to spontaneous power fluctuations in the alpha band of the EEG during eyes closed rest. Here, we explore several possible explanations for this discrepancy by re-analyzing in detail our previously reported data. Using single subject analyses as a starting point, we found that alpha power decreases are associated with fMRI signal increases that mostly follow two distinct patterns: either 'visual' areas in the occipital lobe or 'attentional' areas in the frontal and parietal lobe. On examination of the EEG spectra corresponding to these two fMRI patterns we found greater relative theta power in sessions yielding the 'visual' fMRI pattern during alpha desynchronization and greater relative beta power in sessions yielding the 'attentional' fMRI pattern. The few sessions that fell into neither pattern featured the overall lowest theta and highest beta power. We conclude that the pattern of brain activation observed during spontaneous power reduction in the alpha band depends on the general level of brain activity as indexed over a broader spectral range in the EEG. Finally, we relate these findings to the concepts of 'resting state' and 'default mode' and discuss how - as for sleep - EEG-based criteria might be used for staging brain activity during wakefulness.

Introduction

[1] Own contributions: study design, data acquisition and analysis, result interpretation, entire manuscript preparation; Laufs, H., J. L. Holt, et al. (2006). "Where the BOLD signal goes when alpha EEG leaves." Neuroimage **31**(4): 1408-1418..

The functional connotation of so-called alpha activity, i.e., the predominantly posterior 8 – 12 Hz oscillations that are the prominent characteristic in the human electroencephalogram (EEG) at eyes-closed rest, has remained in the focus of research since its initial description by Hans Berger (Berger 1929). In addition to the classical, posterior rhythm, different types of rhythmic activity in the alpha frequency band (8-12 Hz) have been topographically but also functionally distinguished (Niedermeyer 1997). The Rolandic 'mu-rhythm', for instance, resembles posterior alpha frequency-wise but is linked to sensorimotor function, and the so-called 'third alpha", a mid-temporal alphoid rhythm that is usually not detectable on the scalp, may be modified by acoustical stimuli. Most studies, however, have investigated the Berger rhythm and related it to visual function but also to cognitive processing and vigilance (Berger 1929; Niedermeyer 1997).

Recently, electroencephalography (EEG) has been combined with functional magnetic resonance imaging (fMRI) to study blood oxygen level-dependent (BOLD) signal changes that are systematically associated with changes in power of the alpha rhythm. In summary, these studies have revealed two significant, but different patterns of brain areas where local activity as indexed by BOLD signal is associated with the power of activity in the alpha band. One pattern is characterized by occipital (and parietal) BOLD signal increases during alpha power decreases (Goldman, Stern et al. 2002; Moosmann, Ritter et al. 2003), the other by respective increases in bilateral frontal and parietal cortices (Laufs, Kleinschmidt et al. 2003; Laufs, Krakow et al. 2003). From task-related activation studies these latter areas are known to be involved in attentional control. While both patterns can claim some intuitive plausibility, it has remained puzzling how different results could be obtained in similar settings. Here, we report our findings from detailed re-analyses of the 22 EEG-fMRI data sets acquired during eyes-closed rest in our previous study.

Materials and Methods

Subjects, basic EEG-fMRI analysis

We used the same data as reported in our previous study (Laufs, Kleinschmidt et al. 2003), and acquisition and post processing of EEG and fMRI involved the same steps as

detailed in that report (EEG: BrainAmp MR and Vision Analyzer, Brainproducts, Munich, Germany; fMRI: 1.5 T Siemens Vision, Erlangen, Germany; Statistical Parametric Mapping, SPM, http://www.fil.ion.ucl.ac.uk/spm; MATLAB, Mathworks, Inc., Sherborn, MA, U.S.A.). Twenty-two sessions were analysed. Data from one subject that were excluded from our original analysis due to unsatisfactory correction of fMRI-induced EEG artefacts were successfully recovered for the present analysis by using more than one template for artifact subtraction.

All 11 subjects had undergone two twenty minute sessions of simultaneous EEG and fMRI during resting wakefulness and no other instruction than to stay awake, keep the eyes closed and avoid moving. We determined the spontaneously fluctuating alpha power time course from the mean of the two occipital EEG leads O1 and O2 (referenced to FCz, 10-10 system, frequency/temporal resolution of short time Fourier Transform: 1 Hz/1 s, sliding average with 33% overlap). We convolved this time course with the hemodynamic response function (HRF). After down sampling to the middle of each image volume acquisition, the resulting time courses served as regressors of interest in a general linear model as implemented in SPM, alongside the six rigid body motion parameters, obtained during realignment, as confounds.

In the re-analysis presented here we address the following possible intervening variables: effects of study duration, slow and fast alpha power modulations, peak alpha power variance and mean frequency band power.

Effects of study duration

To assess whether alpha power-associated fMRI maps varied systematically with time, the following analyses were performed based on individual session models (outlined above): i) All pairs of subject sessions were analyzed together in a fixed effects and a second level random effects group analysis in which a linear combination of parameter estimates, reflected by a “contrast image”, from individual session analyses (general linear model) were taken to a second-level by performing a voxel-based t-test (Friston, Holmes et al. 1999). The t-test was performed on the contrast images related to the negatively weighted alpha regressor; ii) all first sessions and 2nd sessions were analyzed

separately (each forming one group); iii) the 1st, 2nd and 3rd thirds of each session were combined in one group each (fixed effects analysis).

Analysis of a temporal shift between EEG alpha power and the hemodynamic response

Convolution of the EEG power time series with the canonical HRF low-pass filters the time series and introduces a delay of approximately 6 seconds between the alpha power and the predicted hemodynamic response. To rule out that this shift might be decisive about which pattern would be detected, we created a flexible model comprising in parallel 5 regressors for each session convolved with a canonical shape of the HRF but shifted from negative 2 to positive 2 seconds in one second steps. For every session, by means of an F contrast (identity matrix across the 5), contrast estimates allowing any linear combination of the [highly correlated] 5 predictors per session were used to derive the estimated hemodynamic response function at every given voxel as the sum of the products of the parameter estimates and the correspondingly shifted canonical HRF initially used when creating the regressor. At regions of interest (frontal left [-50,37,11], frontal right [44,19,30], parietal left [-44, -42, 46], parietal right [32, -68, 46], occipital left [-40,-79,-5], occipital right [42,-81,6], [x, y, z] in mm and Talairach space) these estimated response functions were shifted against the canonical HRF and the correlation coefficients determined.

Power fluctuations within the alpha band

To test for different effects of alpha sub-bands, the 8 - 12 Hz alpha band was split into two halves, an 8 – 10 Hz and a 10 – 12 Hz band. From each band, a regressor was derived, and both were entered into one model as described above. Statistical parametric maps were evaluated for each band separately and for combinations of the two.

Determination of peak alpha frequency variance and mean frequency band power

To characterize the alpha oscillations more, for each thirty second epoch of EEG (in analogy to clinical EEG sleep staging), the peak frequency within the 8 – 12 Hz alpha band was determined resulting in a time series of the peak alpha frequency over time. Its variance was calculated as the square of its standard deviation. In an analogous fashion, the alpha, theta (4 – 7 Hz) and beta (13 – 30 Hz) band power session means

(scalars) were calculated by taking the mean of the time series containing the sum of the respective band power values for every epoch.

Calculation of average group spectrograms and maps of alpha topography

To visualize differences between spectrograms of sessions assigned to different groups (see below), mean group spectrograms were calculated by averaging individual spectrograms. To create average group topographical alpha maps, a common average reference was calculated based on data from and for all scalp electrode positions except Fp1, Fp2, TP9, TP10 which were excluded due to often sub-optimal data quality. Grand average maps are based on individual 8-12 Hz power maps normalized for occipital alpha power.

Regression at the second level

To demonstrate the dependency of the observed alpha-associated fMRI maps on neighbouring frequency bands, based on the second level group analysis described above, a regression (correlation) was performed by extending the design matrix by two regressors. Corresponding to every contrast image, the respective theta (4 – 7 Hz) and beta (13 – 30 Hz) power session means were entered into the second level regression model as implemented in SPM. This allowed us to test at which typically alpha power associated voxels the parameter estimates were positively or negatively correlated with theta or beta power, respectively. Once the regressors have been mean-scaled, positive and negative correlations can be understood as testing for higher and lower power, respectively.

Data driven approach: eigenimage/principal component analysis

Singular value decomposition (principal component analysis) of the fMRI time series was performed using the multivariate linear models toolbox as implemented in SPM99 (Kherif, Poline et al. 2002) after removing the session mean and the variance explained by the realignment parameters. For each subject in the respective analysis, an individual eigenimage analysis was performed. In addition to all eigenvariates (one per image volume), the first 6 spatial modes (eigenimages) were calculated. The one which most resembled the alpha power-associated fMRI map as obtained by the single

subject EEG-fMRI analysis was identified by choosing the first in the order of the 6 eigenimages whose corresponding eigenvariate showed any negative correlation (Pearson's R) with the alpha regressor used in the EEG-fMRI model.

Results

Decreases in alpha power during eyes-closed rest were associated with BOLD signal increases in bilateral frontal and parietal cortices. The reliability and generality of this finding was confirmed in a second level random effects group analysis (Figure 9.1-1). In our previous publication we analyzed all sessions pair-wise before taking one image per subject to the second level (Laufs, Kleinschmidt et al. 2003). Here, to account for intra-subject inter-session differences, all individual sessions were subjected to the group analysis resulting in qualitatively the same, but quantitatively a slightly different map because of an overestimation of the degrees of freedom.

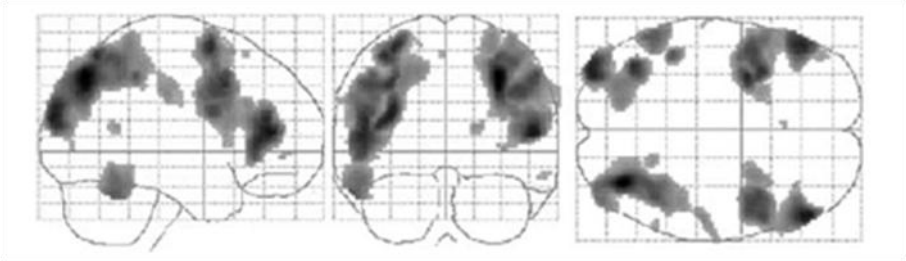

Figure 9.1-1: Correlation of alpha power with fMRI time series leads to robust signal change in bilateral frontal and parietal cortices. Brain areas negatively correlated with alpha band power (i.e. brain areas that activate when alpha power decreases) of 22 sessions (11 subjects) are shown as projections on SPM ‚glass brains'. Statistical parametric maps (SPM{t}) are shown for a random effects group analysis (P<0.0001 uncorrected for multiple comparisons). Coordinates ([X, Y, Z] in approximate Talairach Space) and Z-scores of cluster maxima: frontal left ([-50,37,11], 5.3), frontal right ([44,19,30], 5.5), parietal left ([-44, -42, 46], 5.4), parietal right ([32, -68, 46], 5.84)..

In spite of this robust result at the group level, visual assessment of the individual maps session by session revealed an occipital-parietal activation in 8 single sessions that was negatively correlated with alpha power and that resembled the pattern reported in other studies (Goldman, Stern et al. 2002; Moosmann, Ritter et al. 2003). Our predominant group result with frontal-parietal activation could be identified in 10 of the single sessions. The remaining 4 individual sessions could not be classified with confidence due to weaker and more variable effects (Figure 9.1-2). Usually, both sessions from each subject showed the same characteristic pattern except for two

cases, where in one, the first session showed the “occipital-parietal”, the second a “variable” pattern, and in the other *vice versa*.

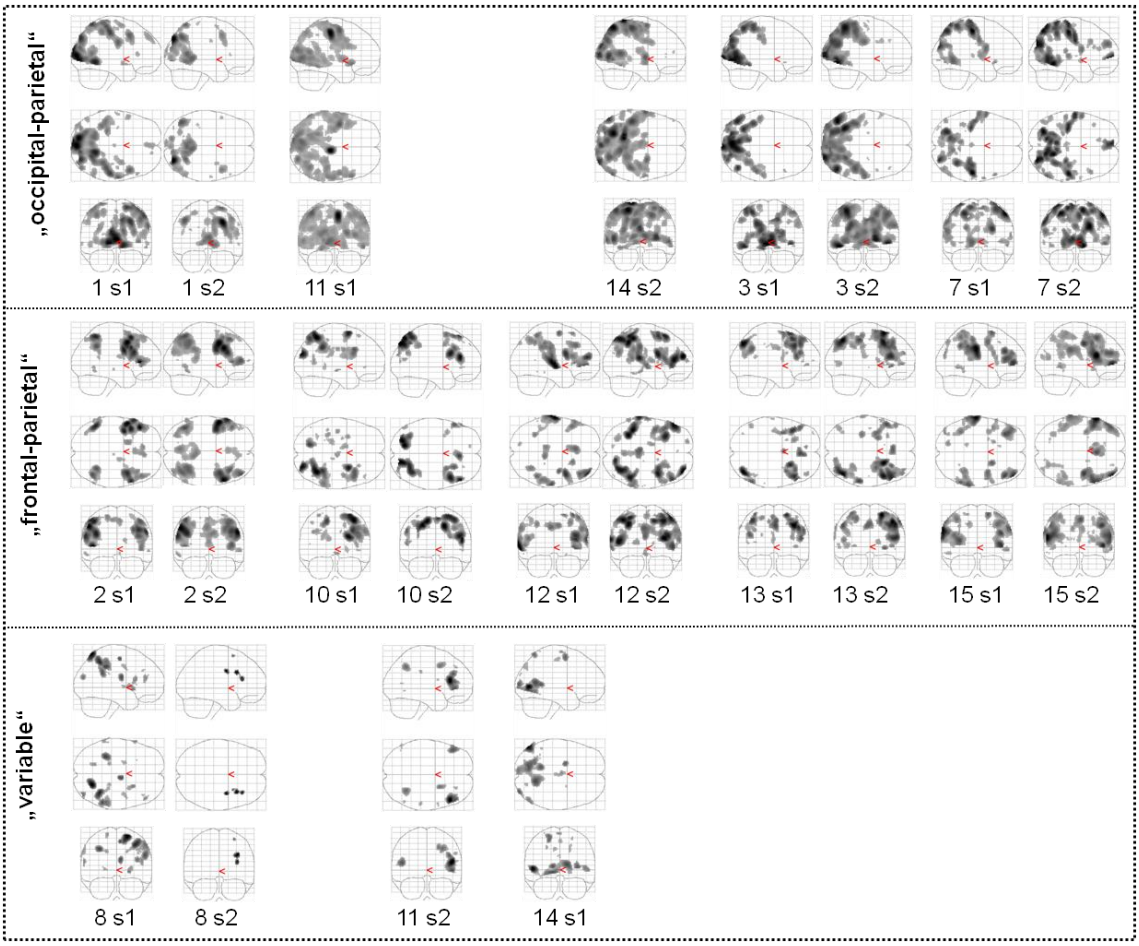

Figure 9.1-2: Individual single session analyses allow visual classification of alpha-correlated deactivations into a „frontal-parietal“, an „occipital-parietal“ and a group „variable“. Glass brain projections (compare Figure 9.1-1; labeled with subject ID followed by „s“ and session number) of statistical parametric maps of negative correlation between alpha power and BOLD signal for each of two sessions from 11 individual subjects (P=0.001 uncorrected for multiple comparisons). Except for subject 11 and 14, session pairs each fall into the same group. The latter two may remotely resemble the „frontal-parietal“ and „occipital-parietal“ pattern respectively.

Inspection of the single session results suggested that both patterns, the occipital-parietal and the frontal-parietal one, were present in our data set. They appeared to be distinct rather than forming a continuum. We therefore sought to identify further variables that might account for why some sessions expressed one rather than the other pattern. We found no systematic difference between first and second sessions, nor within sessions when splitting them into three segments (results not shown). Next, we tried to relate these patterns to higher versus lower peak frequencies in the alpha band, and again found no explanation but that both the frontal-parietal and the occipital-parietal pattern where associated with the upper alpha sub-band (10-12 Hz, Figure 9.1-3). Previously, we had tested whether different modulation frequencies of

alpha power accounted for different topographical patterns and learned that the power modulations of the alpha band accounting for the negative correlation with brain BOLD activity are in a very low frequency range (Laufs, Kleinschmidt et al. 2003).

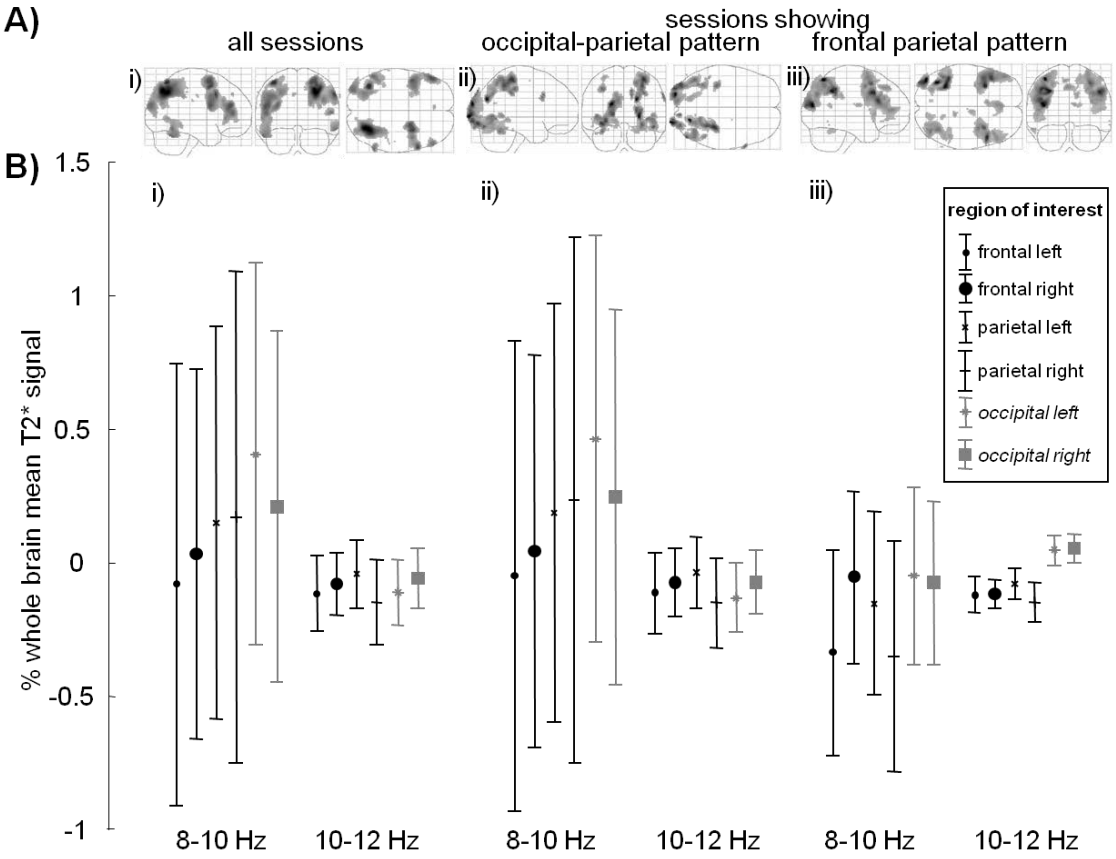

Figure 9.1-3: Not low (8-10 Hz) but high (10-12 Hz) alpha band power is correlated with occipital-parietal and frontal-parietal BOLD signal changes. A) Statistical parametric maps for BOLD signal changes negatively correlated with the high alpha band: Random effects analyses ($p<0.001$, uncorrected) of all 22 sessions (i) and those showing an occipital-parietal (ii) or frontal-parietal (iii) pattern with 8-12 Hz (compare Figure 9.1-2); 8-10/10-12 Hz regressors were part of one fixed effects model. B) Average parameter estimates with 90% confidence intervals for both low (8-10 Hz) and high (10-12 Hz) alpha band power for regions of interest, left and right frontal and parietal cluster maxima, respectively (compare Figure 1) and - in light gray - occipital maxima ([42,-81,6], [-40,-79,-5] (compare A, ii). i-iii same sessions as in A). Note narrower confidence intervals for high alpha band and generally negative means except for the occipital regions of interest in subjects showing the frontal-parietal pattern (iii).

This is in accord with the observation that the exact time delay between the alpha power time series and the BOLD signal is not crucial. In fact we found that the estimated hemodynamic responses at frontal, parietal and occipital regions of interest peaked around 2 seconds later than the canonical HRF Figure 9.1-4). This delay was region of interest specific and was more pronounced at occipital regions, but did not distinguish between sessions showing the occipital- and the frontal-parietal fMRI pattern. Convolution of the EEG regressor with only the canonical HRF allowed to detect both occipital- and frontal-parietal regions (Figure 9.1-2).

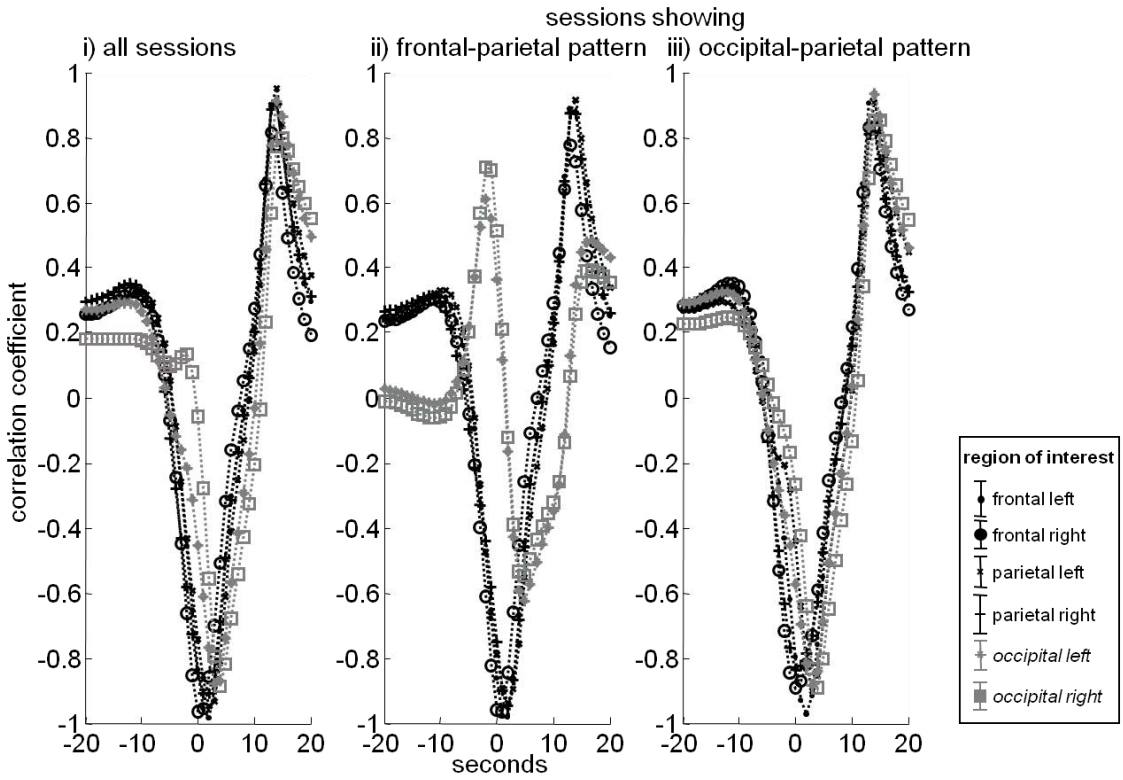

Figure 9.1-4: A delay of the peak of the hemodynamic response to alpha power compared to the canonical hemodynamic response (HRF) is region of interest specific but does not distinguish between the frontal- and the occipital-parietal fMRI patterns. Cross-correlation coefficients of the canonical HRF (as provided by SPM, peak at 6 s) shifted against estimated HRF at regions of interest (compare Methods and Figure 9.1-3 for coordinates; 0 s indicates no shift) for (i) all sessions (mean peak delay with respect to the canonical HRF at frontal and parietal regions: 1.5 +/- 1 s excluding occipital regions (2.2 +/- 1.3 s including occipital regions); at occipital regions 3.5 +/- 2 s; (ii) sessions showing a frontal-parietal pattern at frontal and parietal regions: 1.75 +/- 0.5 s excluding occipital regions (2.8 +/- 1.7 s including occipital regions); at occipital regions 4.2 +/- 2.7 s; (iii) sessions showing an occipital-parietal pattern at frontal and parietal regions: 1.25 +/- 1.5 s excluding occipital regions (2.0 +/- 1.7 s including occipital regions); at occipital regions 3.25 +/- 2.5 s. Note: 1. The positive peaks reflect autocorrelation (peak at 11.5 s for the canonical HRF). 2. While the occipital regions of interest are only part of the occipital-parietal pattern as reflected by the 'distorted' graph (light gray, (i) and (ii)), the parietal – but also the frontal – regions of interest also show correlation with alpha power in sessions showing the occipital-parietal pattern (compare Figure 9.1-2 and random effects group results, Figure 9.1-1).

Because of the observed intra-subject, inter-session differences, we then hypothesized that different brain states might be responsible for the different alpha-related maps, in particular different states of vigilance. We therefore explored spectral content of the related EEG recordings beyond the alpha range. There was a significant difference between the session mean alpha power amplitudes. The group "occipital-parietal" had the lowest, the group "variable" the highest alpha power. More importantly, accounting for this absolute difference, we found that in sessions where alpha power had been negatively correlated with occipital brain activity, the ratio of theta (4 – 7 Hz) over alpha (8 – 12 Hz) power was significantly higher than in sessions showing the

"frontal-parietal" pattern (Figure 9.1-5 A, Table 9.1.1-1). Similarly, 13-16 (13-30) Hz beta power was significantly lower in the "occipital-parietal" versus the "frontal-parietal" group, while a higher variance of the peak alpha frequency was observed in the former compared to the latter (Table 9.1.1-1). The sample size of the group with variable activation patterns ("variable") was too small to perform reliable statistics. A summary fMRI map for each group was created based on the thresholded voxel-wise variance across the individual sessions' 'alpha maps' (Figure 9.1-5 B). Alpha power topographical maps revealed a relatively higher frontal alpha distribution in the "occipital-parietal" compared to the "frontal-parietal" group, while in the "variable" group, a more central emphasis for alpha could be observed (Figure 9.1-6).

	A: occiptal-parietal	B: frontal-parietal	C: variable	t-test A vs B
number of sessions in group	8	10	4	
8-12 Hz alpha power mean	5.709 uV^2	13.061 uV^2	22.659 uV^2	*0.006*
8-12 Hz alpha power variance	0.924 uV^2	2.065 uV^2	3.165 uV^2	*0.011*
4-7 Hz theta power mean	4.808 uV^2	4.952 uV^2	5.962 uV^2	0.409
4-7 Hz theta power variance	0.753 uV^2	0.732 uV^2	0.883 uV^2	0.235
13-16 Hz beta power mean	1.36 uV^2	2.133 uV^2	3.42 uV^2	*0.02*
13-16 Hz beta power variance	0.26 uV^2	0.301 uV^2	0.40 uV^2	0.22
13-30 Hz beta power mean	0.39 uV^2	0.79 uV^2	1.09 uV^2	*0.02*
13-30 Hz beta power variance	0.10 uV^2	0.16 uV^2	0.21 uV^2	0.06
mean theta power / mean alpha pow	0.952	0.683	0.219	*0.001*
alpha band peak frequency mean	9.95 Hz	10.22 Hz	10.48 Hz	0.181
alpha band peak frequency variance	0.98 Hz	0.60 Hz	0.45 Hz	*0.005*
heart rate mean	54.3/min	58.4/min	63.6/min	0.168

Table 9.1.1-1: Group characteristics and statistical comparison of alpha, theta and beta EEG frequency content and heart rate. P-values (right column) are printed in italics if below 0.05.

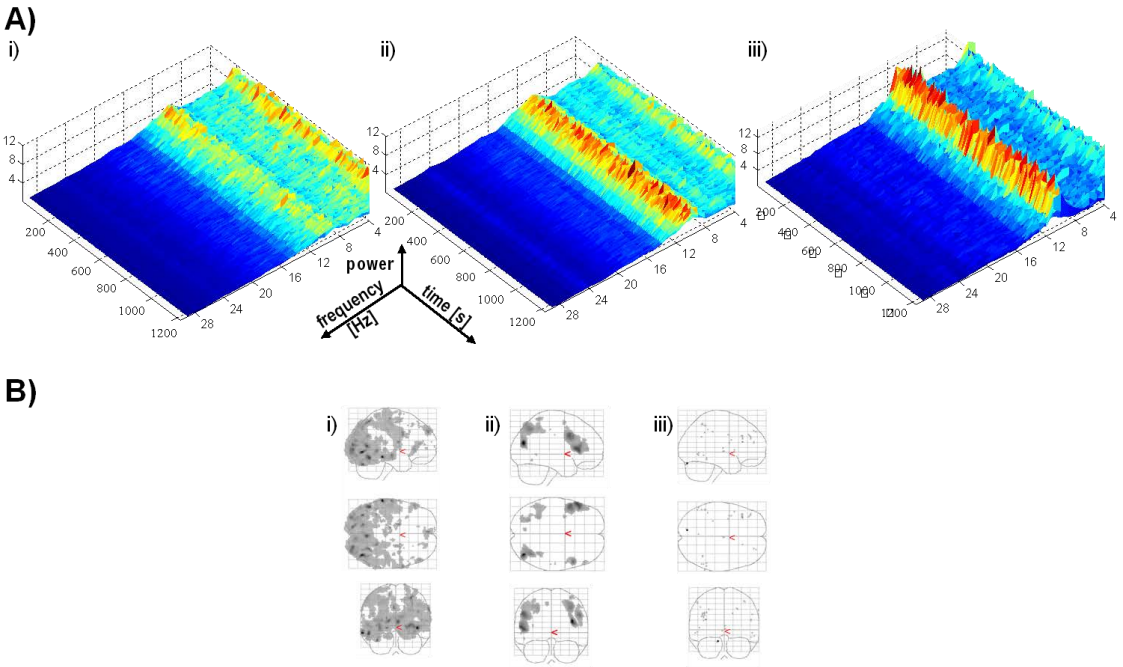

Figure 9.1-5: Summary maps of individual sessions categorized into three groups differing both in their spectrograms (A) and fMRI pattern (B). A) Mean normalised spectrograms corresponding to sessions grouped as: (i) „occipital-parietal“, (ii) „frontal-parietal“, (iii) „variable“. Normalised power is given in units from 0 to 1. B) Brain areas negatively correlated with alpha band power (i.e. brain areas that activate when alpha power decreases) are shown as projections on SPM ‚glass brains‘ (compare Figure 9.1-1). Statistical parametric maps are thresholded at P<0.001, uncorrected. (i) 8 sessions categorized as „occipital-parietal), (ii) 10 sessions as „frontal-parietal“, (iii) 4 sessions as „variable“.

To establish a link between this difference in EEG spectral properties and the fMRI data, we performed a regression analysis at the second level. Testing for a low beta and high theta content across all 22 sessions revealed bilateral occipital and parietal areas (Figure 9.1-7 A), whereas testing for a high beta and low theta content showed bilateral frontal and parietal areas (Figure 9.1-7 B). This established the dependency of the different alpha-related fMRI patterns on theta and beta frequency power at the group level.

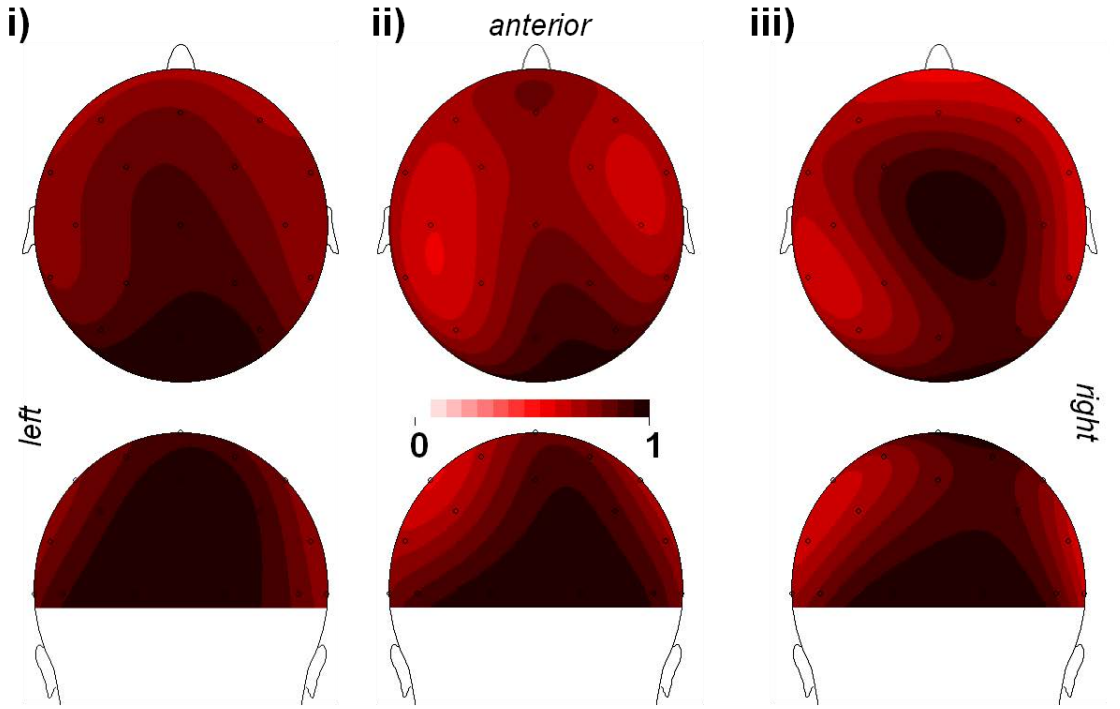

Figure 9.1-6: Spatial distribution of alpha power. Grand average maps of 8-12 Hz power (normalized for O1/O2) distribution of the session averages of subjects grouped as (i) „occipital-parietal" (8 sessions), (ii) „frontal-parietal" (10 sessions), (iii) „variable" (4 sessions) based on fMRI maps. A common average reference was calculated based on data from and for all scalp electrode positions except Fp1, Fp2, TP9, TP10 (international 10-10 system) which were excluded due to often sub-optimal data quality (electrode positions indicated by tiny circles, interpolation by spherical splines; top (row one) and back view (row two)). In (i) relatively high alpha power extends to anterior compared with posterior regions, (ii) shows a different power gradient with less anterior alpha in lateral frontal regions, and in (iii) similar alpha power appears in occipital and central regions, declining towards the front and the sides.

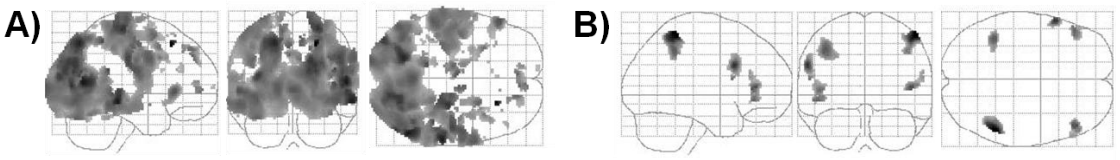

Figure 9.1-7: Alpha power associated deactivations in occipital-parietal regions are typical for high theta and less beta EEG frequency content (A), while alpha deactivations in frontal-parietal brain regions are typical for high beta and less theta power (B). A regression analysis was performed for all 22 sessions on the second level between the mean theta and beta power for each session and the respective „alpha deactivation maps" (negative contrast images corresponding to the HRF-convolved alpha regressor, see Figure 9.1-2). A mask was applied, created by adding the binarized, thresholded summary maps as displayed in Figure 9.1-5 B, and results were thresholded at P<0.05 uncorrected.

Eigenimage analysis (PCA)

As our findings had suggested the existence of two distinct patterns in relation to alpha power decreases and theta and beta EEG spectral content, we applied principal component analysis to our data set. Eigenimage analyses of all sessions revealed two distinct patterns corresponding to the two clusters of brain regions that changed their

activity in relation to alpha power (Figure 9.1-8, Table 9.1.1-2). Although not every session contained both cluster types, "visual" as well as "attentional" patterns could be found across most sessions. For seven out of eight sessions forming the "occipital-parietal" group, an eigenimage could be identified that resembled the statistical parametric map related to alpha power (Table 9.1.1-2). Similarly, eight out of ten eigenimages were identified in the "frontal-parietal" group (Table 9.1.1-2). The two identified spatial modes did not differ significantly in their correlation with the alpha regressor (-0.3 vs. –0.24, see Table 9.1.1-2), but - whenever present - the eigenimages associated with the "occipital-parietal" alpha signature explained significantly more variance in the data (Table 9.1.1-2). In the "occipital-parietal" group we also found eigenimages showing the "frontal-parietal" pattern (Figure 9.1-8), but not *vice versa*. These eigenimages with frontal-parietal patterns were always lower in rank and explained less variance. Finally, two sessions of the "variable" group showed eigenimages resembling the "frontal-parietal", and one in addition the "occipital-parietal" pattern (Table 9.1.1-2).

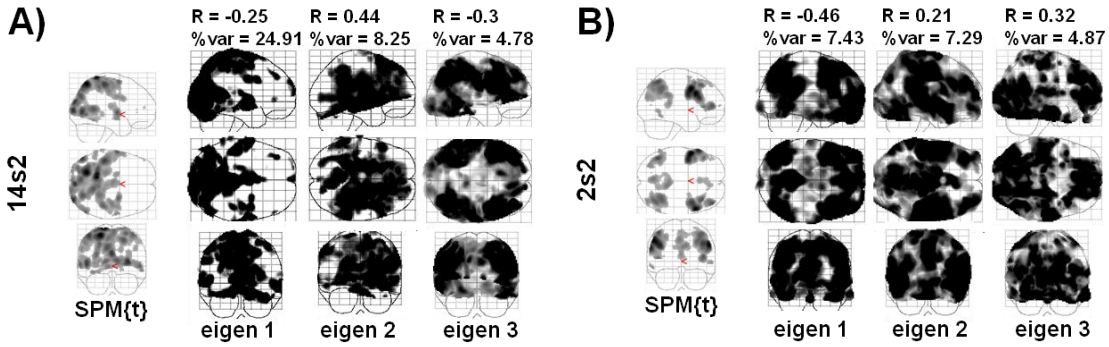

Figure 9.1-8: Eigenimage examples for one session showing activations in occipital-parietal cortices with decreasing 8 - 12 Hz alpha power (A) and one showing respective bilateral frontal and parietal activations (B). SPM{t} indicate the statistical parametric maps as obtained by the general linear model SPM analysis (compare subjects with ID 14s2 and 2s2 in Figure 9.1-2, respectively,), eigen 1, 2 and 3 indicate the first three spatial nodes (eigenimages). In A and B, eigen 1 was judged to show the highest resemblance with the SPM{t}. R: Pearson's correlation between the alpha regressor used to obtain the SPM{t} and the eigenvariate of the respective spatial mode (negative values reflect inverse relationship between alpha power and BOLD signal changes); %var: percent variance explained by the respective spatial mode. Note that in A) the eigenvariate corresponding to eigenimage 3 is highly correlated with the alpha regressor in association with a bilateral frontal and parietal pattern. The variance explained by eigen 3 however is much lower.

subject ID	eigenimage resembling „occipital-parietal“	cross correl. with 8 – 12 Hz power	% variance explained by eigenimage	eigenimage resembling “frontal-parietal”	cross correl. with 8 – 12 Hz power	% variance explained by eigenimage
„occipital-parietal“						
1s1	2	-0.21	7.96	3	-0.24	5.58
1s2	2	-0.11	7.18	n/a		
3s1	1	-0.03	26.10	n/a	-0.20	5.74
3s2	n/a			n/a	0.38	7.39
7s1	1	-0.36	23.89	n/a		
7s2	1	-0.47	14.72	3		
11s1	1	-0.64	20.22	3		
14s2	1	-0.25	24.91	2	-0.30	4.78
mean		**-0.30**	**17.85**		**-0.09**	**5.87**
„frontal-parietal“						
2s1	n/a			n/a		
2s2	n/a			1	-0.46	7.43
10s1	n/a			4	-0.23	4.10
10s2	n/a			1	-0.28	8.61
12s1	n/a			3	-0.31	5.57
12s2	n/a			n/a		
13s1	n/a			1	-0.23	7.47
13s2	n/a			1	-0.20	6.62
15s1	n/a			2	-0.11	6.99
15s2	n/a			2	-0.11	8.28
mean					**-0.24**	**6.88**
“variable”						
8s1	n/a			3	-0.28	6.36
8s2	n/a			3	0.08	5.34
11s2	n/a			n/a		
14s1	1	-0.09	28.07	3	-0.01	7.32
mean		**-0.09**	**28.07**		**-0.07**	**6.34**
“grand” mean		**-0.27**	**19.13**		**-0.17**	**6.50**

“grand” t-test		
“occipital-parietal“ vs. “frontal-parietal”	cross correlation with 8-12 Hz	variance explained
P-value	**0.13**	**0.001**

Table 9.1.1-2: Eigenimage analysis results. Among the first six eigenimages, those were identified which matched either the frontal-parietal or the occipital-parietal activation pattern by comparing it with the individual session SPM{t}. The group summary map was used for comparison to identify the pattern if it was not expressed in the individual's SPM (e.g. “the occipital-parietal” pattern in subjects of the “frontal-parietal” group and vice versa, and both patterns for “variable” subjects). Columns 2 and 5 refer to the rank of the eigenimage, columns 3 and 6 to Pearson's R between the respective eigenvariates and the alpha power regressor.

Discussion

Three studies so far have investigated the correlation of BOLD signal and alpha band power on EEG during task free, eyes-closed rest (Goldman, Stern et al. 2002; Laufs,

Kleinschmidt et al. 2003; Moosmann, Ritter et al. 2003). The topography of BOLD signal increases during spontaneous 8 – 12 Hz alpha desynchronization has been controversial, with two studies mapping this effect mainly to the occipital lobe (Goldman, Stern et al. 2002; Moosmann, Ritter et al. 2003) and our previous study observing signal changes centered in frontal and parietal cortices (Laufs, Kleinschmidt et al. 2003). Occipital deactivation was discussed as a result of synchronization and ‚idling' of cortex or alternatively as linked to other functionally coupled processes, including vigilance (Moosmann, Ritter et al. 2003). We interpreted the frontal-parietal activity, which increases as alpha power decreases in relation to spontaneous fluctuations of attention (Laufs, Kleinschmidt et al. 2003). Here, we reanalyzed 22 EEG-fMRI sessions and found not only that both patterns could be identified in our data set but also that spectral EEG indices accounted for the prevalence of one over the other on a session-by-session basis.

While Moosmann et al. for the main part of their study used both the same MRI scanner and the same MR compatible EEG with the same reference as we did, the experimental set-up differed more for the Goldman et al. study. Nevertheless, those two studies produced similar results (Goldman, Stern et al. 2002; Moosmann, Ritter et al. 2003). Our re-analysis allowed us to affirm that in individual subjects, we could also obtain comparable results. This makes it unlikely, that for instance the use of different EPI sequences or wavelet (Moosmann, Ritter et al. 2003) versus short time Fourier analysis of alpha oscillations led to discrepant results.

We also directly tested in our data set yet another hypothesis pertaining to differences in methodologies across these studies. Discrepant results might have been caused by different session lengths. Goldman and colleagues studied their subjects for 4.5 minutes or a break-down of 9 minutes (Goldman, Stern et al. 2002), whereas Moosmann and colleagues performed one 50 minute and one 25 minute session (Moosmann, Ritter et al. 2003). Probing our data for such duration-dependent effects we found no evidence in favor of this hypothesis. Finally, the average delay of the estimated BOLD response with respect to a canonical HRF (SPM) in our experiment (8.2 +/- 1.3 s) was very similar to that determined by Moosmann et al. using NIRS (8.7

+/- 2.5 s). This delay varied across regions of interest but did not distinguish between the occipital-parietal and the frontal-parietal pattern. Just like that of Moosmann, which by convolution with the canonical HRF (SPM) detected the occipital-parietal set, our model was sensitive to detect both sets of regions probably because low temporal frequency components of the spontaneous power fluctuations account for the correlation with BOLD signal (Laufs, Kleinschmidt et al. 2003; Leopold, Murayama et al. 2003).

Varying experimental set-ups might potentially induce different cognitive states. Previous work has suggested that differences in cognitive function are associated with frequency shifts between different alpha sub-bands (Petsche, Kaplan et al. 1997; Fink, Grabner et al. 2005). We tested for such effects in our data but found that the different fMRI deactivation patterns associated with alpha power were both obtained predominantly in correlation with alpha activity in the high (10-12 Hz) alpha sub-band.

Still, we speculated that different resting brain states had dominated the study groups in the three published experiments. We therefore reanalyzed our findings on a session-by-session basis and found that even within our data set both aforementioned fMRI patterns, and thus presumably both resting brain states that are associated with alpha desynchronization could be identified. Individual sessions were usually dominated by either one or the other of these two patterns. In a study of rest we inevitably lacked behavioral parameters to discriminate the functional significance of these two patterns but instead investigated in more detail the spectral EEG content of individual sessions. In particular, in the absence of any ongoing 'activation' paradigm, we hypothesized to find characteristics of different brain states reflecting fluctuations in vigilance levels.

Different brain states

In addition to the alpha band we determined oscillatory activity in the neighboring theta and beta bands. Theta oscillations are a prominent feature of the normal background EEG in the young population but are generally an indicator for reduced vigilance and early sleep stages in the adult population (Rechtschaffen and Kales 1968; Himanen and Hasan 2000). Age was not significantly different between the occipital-

parietal and the frontal-parietal subjects (and in fact, sessions of the same subject could even fall into different groups, compare Figure 9.1-2). We hence assessed theta power and its relation to alpha power to test whether the occurrence of different fMRI patterns during alpha desynchronization could be related to differences in vigilance. Aside from an increase in slower frequencies with decreasing vigilance (Loomis, Harvey et al. 1935), slowing and thus increased variability of the alpha peak frequency is another indicator of decreasing vigilance (Ota, Toyoshima et al. 1996). The mean amplitude of the alpha power peak in the "occipital-parietal" group was significantly lower than that in the "frontal-parietal" group, and the variance of the peak alpha frequency was significantly higher in the "occipital-parietal" group than in the "frontal-parietal" group (Table 9.1.1-1). Finally, there were significantly more oscillations faster than alpha in the "frontal-parietal" group than the "occipital-parietal". There was a trend of an increasing mean heart rate from the "occipital-frontal" over the "frontal-parietal" to the "variable" group (Table 9.1.1-1). Together, these findings are best accounted for by different vigilance levels.

In this context, it is noteworthy that in the Goldman et al. study only selected epochs were analyzed. To be included, these had to exceed a certain ratio of the epoch's standard deviation over the average alpha power. Given a constant standard deviation (numerator), a relatively low average alpha power (denominator) will facilitate meeting the threshold criterion, which might have biased their analysis towards one brain state. It is also conceivable that session lengths of up to 50 minutes (Moosmann, Ritter et al. 2003) resulted in overall lower levels of vigilance. Finally, topographically, posterior alpha present during the awake state shifts more anteriorly with decreasing vigilance (Zschocke 1995). Both Moosmann's and our choice of the reference (FCz) facilitated sensitivity to frontal alpha power. In fact, the average alpha topography of those individual sessions showing an occipital-parietal pattern reflected a relatively higher anterior alpha prominence than that of the other groups (Figure 9.1-6). This would be in keeping with a potential reduction in vigilance in those subjects – although a pure trait effect could also explain this observation.

A solution: linking broader EEG spectral content to BOLD data

By complementing the information from alpha power with that from the theta and beta bands of the EEG spectrum, we found that these neighboring frequency bands enabled us to dissect the BOLD activation maps associated with alpha power decreases: the "occipital-parietal" could be distinguished from the "frontal-parietal" pattern when pooling all 22 sessions in one second level group analysis and performing a regression with each session's mean theta and beta power content. When mean beta was high and theta power low, the frontal-parietal pattern was revealed, and *vice-versa* the occipital-parietal pattern (Figure 9.1-7).

Recently, Kilner et al. proposed a 'heuristic' linking EEG to hemodynamic measures. Stated simply, BOLD deactivations were speculated to be associated with a shift in the EEG spectral profile to lower frequencies, and BOLD activations with a shift in the opposite direction (Kilner, Mattout et al. 2005). With alpha power dominating the spectrum (Figure 9.1-5 A) this is in line with our prominent alpha-associated BOLD deactivations with an increasing theta/alpha ratio while they cease when the latter ratio decreases and the beta/alpha ratio increases (Table 9.1.1-1, Figure 9.1-7).

A different perspective on BOLD signal decreases associated with alpha power

Based on the observation that alpha is the prominent rhythm during relaxed wakefulness (Berger 1929) we propose the following perspective on the relation between EEG alpha activity and the topography of associated brain activity changes. Brain areas that are less active during high alpha power – in reverse – are more active during epochs of decreased alpha power (Pfurtscheller, Stancak et al. 1996). In other words, associated with higher alpha power, we identify brain areas that have been active 'before' and 'after' epochs of higher alpha power. The intermittent epochs of high alpha power can be seen as an intermediate state, or baseline, between states of either higher degrees of vigilance and activity (characterized by low theta power) or states characterized by lower degrees of vigilance and activity (high theta power) (Loomis, Harvey et al. 1935; Loomis, Harvey et al. 1937; Kinnari, Peter et al. 2000). Hence, it is conceivable to find different topographies of activations when the 'resting alpha state' is left, namely as a function of the direction of this change. Cantero and colleagues suggested "that electrophysiological features of human cortical oscillations

in the alpha frequency range vary across different behavioral states, as well as within state, reflecting different cerebral phenomena with probably dissimilar functional meaning" (Cantero, Atienza et al. 2002).

In summary, we have identified within in a single data set two different modes of brain activity to which the brain can move from baseline alpha activity. This reconciles our findings with those obtained in other studies and moreover suggests the mechanisms that can account for this variability. We found one pattern of alpha-correlated brain activity changes that is coupled with a high amount of theta activity in the EEG spectrum ("occipital-parietal") whereas the other pattern is associated with significantly less power in that band ("frontal-parietal"). It may be that the former state occurs during reduced vigilance compared to alpha baseline as is supported further by the slower and more variable peak alpha frequency (the brain 'climbs back up to alpha').

Vigilance states

In contrast, apart from significantly less theta activity, the frontal-parietal set of brain areas was paired with more activity in the beta band which is characteristic for a higher degree of vigilance and activity (and from which the brain 'falls back down to alpha') (Ota, Toyoshima et al. 1996). If different degrees of vigilance were the causal factor, the brain state reflected by the occipital-parietal pattern would resemble "stage I" sleep (Rechtschaffen and Kales 1968) or "stage A" with "trains" as classified by Loomis (Loomis, Harvey et al. 1935; Loomis, Harvey et al. 1937). In contrast, the state represented by the "frontal-parietal" set of brain areas would appear to be a state of higher vigilance for which fewer classifications exists than for sleep stages (Kinnari, Peter et al. 2000). The group of sessions with variable patterns was associated with even higher content of beta oscillations and less slow activity. Oscillations in the beta band have often been linked to higher order mental processing (Ray and Cole 1985; Neuper and Pfurtscheller 2001). It is conceivable that in this group, during epochs of reduced alpha power – when not 'in alpha mode' – subjects were engaged in various different mental activities (very alert). These were not reflected when contrasted against activity during alpha power because they were too variable to reveal brain

areas significantly and homogenously active. The high amount of variance explained by the "occipital-parietal" pattern in the eigenimages would finally support the notion of a more homogenous (and thus less complex) brain state associated with high theta power (drowsy). In contrast, brain states occurring in association with the "frontal-parietal" pattern may exclusively share transiently heightened attentional levels as their only commonality while the actual content of the 'atoms of thought' (Lehmann and Koenig 1997) might be more variable.

Alpha states and the "default mode" of brain function

Neither of the two presented typical sets of brain areas associated with alpha power changes show the characteristic "default mode" brain areas. This concept has mainly been proposed by Raichle and colleagues and refers to the observation that the retrosplenial, temporo-parietal, and dorso-medial prefrontal cortices are more active during rest both compared to sleep and to perception and action (Mazoyer, Zago et al. 2001; Raichle, MacLeod et al. 2001). Recently, the analysis of resting state fluctuations has shown functional coupling in the default mode network (Greicius, Krasnow et al. 2003; Laufs, Krakow et al. 2003) but also at least one further tightly coupled network that is de- (Laufs, Krakow et al. 2003) or anti-correlated (Fransson 2005) with respect to activity in the default mode system. It has been proposed that intrinsic brain activity such as the interplay between the two is modulated rather than determined by changing contingencies (Fox, Snyder et al. 2005). Alpha power changes might be linked to such modulations and in fact frontal and parietal regions were prominent among the "anti-correlated nodes" identified by Fox et al. and Fransson (Fox, Snyder et al. 2005; Fransson 2005). While activity in "default mode" brain regions decreases during states of reduced vigilance (Laureys, Perrin et al. 2004), we have previously demonstrated that its dynamics during resting wakefulness are associated with beta oscillations (Laufs, Krakow et al. 2003). This may indicate that activity in these regions is related to a more complex set of variables than mere alpha power, a view that would explain why they did not appear in our "negative alpha"-oriented analyses. However, it is noteworthy that "default mode" regions as the precuneus did appear on some eigenimages within the "frontal-parietal" group (Figure 9.1-8).

Conclusion

We have demonstrated the existence of two prominent and distinct alpha power-associated BOLD signal patterns during eyes-closed rest as well as the occurrence of cases that resist classification into either category. The occurrence of either of the two distinct patterns could be related to oscillations in frequency bands adjacent to that of alpha. We hence propose that BOLD patterns during alpha desynchronization depend on where brain activity is heading. This can be towards a relatively stable, more homogenous, globally organized brain state in association with slower (4 – 7 Hz theta) oscillations on one end, reflected by occipital BOLD signal increases. Conversely, on the other end, the brain states with the strongest EEG acceleration appear to be too heterogeneous to yield consistent BOLD patterns. Finally, an intermediate pattern - and overall the most reliable one in our sample – corresponds to a state where the onset of generic attention-demanding cognitive processes dominates and results in the activation of frontal and parietal areas. These observations suggest that analysis of the entire spectral EEG information in conjunction with fMRI may permit to delineate neuroanatomically defined sub-stages of brain activity during resting wakefulness.

9.2 Mapping of ongoing pathological EEG information identifies the irritative zone in a patient with epilepsy

9.2.1 EEG-fMRI mapping of asymmetrical delta activity in a patient with refractory epilepsy is concordant with the epileptogenic region determined by intracranial EEG[2]

Abstract

We studied a patient with refractory focal epilepsy using continuous EEG-correlated fMRI. Seizures were characterised by head turning to the left and clonic jerking of the left arm suggesting a right frontal epileptogenic region. Interictal EEG showed occasional runs of independent, non-lateralized slow activity in the delta band with right fronto-central dominance. and had no lateralizing value. Ictal scalp EEG suggested right sided central slow activity preceding some seizures. Structural 3 Tesla MRI showed no abnormality. There were no clear epileptiform abnormalities during simultaneous EEG-fMRI. We therefore modeled asymmetrical 1-3 Hz EEG delta activity near fronto-central electrode positions. Significant Blood Oxygen-Level Dependent (BOLD) signal changes in the right superior frontal gyrus correlated with right frontal oscillations at 1-3 Hz but not at 4-7 Hz and with neither of the two frequency bands when derived from contralateral or posterior electrode positions which served as controls. Motor fMRI activations with a finger tapping paradigm were asymmetrical: they were more anterior for the left hand compared to the right, and near the aforementioned EEG-correlated signal changes. A right fronto-central, peri-rolandic seizure onset was identified with a subdural grid recording, and electrical stimulation of the adjacent contact produced motor responses in the left arm and afterdischarges. The fMRI localization of the left hand motor and the detected BOLD activation associated with modeled slow activity suggest a role for localization of the epileptogenic region with EEG-fMRI even in the absence of clear interictal discharges.

[2] Own contributions: conceptualization of study, patient selection, method development, analyses; entire manuscript preparation; Laufs, H., K. Hamandi, et al. (2006). "EEG-fMRI mapping of asymmetrical delta activity in a patient with refractory

Introduction

EEG-fMRI can map interictal EEG activity in focal epilepsy (Warach, Ives et al. 1996; Krakow, Woermann et al. 1999; Al-Asmi, Benar et al. 2003; Gotman, Benar et al. 2004; Hamandi, Salek-Haddadi et al. 2004). An important methodological constraint is the necessity of determining unequivocal interictal epileptic activity during scanning to model the fMRI data (Hamandi, Salek Haddadi et al. 2005): Model-free analysis of fMRI independent of EEG may provide localizing information (Morgan, Price et al. 2004; Ricci, De Carli et al. 2004; Federico, Abbott et al. 2005), however, both caution against methodological confounds and also careful validation with EEG are necessary (Hamandi, Salek Haddadi et al. 2005). In addition, there should be validation against a gold standard, such as invasive EEG monitoring, and surgical outcome where possible (Al-Asmi, Benar et al. 2003).

Here, we show how EEG-fMRI in the absence of clear epileptiform discharges may be helpful in identifying the seizure onset zone (Rosenow and Luders 2001) as validated by intracranial EEG and supported by task-related fMRI.

Case report

We studied a 40 year old right-handed patient who experienced the first seizure at age 6 years. Neurological examination revealed mild pyramidal weakness affecting the left arm. Daily doses of medication at the time of the investigation consisted of Carbamazepine (1600 mg), Levetiracetam (2000 mg), Phenobarbitone (75mg), Phenytoin (350 mg), Lamotrigine (200mg), and Lorazepam (3mg). Seizures began with eye and head deviation to the left accompanied by tonic extension and posturing of the left arm and leg, with impaired consciousness and frequent secondary generalization. Interictal scalp EEG demonstrated symmetrical post-central alpha rhythm and occasional runs of independent, non-lateralized slow activity with right fronto-central predominance. Ictal scalp EEG was not sufficiently localizing and high resolution structural MRI was normal (see Methods for details), so intracranial EEG studies were undertaken. One subdural 48 contact grid and two 8 contact strips were placed (Figure 9.2-1 A, B; AD-TECH, Racine, Wisconsin, U.S.A.). During six days of

epilepsy is concordant with the epileptogenic region determined by intracranial EEG." Magn Reson Imaging **24**(4): 367-371..

video-telemetry three stereotyped seizures were captured. Subdural EEG detected a right fronto-central seizure onset with ictal high frequency discharge (at contact 20 on the subdural grid, Figure 9.2-2) anterior to the left hand motor area as identified by cortical stimulation studies which lead to tonic extension of the left arm when stimulating at nearby electrode positions (contacts 30,31, 38, 39, see Figure 9.2-1 C and Table 9.2.1-1). Resective surgery was not pursued in view of the close proximity of the seizure onset zone to eloquent motor cortex and because the clinical onset of some seizures preceded EEG changes.

Grid contact number(s)	**Clinical / *EEG* features**
7, 8	no response (1-3 mA)
15, 16	no response (3 mA)
23, 24	no response (3 mA)
31, 32	slight sensation in left hand (3 mA)
	stronger sensation in left hand (3.5 mA)
39, 40	"weird feeling" in left hand (3.5 mA)
47, 48	strong discomfort in head (3.5 mA)
46, 47	strong discomfort in head (3 mA)
38, 39	motor response in left hand (3 mA)
30, 31	twitch in left index finger (2.5 mA)
22, 23	after discharges (twitch in left index finger)
20	*fast activity at seizure onset*
8, 12	*spread of fast activity following contact 20*
8, 11, 12	*low amplitude fast after seizure onset*

Table 9.2.1-1: Summary of cortical stimulation and ictal EEG features (compare Figure 1C). Electrical stimulation was performed with 0.5 ms 1-3 mA bipolar stimuli at 50 Hz.

Methods

The patient gave written informed consent to this study which was approved by the joint ethics committee of the National Hospital for Neurology and Neurosurgery and Institute of Neurology (04/Q0512/77).

Imaging was performed on a 3T GE Horizon EchoSpeed system using a standard head coil. Two 20 minute eyes-closed rest and one 5 minute finger tap session were acquired with EEG-fMRI (T2*-weighted gradient-echo EPI sequence, TE=40ms; TR=3000ms; interleaved acquisition of 47x5mm slices; Field of View 24x24 cm2; 64x64matrix). The first 4 images/session were discarded to allow for T1-saturation effects. Finger tap was self-paced at around 2 Hz, alternating between left and right in 30-second blocks, modelled using a block design. Subject motion was modelled as confound using the rigid body motion parameters obtained during the realignment procedure (Friston, Williams et al. 1996; Lund, Norgaard et al. 2005). All fMRI data were pre-processed and analyzed using SPM2 (Statistical Parametric Mapping) (http://www.fil.ion.ucl.ac.uk/spm/). Structural imaging comprised coronal volumetric T1-weighted Inversion Recovery-prepared Spoiled Gradient Recalled (IR-SPGR), oblique coronal dual-echo proton density, T2-weighted, and oblique coronal fast fluid-attenuated inversion recovery (Fast-FLAIR) sequences. BOLD images were realigned, normalised (along with the T1 structural scan, based on the MNI template brain) and spatially smoothed with a Gaussian Kernel of 8 mm full width at half maximum.

Using MR-compatible equipment, ten EEG channels (gold disk electrodes with 10 kOhm safety resistors) were recorded at electrode positions Fp2/Fp1, F8/F7, T4/T3, T6/T7, O2/O1, Fz (ground) and Pz as the reference (10-20 system), and bipolar ECG. In-house EEG recording equipment with a 5kHz sampling rate, 33.3 mV range at 2µV resolution was used, with online pulse and imaging artefact subtraction (Lemieux, Allen et al. 1997; Allen, Polizzi et al. 1998; Allen, Josephs et al. 2000; Krakow, Allen et al. 2000; Lemieux, Salek-Haddadi et al. 2001). Further offline imaging and pulse artifact removal was performed using the Brain Vision Analyzer (Laufs, Kleinschmidt et al. 2003). Remaining gross artifacts (motion, electrode contact) were marked semi-automatically. For each session, the EEG was segmented into 1 s epochs (50% overlap), and FFTs (10% hanning window, power) were performed interpolating at the artifact-marked epochs. For each of the bipolar channels F8-T4, F7-T3, T6-O2, T5-O1 one 1-3 Hz and one 4-7 Hz regressor was derived, convolved with the canonical haemodynamic response function and entered into a single general linear model alongside motion confounds (see above). F8-T4/F7-T3 and 1-3 Hz were picked as the band and channels

of interest based on the scalp interictal EEG findings while the contralateral and posterior electrode positions served as controls. Similarly, another slow frequency band, 4-7 Hz, below background EEG activity was chosen to facilitate testing for band-specificity of the presumed 1-3 Hz asymmetrical slow activity. An F-contrast was used to test for BOLD signal changes related to differences in 1-3 Hz power changes occurring in F8-T4 vs. F7/T3, but not at other electrode positions or at 4-7 Hz. fMRI activations were compared with ictal onset and corticography from the subdural grid recordings undertaken during presurgical workup.

Results

Left hand motor mapping by fMRI lead to a contralateral BOLD activation; this was lateral and anterior to the assumed normal functional anatomy as demonstrated for the right hand in the left precentral gyrus (Figure 9.2-1 B). No coregistration of CT, MRI and the grid position was possible. Thus, carefully stated, the right-sided fMRI motor activation lay at least in very close proximity to the corticographically identified hand area (Figure 9.2-1 B, C). Slightly anterior and lateral to this, stimulation at contact 11 led to tonic posturing of the left arm. Neighbouring this electrode was contact 20, the site of seizure onset (Figure 9.2-1 C, Table 9.2.1-1, Figure 9.2-2).

Modelling 1-3 Hz EEG oscillations in right anterior temporal electrodes versus left revealed BOLD signal changes in the supramarginal gyrus (Figure 9.2-1 B), anterior and medial to the motor hand area and medial to the seizure onset zone detected by intracranial EEG (Figure 9.2-1 C). BOLD activations were specific for electrode position and frequency band.

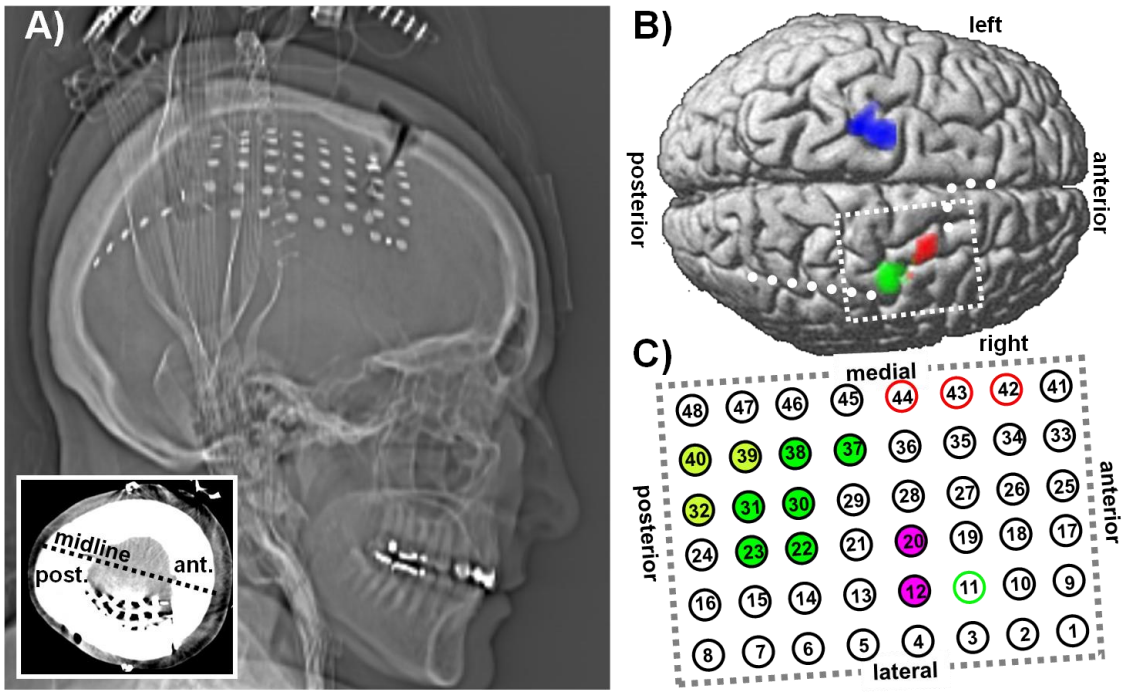

Figure 9.2-1: Position of the subdural grid and strips (A), their approximate relation to fMRI motor mapping and EEG-fMRI activations in response to right fronto-central 1-3 Hz slow activity (B), and cortical stimulation results (C). A) Sagittal Computed Tomography (CT) localizer showing the position of the 48 contact subdural grid over the right anterior frontal lobe and one 8 contact subdural strip overlapping the grid and extending posteriorly. Another 8 contact strip was placed extending medially from contact 34 of the grid (compare C) into the interhemispheric fissure. The insert shows a CT slice reflecting the position of the grid in the axial plane. B) Overlay of fMRI activations onto a surface rendering of a template brain in normalized space, all corrected for multiple comparisons (family wise error, $P<0.05$, extent threshold 30 voxels). Right finger tap fMRI activation is shown in blue (coordinates in Talairach space, maximum at [XYZ] =[-25,-18,61], left precentral gyrus), left tapping in green ([40,-5,63], right precentral gyrus and superior frontal gyrus). Indicated in red ([26,7,65], right superior frontal gyrus) are fMRI signal changes in response to the difference of 1-3 Hz EEG activity recorded at F8-T4 versus F7-T3, masked by signal changes occurring in response to 1-3 Hz EEG slowing at contralateral and posterior electrode positions (T6-O2, T5-O1) and to 4-7 Hz oscillations recorded at F8-T4, F7-T3, T6-O2 and T5-O1. Dashed and dotted lines indicate positions of the subdural grid and strips, respectively. C) Schematic of 48 contact subdural grid with colour-coded elcetrocorticography results (see Table for details). Dark green indicates a motor response from the left hand, lighter green implies the border between motor and somatosensory cortex. Stimulation at contact 11 (green circle) provoked stiffening of the left arm. Pink indicates contacts at which seizure onset or early spreading was seen (compare Figure 9.2-2), and red circles mark contacts which by estimation overly the area of EEG-fMRI activation (compare B, red).

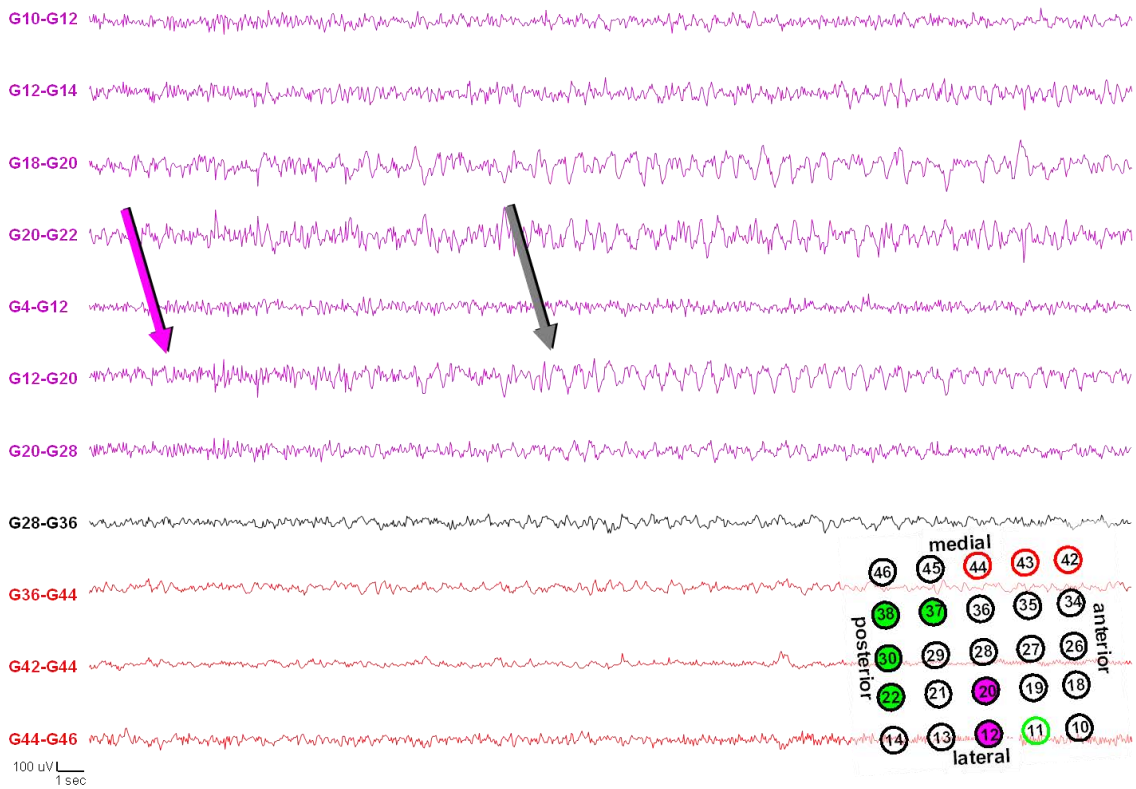

Figure 9.2-2: Bipolar montage of EEG recorded during seizure onset from the 48 contact subdural grid. An increase in background low amplitude fast activity is seen at contact G20 (pink arrow) evolving into higher amplitude fast activity interspersed with low amplitude (100 uV) spikes, before an underlying semi rhythmic slow activity occurs (grey arrow). The discharge is maximal at contact G20, and there is some spread to G12. The bipolar derivations near the suspected area of slowing-associated fMRI activation (G42, G44, red) have a very low amplitude signal implying synchronous activity at respective electrode pairs. Compare Figure 1C for insert in right lower hand corner.

Discussion

We used motor fMRI and EEG-fMRI to investigate a patient with refractory frontal lobe seizures. The absence of clear interictal discharges on scalp EEG recorded during fMRI lead us to develop a strategy for analysis of fMRI based on localised EEG frequency changes, in addition to a close inspection of motor fMRI employing a paradigm (finger tap) that was expected to activate cortex adjacent to the seizure onset zone.

Localized slow activity in focal epilepsy is a lateralizing, and sometimes localizing, finding in temporal (Gambardella, Gotman et al. 1995; Koutroumanidis, Binnie et al. 1998) and extratemporal lobe epilepsy (Geyer, Bilir et al. 1999; Koutroumanidis, Martin-Miguel et al. 1999). The value of slow activity for localization in patients without lateralizing spikes has been demonstrated (Gallen, Tecoma et al. 1997; Koutroumanidis, Martin-Miguel et al. 2004). In addition, cortical ictal and postictal EEG

slowing has been proposed to signify physiologic impairment contributing to altered cerebral function (Blumenfeld, Rivera et al. 2004). This last aspect highlights another role of specific EEG frequency bands as reflections of cognitive processes which when modeled in fMRI studies only indirectly reflect the neural sources of the observed EEG phenomena (Laufs, Kleinschmidt et al. 2003; Laufs, Krakow et al. 2003; Kobayashi, Bagshaw et al. 2005; Laufs, Lengler et al. 2005).

Although no structural cortical lesion could be identified on MRI, functional motor cortex asymmetry with relative antero-lateral displacement of the left hand area compared to the right may suggest an underlying abnormality linked to the seizure onset zone. Previously, motor mapping and EEG-fMRI in a patient with grey matter heterotopia visible on structural MRI and close to the sensorimotor area found activations linked to interictal discharges in close proximity to the lesion, with displaced fMRI motor activation (Diehl, Salek-Haddadi et al. 2003).

We demonstrate that in the absence of interictal epileptic discharges which are normally used to model fMRI data, automated EEG frequency analyses in EEG-fMRI may prove useful for planning the placement of intracranial electrodes to map epileptogenic areas. As with any clinical work-up, information available from other investigations should be taken into account when designing and interpreting studies of individual patients.

9.3 Epilepsy syndromes characterized by impaired consciousness are accompanied by epileptic discharge-associated activity changes in the default mode network

9.3.1 Linking generalized spike-and-wave discharges and resting state brain activity by using EEG-fMRI in a patient with absence seizures[3]

Abstract

Purpose: To illustrate a functional interpretation of blood oxygen level-dependent (BOLD) signal changes associated with generalized spike and wave discharges in patients with absence seizures and to demonstrate the reproducibility of these findings in one case.

Methods: In a 47 year-old patient with frequent absence seizures BOLD signal changes during generalized spike and wave discharges (GSWD) were mapped using simultaneous and continuous electroencephalography (EEG) and functional magnetic resonance imaging (fMRI) at 1.5 T and 6 months later at 3 T. GSWD were modelled as individual events and as blocks.

Results: The patient studied exhibited frequent generalized spike wave activity with temporal properties ideal for study with EEG-fMRI. Highly reproducible GSWD associated fMRI signal decreases (‘deactivations’) were seen in bilateral frontal and temporo-parietal cortices and the precuneus, in addition to activations in occipital cortex and, at 3 T, the posterior thalamus.

Discussion: The GSWD associated changes seen here involve cortical regions that have been shown to be more active at conscious rest compared to sleep and to various types of extroverted perception and action. These regions have been proposed to constitute the core of a functional ‘default mode’ system. We propose that the findings of 'deactivation' of this distributed brain system during GSWD mirrors the

[3] Own contributions: study design, data acquisition and analysis, result interpretation, entire manuscript preparation; Laufs, H., U. Lengler, et al. (2006). "Linking Generalized Spike-and-Wave Discharges and Resting State Brain Activity by Using EEG/fMRI in a Patient with Absence Seizures." Epilepsia **47**(2): 444-448..

clinical manifestation of GSWD, i.e. absence seizures. Furthermore, we suggest that these deactivations may reflect the functional consequences of GSWD on physiological brain activity at rest rather than direct hemodynamic correlates of epileptic discharges.

Introduction:

When combined with simultaneous EEG recording, BOLD fMRI techniques permit the identification of brain regions affected by GSWD (Warach, Ives et al. 1996; Baudewig, Bittermann et al. 2001; Archer, Abbott et al. 2003; Salek-Haddadi, Lemieux et al. 2003; Aghakhani, Bagshaw et al. 2004). Ictal symptoms are not necessarily 'positive', such as movements or sensations but can be 'negative', e.g. absences. One question is whether such negative symptoms are associated with 'deactivation' as indexed by hemodynamic signals. Another current question concerns the topographical relation between electrical and hemodynamic brain signals. If for instance epileptic activity on surface EEG is not focal but generalized, would one predict that activation or deactivation occur reproducibly and globally throughout the brain?

Methods

Patient

We studied a 47 year-old male (written informed consent, ethics committee approval) with juvenile absence epilepsy, onset at age 8, with frequent absence seizures and less than one generalized tonic-clonic seizure per year. Intellectual development, neurological examination and structural imaging findings were all normal. At the time of investigation, more than 10 typical absence seizures per hour were seen on clinical observation as a sudden cessation of activity but without additional motor symptoms. EEG showed a normal background interrupted by frequent 2-3/s GSWD lasting between <1 and 20 seconds, and occasionally up to 40 seconds. Absence seizures had proven refractory to treatment with phenytoin, valproate, phenobarbitone, clonazepam, ethosuximide and primidone. The patient was taking 750 mg of Primidone at the time of both experiments. He was resistant to further changes in medication.

fMRI data acquisition

The patient was studied at 1.5 T (experiment I) and, for reproducibility at follow-up 6 months later at 3 T (experiment II). Two 20 minutes imaging sessions were acquired at each experiment. During scanning the instruction was to lie still with eyes closed ("rest"). Imaging parameters: T2*-weighted echo-planar images covering the entire cerebrum; *1.5 T* Siemens Vision (Erlangen, Germany), voxel size 3.44 x 3.44 x 4 mm, 19 slices with 1 mm gap in 2.8 s, 300 volumes, TR/TE 4000/50; *3 T* Siemens Trio (Erlangen), voxel size 3 x 3 x 4 mm, 20 slices with 1 mm gap in 1.3 sec, 300 volumes, TR/TE 2666/20, vacuum head cushion.

EEG and artifact reduction

EEG was recorded using the BrainAmp MR EEG amplifier (5 kHz), Brain Vision Recorder software (Brainproducts, Munich, Germany) and the BrainCap electrode cap (Falk Minow Services, Herrsching-Breitbrunn, Germany) with 29 electrodes (10-20 system, reference between Fz and Cz). Off-line EEG artifact subtraction was performed, as implemented in the Brain Vision Analyzer (Brainproducts) (Laufs, Kleinschmidt et al. 2003).

Data analysis

We used statistical parametric mapping (SPM2 [http://www.fil.ion.ucl.ac.uk/spm]) for image realignment, normalization, spatial (10 mm full width at half maximum Gaussian kernel) and temporal (128 s high pass filter) smoothing and statistical analysis. Epochs of GSWD were visually identified and used to define a boxcar which was convolved with the hemodynamic response function (HRF; block design). In addition, a template matching algorithm (based on amplitude and correlation measures, Ingmar Gutberlet, VisionAnalyzer, Brain Products) was used to individually mark the spikes of GSWD. These markers were treated as events and convolved with the HRF and used as a regressor for an event-related fMRI analysis. In a third model we grouped runs of GSWD into two event types, depending on whether they lasted for longer or less than 1 second to test for differences in the fMRI response to short and long runs. Motion parameters obtained from realignment were always included as confounds.

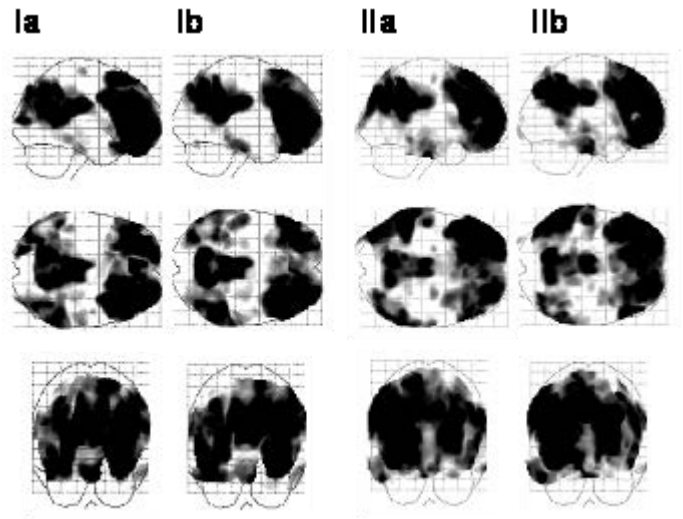

Figure 9.3.1-1: Spatial modes showing highest correlation with generalized spike and wave discharges. Spatial modes (eigenimages) from a data driven analysis are displayed on glass brains. For each session (a and b, respectively) of the experiments I and II, the second eigenimage is shown and its component score showed the highest correlation with the occurrence of GSWD.

An eigenimage analysis was undertaken (Figure 9.3.1-1) by means of Singular value decomposition (principal component analysis) of the fMRI time series. This was performed using the multivariate linear models toolbox as implemented in SPM99 (Kherif, Poline et al. 2002) after removing the session mean and the variance explained by the realignment parameters. The correlation coefficients between the computed eigenvariates and the smoothed, filtered and hrf-convolved regressor modelling each GSWD as a single event were calculated using MATLAB (Mathworks, Inc., Sherborn, MA).

In every session, the second BOLD-eigenvariate showed the maximum correlation with the GSWD regressor, ranging from –0.7 to –0.8, the negative values reflecting their inverse relationship. The related eigenimages very closely matched the topographical "deactivation" pattern that we determined (Figure 9.3.1-2 D), whose appearance in one single eigenimage suggests functional connectivity as demonstrated previously in this network. The high variance of 9% to 14% of the variance in the fMRI data set explained by this spatial mode points to the prominence of activity in these areas during conscious rest, which is then suspended.

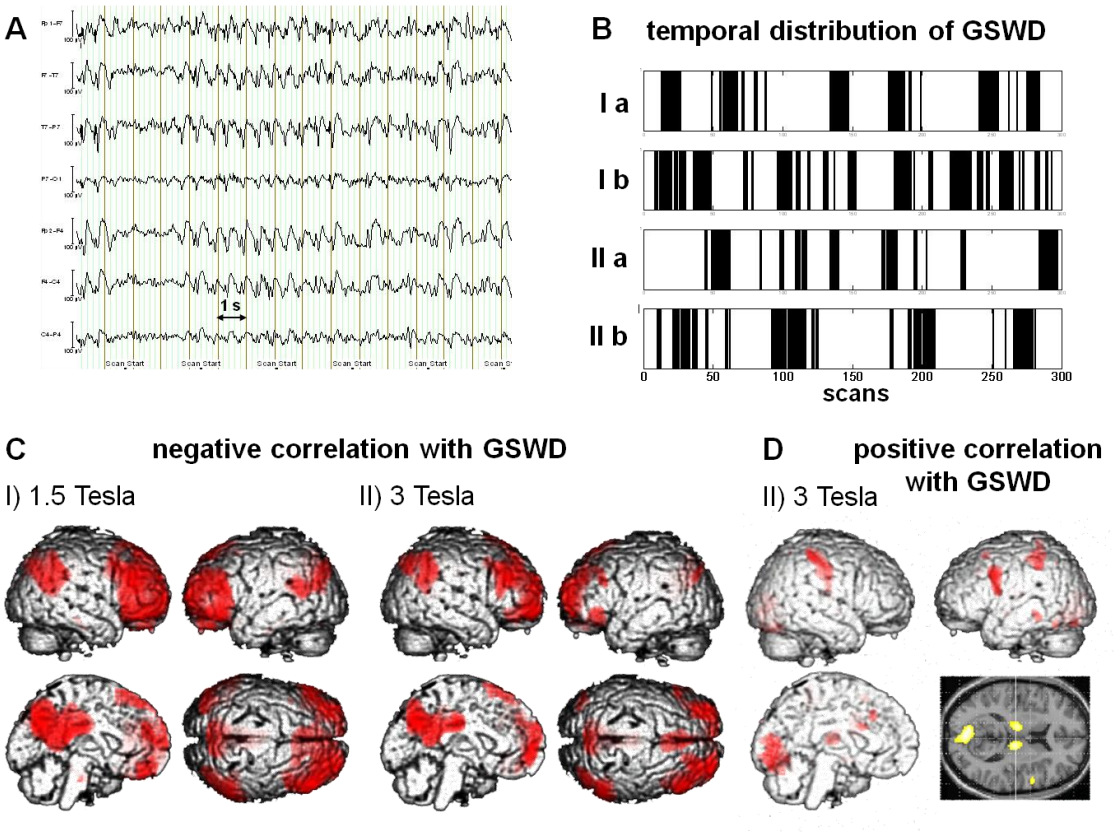

Figure 9.3.1-2: A, B: Generalized spike and wave discharges on EEG and their occurrence in time. A) Electroencephalogram recorded during functional magnetic resonance imaging after image artifact reduction showing intermittent ~ 2/sec generalized spike and wave discharges with frontal emphasis. Bipolar montage (clipped and filtered [0.5-30 Hz] for display), following 10-20 system, Reference between Fz and Cz; 'Scan Start' = start of individual volume acquisition; B) Occurrence of generalized spike and wave discharges (black bars) during experiment I and II, sessions a and b respectively (abscissa in scans): there were on average 369 individual GSWD/session, the mean block length of GSWD per session ranged from 4.5 to 5.9 image volumes/GSWD epoch.

C, D: Maps of fMRI signal changes during generalized spike and wave discharges on EEG. Brain areas where fMRI signal is significantly negatively (C) or positively (D) correlated with generalized spike and wave discharges (event-related design) during experiment I and II (p=0.05 corrected for multiple comparisons, family wise error) are projected onto a rendering of a template brain (colour intensity is a function of depth) or axial slices of a T1-weighted template brain (z=14). Note that positive correlations in experiment I and II are alike except for additional positive thalamic activation which was only detected in experiment II performed at 3 T (data for experiment I not shown in panel D).

Results

In all 4 sessions frequent GSWD were seen (Figure 9.3.1-2 A, B) and the patient was in 'quiet rest' as monitored by the EEG showing a normal awake background with continuous 9 Hz posterior alpha rhythm. There were no drops in vigilance as assessed by looking for vigilance/sleep criteria on the EEG (alpha amplitude variation, slowing, eye movements, sleep grapho-elements, heart rate). Reproducible negative correlations with GSWD were detected bilaterally in dorsal prefrontal and temporo-parietal cortices and the precuneus and posterior cingulum (Figure 9.3.1-2 C) with

positive correlations in the occipital cortex and bilateral inferior parietal areas. At 3 T, additional significant activations were found in the posterior thalamus (Figure 9.3.1-2 D). The block and the event related design showed the same signal changes. The deactivation patterns from short and long runs of GSWD were similar to the above analyses and to one another (significance was lower for short runs as they were less in number). Eigenimage analysis confirmed high reproducibility of the findings and demonstrated functional connectivity of the areas found to deactivate during GSWD (Figure 9.3.1-1).

Discussion

In accordance with our findings, previous fMRI studies have reported predominantly negative cortical BOLD responses or 'deactivation' in association with GSWD in patients with idiopathic generalized epilepsy (IGE, Table 9.3.1-1) (Archer, Abbott et al. 2003; Salek-Haddadi, Lemieux et al. 2003; Aghakhani, Bagshaw et al. 2004). Yet, an interpretation of the functional significance of deactivations during GSWD remains lacking, in particular of those regions reported here.

Study	patients	bilateral activation	bilateral deactivation
this study	1 IGE	thalamus (at 3T), lingual gyrus	precuneus, posterior cingulate, temporo-parietal junction, prefrontal cortex
Salek-Haddadi et al.(Salek-Haddadi, Lemieux et al. 2003)	1 IGE	Thalamus	frontal and parietal cortices with frontal emphasis, retrosplenial areas
Archer et al.(Archer, Abbott et al. 2003)	1 IGE, 4 CAE	variable and scattered at group level	posterior cingulate significant at group level; bilateral temporo-parietal cortex
Aghakhani et al.(Aghakhani, Bagshaw et al. 2004)	15 IGE	group level: deactivation predominant over activation, both found in thalamus and cortex: mainly frontal and parietal cortex, followed by temporal, central and occipital cortex	
(Aghakhani, Bagshaw et al. 2004)	1 CAE	signal changes in thalamus, parietal and [pre-]frontal cortex, precuneus (taken from the figure of one individual case)	

IGE: idiopathic generalized epilepsy, CAE: childhood absence epilepsy

Table 9.3.1-1: Literature evidence for signal changes in 'default mode' brain areas and thalamus during generalized spike and wave discharges.

Meta-analyses of studies in healthy subjects have established that across different functional activation paradigms a similar set of brain areas will consistently display deactivations (Mazoyer, Zago et al. 2001; Raichle, MacLeod et al. 2001): activity in bilateral medial frontal and parietal areas and the precuneus is spontaneously higher when the brain is at 'rest' than when the brain is engaged in extroverted perception and action. Activity in this functional network has thus been termed a "default mode" of brain function, when cognitive processes revolve about the self, its past and its future (Raichle, MacLeod et al. 2001).

This introspective cognitive state can be regarded a cornerstone of consciousness. The pattern of cortical deactivation we observed in these "default mode" areas (Figure 9.3.1-2 C) has also been identified in slow wave sleep compared to wakefulness (Maquet 2000); and the precuneus has been reported to reflect the difference between wakefulness and clinical states where consciousness is impaired as in coma and anaesthesia (Laureys, Owen et al. 2004).

We could recently link the "default mode" areas to another EEG feature, namely activity (power) in the range of 17-23 Hz during conscious rest and also show their connectivity (Laufs, Krakow et al. 2003). Here, in the context of GSWD, we also found these areas to be functionally connected (see supporting material). We suggest that the regions of BOLD signal decreases indicate areas where GSWD are associated with a disturbance or suspension of this physiological conscious rest. The particular deactivations might not be specific for or causally related to GSWD per se. Instead, they may provide an fMRI signature of the negative clinical phenomenology of absence seizures similar to sleep, anaesthesia or coma - impaired consciousness, dynamically occurring even on a second-by-second basis.

We hypothesize that whilst our patient was at rest and not experiencing absence seizures, the 'default mode' brain areas were active as part of normal processing during conscious rest. This conscious rest (with normal background EEG activity) was interrupted by GSWD, presenting in fMRI as a relative deactivation of that mode. Clinical absences during prolonged runs of GSWD were evident outside the scanner. Nevertheless, the same pattern of deactivation was found for short and long runs of GSWD. We suggest that in our patient even short discharges might lead to a (subclinical) interruption of cognitive processes (as reported by others (Aarts, Binnie et al. 1984)). However, any experimental interference to confirm this assumption would have obliterated the resting state. For example, a simple button press-task to monitor the patient's state of consciousness in the scanner would have suspended the default mode in the first place, and during GSWD one might, for instance, have seen deactivations in the [motor] areas recruited by that task.

Apart from the common pattern of deactivation discussed here, there is variability in the findings of EEG-fMRI studies of IGE (Archer, Abbott et al. 2003; Aghakhani, Bagshaw et al. 2004). This can be explained by the fact that different syndromes of IGE have been studied and the clinical manifestation of different types of absences is not uniform (Gloor 1986). Reflecting these clinical differences, varying brain areas may be influenced by GSWD and may explain the different activations seen, including the

occipital activation in this patient (Figure 9.3.1-2 D). An alternative account of this variability, however, is that it expresses the physiological (and between session) variability of resting state brain activity rather than differences between absence syndromes. In this context, the fMRI activations represent brain areas involved in the mental activity disrupted by GSWD. Combining cognitive paradigms with EEG-fMRI experiments might lead to a more realistic characterization of how epileptic EEG activity interferes with the patients' cognitive function.

The presence of thalamic activation seen here at 3 T - but not at 1.5 T - is in keeping with higher sensitivity of fMRI at 3 T and supports the involvement of the thalamus in generating GSWD. A reciprocal relation between thalamo-reticular and cortical structures in generalized epilepsies has been supported by findings in animal models, electrophysiological and functional imaging experiments (Salek-Haddadi, Lemieux et al. 2003; Aghakhani, Bagshaw et al. 2004; Timofeev and Steriade 2004). Studies using deep brain stimulation and PET have demonstrated an inhibitory input to the thalamus being associated with an increase in thalamic but a decrease in frontal, parietal and temporal blood flow, probably caused by inhibiting thalamo-cortical connections (Hershey, Revilla et al. 2003).

As one potential explanation we suggest on the basis of our observations and that of others (Table 9.3.1-1) that functional changes in the 'default mode' network reproducibly occur during GSWD and might be related to the clinical manifestation of absence seizures.

9.3.2 EEG-fMRI of idiopathic and secondarily generalized epilepsies[4]

Abstract

We used simultaneous EEG and functional MRI (EEG-fMRI) to study generalized spike wave activity (GSW) in idiopathic and secondary generalized epilepsy (SGE). Recent studies have demonstrated thalamic and cortical fMRI signal changes in association with GSW in idiopathic generalized epilepsy (IGE). We report on a large cohort of patients that included both IGE and SGE, and give a functional interpretation of our findings. Forty six patients with GSW were studied with EEG-fMRI; 30 with IGE and 16 with SGE. GSW-related BOLD signal changes were seen in 25 of 36 individual patients who had GSW during EEG-fMRI. This was seen in thalamus (60%) and symmetrically in frontal cortex (92%), parietal cortex (76%) and posterior cingulate cortex / precuneus (80%). Thalamic BOLD changes were predominantly positive and cortical changes predominantly negative. Group analysis showed a negative BOLD response in the cortex in the IGE group and to a lesser extent a positive response in thalamus. Thalamic activation was consistent with its known role in GSW, and its detection with EEG-fMRI may in part be related to the frequency and duration of GSW epochs recorded. The spatial distribution of the cortical fMRI response to GSW in both IGE and SGE involved areas of association cortex that are most active during conscious rest. Reduction of activity in these regions during GSW is consistent with the clinical manifestation of absence seizures. (Henson, Price et al. 2002)

Introduction

Generalized spike wave (GSW) activity, is the electroencephalographic (EEG) hallmark of idiopathic generalized epilepsy (IGE), occurring in runs of 2.5-4 Hz spike and slow wave activity, typically arising from a normal background EEG (Duncan 1997). GSW is also seen in symptomatic generalized epilepsies where it is usually associated with an

[4] Own contributions: analysis design, data analysis (MATLAB scripts for fully automated analysis), result interpretation, manuscript preparation; Hamandi, K., A. Salek-Haddadi, et al. (2006). "EEG-fMRI of idiopathic and secondarily generalized epilepsies." Neuroimage **31**(4): 1700-1710..

abnormal background EEG, and clinical evidence of other neurological dysfunction (Holmes, McKeever et al. 1987).

The pathophysiological substrate of GSW remains enigmatic. The debate between a sub-cortical origin "the centrencephalic hypothesis" (Jasper and Drooglever-Fortuyn 1947) versus a cortical origin (Marcus and Watson 1968) was reconciled to an extent by the corticoreticular hypothesis. This proposed a role for both cortex and subcortical structures (Gloor 1968), with aberrant oscillatory rhythms in reciprocally connected thalamocortical loops normally involved in the generation of sleep spindles (Gloor 1968), leading to GSW. The primary neuroanatomical and neurochemical abnormality in IGE remains undetermined with evidence and arguments for onset in either cortex (Timofeev and Steriade 2004) or thalamus (Avoli, Rogawski et al. 2001).

Much of the evidence pertaining to the pathophysiology of GSW comes from invasive electrophysiological and neurochemical recordings in animals (Avoli, Rogawski et al. 2001). A small number of intracranial studies have been reported in man in which spike wave activity was recorded in both thalamus and cortex (Williams 1953; Niedermeyer, Laws et al. 1969; Velasco, Velasco et al. 1989). The spatial sampling of depth studies is limited to the immediate vicinity of the implanted electrodes, and their invasiveness, in the absence of clinical benefit precludes their current use in IGE.

Combining EEG recording with fMRI (EEG-fMRI) enables the non-invasive mapping of haemodynamic correlates of specific EEG events or rhythms (Salek-Haddadi, Friston et al. 2003), by means of the blood oxygen level dependent (BOLD) contrast (Ogawa, Lee et al. 1990). Studies in patients with focal epilepsy have demonstrated spatially concordant BOLD activations in relation to focal epileptiform discharges (IED), evidence that EEG-fMRI can provide localizing information on generators of these discharges (Warach, Ives et al. 1996; Seeck, Lazeyras et al. 1998; Lemieux, Salek-Haddadi et al. 2001; Jäger, Werhahn et al. 2002; Al-Asmi, Benar et al. 2003). Whether EEG-fMRI is able to shed further light on the pathophysiology of GSW, by localizing generators of these discharges remains to be seen.

Salek Haddadi et al (Salek-Haddadi, Lemieux et al. 2003), using continuous EEG-fMRI at 1.5T, described bilateral thalamic BOLD signal increase, and widespread cortical decrease in a patient with juvenile absence epilepsy (JAE). Aghakhani et al. (Aghakhani, Bagshaw et al. 2004) with continuous EEG-fMRI at 1.5T found thalamic haemodynamic

signal change, predominantly activation, in 12 of 15 patients who had GSW during scanning, in addition to symmetrical cortical activation or deactivation associated with GSW. Archer et al. (Archer, Abbott et al. 2003) found posterior cingulate cortex (PCC) deactivation in association with GSW in four of five IGE patients studied with EEG-triggered fMRI at 3 T. Laufs et al. (Laufs, Lengler et al. 2006) noted thalamic activation and widespread cortical deactivation in a patient studied on two occasions, and emphasized the distribution of the cortical deactivation; being cerebral areas thought to be most active during the conscious resting state, the "default mode" hypotheses (Raichle, MacLeod et al. 2001).

We report on a large consecutive series of patients with GSW, including patients with different subtypes of IGE as well as SGE. We hypothesized that population specific BOLD effects to GSW could be identified using EEG-fMRI and a random effects group analysis in a large group of patients

Materials and Methods

Patients

Forty six patients, 30 with IGE and 16 with SGE, and frequent GSW discharges on recent interictal EEG were recruited from the epilepsy clinics at the National Hospital for Neurology and Neurosurgery, London, the National Society for Epilepsy, Chalfont St Peter and St Thomas' Hospital, London. The study was approved by the National Hospital for Neurology and Neurosurgery and the Institute of Neurology Joint Research Ethics Committee. Patients gave written informed consent.

Patients were grouped according to the ILAE 1989 classification scheme (Commission on Classification and Terminology of the International League Against Epilepsy 1989). These were IGE and its sub classifications - juvenile myoclonic epilepsy (JME), juvenile absence epilepsy (JAE), childhood absence epilepsy (CAE), and epilepsy with generalized tonic clonic seizures only (IGE-GTCS) - and secondary generalized epilepsy (SGE). The latter group had one or more of the following: atypical absences, an abnormal background EEG, and irregular GSW. In one patient there was electrographic evidence of a unilateral frontal focus (patient 43, see Table 9.3.2-1, Figure 9.3.2-1 and Figure 9.3.2-3 B). All patients had normal structural MRI.

EEG acquisition

Ten channels of EEG referenced to Pz and two channels of precordial ECG were recorded using in house recording equipment (Allen, Polizzi et al. 1998; Allen, Josephs et al. 2000). Gold disk electrodes fitted with 10 kOhm resistors, to reduce possible MR induced currents (Lemieux, Allen et al.), were applied to the scalp, at FP2/ Fp1, F8/ F7, T4/ T3, T6/ T7, O2/O1, Fz (ground) and Pz according to the international 10-20 system (for methods see (Krakow, Allen et al. 2000)). An impedance of <22 kOhm across each electrode pair was typically achieved (20 kOhm attributable to the resistors in each electrode). Algorithms for pulse and image artifact reduction, that calculate and subtract an averaged artifact waveform, were used to recover the underlying EEG, allowing the visualization of the EEG during the image acquisition (online) and subsequent review (off-line) (Allen, Polizzi et al. 1998; Allen, Josephs et al. 2000).

ID no.	Age (yrs)	Seizure type frequency (age onset/yrs)	Antiepileptic drugs	Frequency of GSW (Hz)
JAE				
1	19	Abs daily (11) GTCS 5/yr (15)	LEV, LTG	2.5–3
2[a]	24	Abs 15 d (10) GTCS 4/yr (13)	CBZ, ESM, LTG, TPM	3
3[a]	18	Abs (10) GTCS 2/mth (14)	LTG	3–4
4	43	Abs 2/wk (9) GTCS 5/yr (9)	CBZ, LTG	3
5[a]	43	Abs daily (8) GTCS 4/yr (13)	CLB, LTG, VPA	3
6[a]	22	Abs 4–5 wk (9) GTCS 6/yr (16)	LTG, VPA	4
7	22	Abs 2–3 day (8) GTCS 2/mth (19)	ESM, LTG, TPM	3–4
8	54	Abs 1/mth (19) GTCS none for 10 yrs (19)	CBZ, PHT, PB, VPA	3–4
9[a]	18	Abs weekly (15)	Nil	2.5–3
10	19	Abs daily (7) GTCS <1 yr (7)	CBZ, VPA	2.5–3
11	33	Abs daily (teens)	LTG, VPA	3
12[b]	33	Abs 10/day (10) GTCS 5/yr (14)	LTG, VPA	3
13[b]	37	Abs 1/mth (4) GTCS 2/yr (11)	LTG, OXC, PB, VPA	3
14[a,b]	36	Abs weekly (3) GTCS 3 in total (6)	LTG	3
Age range: 18–54 yrs, mean 30, median 28.5, sex ratio M:F 4:3				
JME				
15	55	Abs resolved (13) GTCS 1–2/yr (13) MJ 2–3/wk (teens)	CLB, LEV, LTG	3
16[c]	20	Abs daily (13) GTCS 2/mth (13) MJ daily (18)	CLN, TPM, VPA	2–3
17[a]	59	GTCS 1/wk (5) MJ several/wk (10)	CBZ, PB, VPA	4
18	20	Abs 3/d (<10) GTCS 1/mth (13) MJ resolved (14)	LEV	3
19	41	Abs nil GTCS 1/mth (15) MJ resolved (15)	CLB, LTG, PHT, VPA	3
20[a]	18	Abs 2–3/wk (15) GTCS <1/yr (16) MJ daily (15)	LEV, LMT, VPA	4–5
21[a]	37	Abs 10 d (7) GTCS 2/yr (12) MJ (teens)	CLB, GBP, VPA	2–3
22	18	Abs nil GTCS 1/yr (14) MJ resolved (14)	VPA	3
23[a,b]	20	Abs 3 wk (19), GTCS 1/yr (18) MJ daily (18)	CLN, LTG	2–3
Age range 18–59 yrs, mean 34, median 33, M:F 5:4				
IGE-GTCS				
24	33	GTCS free 2 yrs (11)	LTG	4
25[a]	34	GTCS 3 in total (12)	CBZ	3
26	32	GTCS 4 in total (22)	CBZ, CLN	3–4
27[b]	21	GTCS 1/mth (1)	CLB, LTG, VPA	2.5–3
28[b]	48	GTCS 1 <10 yrs (7)	VPA	2–3
29[a,b]	24	GTCS 1 in total	Nil	2–3
Age range 21–48, mean 32, median 32, M:F 2:1				
CAE				
30	23	Abs 10/d (4) GTCS 1/mth (12)	LEV	3
31[c]	26	Abs 15/d (8)	Nil	3
32[c]	53	Abs several/day (10)	DZP	4
Age range 26–53 yrs, mean 34, median 26, M:F 8:5				
SGE				
33	29	Abs daily (20) GTCS <1 yr (23)	LTG, VPA	2–3 abn bkgd
34	29	Abs 3/d (16) GTCS <1 yr (14)	ACE, CBZ, VPA	1.5–2
35	21	Abs daily (10) GTCS <1 yr (10) tonic sz 1/wk (10)	ACE, CBZ, CLN	2–3
36	19	Abs 6–8/d (7) GTCS 6/yr (7)	LEV, LTG, TGB	3 abn bkgd
37	22	Abs 2/wk (8) GTCS resolved (9) MJ 2/wk	CLN, LTG, OXC, VPA	2–3
38	26	GTCS 2–3/yr (14) drop attacks 6/yr (26)	LTG, TPM	2–3
39	26	Abs 2–3/wk (9) GTCS <1/yr (12) atonic sz 1/wk (10)	CLN, LTG, OXC	2 abn bkgd
40	74	Abs daily (teens) GTCS 2/mth (14)	PHT, TPM	2.5–3
41	22	GTCS 6/mth (11)	CBZ, TPM	3
42	38	Abs 10–20/d (7) GTCS 0–4/mth (11)	CBZ, LEV	2–3
43	21	Abs 8/mth (13) GTCS 4/yr (18)	CBZ, LEV, VPA	2 L > R, max F3
44[b]	40	Abs 1–2/mth (11) GTCS 2/yr (11)	CBZ, PHT, TGB	3
45[b]	19	GTCS 2/mth (2)	LTG, TPM	2–3 abn bkgd
46[a,b]	47	Abs 15/d (2) GTCS 3/mth (4)	PHT	3–4
Age range 19–74 yrs, mean 31, median 26, M:F 4:3				

Table 9.3.2-1: Clinical details of patients studied based on ILAE diagnostic categories, showing seizure type and frequency, age at onset, medication at time of study, and frequency of GSW.

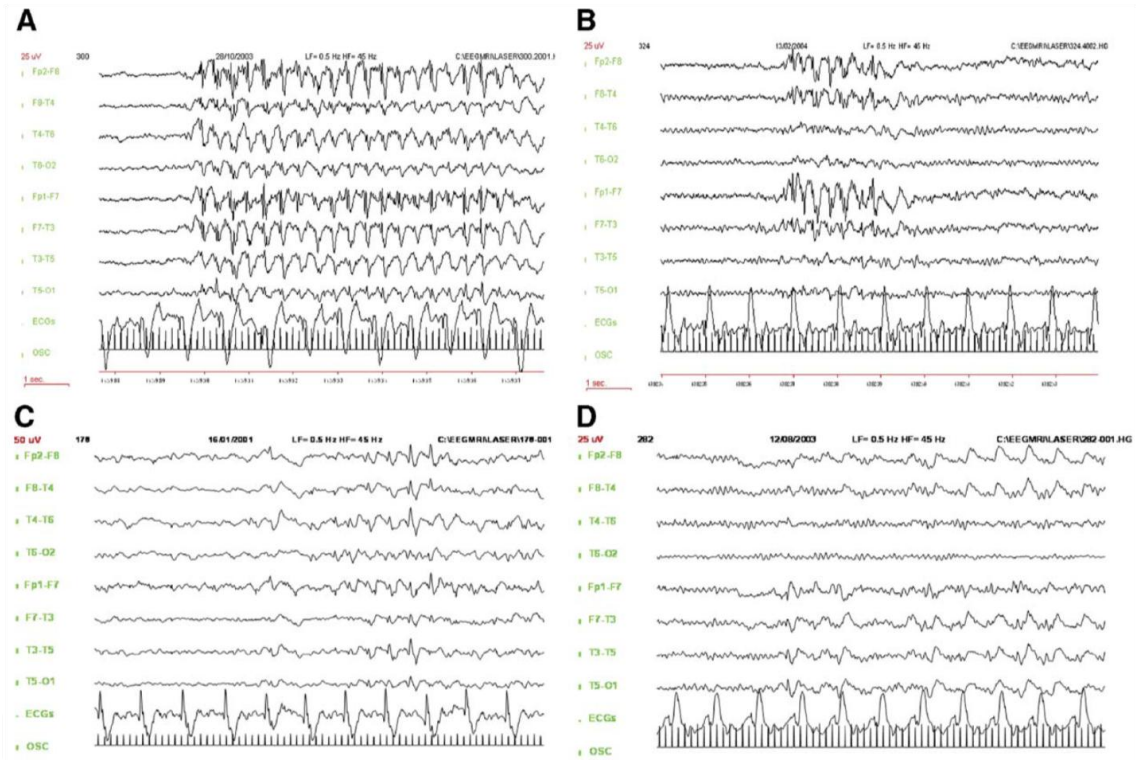

Figure 9.3.2-1: Examples of EEG recorded during scanning following pulse and image artifact subtraction, displayed as bipolar montage showing runs of generalized spike wave activity. (A) Patient #1, JAE; (B) patient #25, IGE-GTCS; (C) patient #35, SGE; (D) patient #43, SGE with evidence of L frontal epileptogenicity. ECG electrocardiogram, OSC scanner slice pulse used for EEG artifact correction, and EEG–fMRI synchronization (7/s).

MRI acquisition

A 1.5T GE Horizon echospeed MRI scanner (Milwaukee, Wisc.) was used to acquire 700 BOLD sensitive echo-planar images (EPI) images (TE/TR 40/3000, 21 x 5 mm interleaved axial slices (acquired parallel to the intercommissural line), FOV 24 x 24 cm, 64x64 matrix) over a 35 minute session with continuous, simultaneous EEG. An additional four images were acquired at the start of each session and discarded to allow for T1 equilibration effects. Foam padding or a vacuum head cushion was used to help secure the EEG leads, minimize motion, and improve patient comfort. Two successive 35 minute scan sessions at the same sitting were acquired in 13 patients, giving 59 sessions in 46 patients.

Data Analyses

The SPM2 software package (www.fil.ion.ucl.ac.uk/spm/) was used for all image pre-processing and voxel based statistical analyses. Images were slice-time corrected to the middle slice and spatially realigned to the first scan of the series, and then spatially

normalized to the MNI template supplied by SPM. Finally images were spatially smoothed using an isotropic Gaussian kernel (10 mm full width at half maximum).

The artifact corrected EEG was reviewed off-line and the onset and offset of GSW epochs were identified relative to the fMRI time series. These were used to construct a boxcar model of the active (GSW) versus rest (background) EEG state. This model was convolved with the canonical haemodynamic response function (HRF), as supplied by SPM2 (peak at 6 seconds relative to inset, delay of undershoot 16 seconds and length of kernel 32 seconds), its time and dispersion derivatives, to form regressors testing for GSW-related BOLD changes. The temporal derivative (TD) and dispersion derivative (DD) were used to accommodate variations in the canonical HRF (Handwerker, Ollinger et al.) (Henson, Price et al.). Spatial realignment parameters and their first order expansion were included as effects of no interest to model the linear and non-linear effects of motion (Friston, Williams et al.). Data and design matrices were high pass filtered at 128 seconds cutoff. An auto regression (AR(1)) model was used to estimate the intrinsic autocorrelation of the data (Friston, Josephs et al.). No global scaling or normalization was performed, to preclude introducing apparent deactivations in the analysis that would be artifactual.

An F-contrast was used to assess the variance at each voxel explained by GSW. The resulting SPMs were thresholded at $p<0.05$ using the correction for multiple comparisons based on random field theory (Friston, Frith et al.). The contrast estimate pertaining to the canonical HRF (Henson, Price et al.) was used to ascertain the direction of the BOLD response at the global maxima and at the local maxima of frontal, posterior superior parietal, and posterior cingulate cortices.

A random effects group analysis was performed on each of the groups IGE, and SGE using the following two stage procedure to infer the average pattern at a population level (Friston, Holmes et al.). The contrast estimates pertaining to HRF, TD and DD, were taken to a second level random effects group analysis using a one-way analysis of variance. The inter-session variability in the number of EEG events requires particular consideration for group analyses due to the risk of unbalanced designs (Friston, Stephan et al.). We therefore selected patient sessions in which the number of GSW events fell within one order of magnitude of each other (see Table 9.3.2-2, sessions marked *), giving 18 IGE cases and 10 SGE cases for the group analyses. An F contrast

at the second (i.e. the between subject) level was used to test for the variance explained by GSW across the group. We had insufficient patient numbers (Desmond and Glover 2002) with GSW during scanning for group analysis in JME and JAE.

Diagnostic category	Id no.	No. of GSW events	Duration of GSW events. median (range) (seconds)	Regions of significant fMRI signal change				
				Thalamus	Frontal	Parietal	Posterior cingulate/ precuneus	Other
JAE	1	9	2.1 (1.6–8.1)	–	↑ B (L **m**)	↓ B	↑B	↑ ss, cereb, temp
	2a	3	7.3 (4.4–7.7)	–	↑ B (L **m**)	↓ B	–	↑ L temp
	2b	1	5.9	–	↑ R m	–	–	↑ B temp
	3*	7	1.3 (0.9–3.3)	↓ R	↕ B	–	–	↕ B head caudate (R **m**)
	4*	4	2.6 (1.0–3.0)	–	–	–	–	–
	5a	18	0.6 (0.4–3.6)	↑ B	↑ B	–	↑ B	↑ ss, cereb (R **m**), B occ
	5b*	16	0.7 (0.4–1.7)	–	–	–	↕ B	↑ cereb (L **m**), B occ
	6a	4	1.9 (1.3–3.0)	–	–	–	–	–
	6b*	17	1.3 (0.4–4.3)	–	–	–	–	↓ L inf occ **m**
	7	2	4.3 (3.4–5.3)	↑ B	↑ B (L **m**)	↑ R	–	↑ ss
	8*	8	2.1 (1.0–5.3)	–	↓ B (L **m**)	↓ B.	↓ B	–
	9a*	8	1.9 (0.7–3.6)	–	↕ B	↓ B	↓ B	↑ ss **m**
	9b	2	0.6 (0.6–0.7)	–	–	–	–	–
	10*	11	1.3 (0.9–2.6)	–	–	–	–	–
	11	189	1.6 (0.3–73.9)	↕ B	↓ B (L **m**)	↓ B	↓ B	↓ ss, cereb
JME	15*	17	0.7 (0.4–5.3)	–	–	–	–	↓ occ **m**, ↕ R BS
	17a*	7	1.4 (1.1–1.6)	–	–	–	–	–
	17b	1	1.4	–	–	–	–	–
	18*	25	1.3 (0.4–3.4)	↑ B (L **m**)	↑ B	–	↑ B	↑ occ, B temp
	19*	4	0.6 (0.6–0.9)	–	–	–	–	–
	20*	7	1.6 (0.7–1.7)	–	–	–	–	–
	21a	60	1.4 (0.4–8.4)	↓ B (L **m**)	↓ B	↓ B	↓ B	↓ BS
	21b	89	1.0 (0.3–5.4)	↑ B	↓ B	↓ R	↓ B	↑ BS **m**
	22*	11	9 (2.4–15.7)	–	↓ B	↓ B (L **m**)	↓ B	–
IGE-GTCS	24*	6	1.1 (0.9–1.7)	–	–	–	–	–
	25a	33	1.6 (0.6–3.9)	–	↓ B	↓ B (L **m**)	↓ B	–
	25b*	24	1.4 (0.6–4.1)	–	↓ B	↓ B (L **m**)	–	–
	26*	5	1.1 (0.7–1.4)	–	–	–	–	–
CAE	32*	17	2.1	↑ B	↓ B	↓ B	↓ B	↑ cereb **m**
SGE	33*	25	1.1 (0.3–2.0)	↕ R	↓ B	↓ B (R **m**)	↓ B	–
	34*	55	13.7 (1.0–82.4)	↑ B	↓ B	B	↓ B (R **m**)	↓ all lobes, cereb, BS, BG
	35*	32	10.9 (1.3–82.4)	↓ B	↓ B (L **m**)	↓ B	↓ B	↓ ss, cereb., temp, BS
	36*	9	7.1 (5.0–12.6)	–	↑ B (R **m**)	↓ B	↓ B	↑ ss, ↓ BS
	37*	78	2.6 (0.6–15.0)	↕ B	↑ B	–	↑ B (L **m**)	↕ occ
	38*	43	5.7 (0.7–12.3)	↑ B (R **m**)	↑ B	↑ B	↑ B	↑ ss, cereb, ↕ BS
	39*	68	6.6 (0.4–39)	↑ B (R **m**)	↑ B	↑ B	↑ B	↑ cereb, temp, BS, BG
	40	3	6.9 (1.9–8.6)	–	–	–	–	–
	41*	46	0.7 (0.3–12.9)	↕ B	↓ B midline (L **m**)	↓ B	↓ B	↓ cereb, ↑ BS, temp, occ
	42*	57	4.1 (1.1–24.6)	–	↓ B	↓ B (R **m**)	↓ B	↓ temp
	43*	46	5.2 (1.1–29.3)	↑ L	↓ B + area of L ↑	↓ B (R **m**)	↓ B	↓ BS

All SPMs corrected for multiple comparisons using random field theory ($P < 0.05$).
Id no.—identification number, corresponds to that in Table 1. (a) and (b) are given for those studied with two sessions.
↑—increase, ↓—decrease, ↕—biphasic, B—bilateral, L—left, R—right, m—global maxima, BG—basal ganglia, BS—brainstem, BG—basal ganglia, cereb—cerebellum, temp—temporal lobes, occ—occipital lobes, ss—sagittal sinus (draining vein), *indicates sessions included in second level group analysis.

Table 9.3.2-2: Summary of results for all sessions during which GSW activity occurred, detailing number and duration of GSW epochs, and regions of significant BOLD signal change labeled in accordance with direction of HRF loading.

Results

Clinical features

See Table 9.3.2-1 for the patients' clinical features. Good quality EEG was obtained following pulse and gradient artifact subtraction, allowing identification of epileptiform discharges (for examples see Figure 9.3.2-1). In 16 sessions (10 patients, marked † in Table 9.3.2-1) no GSW was seen; these sessions were not considered further. Three further patients were excluded due to correlation between head motion and GSW events (marked ‡ in Table 9.3.2-1). The rate of occurrence of GSW events in the

remaining 40 sessions (in 33 patients) varied between 1 and 189 per 35-minute scan session (mean 28, median 11).

Single subject results

Significant BOLD signal changes were seen in 25 patients, (29 sessions, 73% of sessions containing GSW): in thalamus (15 patients), frontal cortex (FC) (23 patients), posterior parietal cortex (PPC)(19 patients) and PCC / precuneus (20 patients), with one or typically more of these areas involved in each case (Table 9.3.2-2). In addition, BOLD change was also seen, to a variable extent in some patients in basal ganglia, cerebellum, brainstem, the sagittal sinus, or all lobes.

Figure 9.3.2-2 shows examples of BOLD response patterns in 3 patients with the different IGE syndromes JME, IGE-GTCS, JAE, and Figure 9.3.2-3 in one case with SGE, illustrating the similarities of the cortical pattern in these distinct syndromes. Negative cortical changes predominated, although positive, and biphasic changes, were also seen (Table 9.3.2-2). BOLD decreases in FC were seen in 14 sessions (8 IGE, 6 SGE), increases in 10 (5 IGE, 5 SGE), and biphasic changes in 2 (IGE), PPC decreases were seen in 17 (11 IGE, 6 SGE), increases in 3 (1 IGE, 2 SGE), and biphasic changes in 1 (SGE), and PCC / precuneus decreases in 15 (8 IGE, 7 SGE), increases in 6 (3 IGE, 3 SGE) and biphasic changes in 1. The signal change in the thalamus was positive in 9 sessions, biphasic in 4 and negative in 3 sessions. In patient 43, with SGE and EEG evidence of left frontal epileptogenicity a small area of frontal activation was seen in addition to a more widespread fronto-parietal cortical negative response (Figure 9.3.2-3).

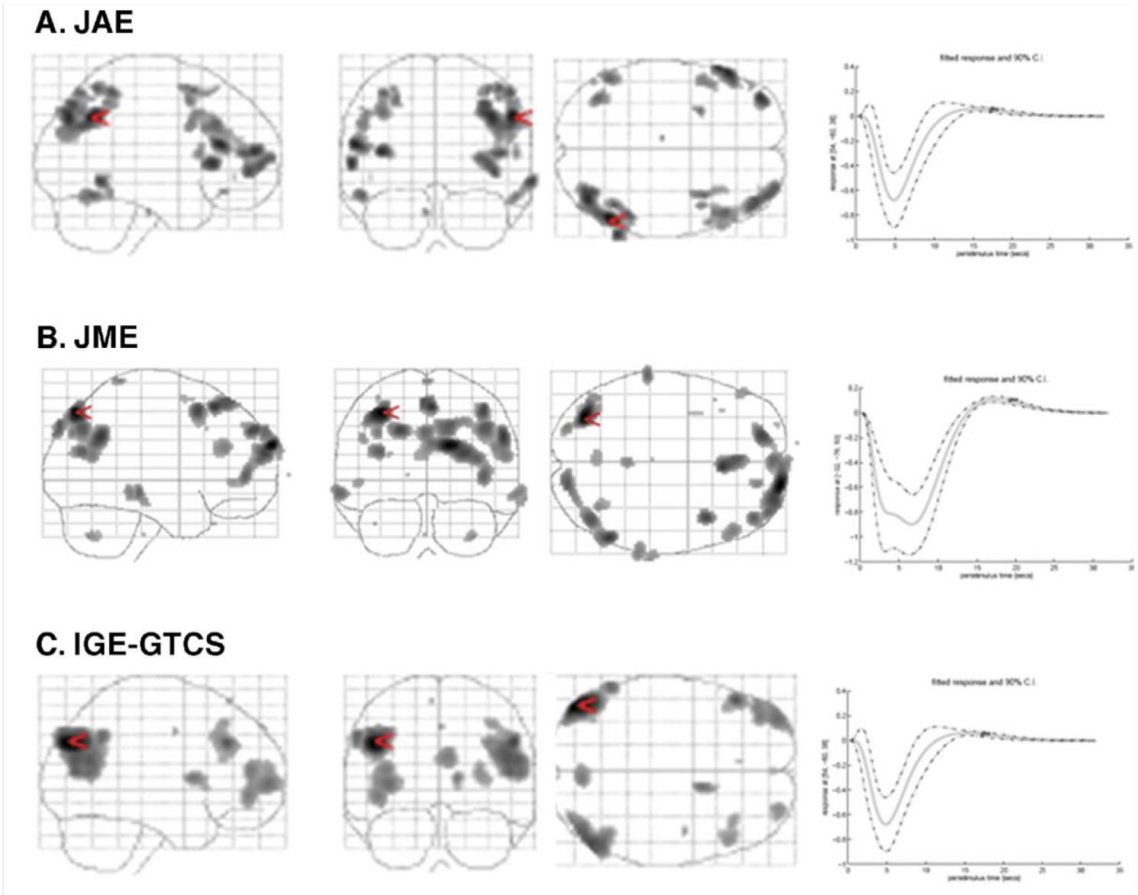

Figure 9.3.2-2: Examples of mean intensity projections from single subject SPM analyses showing cortical signal change with GSW involving symmetrical bifrontal, biparietal, posterior cingulate/precuneus in three patients with different diagnostic syndromes. (A) Patient #10, JAE; (B) patient #22 JME; (C) patient #25 IGEGTCS. The fitted response for each global maximum (marked with red arrow on the SPM) is plotted on the right indicating the peristimulus time course and percent signal change (SPMs corrected, $P < 0.05$).

Group results

Table 9.3.2-3 gives the regions of significant BOLD changes revealed by the group analysis, with coordinates of local maxima and their respective Z score. This shows a group effect of thalamic signal increase in IGE, a biphasic change in SGE, and cortical signal decrease in a characteristic distribution of PPC, PCC / precuneus and FC in the IGE group and medial FC / anterior cingulate increase in the SGE group and biphasic thalamic change in the SGE group. Figure 9.3.2-4 shows the SPM{t} of the HRF for the group analyses of the IGE, illustrating the cortical distribution of signal decrease and the thalamic activation.

Discussion

BOLD signal changes were detected in 73% of sessions, a yield comparable to that previously reported (Aghakhani, Bagshaw et al.). Those with no BOLD response had 7 events or less, all of which were of less than 2 seconds duration (Table 9.3.2-2). The most striking feature of our results is the lack of changes in the primary cortices, except in a few cases, the primary visual cortex. Aghakhani et al (2004) similarly, found the cortical BOLD changes predominantly in a frontal and posterior distribution, similar to those seen here. They highlighted the symmetrical nature of their findings as well as the predominance of negative changes in cortex as seen here. We used a second level random effects group analysis to look for population specific BOLD effects to GSW. Sub threshold signal changes that are not seen at the individual level will become significant if they are present across subjects. Similarly if there is a high degree of variance at a particular voxel then activations that are seen on the individual level will not reach significance at the group level. We chose to show the results for both the individual analyses and the random effects group analysis to demonstrate 1) the degree of intersubject similarity, in different syndromes and variability within the same syndrome, at the individual level, that, at this present time preclude the use of EEG-fMRI as a clinical tool, and 2) population specific effects that allow inferences to be made about neuronal activity during GSW.

Region		*x*, *y*, *z*	Peak *Z*	Weighting on score contrast estimate
A. IGE group analysis				
Parietal				
L	Angular gyrus	−44, −62, 34	5.96	↓
R	Supramarginal gyrus	46, −51, 32	5.86	↓
R	Posterior cingulate	6, −48, 17	5.23	↓
Frontal				
L	Inferior frontal gyrus	−51, 16, 16	4.75	↓
L	Inferior frontal gyrus	−50, 26, −15	4.11	↓
R	Inferior frontal gyrus	53, 35, 7	3.86	
L	Inferior frontal gyrus	−38, 49, 1	3.82	↓
R	Middle frontal gyrus	53, 23, 23	5.47	↓
L	Superior frontal gyrus	−12, 61, 23	3.76	↓
R	Superior frontal gyrus	18, 48, 29	3.59	↓
Temporal				
L	Fusiform gyrus	−51, −34, −20	4.21	↓
R	Middle temporal gyrus	67, −28, −12	4.51	↓
L	Middle temporal gyrus	−46, −52, 3	3.78	
L	Parahippocampal gyrus	−16, −10, −13	3.98	
Subcortical				
L	Caudate	−14, 10, 5	4.68	↓
R	Caudate	10, 8, 5	4.13	↓
R	Thalamus	12, −11, 4	3.67	↑
B. SGE group analysis				
Frontal				
L	Cingulate gyrus	−8, 10, 42	5.56	↑
L	Anterior cingulate	−8, 33, 2	3.94	
L	Inferior frontal gyrus	−50, 5, 27	3.98	
R	Cingulate gyrus	10, 9, 33	3.89	
Subcortical				
L	Thalamus	−14, −15, 4	4.15	
R	Thalamus	10, −15, 3	3.92	

The weighting on the contrast is given to show the direction of BOLD signal change. L, left; R, right; hrf, canonical hemodynamic response; td, temporal derivative.

Table 9.3.2-3: Brain regions that showed significant change on the group analysis.

The selection of patients for this study was necessarily biased to those at the severe end of the spectrum often referred for optimization of medical treatment. Rarely were patients on no medication. Carbemazepine (CBZ) and gabapentin (GBP) are known to increase the amount of GSW in patients with IGE (Kochen, Giagante et al. 2002), however they used if the initial diagnosis is incorrect, or in some improvements in generalized seizures are seen despite the relative contraindication. It is notable that 7 of 34 of our IGE patients with frequent discharges were taking CBZ or GBP at the time of the study. In the other EEG-fMRI studies 4 of 15 were taking CBZ in (Aghakhani *et al.* 2004) and 4 of 5 in (Archer *et al.*2003). The effect of anti epileptic medication on the neurovascular response is not known, although any effect is lessened by the fact that comparisons made here are within sessions. Even with optimal patient selection, the unpredictability and in cases paucity of GSW during scan sessions remains a limitation of EEG-fMRI. Activating procedures such as hyperventilation could be employed but are likely to introduce confounds due to variable effects on cerebral circulation and the BOLD response (Kemna and Posse 2001), whilst photic stimulation, sleep deprivation or drug withdrawal would run the risk of provoking generalized tonic clonic seizures.

The predominant finding in individual subject and group analyses was of thalamic activation and cortical BOLD negative response, consistent with recent EEG-fMRI reports (Archer, Abbott et al. 2003; Salek-Haddadi, Lemieux et al. 2003; Aghakhani, Bagshaw et al. 2004; Laufs, Lengler et al. 2006). Thalamic signal change was seen in less than half of patients with IGE and almost all patients with SGE. This may be due to the greater occurrence of GSW in SGE cases compared to IGE (median SGE 44.5 versus IGE 8), and tended to be seen in those individual IGE cases with a higher number or longer duration of GSW. Primary cortical areas were spared, with changes occurring in frontal, parietal and temporal association areas. At the single subject level similar BOLD responses were seen across IGE syndromes and in SGE, suggesting that the predominant BOLD findings represent generic changes associated with GSW per se rather than syndrome specific patterns. This is unlikely due to syndrome misclassification (Berkovic, Andermann et al.) given the similarity of our findings in cases with very clear syndromic differences (Figure 9.3.2-2, Figure 9.3.2-3).

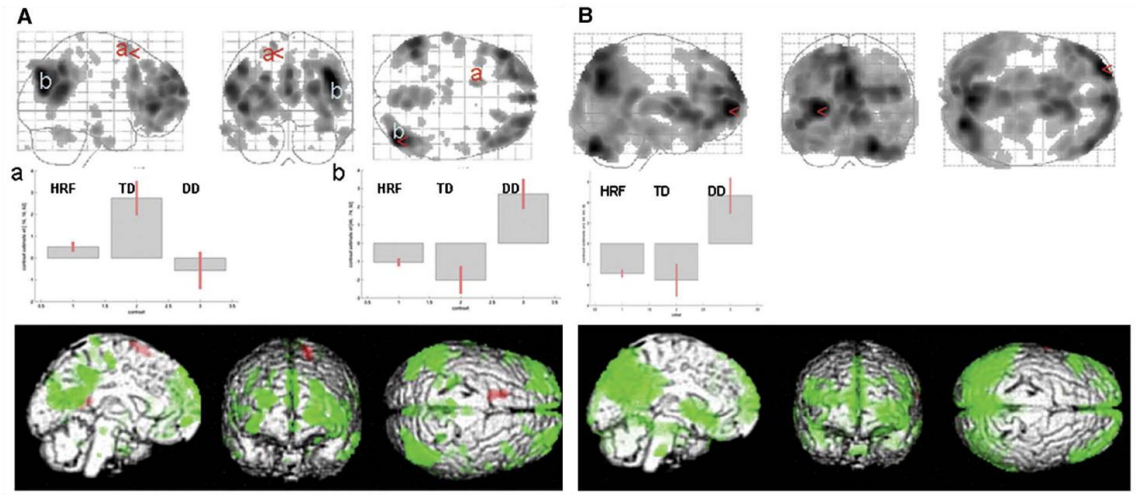

Figure 9.3.2-3: Examples of mean intensity projections SPM{F} from 2 patients with SGE whose EEGs are shown in Figure 9.3.2-1. A color coded overlay of SPM{t} (redactivation and green deactivation) onto the surface render is shown for display purposes and a plot of the weighting on the contrast estimates also shown to indicate the direction of the signal change; both show a similar distribution on negative BOLD to the IGE cases shown in Figure 9.3.2-2, although to a greater extent due to the higher number of events during the scan session. (A) Patient #35 shows widespread cortical deactivation sparing primary cortical areas. (B) Patient #43 illustrates in addition to the negative BOLD changes a small area of left frontal activation concordant with the EEG abnormality.

It is not possible to infer causality of the BOLD changes relative to our modeled covariate, GSW; they may represent areas generating GSW, or alternatively reflect areas secondarily affected by GSW. This difficulty in inferring causality is in contrast to paradigm driven fMRI where it is generally safe to assume a primary association

between the task or stimulus and the observed fMRI changes; in addition a prior hypothesis about a relatively well defined location of expected neural activity usually exits. In GSW however we have little prior anatomical hypothosis regarding the spatial extent of BOLD changes. We propose that thalamic activation seen here represents subcortical activity necessary for the maintenance of GSW (Avoli, Rogawski et al. 2001). The absence of thalamic activation in a number of our cases may reflect low sensitivity of our model at 1.5 T (Laufs, Lengler et al. 2006). The left frontal cortical activation in case 43 (Figure 9.3.2-3 B) requires further validation but likely represent an area of initiation of GSW, given its concordance with the left frontal EEG onset of GSW (Figure 9.3.2-1 d).

The cortical distribution of signal change, FC, PPC and PCC / precuneus, comprises areas of association cortex that are hypothesized, at rest, to be involved in an organized, baseline level of activity, a “default mode” of brain function (Mazoyer, Zago et al. 2001; Raichle, MacLeod et al. 2001). The default mode concept came from observations of consistent deactivations in meta analyses of different task related paradigms in fMRI, in addition to independent PET measurements of increased blood flow to these areas during awake conscious rest (Raichle, MacLeod et al. 2001). Activity in these areas as measured by PET is also altered during sleep, coma and anaesthesia (Laureys, Owen et al. 2004). Default mode areas likely represent part of a neural network subserving human awareness. Our study and others (Archer, Abbott et al. 2003; Aghakhani, Bagshaw et al. 2004; Laufs, Lengler et al. 2006) show alteration of activity in these regions during GSW, which would be consistent with the clinical manifestation of absence seizures. These findings are also consistent with PET findings of opioid release in association neocortex, most marked in parietal cortex and posterior cingulate, following absence seizures (Bartenstein, Duncan et al. 1993).

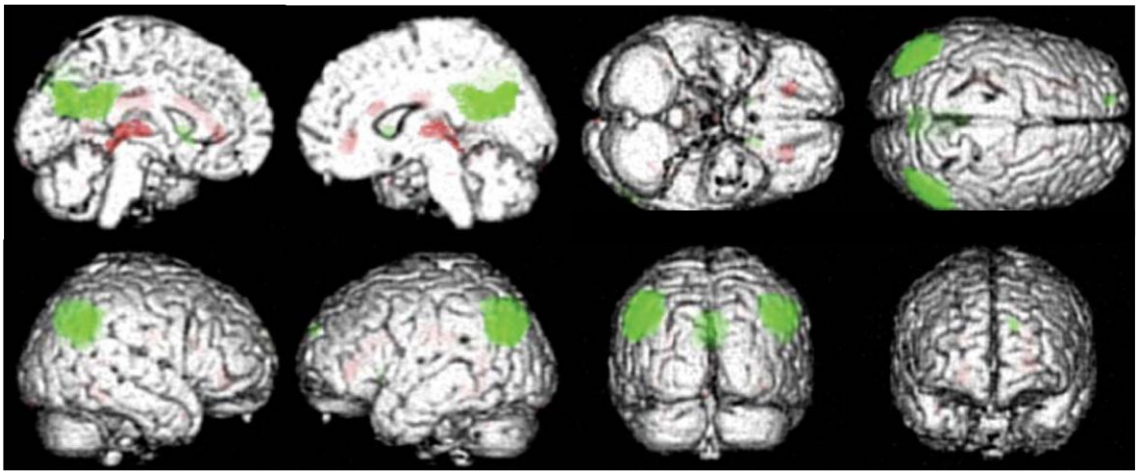

Figure 9.3.2-4: SPM{t} overlaid onto canonical brain of positive HRF (red) and negative HRF (green) (uncorrected P < 0.001) illustrating the thalamic and cortical distribution of BOLD changes to GSW in the IGE group analysis. This shows bilateral parietal (46, -51, 32), (-44, -62, 34) and posterior cingulate/precuneus (6, -48, 17) deactivation and thalamic activation (12, -11, 4); the activation around the ventricles, we suspect is due to modelled changes in CSF pulsation as a result of the widespread hemodynamic changes occurring during GSW.

The majority of cortical BOLD responses were negative (Table 9.3.2-2), in keeping with other fMRI (Salek-Haddadi, Lemieux et al. 2003; Aghakhani, Bagshaw et al. 2004; Laufs, Lengler et al. 2006) as well as transcranial Doppler (TCD) (Sanada, Murakami et al. 1988; Klingelhofer, Bischoff et al. 1991; Bode 1992; De Simone, Silvestrini et al. 1998; Diehl, Knecht et al. 1998) and near infrared spectroscopy studies (Haginoya, Munakata et al. 2002; Buchheim, Obrig et al. 2004). A number of lines of evidence suggest that BOLD negative responses represent a reduction in neural activity. In visual cortex, a reduction of BOLD signal, elicited by stimulating part of the visual field is due, primarily, to a reduction of neuronal activity (Shmuel, Augath et al. 2006). A decrease in BOLD signal is seen in the occipital cortex during auditory induced saccades (Wenzel, Wobst et al. 2000), a manipulation known to suppress neuronal activity (Duffy and Burchfiel 1975). BOLD decreases have also been observed in the context of neuronal synchronization, modulated by sub-cortical structures (Parkes, Fries et al. 2004). Visual stimulation during sleep leads to occipital BOLD negative responses, confirmed as a decrease in rCBF with $H_2{}^{15}O$ PET (Born, Law et al. 2002). Similarly auditory BOLD negative responses occur on auditory stimulation during sleep, the amplitude and extent of which correlate positively with measures of EEG synchronization in sleep (Czisch, Wetter et al. 2002; Czisch, Wehrle et al. 2004; Czisch, Wehrle et al. 2009).

Although the majority of our cases showed cortical negative response a number of cases showed activation or biphasic time courses in the same areas. These did not

differ significantly (2-sample t-tests, all $p > 0.8$) from those with negative response in terms of the frequency of GSW, the number of events, their median duration or total duration during the scan session. Nevertheless activations were seen in a greater proportion of SGE than IGE patients. This would explain the absence of widespread cortical change in the SGE group analysis, where positive signal changes in some subjects and negative in others in the same region lead to a loss of this effect at the group level.

Our cases of cortical activation are compatible with the findings of others; cortical increases were seen in some cases with fMRI (Aghakhani, Bagshaw et al. 2004) and in TCD an initial increase was seen prior to the more prolonged decrease (De Simone, Silvestrini et al. 1998; Diehl, Knecht et al. 1998). Similarly, SPECT and PET showed increases as well as decreases in cortical activity to spike wave (Engel, Lubens et al. 1985; Theodore, Brooks et al. 1985; Ochs, Gloor et al. 1987; Prevett, Duncan et al. 1995; Yeni, Kabasakal et al. 2000). The terms “activation” and “deactivation” are operational terms that reflect measured vascular or metabolic responses from which inferences about neuronal activity are made, we have preferred to use the term negative BOLD response rather than deactivation as the neural correlates of these responses aren’t yet clear. The terms have their origins in the field of PET (Friston, Frith et al. 1990), in which measures are quantitative and more direct. In fMRI the modeling of signal changes is relative, i.e. a comparison between two states (Bandettini, Wong et al. 1992). Given that 1) we, and others (Salek-Haddadi, Lemieux et al. 2003; Aghakhani, Bagshaw et al. 2004) model GSW against an implicit baseline, i.e. active (GSW) against rest (background resting state activity), and 2) we detect changes in areas of association cortex, then the level of arousal or sleep reflecting resting state activity in these regions may affect the direction of detected BOLD signal changes. A negative response is therefore seen where there is a decrease or interruption of awake resting state activity; if however the patient is drowsy or asleep activity in these areas may be lower than that engendered by GSW thus giving rise to activations. Future studies of GSW with EEG-fMRI need to take this into account, by modeling the background EEG in more detail or presenting the subject with a low grade task designed to maintain and monitor a constant level of vigilance.

Conclusion

In conclusion, we have shown that the main BOLD fMRI correlates of GSW consist of widespread cortical negative response in areas associated with normal brain activity during conscious rest. These likely reflect a decrease in neural activity, as a result of either synchronization or inhibition of cortical activity due to thalamo-cortical interactions. This is in keeping with the clinical features of absence seizures, i.e. a brief alteration of consciousness with minimal somatosensory or motor manifestations.

9.3.3 Temporal lobe interictal epileptic discharges affect cerebral activity in "default mode" brain regions[5]

Abstract

A cerebral network comprising precuneus, medial frontal and temporo-parietal cortices is less active both during goal-directed behaviour and states of reduced consciousness than during conscious rest. We tested the hypothesis that interictal epileptic discharges affect activity in these brain regions in patients with temporal lobe epilepsy who have complex partial seizures. At the group level, using electroencephalography-correlated functional magnetic resonance imaging in 19 consecutive patients with focal epilepsy, we found common decreases of resting state activity in nine patients with temporal lobe epilepsy (TLE) but not in ten patients with extra-TLE. We infer that the functional consequences of TLE interictal epileptic discharges are different from those in extra-TLE and affect ongoing brain function.

Activity increases were detected in the ipsilateral hippocampus in patients with TLE, and in sub-thalamic, bilateral superior temporal and medial frontal brain regions in patients with extra-TLE, possibly indicating effects of different interictal epileptic discharge propagation.

Introduction

Simultaneous electroencephalography (EEG) and functional magnetic resonance imaging (fMRI) has been used in individual patients to map the brain areas involved in interictal epileptic discharges (IED) (Salek-Haddadi, Friston et al. 2003) and in particular the area giving rise to the discharge - the 'irritative zone' (Rosenow and Luders 2001). In addition however, EEG-fMRI allows the impact of epileptic discharges on ongoing brain function to be assessed (Gotman, Grova et al. 2005; Laufs, Lengler et al. 2006) and the effects of epileptic activity across different patient groups to be studied (Hamandi, Salek-Haddadi et al. 2006).

[5] Own contributions: study design, data analysis, result interpretation, manuscript preparation; Laufs, H., K. Hamandi, et al. (2007). "Temporal lobe interictal epileptic discharges affect cerebral activity in "default mode" brain regions." Human Brain Mapping **28**(10): 1023-1032..

Brain areas preferentially active on functional imaging during conscious rest include the precuneus and posterior cingulate, bilateral temporo-parietal and medial prefrontal cortices (Shulman, Fiez et al. 1997; Mazoyer, Zago et al. 2001; Raichle, MacLeod et al. 2001). This network expresses strong functional connectivity at rest (Greicius, Krasnow et al. 2003; Laufs, Krakow et al. 2003) and has higher overall activity during resting wakefulness than in states of impaired consciousness such as sleep, anaesthesia and coma (Laureys, Owen et al. 2004) or during generalized spike and wave discharges (GSW) (Archer, Abbott et al. 2003; Gotman, Grova et al. 2005; Hamandi, Salek-Haddadi et al. 2006; Laufs, Lengler et al. 2006). Activity in these regions also decreases during a wide range of cognitive tasks (Mazoyer, Zago et al. 2001; Raichle, MacLeod et al. 2001) and this observation of "task-independent deactivation" has led to the proposal that activity in these structures serves as a 'default mode' of brain function that predominates whenever subjects are awake, but not performing any explicit task (Raichle, MacLeod et al. 2001).

Functional connectivity in the default mode network has been shown to be affected in patients with Alzheimer's disease (Greicius, Srivastava et al. 2004), and temporal lobe connectivity in particular (Wang, Zang et al. 2006). Recently, spontaneous alteration of functional connectivity between language areas was also demonstrated in patients with temporal lobe epilepsy (TLE) (Waites, Briellmann et al. 2006).

We sought to test the hypothesis that IED occuring during the resting state would result in a relative BOLD signal decrease in default mode brain areas. In patients lying at rest with their eyes closed in the scanner we expect the default mode network to be active. Interruption of resting state activity as a direct consequence of IED should then result in a relative decrease in BOLD signal within the default mode areas. Aside from testing this hypothesis we also set out to explore any BOLD signal increases common to the group, as these may reveal underlying networks not detectable at the individual level. We investigate the effects of IED in two groups of patients with focal epilepsy, namely with TLE and extra-TLE.

Material and Methods

Patients

63 patients with focal epilepsy underwent EEG-fMRI (Salek-Haddadi, Diehl et al. 2006). Of those, we selected all scanning sessions with a spiking rate of between one and twenty IED per minute during data acquisition, corresponding to the mid-range level of activity in the group. This selection was necessary to facilitate a balanced design for the purpose of group analysis (Friston, Stephan et al. 2005). All patients gave written informed consent (Joint Ethics Committee of the National Hospital for Neurology and Neurosurgery and Institute of Neurology). Clinical and experimental details are listed in Table 9.3.3-1.

Case	Number of IED during 35 min fMRI	Description of clinical EEG		Clinical localization	Seizure type	Structural MRI	Etiology	Epilepsy syndrome	
		Ictal	Interictal					TLE	xTLE
1	404	No lateralization	L Ant Temp Sp	L Temp	SPS (epigastric), CPS,	L-HS	L-HS	X	
2	638	No lateralization	L Ant Temp Sp	L Temp	SPS, CPS, SGTCS	L-HS	L-HS	X	
3	630	No clear change	L Ant Temp Sp	L Temp	CPS, SGTCS	L hippocampal, parahippocampal and amygdala mass	glioma	X	
4	72	Independent R and L seizure onsets	L Ant mid-Temp SW	Temp, uncertain laterality	CPS	L-HS	L-HS	X	
5	45	Subdural electrodes: seizure onset outside of the resected areas, possibly contralateral	Widespread theta, frequent Temp shW, and redominantly L mid Temp Sp	L Temp	CPS, SGTCS	L Temp lobe resection	Post L Temp lobe resection for DNET, plus R-HS	X	
6	58	Initially bilateral theta, then left sided rhythmic shWs	L Temp slow waves, and Sp plus R Temp Sp during sleep	Temp	CPS, SGTCS	MRI negative	Cryptogenic	X	
7	190	–	L Temp slowing with frequent L Ant Temp Sp	L Lateralised	SGTCS	MRI negative	Post-traumatic	X	
8	79	L hemisphere	L Temp slow and shWs	L Temp	CPS	L-HS	L-HS	X	
9	166	No clear lateralisation	L slow activity, Bil SW, pSpW, L Temp Sp	Diffuse	CPS, SGTCS	Focal lesion L middle Temp gyrus, L Temp lobe smaller than R	DNET	X	
10	82	–	Widespread, R Sp, shW, and sharp and slow waves maximal frontocentral	R Lateralised	SPS (motor)	Diffuse cortical thickening R hemisphere, within Par and Occ lobes, extending to frontal region	MCD		X
11	50	No clear changes	Bil, Post Temp/Occ sharp and slow wave complexes with L Sp	Bilateral	CPS, SGTCS	Widespread band and subcortical nodular heterotopia, predominantly posterior	MCD	X	
12	230	–	L slow activity with L Post Temp Sp	L Lateralised	CPS, SGTCS	L cystic encephalomalacia	Perinatal subarachnoid haemorrhage	X	
13	73	–	Over central region Bil SW	R Frontal	SPS (focal motor), SGTCS	R parietal open leptoschizencephaly	MCD	X	
14	477	No change	Continuous L Par Sp	L Parietal	SPS (sensory)	Thickened cortex in the L Ant-inferior Par region just extending into the inferior Front gyrus (FCD)	MCD	X	
15	97	–	L Sp, shW, and slow waves, some Bil synchronous and occasionally R-sided	Diffuse	CPS, SGTCS	Extensive polymicrogyria involving both hemispheres, R > L	MCD	X	
16	103	Bilateral onset	L and Bil Front shWs (R > L), and occasional L Temp Sp	Uncertain	CPS (extra-temporal semiology), SGTCS	MRI negative	Cryptogenic	X	
17	198	–	R pSp and slow wave discharges, single and bursts, maximal centro-Temp	R Frontal	CPS, SGTCS	R middle Front gyrus cortical scar	Post- traumatic	X	
18	483	Widespread over left hemisphere	L mid-Temp SW	L Cent-Temp	SPS (focal motor), CPS, SGTCS	Mild atrophy of L cerebral hemisphere	Chronic encephalitis	X	
19	371	Widespread over L hemisphere	L front Sp	L Front	SPS, CPS	Focal scarring of L middle Front gyrus	Low-grade astrocytoma (post surgery and radiotherapy)	X	

shW: sharp wave; SW: spike and wave; Sp: spikes; pSp: poly spikes; pSpW: poly SW; Temp: temporal; Par: parietal; Occ: occipital; Front: frontal; R: right; L: left; Bil: bilateral; Cent: central, Mid: midline; CPS: Complex partial seizure; SGTCS: Secondarily generalized tonic-clonic seizure; SPS: Simple partial seizure; DNET: Dysembryoblastic neuro-epithelial tumour; FCD: Focal cortical dysplasia; HS: Hippocampal sclerosis; MCD: Malformation of cortical development; Ant: Anterior; Post: Posterior; TLE: temporal lobe epilepsy; xTLE: extra temporal lobe epilepsy; "–" data not available.

Table 9.3.3-1: Experimental, electroclinical, and imaging patient details

Simultaneous acquisition of EEG and fMRI

The methods and results pertaining to single-subject analyses are reported elsewhere (Salek-Haddadi, Diehl et al. 2006). Briefly, using MR-compatible equipment, ten EEG

channels were recorded at Fp1/Fp2, F7/F8, T3/T4, T5/T6, O1/O2, Fz (ground) and Pz as the reference (10-20 system), and bipolar electrocardiogram (Krakow, Allen et al. 2000). Seven hundred and four T_2*-weighted single-shot gradient-echo echo-planar images (EPI; TE/TR 40/3000, flip angle: 90º, 21 5 mm interleaved slices, FOV=24 x 24 cm^2, 64^2 matrix) were acquired continuously over 35 minutes on a 1.5 Tesla Horizon EchoSpeed MRI scanner (General Electric, Milwaukee, USA). Patients were asked to rest with their eyes shut and to keep their head still. After gradient and pulse artifact reduction (Allen, Polizzi et al. 1998; Allen, Josephs et al. 2000), IED were individually identified and the fMRI data were pre-processed and analyzed using SPM2 (http://www.fil.ion.ucl.ac.uk/spm/). After discarding the first four image volumes, the EPI time series were realigned, normalized (MNI305 space, SPM2) and the images spatially smoothed with a cubic Gaussian Kernel of 8 mm full width at half maximum.

Brain region of interest	Brodmann area (BA)	Center of region of interest (mm)			Z-score	*P* value
		X	*Y*	*Z*		
9 patients with TLE						
Precuneus	BA 7	−5	−49	40	2.9	0.030
Posterior Cingulate	BA 31	1	−35	34	2.7	0.048
Frontal Gyrus, left	BA 8/9	−11	41	42	2.0	0.135
Frontal Gyrus, right	BA 8/9	5	49	36	2.7	0.043
Inferior Parietal Lobule, left	BA 40	−53	−39	42	2.7	0.047
Inferior Parietal Lobule, right	BA 40	45	−57	34	2.0	0.144(1)
(1)	BA 40	56	−48	40	2.7	0.049
10 patients with extra-TLE						
No deactivations found in regions of interest nor across the whole brain at $P < 0.001$ uncorrected for multiple comparisons						

Table 9.3.3-2: Blood oxygen level-dependent signal decreases in regions of interest in 9 patients with temporal lobe epilepsy (TLE) and respective findings in 10 patients with extra-TLE. Results of region of interest analyses (random effects group analyses). Z-scores are reported for activations within spherical search volumes (1 cm in diameter) centered at coordinates taken from (Shulman, et al. 1997); P values are corrected for multiple comparisons within these volumes. Note that although the activation in the region of interest positioned in the right inferior parietal volume did not reach significance, a nearby area of activation did (indicated by (1)). All coordinates are given in Talairach space, converted from Montre´al Neurological Institute space using mni2tal (http://imaging.mrc-cbu.cam.ac.uk/imaging/MniTalairach).

Statistical parametric mapping

IED onsets were used to build a linear model of the effects of interest by convolution with a canonical hemodynamic response function (HRF, event-related design) and its temporal derivative to account for possible variations in the blood oxygen level-dependent (BOLD) response delay. Motion realignment parameters were modelled as a confound (Friston, Williams et al. 1996).

A single T-contrast image was generated per subject from the first (single-subject) level and the images used to inform a second level (group effect) analysis to test for any

common patterns. Analyses were performed for both TLE and extra-TLE groups. A random effects model was used to identify any *typical* responses consistent across the patients (Friston, Holmes et al. 1999) We used this approach to test the hypothesis that *negative* responses arose in one or more of the default mode areas: precuneus, posterior cingulate, frontal, and inferior parietal cortices bilaterally. For this purpose, regions of interest were defined as spheres with 1 cm in diameter centered on coordinates given in Table 9.3.3-2, taken from (Shulman, Fiez et al. 1997; Raichle, MacLeod et al. 2001). The statistical images were thresholded at $P < 0.05$ (family wise error-corrected for multiple comparisons within the search volume). Any *positive* responses were further explored at a threshold of $P<0.001$ (uncorrected at the single voxel level), and declared significant at $P<0.05$ (corrected for multiple comparisons at the cluster level) as we were not testing a specific hypothesis.

Results

Common IED-related deactivations in default mode areas in TLE but not in extra-TLE

Based on the inclusion criteria for group analysis, 19 scanning sessions were analysed. They were divided into two groups: one group with TLE (n=9) and one with extra-TLE (n=10). The TLE group as a whole showed significant IED-related deactivation in the posterior cingulate, the precuneus, the left and right frontal and parietal lobes (Figure 9.3.1-1,Table 9.3.3-2). The extra-TLE group did not show any significant IED-related deactivations (Figure 9.3.3-2). There was no statistically significant difference between the two groups in terms of the number of IED during fMRI (P=0.48, T-test).

Brain region, cluster maxima (>8 mm apart)			Talairach coordinates (mm)			Z-score
			x	*y*	*z*	
9 patients with TLE						
Left	Cerebrum	Hippocampus	−26	−35	−1	3.7*
Left	Cerebrum	Parahippocampal gyrus	−26	−11	−25	3.7*
10 patients with extra-TLE						
Left	Cerebrum	Superior Temporal Gyrus	−48	4	−6	3.9
Right	Cerebrum	Medial Frontal Gyrus Lobe	2	−8	52	3.7
Right	Cerebrum	Anterior Cingulate	10	26	−6	3.4
Left	Midbrain	Subthalamic nucleus	−2	−16	−6	3.3
Right	Cerebrum	Superior Temporal Gyrus	64	−8	0	3.4
Right	Cerebrum	Middle Temporal Gyrus	56	−8	−6	3.2
Right	Cerebrum	Postcentral Gyrus	8	−40	66	3.1

Table 9.3.3-3: Common blood oxygen level-dependent signal increases in 9 patients with temporal lobe epilepsy (TLE) and respective findings in 10 patients with extra-TLE. Results of explorative ($P < 0.001$ uncorrected for multiple comparisons) random effects group analyses. Main cluster grey matter coordinates are given as Talairach coordinates (compare Table II) and automatically labelled using Talairach Daemon V1.1 (Research Imaging Center, University of Texas Health Science Center at San Antonio). Z-scores are reported for local voxel maxima (extent threshold: 15 voxels). *$P < 0.05$ corrected for multiple comparisons.

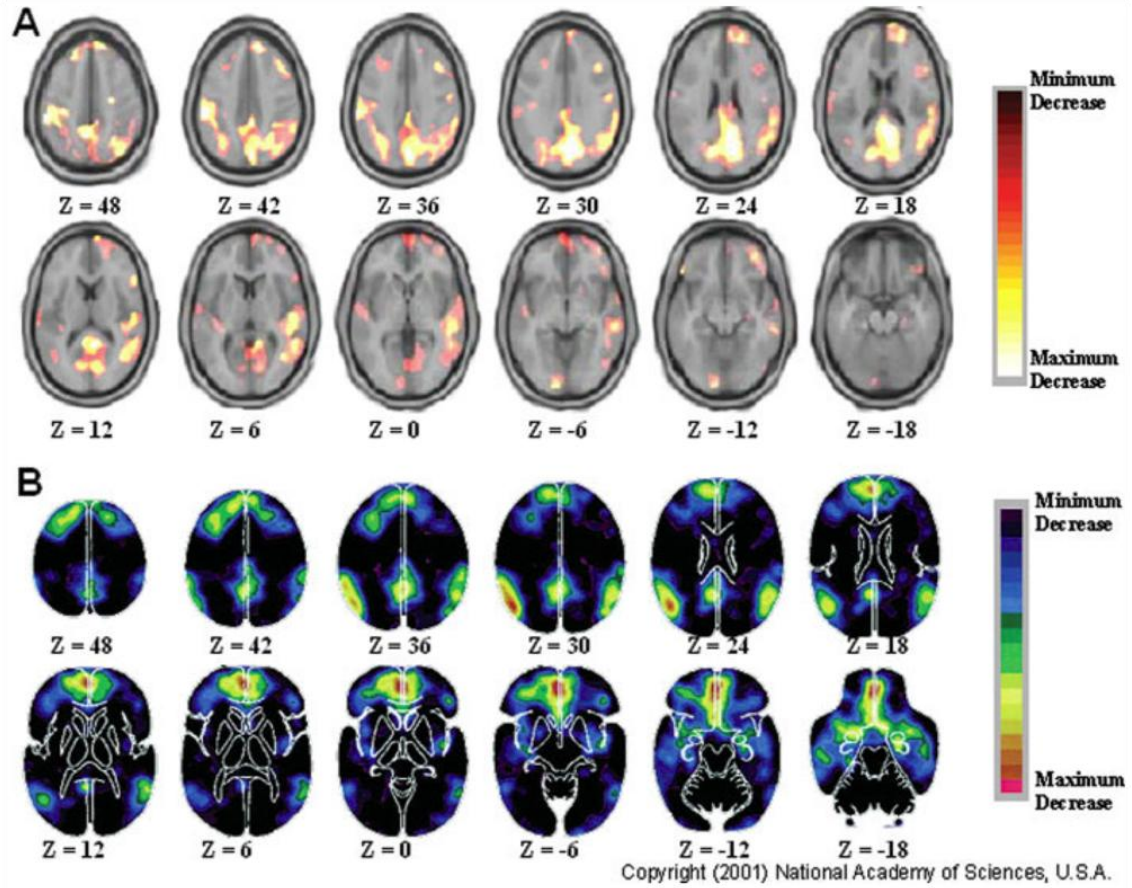

Figure 9.3.3-1: Random effects group analysis blood oxygen level-dependent signal decreases in temporal lobe epilepsy with focal interictal epileptic discharges (IED) in comparison with classic ''default mode'' brain regions. A: Brain areas where blood oxygen level-dependent signal is significantly negatively correlated with IED are projected onto axial slices (Z coordinates given below each slice) of a template average brain. B: Corresponding display of brain regions to which the term ''default mode'' was originally applied. Taken from (Raichle, MacLeod et al. 2001). Note that despite spatial normalization there is slight anatomical discrepancy between slices displayed in panel A versus panel B.

Common IED-related activations specific to TLE and extra-TL

All 9 TLE patients had left-sided IED (some bilateral and one additional diffuse IED, see Table 9.3.3-1). We looked for common activations across this group of patients and found significant positive IED-related BOLD signal changes in the left anterior medial temporal lobe (Figure 9.3.3-2, Table 9.3.3-3). The same analysis for the heterogeneous group of patients with extra-TLE showed common activations in the left subthalamic nucleus, superior temporal gyrus bilaterally, right middle temporal gyrus, medial frontal gyrus bilaterally, anterior cingulate and the right postcentral gyrus (Figure 9.3.3-3, Table 9.3.3-3).

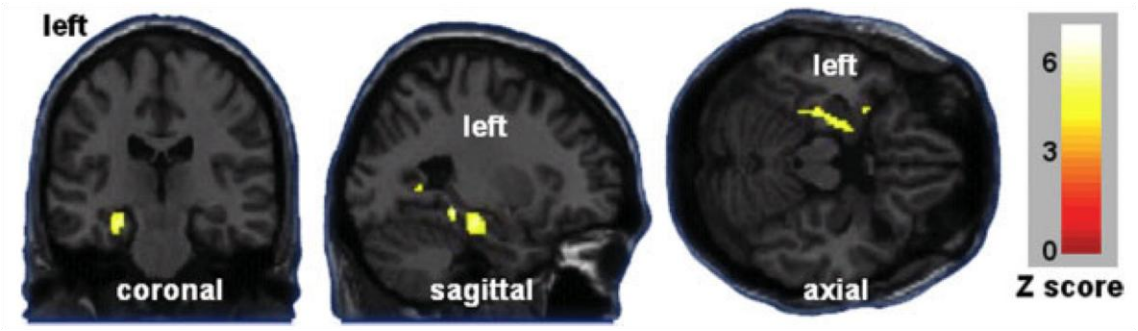

Figure 9.3.3-2: Statistical parametric maps of a random effects group analysis of 9 patients with temporal lobe epilepsy. Brain areas where blood oxygen level-dependent signal is significantly ($P < 0.001$) positively correlated with interictal epileptic discharges are overlaid onto a T1-weighted anatomical brain template (slice planes [x,y,z] = [-26, -35,1]).

Complex versus simple partial seizures

Activity in default-mode brain regions is correlated with consciousness (Laureys, Owen et al. 2004) and so we looked at the differences in habitual seizure-types between these groups. We found that simple partial seizures (SPS) were more frequent in the patients with extra-TLE (5/10 patients) and were the single focal seizure type in three of them. Only three of nine patients with TLE had SPS, and these always occurred in addition to complex partial seizures (CPS).

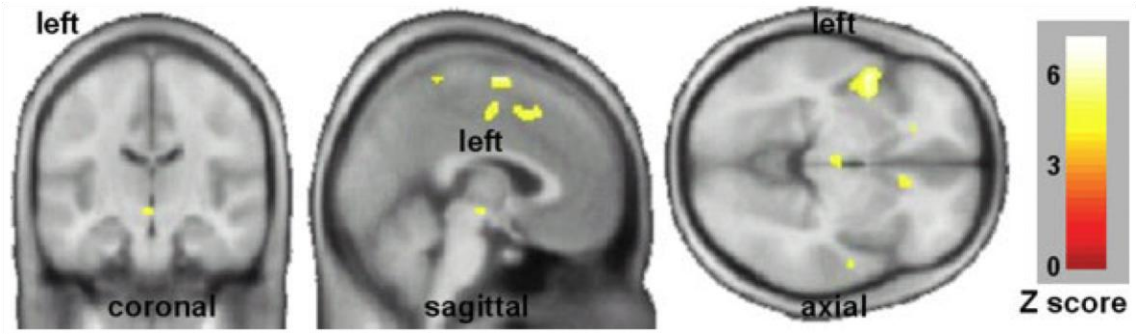

Figure 9.3.3-3: Statistical parametric maps of a random effects group analysis of 10 patients with extratemporal lobe epilepsy. Brain areas where blood oxygen level-dependent signal is significantly ($P < 0.001$) positively correlated with interictal epileptic discharges are overlaid onto an average T1-weighted anatomical brain template (slice planes [x,y,z] = [-2, -16, -6]—note different slice planes compared with Figure 9.3.3-2 despite analogous format of display).

Aetiology

Apart from localization, aetiology was assessed as a possible explanatory variable accounting for the differing BOLD response patterns. We found hippocampal sclerosis to be the prevalent pathology in the TLE group (five of nine patients), whilst malformations of cortical development (MCD) were the prominent pathology in the extra-TLE group (five of the ten patients, Table 9.3.3-1).

Discussion

Principal findings

In patients with TLE, IED were associated with significant deactivation in default mode brain areas and with significant activation in the ipsilateral medial temporal lobe. In the patients with extra-TLE no significant deactivations were found; and there were activations in the sub-thalamic nucleus, the superior aspects of both temporal, and medial frontal lobes. The findings indicate that deactivations in default mode brain regions are characteristic of IED in TLE whilst not seen in extra-TLE, and that different common activation patterns were seen in the two groups.

Methodological considerations

EEG-fMRI can be used to investigate the electrical and haemodynamic aspects of brain activity changes during task-free rest such as those associated with individual IED. To facilitate inter-subject comparison we restricted our analyses to experiments with 1-20 IED per minute. This enabled us to make valid inferences at the group level using a two-stage procedure but restricted the group size to 19 patients (Friston, Stephan et al. 2005).

Violations of homoscedasticity implicit in the loss of balance at the first level can make the second level inference less efficient, but would not bias or invalidate it. A full mixed-effects analysis could improve the power of the inference but this is not necessary because we already have significant results using the more conservative summary-statistic approach (Penny and Holmes 2006).

The distributed and distinct areas of the brain involved in default mode activity were originally identified by positron emission tomography and fMRI meta analyses that included studies with block designs (Gusnard and Raichle 2001). Stimulus-correlated motion and circulation or respiration effects are thus unlikely to cause the observed signal changes. Nevertheless we took the precaution of modelling realignment parameters reflecting motion as a potential confound. Likewise, the signal changes observed during resting state brain activity do not originate from the aliasing of physiological noise (De Luca, Beckmann et al. 2006).

A group analysis emphasizes features common to all group members while supressing the individual variability at the same time. Such an approach will be less sensitive to IED-correlated BOLD signal changes reflecting potentially different irritative zones but will rather indicate common pathways of IED propagation or their associated effects on ongoing brain function, that fail to reach statistical significance at the single subject level. A group analysis will therefore highlight common features ("typical effects") for a group of patients investigated.

Previous work

Deactivations in relation to IED were found in default mode brain areas in 10 of a series of 60 analyzed scanning sessions, mostly associated with bilateral or generalised bursts of spikes (Kobayashi, Bagshaw et al. 2005). IED localization however was not further specified nor a group analysis performed. Meanwhile, the same group has recently also found ipsilateral medial temporal activation in a group of patients with temporal lobe IED (Grova, Kobayashi et al. 2006).

Using Single Photon Emission Computed Tomography (SPECT), Van Paesschen and co-workers described significant *ictal* hypoperfusion in the superior frontal gyrus and the precuneus in 90% of TLE patients with complex partial seizures studied, plus hypoperfusion in temporal, occipital and cerebellar regions (Van Paesschen, Dupont et al. 2003). Blumenfeld et al. using EEG-SPECT found that temporal lobe seizure-related loss of consciousness was associated with bilateral decreases in cerebral blood flow in the frontal and parietal association cortex and retrosplenium. In contrast however, when consciousness was preserved, such widespread changes were not seen (Blumenfeld, McNally et al. 2004). The distribution of these ictal perfusion decreases is consistent with our interictal findings in those with TLE who mainly had CPS. Although failure to detect deactivations in default mode brain areas in those with extra-TLE does translate to their absence, it does suggest that IED do not influence brain function in this network to the degree IED do in TLE.

IED propagation affects default mode network in TLE

In TLE, epileptic activity may spread from the temporal lobe into one or more functionally interconnected default mode brain regions and the effect of propagated activity can be measured by fMRI. Epileptic networks can lead to widespread secondary inhibition of non-seizing cortical regions via subcortical structures (Norden and Blumenfeld, 2002). It has previously been reported that - even very short (Laufs, Lengler et al. 2006) - GSW were associated with deactivations in default mode brain regions (Salek-Haddadi, Lemieux et al. 2003; Gotman, Grova et al. 2005; Hamandi, Salek-Haddadi et al. 2006; Laufs, Lengler et al. 2006).

Alarcon and colleagues proposed that in TLE a lesion may affect remote, functionally coupled normal brain regions and that IED may originate from separate regions, resulting in propagation to and recruitment of other neuronal assemblies (Alarcon, Garcia Seoane et al. 1997). Indeed Ebersole and colleagues suggested that scalp EEG changes in TLE principally reflect propagated epileptic activity (Pacia and Ebersole 1997). The current study supports the notion that temporal lobe IED affect an epileptic network rather than a circumscribed focus. Further, it may be inferred that the medial anterior temporal lobe structures are a crucial part of such a network in this group of patients with TLE, who had a variety of underlying pathologies at varying locations within the temporal lobe.

The (left) temporal lobe and the default mode brain network

Functional connectivity studies have identified the temporal lobe (Fox, Snyder et al. 2005; Fransson 2005), and more specifically the hippocampus (Greicius and Menon 2004) as another part of the default mode network. Activity changes in the default mode network could thus be a consequence of IED-effects on the functionally connected hippocampus, or – as was demonstrated in the case of Alzheimer's disease (Wang, Zang et al. 2006) – the result of disturbed functional connectivity between the hippocampus and other default mode regions. In patients with left TLE, Waites and colleagues have recently demonstrated that functional connectivity in the 'language network' was disturbed (Waites, Briellmann et al. 2006). As our subjects all had left-biased IED, we could not investigate laterality influences on default mode activity. This would be interesting especially since verb generation tasks, for example, lead to left-

lateralized temporal lobe activations (Rowan, Liegeois et al. 2004) and classically deactivate default mode brain regions (Burton, Snyder et al. 2004).

Our findings do not address the issue of causality, but indicate a correlation between IED in TLE and default mode network fluctuations. A hypothetical alternative explanation is that alteration of the default mode (e.g. by an external cause) facilitates IED. In the case of GSW, a link with sleep spindles and arousal has already been demonstrated (Steriade 2005).

An analogy between the thalamus in GSW and the hippocampus in TLE

The hippocampus plays a central role in propagation of epileptic activity in TLE, and hippocampal sclerosis often accompanies different pathologies in the temporal lobe (Duncan and Sagar 1987; Thom, Zhou et al. 2005). An analogy could be drawn between the role of the thalamus in the propagation of GSW and the role of the hippocampus in the propagation of IED in TLE, with both resulting in antidromic deactivation of default mode brain regions.

Similarly, the activations seen in association with IED in the extra-TLE group suggest a different 'propagation network' consisting of sub-thalamic nuclei, superior temporal lobe and medial frontal structures (Table 9.3.3-2). This group however was more heterogeneous and this possibility remains speculative until a higher number and more defined groups of epilepsy syndromes have been studied.

Lack of default mode deactivation in extra-temporal lobe epilepsy

Possible reasons for the lack of deactivations associated with IED in extra-TLE need consideration. These include a lack of sensitivity and the failure of scalp EEG to detect deep IED. Extra-temporal IED propagation might not occur so readily and so may not have distant effects: Blume at al. showed that interictal activity in extra-TLE mainly remains within the lobe of origin (Blume, Ociepa et al. 2001).

As much as propagation of IED might depend on the lobe of origin, it may also be a function of underlying pathology. In this series, MCD was the prominent pathology in

the extra-TLE group, and their patho-neurophysiology will be different to that of hippocampal sclerosis, for example. Further EEG-fMRI studies of patients with MCD and those with acquired lesions in temporal and extra-temporal lobes are needed to resolve this issue.

IED location-independent deactivation of the default mode brain areas

Our data suggest that activation of an epileptic network associated with TLE-IED is associated with deactivation of the cerebral areas that are active during conscious rest, in the same way as deactivation occurs consequent to a cognitive activation paradigm (Gusnard and Raichle 2001). Our results suggest that default mode brain areas deactivate irrespective of the IED location within the temporal lobe. Such decreases are therefore not epilepsy-specific, but may instead reflect an alteration of the mental state, in particular consciousness (Salek-Haddadi, Lemieux et al. 2003; Gotman, Grova et al. 2005; Laufs, Lengler et al. 2006). In focal epilepsy, fMRI *deactivations* have been found to correlate less with spike location and generally occur later than activations (Bagshaw, Aghakhani et al. 2004; Aghakhani, Kobayashi et al. 2005) and may thus reflect such 'downstream' cognitive effects. In contrast, the *activations* we found in TLE are closer to the spike origin (Salek-Haddadi, Diehl et al. 2006).

Possible implications of common (de-)activation of brain areas

Although generally considered a sub-clinical and purely an EEG event, TLE-IED have been shown to be associated with transient cognitive impairment and a decrease in reaction time (Shewmon and Erwin 1988; Binnie 2003). Our finding that IED in TLE were associated with an alteration of resting state brain function raises the possibility that IED might also affect activity in regions supporting specific cognitive functions during a task. In this study, when patients were at rest, no task was presented and only default mode but no explicit task-specific brain regions could be expected to deactivate in response to IED.

The region of the brain that generates IED defines the irritative zone, which does not necessarily coincide with the epileptogenic zone (which by definition is indispensable for the generation of epileptic seizures) (Rosenow and Luders 2001). Our finding of

IED-concomitant activation of the medial temporal lobe might explain the higher seizure free rates of patients in whom the hippocampus is removed in an anterior temporal lobe resection compared to those who have a temporal lesionectomy without hippocampal resection.(Wyler, Hermann et al. 1989).

Conclusion

We found that brain areas which are active when a subject is in a state of relaxed wakefulness deactivate during IED of temporal lobe origin but not in extra-TLE. We show that EEG-fMRI group analysis can be used to explore networks associated with interictal discharges. Our data suggest that medial temporal lobe structures are central in generating or propagating IED in TLE, and superior temporal, while superior temporal, sub-thalamic and mesial frontal brain regions are involved in extra-TLE.

9.4 Probing the interaction of interictal epileptic activity and the default mode network

9.4.1 Causal hierarchy within the thalamo-cortical network in spike and wave discharges[6]

Background

Generalised spike wave (GSW) discharges are the EEG hallmark of absence seizures, clinically characterised by a transitory interruption of ongoing activities and impaired consciousness, occurring during states of reduced awareness.

Several theories have been proposed to explain the pathophysiology of GSW discharges and the role of thalamus and cortex as generators. In this work we extend the existing theories by hypothesizing a role for the precuneus, a brain region neglected in previous works on GSW generation but already known to be linked to consciousness and awareness. We analysed fMRI data using dynamic causal modelling (DCM) to investigate the effective connectivity between precuneus, thalamus and prefrontal cortex in patients with GSW discharges.

Methodology and Principal Findings

We analysed fMRI data from seven patients affected by Idiopathic Generalized Epilepsy (IGE) with frequent GSW discharges and significant GSW-correlated haemodynamic signal changes in the thalamus, the prefrontal cortex and the precuneus. Using DCM we assessed their effective connectivity, i.e. which region drives another region. Three dynamic causal models were constructed: GSW was modelled as autonomous input to the thalamus (model A), ventromedial prefrontal cortex (model B), and precuneus (model C). Bayesian model comparison revealed Model C (GSW as autonomous input to precuneus), to be the best in 5 patients while model A prevailed in two cases. At the group level model C dominated and at the population-level the p value of model C was ~1.

[6] Own contributions: study design, models, principle of DCM analysis (mainly performed by Anna Vaudano), EEG/fMRI data collection, review of clinical data,

Conclusion

Our results provide strong evidence that activity in the precuneus gates GSW discharges in the thalamo-(fronto) cortical network. This study is the first demonstration of a causal link between haemodynamic changes in the precuneus - an index of awareness - and the occurrence of pathological discharges in epilepsy.

INTRODUCTION:

The existence of a link between physiological and environmental factors and the occurrence of epileptic seizures is well documented in the literature (Niedermeyer 1966; Guey, Bureau et al. 1969; Kostopoulos 2000; Andermann and Berkovic 2001). However, the brain networks through which these factors influence the epileptic state remain unclear.

Such a link is particularly evident in patients affected by Idiopathic Generalized Epilepsy (IGE) in whom, for example, sleep deprivation, alcohol and stress seem to act as activating factors for seizures occurrence (Andermann and Berkovic 2001) and a close relationship between absences and the sleep-wake cycle has been demonstrated (Niedermeyer 1966; Kostopoulos 2000; Andermann and Berkovic 2001).

The prototypical seizure type in IGE is the absence with its electroencephalographic hallmark, generalised spike and wave (GSW) discharges. Clinically, absences are characterized by a blank stare and impaired consciousness. Activities requiring vigilant attention have been coupled with a lesser likelihood of absences whereas an increased frequency of these seizures during relaxation is well established (Guey, Bureau et al. 1969; Andermann and Berkovic 2001). These findings suggest a causal link between changes in the level of awareness and the occurrence of GSW discharges.

Recent functional imaging studies have revealed the existence of a set of brain regions which show increased functional and metabolic activity during rest, compared to attention-demanding tasks (Mazoyer, Zago et al. 2001; Raichle, MacLeod et al. 2001). Involved brain areas include the posterior cingulate cortex, the precuneus, the medial prefrontal cortex, mid-dorsolateral prefrontal and anterior temporal cortices and have

manuscript writing; Vaudano, A. E., H. Laufs, et al. (2009). "Causal hierarchy within the thalamo-cortical network in spike and wave discharges." PLoS One **4**(8): e6475..

been hypothesized to constitute the so-called “default mode network” (DMN) (Raichle, MacLeod et al. 2001). DMN activity decreases during various cognitive tasks indicate that this network sustains the spontaneous thought processes or self-oriented mental activity that characterizes the brain’s resting state. Mental processes subservient to consciousness have been linked to DMN activity such as random episodic memory (Andreasen, O'Leary et al. 1995), conceptual processing (Binder, Frost et al. 1999), stimulus independent thought (McGuire, Paulesu et al. 1996) and self-reflection (Gusnard, Akbudak et al. 2001; Johnson, Baxter et al. 2002; Cavanna and Trimble 2006; Cavanna 2007). Although most neuroimaging studies characterize the DMN as a homogeneous network, recent work has suggested a functional differentiation within it: particularly, of the two main nodes in the DMN, the posteromedial cortical region (precuneus and posterior cingulate cortex) seems linked specifically with visual-spatial and attention networks while the medial prefrontal cortex is more engaged in motor control circuits (Uddin, Clare Kelly et al. 2008). Additionally, the precuneus/posterior cingulate node has been recently demonstrated to have the highest degree of interactions (using a partial correlation approach on fMRI data) with the rest of the DMN (Fransson and Marrelec 2008) suggesting a pivotal role of this area within the network. This interpretation is in line with the evidence from previous PET studies that this brain region, and in particular the precuneus, shows the highest metabolic rate consuming 35% more glucose than any other area of the cerebral cortex (Gusnard and Raichle 2001) at rest.

The DMN shows decreased activity both during attention-demanding tasks and equally during states of reduced vigilance and, especially the posteromedial cortical regions, during altered states of consciousness (Laureys, Owen et al. 2004; Faymonville, Boly et al. 2006). Based on these observations, several authors (Cavanna and Trimble 2006; Cavanna 2007; Boly, Phillips et al. 2008) suggested a pivotal role of the posteromedial cortical region in self-consciousness inside the DMN.

EEG-correlated functional magnetic resonance imaging (EEG-fMRI) studies have shown a common pattern of blood oxygen level-dependent (BOLD) signal decrease in the precuneus and the other default mode areas, together with a thalamic BOLD signal increase, during ictal and interictal GSW discharges (Archer, Abbott et al. 2003; Salek-

Haddadi, Lemieux et al. 2003; Aghakhani, Bagshaw et al. 2004; Gotman, Grova et al. 2005; Labate, Briellmann et al. 2005; Hamandi, Salek-Haddadi et al. 2006; Laufs, Lengler et al. 2006; De Tiege, Harrison et al. 2007). Decreased cerebral blood flow consistent with a decrease in neuronal activity was demonstrated in DMN regions during GSW (Hamandi, Laufs et al. 2008). Therefore, these relative BOLD signal decreases can be interpreted as a transitory suspension of the "default state" of the brain which occurs in association with an altered level of awareness observed during GSW discharges and absences, respectively (Salek-Haddadi, Lemieux et al. 2003; Aghakhani, Bagshaw et al. 2004; Gotman, Grova et al. 2005; Hamandi, Salek-Haddadi et al. 2006; Laufs, Lengler et al. 2006).

The pathophysiological substrate of GSW remains enigmatic and several studies, both in animals and humans, have tried to answer the historical debate regarding the putative role of the thalamus and cortex as generators. Data from invasive recordings and manipulations in well-validated genetic models of absence epilepsy have supported the hypothesis that absence seizures are of cortical origin. Depth electrode recordings from the thalamus and suprasylvian cortex in cats have shown a primary role of the neocortex in producing seizures consisting of spike and wave complexes (Steriade and Contreras 1998). More recently, electrophysiological recordings in a rat (WAG/Rij) genetic model of absence epilepsy demonstrated the existence of a cortical focus within the perioral regions of somatosensory cortex (Meeren, Pijn et al. 2002; Meeren, van Luijtelaar et al. 2005). Using *in vivo* intracellular recordings in the GAERS rat model (Genetic Absence Epilepsy Rats from Strasbourg), Polack and colleagues (Polack, Guillemain et al. 2007) demonstrated pathological activity originating in the perioral region of somatosensory cortex. Those findings led to renewed interest in the role of the cortex in human GSW. Using source reconstruction methods based on high-density EEG data acquired during the propagation of ictal GSW discharges, Holmes et al. (Holmes, Brown et al. 2004) showed the involvement of the orbital frontal and mesial frontal regions. Recent work using advanced EEG data analysis provided evidence in favour of a primary role of ventromedial prefrontal cortex (vmPFC) and particularly Brodmann area 10 in the generation of GSW discharges during absences (Tucker, Brown et al. 2007).

However, despite the suggestion of the involvement of dorsal cortical regions (particularly posterior-medial cortical regions) in GSW discharges from neuroimaging studies (Salek-Haddadi, Lemieux et al. 2003; Gotman, Grova et al. 2005; Hamandi, Salek-Haddadi et al. 2006; Laufs, Lengler et al. 2006) and their role in conscious awareness (Faymonville, Boly et al. 2006; Boly, Phillips et al. 2008), no work attempting to understand the interaction between these areas and the (frontal)cortical-thalamic loop has been performed to date. This is what we propose to evaluate here using Dynamic Causal Modelling to study effective connectivity based on simultaneously recorded EEG-fMRI data in patients with GSW discharges.

Dynamic Causal Modelling (DCM) offers the possibility of characterising the effective connectivity, defined as "the influence that one neural system exerts over another", in other words: it can be used to test which brain region drives which (Friston, Harrison et al. 2003). The aim of DCM is to estimate the effective connectivity between brain regions and more generally, to adjudicate among a set of models describing connectivity using model comparison (Penny, Stephan et al. 2004). In brief, DCM for fMRI data combines a model of neural dynamics with an experimentally validated haemodynamic model that describes the transformation of neuronal activity into a BOLD response (Stephan, Harrison et al. 2007). Both sets of parameters describing the neuronal state and those determining the forward model of BOLD signal generation (Penny, Stephan et al. 2004) are estimated from the data within a Bayesian framework for each brain area included in the model. Hence, crucially, the possibility for differing haemodynamic responses (e.g. latency between regions) is included within the DCM. The Bayesian framework allows an inference to be made as to whether the data is best explained by variations in the haemodynamic response or instead by changes in the underlying neural system. This means valid inferences can be made about, for example, which brain region drives which, despite the limitations of temporal resolution inherent to fMRI. This could be particularly interesting in epilepsy where identifying the drivers of the pathological activity and their "causal" relationships in the epileptic network is essential for improving neurophysiopathological understanding of epileptic syndromes. Hamandi et al. (Hamandi, Powell et al. 2008)

used DCM to show propagation of neuronal activity from the irritative zone to ipsilateral posterior brain regions in a patient with temporal lobe epilepsy. More recently David and colleagues (David, Guillemain et al. 2008) applied effective connectivity analysis techniques including DCM to fMRI data from (GAERS) rats to demonstrate concordance between the drivers revealed by DCM and the trigger identified using intracranial recordings.

We applied DCM to EEG-correlated fMRI data to understand the dynamic interaction between brain regions known to be involved in the initiation and cessation of GSW discharges and with a brain region known to be related to conscious awareness, the precuneus. We compared a family of models of effective connectivity focusing on a set of cortical regions and the thalamus. We tested and compared the following models in relation to the GSW discharges: when treated as autonomous input GSW activity enters the cortico-thalamic loop: 1. via the thalamus (following the centrencephalic theory); 2. via the ventromedial prefrontal cortex (vmPFC) (following the cortical focus theory); or 3. via the precuneus (i.e. the state of the precuneus – a key region for the sustenance of consciousness - gates pathological activity via the cortico-thalamic network); see Fig.1 for an illustration of the models.

MATERIALS and METHODS:

Patients

In order to apply DCM analysis, we re-analysed the resting-state EEG-fMRI data of 32 IGE patients already studied, as reported elsewhere (Hamandi, Salek-Haddadi et al. 2006). Ten patients from the original population did not have any GSW discharges during the 35-min fMRI session and hence the data discarded. The EEG-fMRI data of the remaining 22 patients were pre-processed and analysed using SPM8b. In 15 cases no GSW-related BOLD changes were found in the thalamus (14 cases) and in the precuneus (one case), leaving data from 7 patients (5 females) in whom significant GSW-related BOLD signal changes (increase and/or decrease) were revealed in all three regions of interest (Table 9.4.1-1): the thalamus, vmPFC (Brodmann Area 10) and precuneus (BA7). The 7 selected patients represent all the cases who satisfied the criteria. According to the ILAE 1989 classification scheme (Commission on Classification and Terminology of the International League Against Epilepsy 1989) five patients were

affected by Juvenile Absence Epilepsy (JAE) (patients # 2a, 5, 7, 9a, 11 in (Hamandi, Salek-Haddadi et al. 2006)) and two patients by Juvenile Myoclonic Epilepsy (JME) (patients # 18, 21a in (Hamandi, Salek-Haddadi et al. 2006), Table 9.3.2-1). Structural MRI was normal in all patients.

Id no.	Age/Gender	Epilepsy syndrome/Syndrome subtype	Seizure type frequency (age onset/yrs)	Therapy
2a	24/F	IGE/JAE	abs 15/d (10), GTCS	LTG,ESM, CBZ,TPM
5	43/F	IGE/JAE	abs daily (8) , GTCS 4/yr (13)	VPA,LTG,CLB
7	22/F	IGE/JAE	abs 2–3/d (8), GTCS 3/mth (19)	LEV, ESM, TPM
9a	18/M	IGE/JAE	abs weekly (15)	nil
11	33/F	IGE/JAE	abs daily (teens)	VPA, LTG
18	20/M	IGE/JME	abs 3/d (<10), GTCS 1/mth (13), MJ(teens)	LEV
21a	37/F	IGE/JME	abs 10 d (7) GTCS 2/yr (12), MJ teens	VPA, GBP, CLB

ID no: patient identification as in Hamandi et al., 2006, table 1.
JAE, juvenile absence epilepsy; JME, juvenile myoclonic epilepsy; abs, absence seizures; MJ, myoclonic jerks; GTCS, generalized tonic clonic seizures; CBZ, carbamazepine; CLB, clobazam;; ESM, ethosuximide; GBP, gabapentin; LEV, leviteracetam; LTG, lamotrigine; TPM, topiramate; VPA, sodium valproate; M, male; F, female; d, day; wk, week; mth, month; yr, year.
[a]patients studied in two successive sessions.

Table 9.4.1-1: Clinical details of patients studied based on ILAE diagnostic categories.

EEG-fMRI acquisition and analysis

The methods pertaining to data acquisition are described elsewhere (Hamandi, Salek-Haddadi et al. 2006). In brief, ten-channel EEG was recorded using MR-compatible equipment, at Fp1/Fp2, F7/F8, T3/T4, T5/T6, O1/O2, Fz (ground) and Pz as the reference (10–20 system), along with bipolar electrocardiogram (Krakow, Allen et al. 2000). Seven hundred and four T2*-weighted single-shot gradient-echo echo-planar images (EPI; TE/TR: 40/3000, 21 interleaved axial slices of 5 mm thickness, acquired continuously and parallel to the inter-commissural line, FOV 24x24 cm^2, 64 x 64 matrix) were acquired over a 35-min session on a 1.5 Tesla Horizon EchoSpeed MRI scanner (General Electric, Milwaukee, WI). Patients were asked to rest with their eyes closed and to keep still.

FMRI data were processed and analysed using SPM8b (http://www.fil.ion.ucl.ac.uk/spm/).

After discarding the first four image volumes, the EPI time series were realigned and spatially smoothed with a cubic Gaussian Kernel of 8 mm full width at half maximum and normalised to MNI space.

A general linear model (GLM) was constructed to assess the presence of regional GSW-related BOLD signal changes. GSW events were represented as variable-duration

blocks beginning at the onset of GSW as identified on the MR-synchronised EEG by two expert observers (AEV and RT) and ending upon GSW cessation.

Motion-related effects were modelled in the GLM by 24 regressors of the 6 scan realignment parameters and a Volterra expansion of these (Friston, Williams et al. 1996), plus scan nulling Heaviside terms for large (inter-scan displacement > 0.2mm) motion effects (Salek-Haddadi, Diehl et al. 2006; Lemieux, Salek-Haddadi et al. 2007). No global scaling was employed. In addition, confounds were included to account for cardiac-related signal changes (Liston, Lund et al. 2006).

The GSW event blocks were convolved with the canonical hemodynamic response function (HRF), and its temporal and dispersion derivatives, to form regressors testing for GSW-related BOLD signal changes. Significant positive and negative BOLD signal changes correlated with GSW were identified by means of an F-contrast across the three regressors of interest and recorded as activation and deactivation depending on the response shape. The resulting SPMs were thresholded at $p<0.001$ (Friston, Frith et al. 1991) to define regions of interest (inference on these regional effects using multiple comparison correction are reported in (Hamandi, Salek-Haddadi et al. 2006).

Effective connectivity

The DCM analysis was performed for three ROI: thalamus, vmPFC, precuneus. For all ROI we used spherical volumes with a 5mm radius. For ROI selection within the thalamus we chose the axial slice that showed the largest cluster and placed the ROI so as to cover the region. In patients with bilateral thalamus involvement, we selected only one ROI, on the side of the largest cluster. For ROI selection within vmPFC, we placed the ROI in the axial slice within the Brodmann Area 10 and the side containing the largest area of signal BOLD change. The precuneus ROI was placed within the medial sagittal slice, rostrally to the middle of the parieto-occipital sulcus. In patients showing bilateral precuneus involvement, we placed the ROI on the side of the largest cluster. The ROI positions were defined using Talairach Daemon, http://ric.uthscsa.edu/project/talairachdaemon.html); the Talairach coordinates and equivalent Z-scores of the selected regions are listed in Table 9.4.1-2. Following the standard DCM procedure in SPM, a summary time series was derived for each ROI by

computing the first principal eigenvariate of all super-threshold voxel time series within the ROI.

Id no.	Talairach coordinates of ROIs			Cluster size (voxels)/Z-score		
	Thalamus	vmPFC	Precuneus	Thalamus	vmPFC	Precuneus
2a	x = 4 y = −16 z = 2	x = −24 y = 62 z = 14	x = −22 y = −76 z = 50	19/3.42	81/5.55	81/4.27
5	x = −2 y = −24 z = 4	x = 26 y = 46 z = 26	x = 14 y = −80 z = 4	81/4.3	73/3.78	81/4.90
7	x = 10 y = −12 z = 8	x = 30 y = 42 z = 22	x = 8 y = −54 z = 64	81/7.05	81/7.07	81/>7.53
9a	x = 2 y = −16 z = 0	x = 12 y = 52 z =	x = 10 y = −58 z = 20	14/3.24	81/5.28	81/5.64
11	x = 4 y = −14 z = 0	x = −2 y = 66 z = 24	x = −4 y = −70 z = 40	78/4.13	81/3.98	81/4.74
18	x = −16 y = −14 z = 2	x = −24 y = 46 z = 14	x = 16 y = −72 z = 40	81/7.29	81/6.07	78/4.58
21a	x = 8 y = −18 z = 8	x = 44 y = 56 z = 4	x = 0 y = −72 z = 52	81/>7.53	64/7.53	61/5.60

ID no: patient identification as in Hamandi et al., 2006, table 1.
vmPFC: Ventromedial Prefrontal Cortex. Talairach Coordinates of the ROIs selected (obtained using Talairach Daemon, http://ric.uthscsa.edu/project/talairachdaemon.html); Z-scores are reported for local voxel maxima.
doi:10.1371/journal.pone.0006475.t002

Table 9.4.1-2: DCM regions of interest.

The regional responses were filtered, whitened and the nuisance effects (motion, cardiac) were subtracted to leave only GSW-related effects. To account for the effect of scan nulling of large motion events (which effectively removes any signal change in the affected volumes) (Lemieux, Salek-Haddadi et al. 2007), the GSW epoch was removed when it occurred during these motion-laden periods. The net effect of this procedure was to remove any events associated with large-scale head motion from consideration within the DCM.

Using the DCM module as implemented in SPM8b three linear models were constructed. Each comprised the three ROI as reciprocally (forward and backward) connected regions and GSW event blocks considered as autonomous input to each of the three regions, one at a time a) GSW as autonomous input on the thalamus (Model A), b) GSW as autonomous input on vmPFC (Model B), c) GSW as autonomous input on the precuneus (Model C). Hence, three models were evaluated per subject (see the schematic in Figure 9.4.1-1).

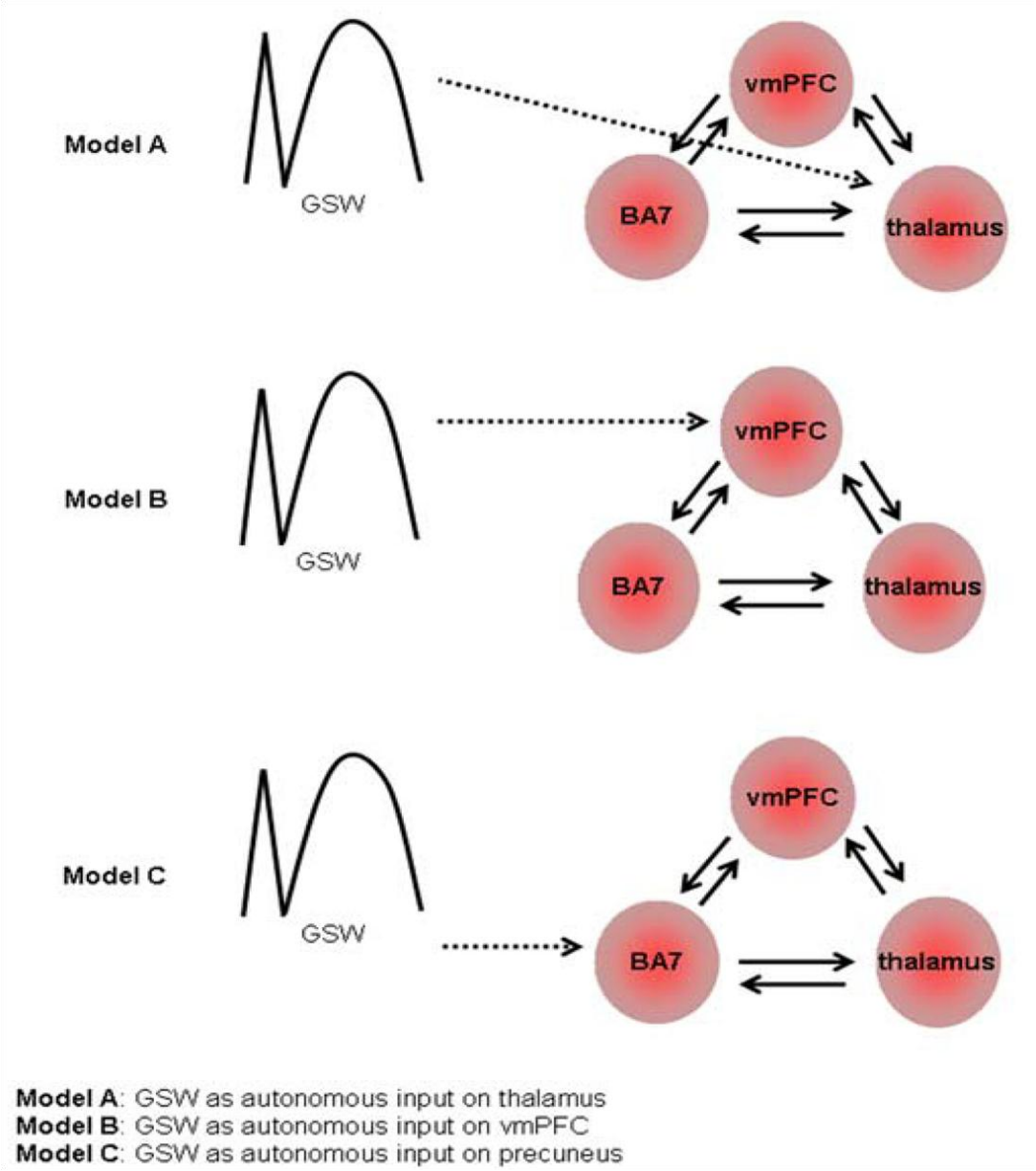

Figure 9.4.1-1: Effective connectivity models. Effective connectivity (DCM) models showing GSW discharges as autonomous input on three different regions (dotted arrows) within the cortical thalamic system: 3 ROI are structurally (forward and backward) connected (solid arrows). Model A: GSW as autonomous input on the thalamus; Model B: GSW as autonomous input on the ventromedial prefrontal cortex (vmPFC). Model C: GSW as autonomous input on the precuneus (BA 7). GSW: Generalised Spike and Wave discharges; BA: Brodmann Area.

After the estimation of parameters of each competing model, they were compared using Bayesian Model Comparison (BMC) where the evidence of each model, computed from estimated parameters distributions, is used to quantify the model plausibility (Penny, Stephan et al. 2004; David, Guillemain et al. 2008). Given two models m_1 and m_2, one can compare them by computing the difference in their log-evidence ln $p(y \mid m_1)$- ln $p(y \mid m_2)$. If this difference is greater than about 3 (i.e. the relative likelihood is greater than 20:1) then one asserts that there is strong evidence

in favour of one of the models. This is commonly calculated based on the *F* value of each model, which is the negative marginal log-likelihood or negative log-evidence: $F = -\ln p(y \mid m)$. For more details about BMC, see (Garrido, Kilner et al. 2007; Kiebel, Garrido et al. 2008).

Assuming that data from each subject are conditionally independent, the evidence at the group level is obtained by multiplying the marginal likelihood, or, equivalently, by adding the log-evidences from each subject (Garrido, Kilner et al. 2007).

RESULTS:

GSW-related BOLD patterns

Good quality EEG was obtained following pulse and gradient artefact subtraction, allowing reliable identification of epileptiform discharges (see Figure 9.3.1-1). EEG discharge features are summarized in Table 9.4.1-2. The reader should refer to Table 9.4.1-2 and (Hamandi, Salek-Haddadi et al. 2006) for the detailed patterns of the GSW-related BOLD signal changes in each patient. Figure 9.4.1-3 shows a representative example of a BOLD map for one patient with JME (#21a).

Id no./Epilepsy syndrome	No. of GSW events	Duration of GSW events, median (range) (seconds)	EEG-fMRI results for DCM ROIs		
			Thalamus	vmPFC	Precuneus
2a/JAE	3	7.3 (4.4−7.7)	B **(i)**	B (>L) **(d)**	L **(d)**
5/JAE	18	0.6 (0.4−3.6)	B(>L) **(i)**	R **(i)**	B **(i)**
7/JAE	2	4.3 (3.4−5.3)	B(>R) **(i)**	B **(i)**	B **(i)**
9a/JAE	8	1.9 (0.7−3.6)	R **(i)**	R **(d)**	B **(d)**
11/JAE	189	1.6 (0.3−73.9)	B(>L) **(i)**	B **(d)**	B **(d)**
18/JME	25	1.3 (0.4−3.4)	B(>L) **(i)**	B(>L) **(i)**	B **(i)**
21a/JME	60	1.4 (0.4−8.4)	B **(d)**	R **(d)**	B **(d)**

ID no: patient identification as in Hamandi et al., 2006, table 1. Summary of results for all EEG-fMRI sessions: number and duration of GSW epochs, regions of BOLD signal change labelled in accordance with direction of HRF loading, vmPFC: Ventromedial Prefrontal Cortex;
(i) BOLD signal increase;
(d) BOLD signal decrease; B: bilateral, L: left, R: right. All SPMs corrected for multiple comparisons using random field theory ($p<0.001$, patients 2a, 7, 9a, 18; $p<0.05$, patients 5, 11, 21a).
doi:10.1371/journal.pone.0006475.t003

Table 9.4.1-3: EEG-fMRI results.

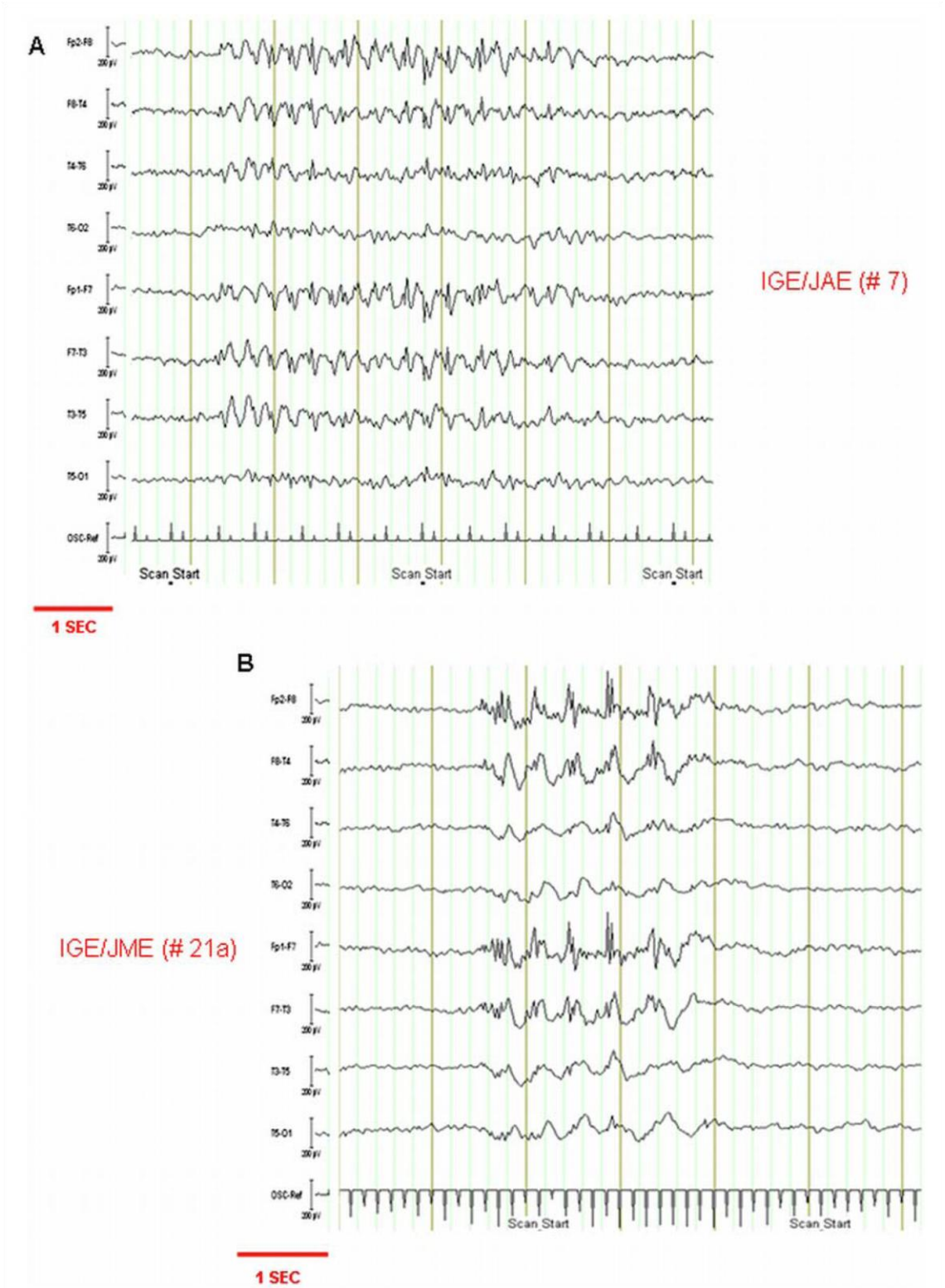

Figure 9.4.1-2: Representative example of EEGs recorded during scanning after scanning artefact subtraction. The EEG traces were analysed following pulse (not shown) and image artifact subtraction; EEG traces are displayed as bipolar montage. OSC: scanner slice pulse used for EEG artifact correction, and EEG-fMRI synchronization (7/s). (A) IGE/JAE: patient (ID #7). The trace shows an epoch of 3.5 Hz generalised spike-wave complexes (length ,4 seconds) with anterior predominance. (B): IGE/JME: patient (ID #21a).The trace shows an epoch of 2.523 Hz generalised multispike-wave complexes (length ,2.5 seconds) with anterior predominance.

In accordance with the selection criteria, significant GSW-associated BOLD signal changes were found in the thalamus, in the frontal lobe limited to the vmPFC, and precuneus (see Table 9.4.1-2 and (Hamandi, Salek-Haddadi et al. 2006)). Frontal cortex and precuneus showed a positive BOLD response in 3 patients (2 JAE and 1 JME) and a negative BOLD response in the remaining 4 patients (3 JAE and 1 JME). In two cases (#2a, #9a) our results were different from Hamandi's previous

single-subject analysis results when fewer confounds were included (no global scaling and 6 scan realignment parameters with their first order expansion in (Hamandi, Salek-Haddadi et al. 2006)). We note that Hamandi et al., showed a consistent pattern of thalamic signal increase and a cortical signal decrease which involved the precuneus and prefrontal cortex.

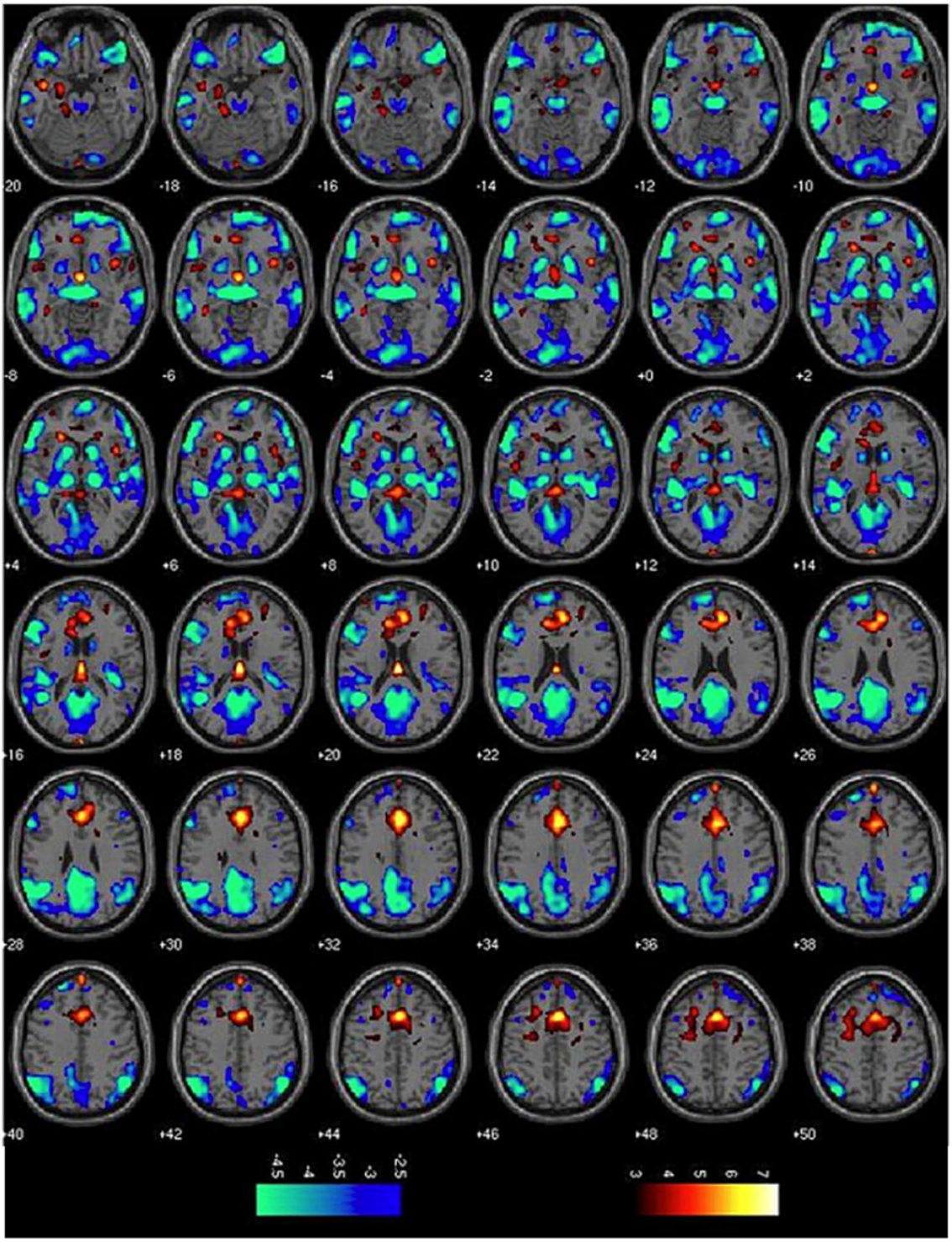

Figure 9.4.1-3: EEG-FMRI statistical parametric map in a patient with JME. A colour-coded overlay of SPM{t} (red: positive BOLD response; green: negative BOLD response) (p,0.05 corrected for Family-Wise Error-FWE) onto the slices overlay shows, BOLD signal increase in bilateral cingulated gyrus (BA32) and BOLD signal decrease in bilateral thalamic, bilateral caudate, right medial frontal gyrus (BA10), left superior temporal gyrus (BA39), right precuneus (BA7), bilateral inferior parietal lobuli (BA39). Clusters labelling according to Talairach Daemon, (http://ric.uthscsa.edu/project/talairachdaemon.html). BA: Brodmann Area

Effective connectivity

Figure 9.4.1-4 a shows the log-evidence for the three models, in each subject. Bayesian Model Comparison (BMC) identified model C (GSW immediately influences the precuneus) to be the best in 5 cases. In patients #5, #7, #18 model C was found to be significantly more likely than both models A (GSW immediately influences the thalamus) and B (GSW immediately influences the vmPFC), whereas in patient #2a it was significantly better than model A and in patient #21a better than model B only. In the remaining two cases (#11, #9a) model A was better than models B and C. Interestingly model B was never significantly better than model C and in only one subject (# 7) was it more likely than model A. Table 9.4.1-4 shows the *F* values (i.e. the negative log-evidence) in absolute numbers. Figure 9.4.1-4 b shows the log-evidence for the three models at the group level. Models C and A are clearly more likely than model B and over patients, there is strong evidence in favour of model C over model A and B.

Assuming that all patients in the group are representative of IGE we generalized the results of group analysis to the population level. The *p* value calculated for each model were extremely close to zero for models B and A, and close to 1 for model C, demonstrating the latter to be very likely at the population level.

Id n°	Model A	Model B	Model C
2a	F = −3427.2898	F = −3422.9665	F = −3420.6739
5	F = −3039.0606	F = −3036.7609	F = −3023.5675
7	F = −1762.445	F = −1758.6259	F = −1754.9096
9a	F = −2972.7801	F = −2976.9679	F = −2976.0056
11	F = −3089.2781	F = −3093.2254	F = −3094.3386
18	F = −3210.5648	F = −3217.2931	F = −3205.6735
21a	F = −2377.5158	F = −2383.6488	F = −2374.9833

ID no: patient identification as in Hamandi et al., 2006, table 1.
F value (i.e. the negative log-evidence) for each model at single subject level analysis. See the text for details.

Table 9.4.1-4: DCM F values.

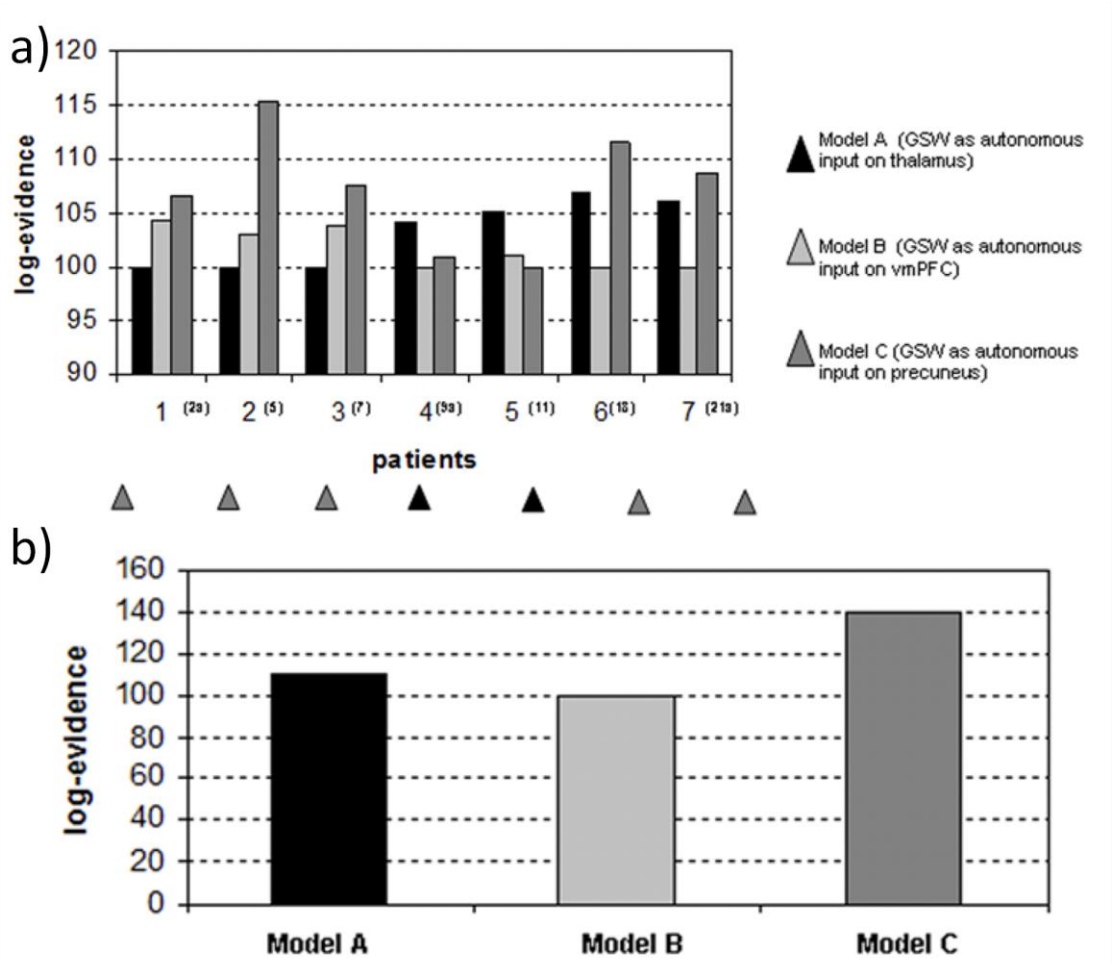

Figure 9.4.1-4: Effective connectivity model comparison results. Bayesian Model Selection (BMC) among DCMs for the three models tested. (a): differences between log-evidences for model A, B, C for each subject. The triangles identify the best model on the basis of the subject's highest logevidence difference. A difference greater than 3 is highly significant. For illustration purposes we added a constant value of 100 to all log-evidence differences. The numbers inside brackets (on the x-axis) correspond to ID no in Hamandi et al. [23]. (b): graph showing the difference between the log-evidence at the group level, i.e. pooled over subjects, for the three models. For illustration purposes we added a constant value of 100 to all logevidence differences.

DISCUSSION:

We investigated the causal relationship between neuronal activity as reflected by BOLD signals in three brain regions, namely the thalamus, the vmPFC and the precuneus, in relation to the onset and offset of GSW in 7 patients affected by IGE. The thalamus and the frontal cortex are key structures in well established hypotheses on GSW generation (Jasper and Drooglever-Fortuyn 1947; Marcus, Watson et al. 1968; Steriade and Contreras 1998; Meeren, Pijn et al. 2002; Meeren, van Luijtelaar et al.

2005). The inclusion of the vmPFC was motivated by recent evidence for its primary role in the generation of GSW in absences (Holmes, Brown et al. 2004; Craiu, Magureanu et al. 2006; Tucker, Brown et al. 2007) and by the frequent observation of its prominent BOLD increase and/or decrease compared to other frontal cortical areas in EEG-fMRI studies (Salek-Haddadi, Lemieux et al. 2003; Aghakhani, Bagshaw et al. 2004; Gotman, Grova et al. 2005; Hamandi, Salek-Haddadi et al. 2006; Laufs, Lengler et al. 2006). Our results are consistent with the precuneus, as a key region changing its activity with altered states of vigilance, influencing the occurrence of generalized seizures. The precuneus has direct connections with the frontal lobe (prefrontal cortex) (Petrides and Pandya 1984; Goldman-Rakic 1988; Leichnetz 2001) and thalamus (Yeterian and Pandya 1985; Schmahmann and Pandya 1990; Van Hoesen, Maddock et al. 1993).

Applying DCM to fMRI data simultaneously acquired with EEG we found that, for the models tested, in five out of seven patients studied, electroencephalographic discharges first affected the precuneus. This finding became more evident at the group and population level so that the evidence in favour of model C (GSW as autonomous input to precuneus) was significantly higher than for models A (GSW as autonomous input to thalamus) and B (GSW as autonomous input to vmPFC). In the remaining two cases, BMC showed model A to be the best. The discrepancy between the results of the analysis of the single subjects is not unexpected. We note that in one of the pioneer DCM studies on evoked potentials, Garrido et al (Garrido, Kilner et al. 2007) found reproducible results in seven out of eleven patients (in whom one of the models tested was the best over subjects) whereas the consistency of their conclusion is more evident at the group level. In our study, the consistency of the results at both the individual and group level is similar.

Our finding, that GSW onset and offset are more directly linked to the neural activity (as reflected by the BOLD signal) in the precuneus than in the other tested regions, implies a dependency of the cortico-thalamic loop on the precuneus and hence its state, i.e. a causal link. A possible interpretation is that changes in the precuneus state (as increase or decrease of it neuronal activity), which reflects spontaneous fluctuations in awareness, act on the thalamic-(frontal) cortical network facilitating the development of GSW. This is in contra-distinction to previous suggestions (22-24) that

decreases in precuneal activity reflect the semiology of impaired consciousness and are a consequence of GSW.

A similar hypothesis has been already proposed by Archer et al (Archer, Abbott et al. 2003), who observed a significant posterior cingulate negative BOLD response in 5 IGE patients with interictal GSW discharges whereas no BOLD signal changes were detected in thalamus or prefrontal cortex. The authors suggested that decrease in the posterior cingulate activity and associated regions may be involved in initiation of GSW activity.

Additionally, an fMRI study showed BOLD signal decrease in the posterior cingulate in IGE subjects following photic stimulation whether or not GSW occurred, while control subjects showed no change in this region (Hill, Chiappa et al. 1999). Such changes would be consistent with decrease in the posterior cingulate activity being a precursor (or facilitator) of GSW, rather than being a secondary phenomenon. The posterior cingulate cortex is adjacent to precuneus and some authors proposed it as part of precuneal cortical area (Frackowiak 1997; Fransson and Marrelec 2008).

Precuneus, awareness and GSW generation

According to the current thinking of the pathophysiology of GSW, there are two prerequisites for the occurrence of this pathological activity: 1) the pathological thalamo-(frontal) cortical interactions and 2) the so-called mild diffuse epileptogenic state of the cortex (ictogenicity of the cortex; (Gloor, Metrakos et al. 1982; van Gelder, Siatitsas et al. 1983; Gloor, Avoli et al. 1990; Clemens, Bessenyei et al. 2007)). Our findings suggest that changes in the level of awareness and hence precuneal activity, may increase the likelihood of an epileptogenic cortical state to arise and GSW to be generated within the thalamo-(frontal)cortical network.

The precuneus neuronal state, and hence the level of awareness, may, consequentially, reflect a “physiological initiator” of generalized synchronous discharges. The existence of a transient facilitating state of the brain which increases cerebral susceptibility to GSW generation has been recently demonstrated in patients

with absences, by synchronization measures and MEG source imaging methods (Amor, Baillet et al. 2009). This "idle" state is not part of the ictal process itself but allows vulnerable regions to generated epileptic discharges; electrically, it reflects a long-range de-synchronization between cortical sources which takes place few seconds before seizures onset. Fluctuations in the level of awareness, and hence in precuneal activity, could account for this facilitating effect. It is well established that the probability of absences occurrence depends on the level of awareness of the patient. Guey and colleagues, in 1969, identified factors influencing the occurrence of epileptic paroxysms in 30 patients with absences; particularly they found that, when an epileptic patient focused his attention, the likelihood of GSW discharges diminished considerably (Guey, Bureau et al. 1969). Moreover, inactivity or the moment of rest after an accomplished task or monotonous task can be regarded as factors favouring the occurrence of paroxysms. The fact that these processes can be detected also at the observational level implies a time scale of these changes of the order of seconds. This, in turn, makes fMRI a suitable tool to reveal such phenomena. A recent GSW-correlated EEG-fMRI study, indeed, demonstrated BOLD signal and hence neuronal activity changes - including within the precuneus - to occur several seconds before the appearance of the pathological GSW activity on scalp EEG (Moeller, Siebner et al. 2008). Moreover, the application of DCM to fMRI data from animal models with absences (David, Guillemain et al. 2008) has been validated with intracranial recordings.

Previous EEG-fMRI studies showed BOLD signal decrease in the DMN in relation to GSW apparently not correlated with clinical manifestations (Hamandi, Salek-Haddadi et al. 2006; Laufs, Lengler et al. 2006). This also argues for the proposed permissive role of precuneal activity changes contributing to an epileptogenic state and eventually GSW generation rather than DMN changes being a consequence of the semiology of impaired consciousness. A common pattern of negative BOLD responses in the DMN was observed in relation to focal interictal spikes in patients with temporal lobe epilepsy (Laufs, Hamandi et al. 2007). It remains to be seen whether precuneal activity plays a similarly permissive role in patients with focal epilepsy and complex partial seizures, i.e. periods of impaired consciousness.

EEG-fMRI adds to electrophysiological data on GSW generation and precuneal involvement

While there is little evidence of a strict consequentiality between a particular state of vigilance and the occurrence of GSW discharges, there is a notable lack of studies focusing on the possible role of cortical structures (particularly the precuneus) other than the thalamus and frontal cortex in GSW. However, evidence from scalp EEG source reconstruction analysis suggests that the precuneus participates in the generation of fast sleep spindles at 14 Hz (Anderer, Klosch et al. 2001). Animal models of absence epilepsy showed the possibility of a transition between sleep spindles and GSW suggesting a common origin (Gloor 1978; Steriade and Contreras 1998). According to this hypothesis, the circuit which normally generates sleep spindles leads to GSW under the condition of a cortical hyper-excitability (1). The existence of an active cortical spindle source located in the region of the precuneus is in line with our findings of its involvement in GSW discharges. Additionally, source reconstruction of the interictal spontaneous EEG activity has shown elevated bilateral parieto-occipital cortex involvement in patients with IGE compared to healthy subjects (Amor, Baillet et al. 2009). However, as noted previously, we are not aware of the precuneus having been identified in relation to GSW generation in neither EEG nor MEG.

In contrast to surface electrophysiological recordings, fMRI studies with concurrent EEG in patients with GSW discharges have shown common significant haemodynamic changes not only in the thalamus and frontal cortex, but also in the precuneus and other brain regions (encompassing fronto-parietal association cortices) of the DMN (Archer, Abbott et al. 2003; Aghakhani, Bagshaw et al. 2004; Gotman, Grova et al. 2005; Laufs and Duncan 2007).

FMRI's relatively homogeneous sensitivity across the brain relative to that of scalp EEG may explain why recent EEG-fMRI studies have been able to reveal precuneal involvement in epilepsies characterized by impaired consciousness and in particular associated with GSW (Gotman, Grova et al. 2005; Laufs, Lengler et al. 2006).

The application of connectivity analysis techniques based on fMRI data may improve our understanding of the interactions between brain regions haemodynamically involved during GSW discharges. David et al. applied DCM analysis to fMRI data acquired in an animal model of absences (David, Guillemain et al. 2008). They compared alternative neural models including the thalamus, the striatum and the somatosensory cortex, in which each region is modelled in turn as the driver of the pathological activity and showed that the somatosensory cortex to be the more likely driver. This is line with previous findings in animal models (Meeren, Pijn et al. 2002; Meeren, van Luijtelaar et al. 2005). Despite the presence of significance symmetrical activated clusters in retrosplenial cortex the authors assumed the posterior cortical regions to be involved only during the spreading of the pathological activity (downstream effect) and therefore did not include them in their models. No inference can be made on the putative role of regions not included in the models. We note that retrosplenial cortex, together with precuneus and posterior cingulate cortex, has been shown to be a critical node in the network correlates with consciousness in humans and animals (Vogt and Laureys 2005).

Methodological Considerations

Brain connectivity based on fMRI data, can be investigated via two different approaches: functional connectivity and effective connectivity analysis. Functional connectivity is data-driven and assesses statistical dependencies between fMRI signals from different brain regions without consideration of the underlying neuronal activity. In contrast, analyses of effective connectivity test hypotheses based on modelling of neuronal activity and a forward model describing how this activity is translated into the fMRI signals (Friston 2009). DCM of fMRI can thus provide information about the directionality of functional relations between positive or negative BOLD clusters and is context-dependent (Brazdil, Mikl et al. 2007; Friston 2009). Furthermore, our choice of effective connectivity approach rather than a data-driven functional connectivity analysis was motivated by the following considerations: 1) we had clear hypotheses to be tested about the GSW pathophysiology, and 2) the capacity of effective connectivity analyses to determine causality of the interactions between a set of brain regions makes it much more powerful.

There are different approaches for modelling effective connectivity from functional MRI, which include structural equation modelling (SEM), vector-autoregression models and DCM (Friston, Harrison et al. 2003). DCM represents a departure from other existing approaches since it assumes that the responses are driven by known or measurable regional changes that may be controlled experimentally (Friston, Harrison et al. 2003). An important conceptual aspect of DCM for neuroimaging pertains to how experimental or known effects enter the model and cause neuronal responses; designed experimental inputs may elicit responses through direct influences on specific anatomical nodes (driving or autonomous inputs), or they may affect the system by inducing changes in coupling among brain areas (modulatory inputs). In the context of intrinsic brain activity, and in particular brain states defined in relation to paroxysmal discharges such as GSW, the notion of experimental effects requires re-interpretation. In our approach, the GSW epochs, represented as blocks, correspond to the onset and offset of a perturbation of endogenous neuronal activity in the postulated network and epileptic activity is supposed to act as an endogenous autonomous effect, since it can influence directly the neuronal state of the specified anatomical nodes. There is good evidence of the validity of this approach in relation to intra-cerebral electrophysiology in rats (David, Guillemain et al. 2008). Our family of models is designed to compare the causal hierarchy between the three postulated regions of interest, and representing GSW as an autonomous effect must be seen as meeting a requirement of DCM with respect to this aim. We could have increased the number of cases included in the analysis by relaxing the requirement for involvement of the three regions of interest, for example cases that do not include the significant GSW-related BOLD changes in the thalamus; however, we believe that this would have undermined the credibility of the model comparison due to their known importance in GSW generation. Furthermore, in contrast to DCM for M/EEG (Kiebel, Garrido et al. 2009) DCM for fMRI is limited to the comparison of models with identical numbers of nodes. This is because in Bayesian model comparison, the models can be different but the data must be the same. In fMRI the data are derived from the nodes whereas in M/EEG, the data are taken from the sensors.

The causal link revealed in our study (i.e. precuneus activity facilitates GSW) is limited to onset and offset of GSW discharges. Therefore, our findings do not preclude a reverse causal relationship in which GSW accompanied by impairment of consciousness leads to (further) deactivation of the precuneus. This could be addressed by studying ictal GSW data using a similar methodological approach.

In common with all DCM-based inferences, our conclusions are valid solely with respect to the family of tested models; there may be brain areas which are involved in the GSW generation processes that were overlooked because of their apparent lack of haemodynamic involvement.

Conclusion

In this study we have demonstrated an active role in generalised epilepsy for the precuneus, a region previously neglected in electrophysiological studies of GSW. Using Dynamic Causal Modelling based on EEG-fMRI data we showed that the precuneus not only is strongly connected with the frontal cortex and the thalamus but also that the neuronal activity in this area may facilitate epileptic activity within a thalamo-cortical loop, the existence of which is well established. These findings suggest that GSW may arise through the direct influence of the neuronal state of the precuneus associated with spontaneous changes in the level of awareness.

9.5 Insights into the neurobiology of epilepsy

9.5.1 Converging PET and fMRI evidence for a common area involved in human focal epilepsies[7]

Abstract:

Objectives: Experiments in animal models have identified specific subcortical anatomic circuits, which are critically involved in the pathogenesis and control of seizure activity. However, whether such anatomic substrates also exist in human epilepsy is not known.

Methods: We studied two separate groups of patients with focal epilepsies arising from any cortical location either using simultaneous EEG-functional MRI (n=19 patients) or with [^{11}C]-flumazenil positron emission tomography (n=18).

Results: Time-locked with the interictal epileptiform discharges we found significant haemodynamic increases common to all patients near the frontal piriform cortex ipsilateral to the presumed cortical focus. $GABA_A$ receptor binding in the same area was reduced in patients with more frequent seizures.

Conclusions: Our findings of cerebral blood flow and GABA-ergic changes, irrespective of where inter-ictal or ictal activity occurs in the cortex, suggest that this area of the human primary olfactory cortex may be an attractive new target for epilepsy therapy, including neurosurgery, electrical stimulation and focal drug delivery.

Introduction:

Experimental evidence from animal models indicate that, independent of seizure induction, certain subcortical anatomic circuits act as critical modulators of seizure generation and propagation (Piredda and Gale 1985; Gale, Zhong et al. 1992; Gale 1995; Löscher and Ebert 1996; Steriade 2005). Although epileptic seizures may result from a broad array of brain insults, involving various brain areas, seizure activity does not spread diffusely throughout the brain, but propagates along specific anatomic pathways (Piredda and Gale 1985; Gale, Zhong et al. 1992; Gale 1995). During focal

[7] Own contributions: conceptualization, fMRI data analysis, manuscript preparation, Discussion; Laufs, H., M. P. Richardson, et al. (2011). "Converging PET and fMRI

cortical seizure activity, specific cortical-subcortical circuits contribute to sustaining and propagating the seizure discharge. Experiments in animal models have identified specific brain regions such as the substantia nigra and the deep anterior piriform cortex as important for controlling the initiation or propagation of both generalized and focal seizure activity (Piredda and Gale 1985; Depaulis, Vergnes et al. 1994; Deransart, Vercueil et al. 1998; Biraben, Semah et al. 2004; Bouilleret, Semah et al. 2005). In rat and monkey, a discrete site within the deep piriform (primary olfactory) cortex, termed “area tempestas” or “ventrostriatal anterior piriform cortex” is critical for modulating focal seizures (Piredda and Gale 1985; Ekstrand, Domroese et al. 2001). However, there is little experimental evidence to translate these observations to the human situation (Blumenfeld, McNally et al. 2004). Recent observations with deep brain stimulation in a variety of subcortical structures in patients with epilepsy (Morrell 2006) suggest that cortical-subcortical circuits have the potential to be harnessed for therapeutic benefit.

We undertook electroencephalography (EEG) combined with simultaneous functional magnetic resonance imaging (fMRI) in a group of patients with focal epilepsies arising from a wide variety of cortical locations to test whether specific IED-correlated haemodynamic changes occur within the human equivalent of the “area tempestas”. Furthermore, in another group of patients with extra-temporal epilepsy syndromes, we used carbon-11 labeled flumazenil (FMZ) positron emission tomography (PET) to assess seizure-related metabolic GABA-mediated changes within this region.

Methods

Standard Protocol Approvals, Registrations, and Patient Consents

The study was approved by the joint ethics committee of the National Hospital for Neurology and Neurosurgery and UCL Institute of Neurology, London, UK. Subjects gave informed, written consent.

Patients

Sixty-three patients with focal epilepsy underwent EEG-fMRI, following which IED were correlated with the fMRI data in an event-related fashion (Blumenfeld, McNally et al. 2004). Because IED occur spontaneously and unpredictably, the number of events captured varied widely across patients. To ensure the validity of the group analysis described below, i.e. to avoid any violation of homoscedasticity implicit in the loss of balance at the first level, it was mandatory only to include patients with a similar number of IED during fMRI data acquisition (Morrell 2006; Salek-Haddadi, Diehl et al. 2006). Consequently, of the 63 patients with focal epilepsy, those with a spiking rate in the mid-range level of activity in the group (between one and 20 IED per minute) were selected, giving 19 patients (10 female, mean age 38 years, range 25-67 years) for the group analysis (see Table 9.1.1-1 "EEG-fMRI" for patients' demographics).

A different patient group was studied with ^{11}C-FMZ-PET: 18 patients (7 females, mean age 27 years; range: 18 – 47 years) with MRI reported as normal by an experienced neuroradiologist were recruited (see Table 9.1.1-1 "FMZ PET" for patients' demographics). All of these subjects had focal or secondarily generalized seizures. Patients were excluded from the study if taking benzodiazepines. A group of 24 healthy subjects (3 females) of similar age (mean: 31 years, range: 20-51 years) who had no evidence of neurological disorder and were on no medication were studied. Consumption of alcohol was not allowed during 48 hours preceding the scan. Written informed consent was obtained in all cases and approvals of local ethical committees and of the UK Administration of Radioactive Substances Advisory Committee (ARSAC) were obtained.

EEG-fMRI

No	Age	Sex	Duration epilepsy (years)	Seizure type	Interictal / ictal EEG; seizure semiology	MRI	Lateralization	IED per min fMRI
1	47	F	46	SPS, CPS.	L ant temp spikes	HS	Left	12
2	40	M	39	SPS, CPS, SGTCS	L ant temp spikes	HS	Left	18
3	42	F	41	CPS, SGTCS	L ant temp spikes	normal	Left	18
4	67	M	53	CPS	L ant mid-temp spike-wave	normal	Left	2
5	41	F	41	CPS, SGTCS	widespread theta, frequent temp sharp waves predominantly L temp spikes	normal	Left	1
6	30	M	11	CPS, SGTCS	L temp slow waves, spikes, R temp spikes during sleep	MCD	bilateral	2

7	26	F	21	SGTCS	L temp slowing with frequent L ant temp spikes	HS	Left	5
8	38	F	20	CPS	L temp slow and sharp waves	normal	Left	2
9	47	F	44	CPS, SGTCS	L slow activity, bilateral spike-waves, poly-spike wave, L temp spikes	MCD	Left	5
10 F	33	F	26	SPS (motor)	Widespread spikes, sharp waves, sharp and slow waves maximal frontocentral	normal	Right	2
11	34	M	27	CPS, SGTCS	bilateral, post temp/occip sharp and slow wave complexes with L spikes	MCD	Left	1
12	40	M	40	CPS, SGTCS	L slow activity with L post temp spikes	DNT post-op seizure-free	Left	7
13 F	25	M	21	SPS, SGTCS.	bilateral spike wave over central region seizure starts with L arm motor symptoms*	normal	Right	2
14	28	F	25	SPS	continuous L parietal spikes	normal	Left	14
15	31	M	31	CPS, SGTCS	L spikes, sharp waves and slow waves bilateral synchronous and occasionally R	normal	bilateral	12
16	33	M	26	CPS, SGTCS	L and bilateral frontal sharp waves and occasional L temp spikes	normal	Left	3
17 F	36	F	27	CPS, SGTCS	R poly-spike and slow wave discharges, single and bursts, maximal centro-temp	FCD	Right	6
18	57	F	17	SPS, CPS, SGTCS	L mid-temp spike-wave	HS – post-op seizure-free	Left	14
19	36	M	21	SPS, CPS	L front spikes	TBI	Left	11

mean age: 38 years, age range: 25-67 years, 10 female, 9 male subjects

FMZ PET

No	Age	sex	Duration epilepsy (years)	Seizure type	Interictal / ictal EEG (*); seizure semiology	Lateralization	Seizure frequency per month	FMZVD at peak
1	18	M	7	CPS	frequent L frontal IEDs	Left	8	3.4
2	24	F	18	CPS, SGTCS	L frontal seizure onset *	Left	12	3.43
3 F	36	F	29	SPS, CPS, SGTCS	R fronto-temporal IEDs; seizure starts with L sensorimotor symptoms *	Right	31	3.11
4	18	F	11	CPS, SGTCS	L hemishpere: EEG non-localising seizure starts with R arm motor symptoms *	Left	2	3.0
5 F	26	M	21	CPS	R frontal seizure onset *	Right	40	2.88
6 F	24	F	18	CPS	R hemisphere: EEG non-localising seizure starts with L face / limb motor symptoms *	Right	30	3.09
7 F	22	M	21	CPS	continuous R frontal IEDs	Right	3	3.33
8	27	F	23	CPS	L frontal IEDs; seizure starts with R arm dystonia, L hand automatism *	Left	55	3.0
9	21	M	17	CPS	L frontal seizure onset *	Left	30	3.0

					Seizure starts with R limb clonic activity			
10 F	28	F	17	CPS, SGTCS	R frontal IEDs	Right	4	3.15
11 F	37	M	33	SPS, SGTCS	R widespread slow; Seizure starts with left leg sensory symptoms *	Right	10	3.4
12 F	47	M	37	CPS, SGTCS	R post temp seizure onset *	Right	6	3.28
13	26	M	11	CPS	Frontal non-lateralised: Bifrontal high voltage sharp waves; Seizure semiology frontal *	bilateral	12	3.3
14	39	M	30	CPS, SGTCS	Frontal non-lateralised: Bilateral sharp and spikes; Seizure semiology frontal *	bilateral	5	3.33
15	25	M	17	SPS, SGTCS	L post temp: L post temp slow; Seizure starts with right visual field symptoms *	Left	2	3.29
16 F	18	F	10	SPS, CPS	Bilateral independent foci: Two different seizure patterns, clear ictal onsets from each post temp region, with seizure onset from the right more frequent *	Consensus: Right	3	3.14
17	23	M	17	SPS, CPS, SGTCS	Bilateral independent post temp IEDs	bilateral	76	2.42
18	40	M	13	CPS	Bifrontal high voltage sharp waves; EEG non-lateralising, Seizure semiology frontal *	bilateral	4	3.4

Table 9.5.1-1: Patient demographic data. Legend: ant = anterior; post = posterior; temp = temporal; R = right; L = left; CPS = complex partial seizure; SGTCS = secondarily generalised tonic-clonic seizure; SPS = simple partial seizure; F = images flipped for analysis prior to normalisation procedure. Lateralization was based on an interdisciplinary discussion (telemetry meeting, The National Hopsital for Neurology and Neurosurgery, London, UK) mainly based on seizure semiology, interictal and ictal EEG (*), and structural MRI pathology. (see ref 16 for further information).

EEG and fMRI acquisition

Methods and results pertaining to single-subject analyses have been reported elsewhere (Salek-Haddadi, Diehl et al. 2006). In summary, using MR-compatible equipment, 10 EEG channels were recorded using the International 10-20-System, and bipolar electrocardiogram. Over 35 minutes, 704 T_2*-weighted single-shot gradient-echo echo-planar images (EPI; TE/TR 40/3000, 21 slices, voxel size 3.75 x 3.75 x 5 mm^3) were acquired continuously on a 1.5 Tesla Horizon EchoSpeed MRI scanner (General

Electric, Milwaukee, USA). Patients were asked to rest with their eyes shut and to keep their head still. Following removal of artefact on the in-scanner EEG, IEDs were marked by 2 trained observers. fMRI data were pre-processed and analyzed using Statistical Parametric Mapping (SPM) (Friston, Worsley et al. 1994). After discarding the first four image volumes, the EPI time series was realigned, normalized (MNI template brain) and images spatially smoothed with a cubic Gaussian Kernel of 8 mm full width at half maximum. The three datasets of patients in which the presumed electro-clinical location of the epileptic focus was right-sided were flipped along the X-axis prior to normalization.

Spike-correlated EEG-fMRI group analysis

Onsets of interictal epileptiform discharges (IED) were used to build a linear model of effects of interest by convolution with a canonical haemodynamic response function (HRF, event-related design) and its temporal derivative to account for variations in the blood oxygen level-dependent (BOLD) response delay. Motion realignment parameters were modelled as a confound.(Friston, Williams et al. 1996) A single T-contrast image was generated per subject from the first (single-subject) level and the images used in a second level analysis, to test for any common patterns across the group of patients. A random effects model was used to identify any typical responses consistent across patients[16]. We used this approach to test the hypothesis of activation in the region of the presumed *Area tempestas*. Bilateral 0.7 cm x 1.4 cm x 1.4 cm search volumes (totalling 2744 mm^3) were each centred between the tip of the temporal pole and the orbitofrontal gyrus based on the aneurysm case report of Mizobuchi et al. (Mizobuchi, Ito et al. 1999), and in these regions, fMRI signal changes were considered significant at $P<0.05$ family-wise error-corrected for multiple comparisons within the search volume. In addition, positive responses were explored across the whole brain at a significance threshold of $P<0.001$ (uncorrected at the voxel level) to assess the presence of unspecific effects, e.g. sub-threshold bilateral, or covering the entire region of interest or even beyond.

PET acquisition

The method has been described in detail previously (Koepp, Richardson et al. 1996). In brief, scans were performed using an ECAT-953B PET scanner (CTI/Siemens, Knoxville) in 3D mode, with the septa retracted to improve sensitivity. Scatter correction and attenuation correction were employed in reconstruction to produce images with a resolution of 4.8 x 4.8 x 5.2mm. Images containing 31 contiguous slices were produced with voxel dimensions 2.09 x 2.09 x 3.43mm. High specific activity ^{11}C-flumazenil (FMZ) tracer was injected intravenously. A dynamic image sequence of 20 frames was acquired over 90 minutes.

FMZ-PET data analysis

The derivation of an arterial plasma input function was carried out as described previously (Cunningham and Jones 1993). Voxel-by-voxel parametric images of FMZ volume of distribution (FMZ-V_T) were produced using spectral analysis (Piredda and Gale 1986). For group analysis, eight datasets were flipped about the A/P axis to ensure that the epileptogenic focus was on the same (left) side in all patients. SPM was used for spatial transformations and statistical analysis. Firstly, all images were transformed into a standard space. An in-house created FMZ-V_T template that occupies the standard stereotaxic space defined by the Montreal Neurological Institute (MNI) / International Consortium for Brain Mapping (ICBM) 152 templates as supplied with SPM was right-left reversed (flipped), rigid-body co-registered onto itself and averaged using a soft mean, thus creating a symmetrical template approximating MNI/ICBM152 space. Secondly, the images were smoothed using a (10x10x6mm FWHM) Gaussian kernel to reduce high spatial frequency noise. Thirdly, effects were estimated according to the general linear model at every voxel. Global activity was included as a confounding covariate. Patients and normal subjects were compared using a voxel-wise t-test. To test hypotheses about regionally specific effects the estimates were compared using linear contrasts. The resulting set of voxel values for each contrast constituted a statistical parametric map of the t statistic (SPM{t}). For the comparison of the patient and normal groups, the SPM{t} were transformed to the unit normal distribution (SPM{Z}) and, since we had no a priori hypotheses with regard to the regions to be examined, an uncorrected threshold of $p<0.01$ was subjected to a correction for multiple non-independent comparisons in terms of peak height (μ) and

taking into account the shape of the thresholded volume (spatial extent (κ) at p<0.05), in order to allow the entire brain volume to be interrogated.[14] For the analysis of correlation between FMZ-V_T and seizure frequency, the total number of seizures that occurred during the month prior to the PET scan (as determined from patients' prospectively compiled diaries) was included in the model in a voxel-wise linear regression. Effects were significant at p<0.05 corrected for multiple comparisons using both peak height (μ) and spatial extent (κ) across the whole brain (Friston, Worsley et al. 1994).

Results

EEG-fMRI

We identified 19 patients who had well defined focal epilepsy syndromes (see Table 9.1.1-1 "EEG-fMRI" for patients' demographics).

We found a p<0.05 (corrected for multiple comparisons) correlation between IED occurrence and BOLD increase common to all 19 patients (i.e. typical for the group studied with 1-20 IED/min) in an area near the frontal piriform cortex ([X,Y,Z] = [-30, 6, -2], coordinates in Talairach space), on the same side as the presumed cortical epileptic focus (Figure 9.3.1-1, Table 9.5.1-2).

Brain region (approximate BA)	**X**	**Y**	**Z**	**cluster size [voxels]**	**Z-score**
	[Talairach space, mm]				
interictal discharge-correlated					
Region near left frontal prirform cortex, *area tempestas*	*-30*	*6*	*-2*	*162*	*3.55**
region around posterior horn of ventricle, near lingual gyrus, left	*-26*	*-52*	*4*	*117*	*3.70*
idem, right	*32*	*-45*	*-1*	*72*	*3.49*
region around anterior horn of ventricle, near forceps, right	*16*	*27*	*-3*	*72*	*3.46*
idem, left	*-10*	*27*	*-1*	*51*	*3.20*
right middle occipital gyrus (BA19)	*42*	*-77*	*11*	*66*	*3.52*
anterior cingulated	*0*	*32*	*13*	*87*	*3.41*
cingulate gyrus	*0*	*16*	*40*	*123*	*3.40*

* **p≤0.05 corrected**

Table 9.5.1-2: Results from the interictal-discharge correlated EEG-fMRI group analysis. Interictal discharge-correlated group analysis: The activation within the region of interest near the presumed Area tempestas was significant at p<0.05 (family wise error, FWE) when correcting for multiple comparisons across the search region (2744 mm3, see Methods). Across the whole brain and outside the search volume, more clusters reached similar Z-scores (maxima listed in this table in light grey) at an uncorrected threshold of p<0.001 at which figure 1 is displayed.

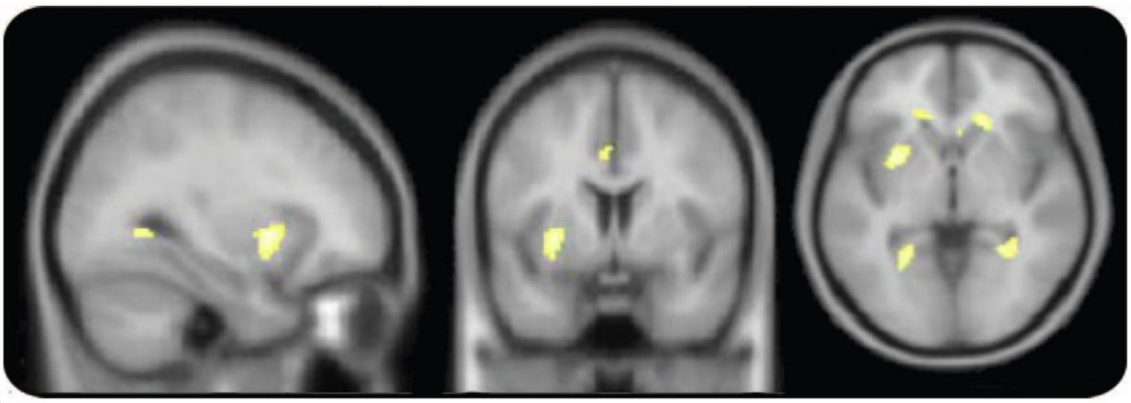

Figure 9.5.1-1: EEG-fMRI group analysis. Results of a second-level random-effects group analysis of 19 patients with focal epilepsy syndromes. For visualization, consistent common activations (p □ 0.001) are overlaid on axial slices of a mean T1-weighted template brain (X, Y, Z = -30, 6, -2, coordinates in Montreal Neurological Institute space). The activation within the region of interest near the presumed area tempestas was significant at $p < 0.05$ (family-wise error), when correcting for multiple comparisons across the search region (2,744 mm^3).

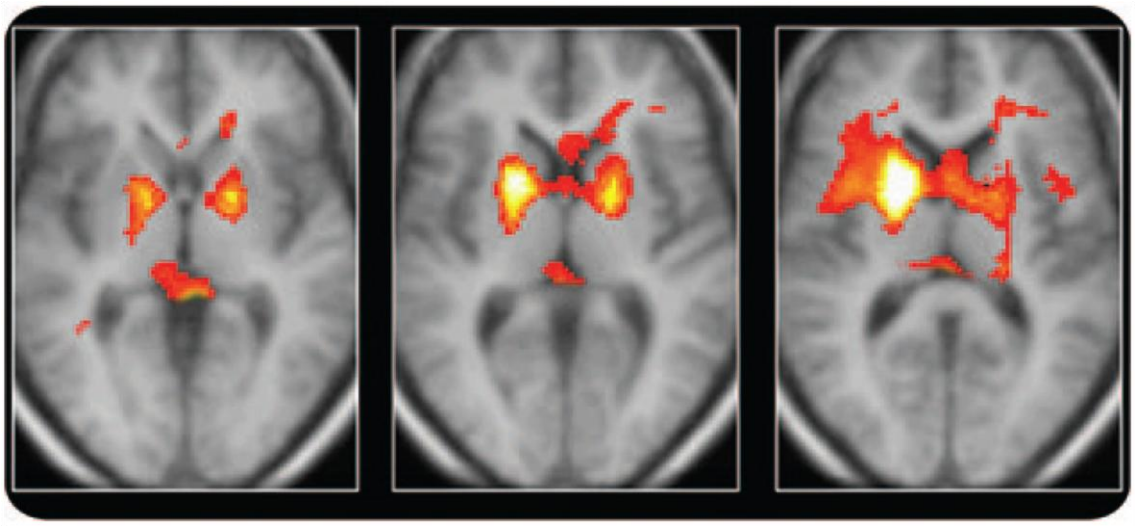

Figure 9.5.1-2: Flumazenil PET group comparison. Regions of significantly increased flumazenil volume of distribution in 18 patients with focal epilepsy syndromes compared with those of 24 normal control subjects. The hot metal color scale displays all voxels falling below $p < 0.01$ for display; increasing intensity corresponds to increased significance.

^{11}C- FMZ PET

The 18 patients had significant increases in FMZ volume of distribution (V_T) compared to the 24 controls, in the ipsilateral putamen (Z=5.21) and the contralateral putamen (Z=4.4) (Figure 9.5.1-2). These increases were apparent on single subject level in 13/18 patients. No regions of decreased FMZ-V_T were found. For comparison with the fMRI data, we analysed the data looking for regions in which FMZ-V_T correlated significantly with seizure frequency, confining attention only to those regions identified in the first

analysis. The lower the FMZ-V_T in the same area near the frontal piriform cortex, the higher was the seizure frequency over the preceding month (Z=3.97) (Figure 9.5.1-3). This correlation remained significant, even when removing the subject with very frequent seizures (>70/month). There were no significant correlations between increasing FMZ-V_T and seizure frequency.

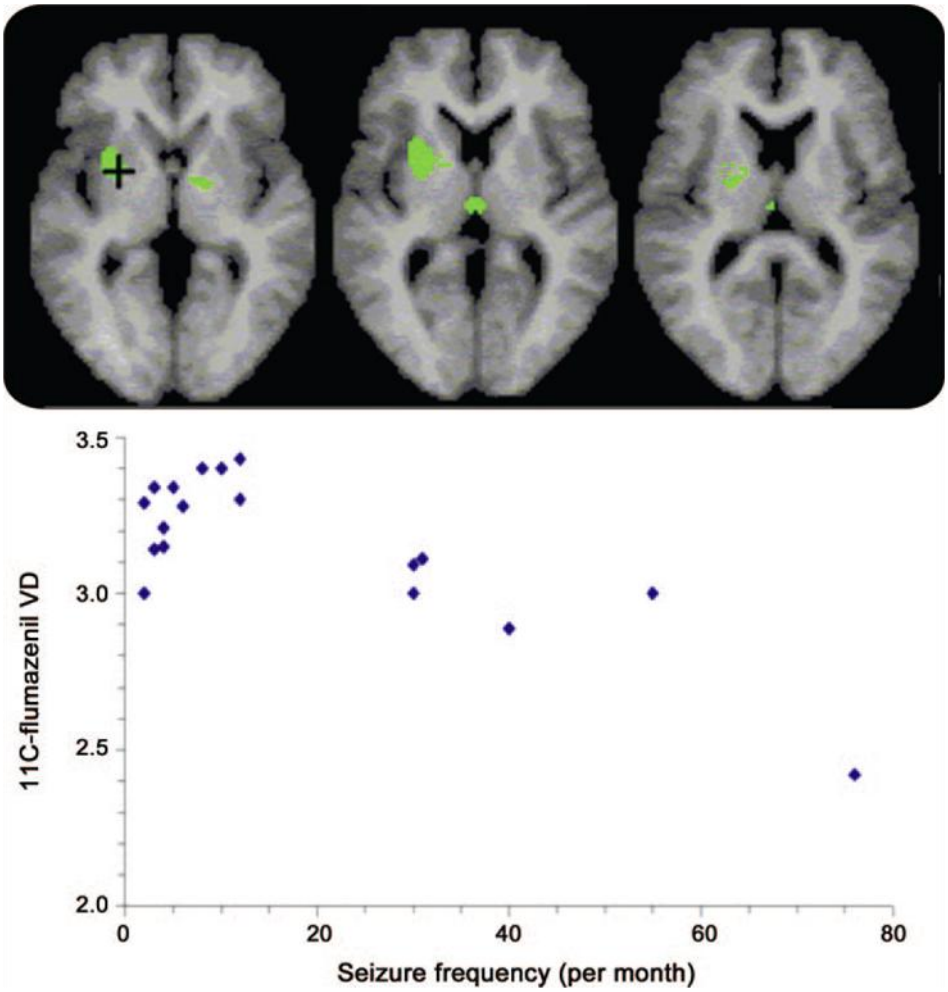

Figure 9.5.1-3: Flumazenil PET correlational analysis. *Top row*: Regions of increased flumazenil volume of distribution (VD) in 18 patients with focal epilepsy syndromes in a parametric analysis of patient data alone that showed reduced flumazenil binding with increased number of seizures per month ($p < 0.05$ corrected). *Bottom*: Scattergraph of seizure frequency vs flumazenil volume of distribution at the voxel with a maximum z score (indicated by + in the left panel).

Discussion

Our study is unique for two reasons: (1) By averaging the imaging data across a group of patients with different sites of seizure onset we were able to eliminate signal changes associated with sites of seizure onset (which varied across the patients), and selectively detect signal changes common to all cases. (2) In two independent data sets using two different imaging modalities, we identified an area in the human piriform (primary olfactory) cortex which was active in association with interictal EEG spikes,

and where benzodiazepine-$GABA_A$ receptor complex expression was reduced the higher the seizure frequency (Figure 9.5.1-4). This region is located in close proximity to the physiologically defined "deep piriform cortex" (or *"Area tempestas"*) from which convulsants are known to initiate temporal lobe seizures (Millan, Patel et al. 1986; Piredda and Gale 1986), and blockade of glutamate (Piredda and Gale 1985; Millan, Patel et al. 1986; Piredda and Gale 1986; Fornai, Busceti et al. 2005) or application of a GABA agonist in this area (Fornai, Busceti et al. 2005) reduce limbic motor seizures in rodents and non-human primates (Gale, Zhong et al. 1992).

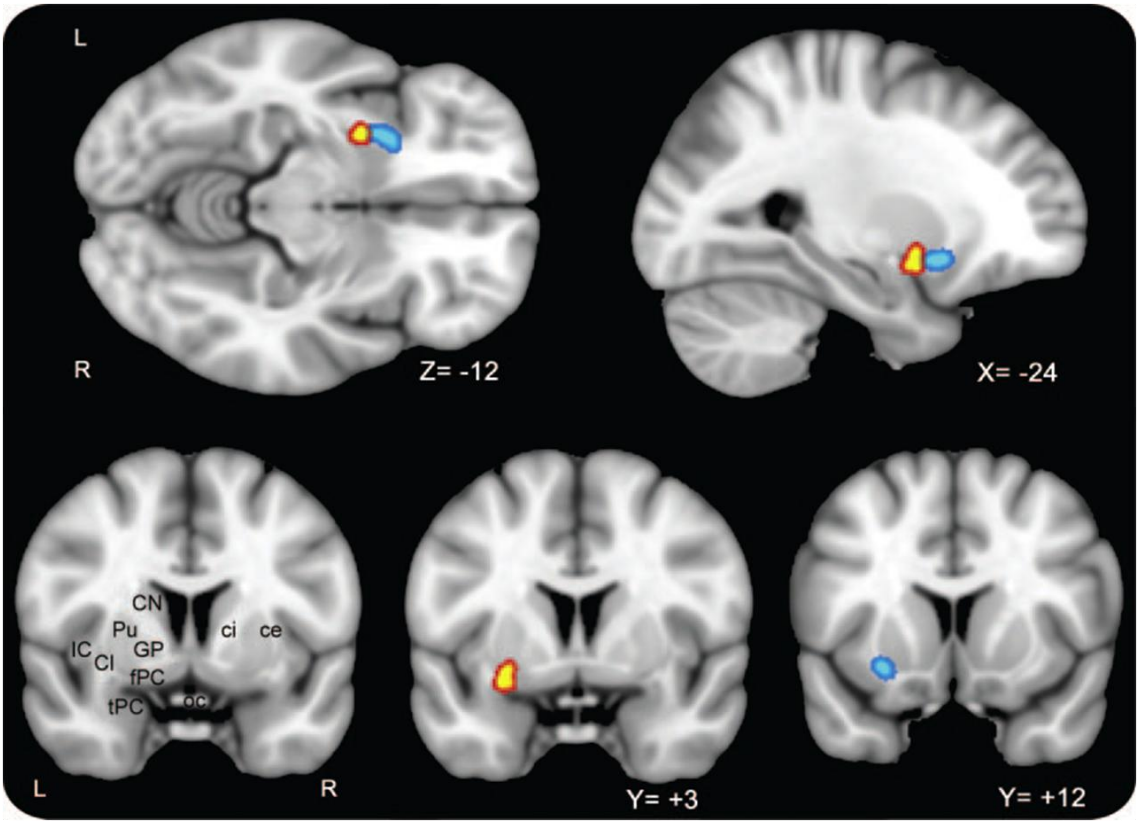

Figure 9.5.1-4: Combined EEG-fMRI/PET results. Clusters around the peak voxels for EEG-fMRI group analysis (yellow) and correlation between flumazenil binding and seizure frequency (blue) are superimposed on a T1 template. ce = capsula externa; ci = capsula interna; Cl = claustrum; CN = caudate nucleus; fPC = frontal piriform cortex; GP = globus pallidus; IC = insular cortex; oc = optic chiasm; Pu = putamen; tPC = temporal piriform cortex.

The piriform / primary olfactory cortex, because of its unique intrinsic associative fiber system and its various connections to and from other limbic nuclei (Löscher and Ebert 1996; Haberly 2001; Gottfried and Zald 2005), might be part of an epileptic network which is pivotal in the genesis of focal seizures, facilitating and intensifying the spread of seizures from a focus in hippocampus or other limbic sites to cortical and subcortical regions along pathways that are also utilized in normal movements (Haberly 2001; Wilson and Stevenson 2003; McIntyre and Gilby 2006; Howard, Plailly et al. 2009). The

deep piriform is a site at which unilateral microinjection of a GABA receptor antagonist or glutamate receptor agonists triggered limbic motor seizures in rats and non-human primates, whereas enhancement of GABA-mediated mechanisms reduced seizure activity. Prior to our study, there was no direct evidence implicating the piriform cortex in the pathogenesis of human epilepsy.

Our observed association of low FMZ-V_T in the human frontal piriform (primary olfactory) cortex with increased seizure frequency is concordant with findings in animal models of focal epilepsies. FMZ-V_T is directly correlated with central benzodiazepine receptor (cBZR) density (B_{max}) and hence may act as an index of $GABA_A$ density. Postsynaptic increases in the number of $GABA_A$ receptors underlying inhibitory potentiation in the kindling model have been described (Nusser, Hajos et al. 1998). Such an increase in available binding sites (or B_{max}) will lead to an increase in FMZ-V_T. Similarly, a recent study using the pilocarpine model has found pre- and postsynaptic changes of GABA transmission involving changes of $GABA_A$ receptor subunit composition (Brooks-Kayal, Shumate et al. 1998). Thus, increased density or affinity of available receptors per neuron, either on abnormal nerve cells or as an adaptive response to the abnormal neuronal activity may explain the observed increases of FMZ binding. If increased FMZ-receptor binding reflects increased GABA-ergic inhibition locally, the increased inhibition in this area would result in reduced cortical excitability in the lobe of seizure origin. Thus, we can speculate that the greater the increase in FMZ binding the fewer the seizures, as observed in this study. Similarly, greater reductions of FMZ binding were found the shorter the interval since the last seizure (Bouvard, Costes et al. 2005). This potential plasticity of receptors following seizures is consistent with our observation of greater reductions of FMZ binding the higher the seizure frequency. This holds true in particular for patients with frequent seizures (>10 / month, see Figure 9.5.1-4), but not necessarily for patients with very few seizures, in whom PET scans were performed at various intervals since the last seizure.

For group comparisons, the images of patients with clear right-sided focus were right-left reversed prior to normalization, making the focus appear on the same side in all patients. We have previously carefully investigated the influence of such right-left

reversals prior to spatial normalisation and we did not find a difference in the statistical results (Hammers, Koepp et al. 2003). In both, fMRI and PET groups, few patients had bilateral, or no localising features on MRI, EEG or seizure semiology, but "wrong" lateralisation would only reduce the likelyhood of observing an unilateral (ipsilateral) effect.

Our findings from combined haemodynamic and neuroreceptor imaging studies support the concept of a network of cortical and subcortical structures modulating epileptiform activity. Our group analysis will be less sensitive to IED-correlated BOLD signal changes reflecting potentially different irritative and seizure-onset zones but will highlight common features ("typical effects") in a group of patients. Despite exhibiting disparate sites of seizure foci, the patients in our study shared a common region of discharge-correlated activity. We restricted our analyses to EEG-fMRI studies with 1-20 IED per minute. This enabled us to make valid inferences at the group level using a two-stage procedure but limited the group size to 19 patients (Friston, Holmes et al. 1999). Violations of homoscedasticity implicit in the loss of balance at the first level can make the second level inference less efficient, but would not bias or invalidate it (Penny and Holmes 2006).

At the single subject level, there may be other areas fulfilling such a role, which failed to reach significance as a result of group averaging. Interestingly, recent PET studies have suggested that increased FMZ binding in one of these areas, the retro-ventricular area (Table 9.5.1-2), is predictive of poor surgical outcome (Hammers, Koepp et al. 2005). Although there is likely to be considerable individual variability in potential "epileptogenic networks", some areas are common to all networks, and may be potential target areas for new therapeutic approaches. Our findings support an understanding of epilepsy moving on from the traditional zone-concept to that of a network theory (Spencer 2002; Berg, Berkovic et al. 2010).

Conclusion

The discussed non-invasive *in vivo* EEG-fMRI epilepsy studies identified brain networks and states associated with (interictal) disease-specific EEG paroxysms highlighting the persistence of altered activity in typical sets of (sub-)cortical brain regions (e.g. thalamus vs. cortex in generalized; hippocampus vs. cortex in temporal lobe; a frontal

near-piriform region universally in focal epilepsies) responsible for the clinical manifestation of the disease and its underlying encephalopathy. Conceptualizing epilepsies as disturbed network interactions motivates – and requires - the development of multi-target and –modal treatments acting on these networks including physiological ones. *In silico* computational and modelling methods (Lytton 2008; Touboul, Wendling et al. 2011) need to be improved further as they should pave the way to the design of literally anti-epileptic therapeutic strategies (Blumenfeld 2011; Loeb 2011; Margineanu 2011; Winden, Karsten et al. 2011). Meanwhile, clinicians should remember that epilepsy is “always on” and all effort should be made not only to achieve seizure control but also to alleviate interictal pathology requiring multidimensional treatment (Laufs and Duncan 2007; Laufs 2012).

10 Overall conclusions and future work

Interictal activity-correlated EEG-fMRI was established as a useful adjunct to the preoperative work up of patients in whom surgery for focal epilepsy is being considered. The multi-modal method has gained its right among other diagnostic tools applied in the pre-surgical evaluation of patients by either spatially approximating the surgical target zone or by making negative predictions w.r.t. surgical success (Zijlmans, Huiskamp et al. 2007; Rosenkranz and Lemieux 2010; Thornton, Laufs et al. 2010; Thornton, Vulliemoz et al. 2011).

The present work is concerned with the use of EEG-fMRI beyond the identification of potentially epiletogenic tissue. It demonstrates the method's usefulness in the understanding of the neurobiology of epilepsy. Taking analyses of individual patients with the same class of epilepsy syndrome to the group level, brain regions commonly affected by interictal epileptic activity could be identified: the hippocampus in lateralized temporal lobe epilepsy, an area near the frontal piriform cortex in an unselected mix of focal epilepsies, and the thalamus in generalized epilepsy syndromes. In the two syndrome classes associated with dyscognitive seizures (temporal lobe and generalized epilepsies), changes were found in default mode brain regions fitting well the ictal semiology, because these are known to reduce their activity during states of reduced consciousness.

Identifying a patient's type of epilepsy based on EEG-fMRI will require an opposite approach: one would need to be able to classify an individual's (resting state) functional EEG-fMRI architecture such that the epilepsy syndrome present could be identified. Until the present day, this has not been achieved. However, after training with group data, a classifier algorithm (support vector machine) has been demonstrated to highly accurately identify specific brain states in individual subjects, and fMRI connectivity patterns have been linked to specific EEG features (Tagliazucchi, von Wegner et al. 2012; Tagliazucchi, von Wegner et al. 2012). Hence, establishing multimodal imaging as an adjunct tool to making a syndrome diagnosis in epilepsy appears a realistic and promising path to pursue.

We demonstrated that interictal epileptic discharges affect activity in a set of brain regions commonly identified also in healthy subjects in the form of a resting state network. The latter term describes brain regions robustly exhibiting coherent activity fluctuations which can be identified with fMRI using data driven methods such as independent component analysis (Fox and Raichle 2007) - including at the individual subject level. Specifically, such analyses can be performed on data recorded from epilepsy patients independent of the identification or presence of interictal scalp EEG changes (Rodionov, De Martino et al. 2007). Grounded on existing evidence that epilepsy affects the brain not only during a seizure but also during the state usually considered interictal (Laufs 2012), alterations in the common structure of resting state network activity in patients with epilepsy can be identified and compared to control data from healthy subjects exhibiting a comparable vigilance state (Tagliazucchi, von Wegner et al. 2012). In epilepsy patients, based on the observation of interictal changes it is intriguing to postulate a connection between them and transient cognitive impairment (Binnie 2003) – an issue deserving future attention.

The resulting implications are twofold: 1) Our understanding of the devastating effect epilepsy can have on the patients' lives beyond those directly caused by or linked to the seizures themselves (e.g. cognitive impairment, psychiatric conditions) can be furthered by identifying effects of the epilepsy syndrome on the resting state architecture of the brain. 2) Subjects with little or no interictal epileptiform activity on scalp EEG posit a fundamental challenge in EEG-fMRI studies (Laufs, Hamandi et al. 2006; Rodionov, De Martino et al. 2007; Grouiller, Thornton et al. 2011). At the same time, these patients are often those for whom the more established clinical investigations also fail to create clear hypotheses. Future studies should compare the resting state functional connectivity pattern of epilepsy patients at rest with that of healthy volunteers in order to pin down "hub regions" as potential therapeutic targets (Laufs 2012).

In conclusion, multimodal data integration has found entry into clinical practice. In addition, EEG-fMRI is a valuable tool in basic research of epilepsy when studying cognitive effects of (inter-)ictal activity, its spread and interaction with global brain

function (Laufs 2012). The recent development of concurrent recordings of intracranial EEG and fMRI (Carmichael, Thornton et al. 2010; Vulliemoz, Carmichael et al. 2011) and faster fMRI acquisition techniques (Zahneisen, Hugger et al. 2012) will open even wider avenues.

11 Bibliography

Aarts, J. H., C. D. Binnie, et al. (1984). "Selective cognitive impairment during focal and generalized epileptiform EEG activity." Brain **107 (Pt 1)**: 293-308.

AASM (2007). The AASM Manual for the Scoring of Sleep and Associated Events- Rules, Terminology and Technical Specifications. Chicago, American Academy of Sleep Medicine.

Achenbach, S., W. Moshage, et al. (1997). "Effects of magnetic resonance imaging on cardiac pacemakers and electrodes." Am Heart J **134**(3): 467-473.

Aghakhani, Y., A. P. Bagshaw, et al. (2004). "fMRI activation during spike and wave discharges in idiopathic generalized epilepsy." Brain **127**(Pt 5): 1127-1144.

Aghakhani, Y., E. Kobayashi, et al. (2005). "Cortical and thalamic fMRI responses in partial epilepsy with focal and bilateral synchronous spikes." Clin Neurophysiol.

Al-Asmi, A., C. G. Benar, et al. (2003). "fMRI activation in continuous and spike-triggered EEG-fMRI studies of epileptic spikes." Epilepsia **44**(10): 1328-1339.

Alarcon, G., J. J. Garcia Seoane, et al. (1997). "Origin and propagation of interictal discharges in the acute electrocorticogram. Implications for pathophysiology and surgical treatment of temporal lobe epilepsy." Brain **120 (Pt 12)**: 2259-2282.

Allen, P. J., O. Josephs, et al. (2000). "A method for removing imaging artifact from continuous EEG recorded during functional MRI." Neuroimage **12**(2): 230-239.

Allen, P. J., G. Polizzi, et al. (1998). "Identification of EEG events in the MR scanner: the problem of pulse artifact and a method for its subtraction." Neuroimage **8**(3): 229-239.

Amor, F., S. Baillet, et al. (2009). "Cortical local and long-range synchronization interplay in human absence seizure initiation." Neuroimage **45**(3): 950-962.

Anami, K., T. Mori, et al. (2003). "Stepping stone sampling for retrieving artifact-free electroencephalogram during functional magnetic resonance imaging." Neuroimage **19**(2 Pt 1): 281-295.

Anderer, P., G. Klosch, et al. (2001). "Low-resolution brain electromagnetic tomography revealed simultaneously active frontal and parietal sleep spindle sources in the human cortex." Neuroscience **103**(3): 581-592.

Andermann, F. and S. F. Berkovic (2001). "Idiopathic generalized epilepsy with generalized and other seizures in adolescence." Epilepsia **42**(3): 317-320.

Andreasen, N. C., D. S. O'Leary, et al. (1995). "Remembering the past: two facets of episodic memory explored with positron emission tomography." Am J Psychiatry **152**(11): 1576-1585.

Angelone, L. M., A. Potthast, et al. (2004). "Metallic electrodes and leads in simultaneous EEG-MRI: specific absorption rate (SAR) simulation studies." Bioelectromagnetics **25**(4): 285-295.

Angelone, L. M., C. E. Vasios, et al. (2006). "On the effect of resistive EEG electrodes and leads during 7 T MRI: simulation and temperature measurement studies." Magn Reson Imaging **24**(6): 801-812.

Archer, J. S., D. F. Abbott, et al. (2003). "fMRI "deactivation" of the posterior cingulate during generalized spike and wave." Neuroimage **20**(4): 1915-1922.

Archer, J. S., R. S. Briellman, et al. (2003). "Benign epilepsy with centro-temporal spikes: spike triggered fMRI shows somato-sensory cortex activity." Epilepsia **44**(2): 200-204.

Archer, J. S., R. S. Briellmann, et al. (2003). "Spike-triggered fMRI in reading epilepsy: involvement of left frontal cortex working memory area." Neurology **60**(3): 415-421.

Avoli, M., M. A. Rogawski, et al. (2001). "Generalized epileptic disorders: an update." Epilepsia **42**(4): 445-457.

Bagshaw, A. P., Y. Aghakhani, et al. (2004). "EEG-fMRI of focal epileptic spikes: analysis with multiple haemodynamic functions and comparison with gadolinium-enhanced MR angiograms." Hum Brain Mapp **22**(3): 179-192.

Bandettini, P. A., E. C. Wong, et al. (1992). "Time course EPI of human brain function during task activation." Magn Reson Med **25**(2): 390-397.

Barkley, G. L. and C. Baumgartner (2003). "MEG and EEG in epilepsy." J Clin Neurophysiol **20**(3): 163-178.

Bartenstein, P. A., J. S. Duncan, et al. (1993). "Investigation of the opioid system in absence seizures with positron emission tomography." J Neurol Neurosurg Psychiatry **56**(12): 1295-1302.

Baudewig, J., H. J. Bittermann, et al. (2001). "Simultaneous EEG and functional MRI of epileptic activity: a case report." Clin Neurophysiol **112**(7): 1196-1200.

Baumann, S. B. and D. C. Noll (1999). "A modified electrode cap for EEG recordings in MRI scanners." Clin Neurophysiol **110**(12): 2189-2193.

Beckmann, C. F., M. DeLuca, et al. (2005). "Investigations into resting-state connectivity using independent component analysis." Philosophical transactions of the Royal Society of London. Series B, Biological sciences **360**(1457): 1001-1013.

Beckmann, C. F. and S. M. Smith (2004). "Probabilistic independent component analysis for functional magnetic resonance imaging." IEEE transactions on medical imaging **23**(2): 137-152.

Beers, C. A. and P. Federico (2012). "Functional MRI applications in epilepsy surgery." The Canadian journal of neurological sciences. Le journal canadien des sciences neurologiques **39**(3): 271-285.

Bénar, C., Y. Aghakhani, et al. (2003). "Quality of EEG in simultaneous EEG-fMRI for epilepsy." Clin Neurophysiol **114**(3): 569-580.

Benar, C. G., D. W. Gross, et al. (2002). "The BOLD response to interictal epileptiform discharges." Neuroimage **17**(3): 1182-1192.

Berg, A. T., S. F. Berkovic, et al. (2010). "Revised terminology and concepts for organization of seizures and epilepsies: report of the ILAE Commission on Classification and Terminology, 2005-2009." Epilepsia **51**(4): 676-685.

Berger, H. (1929). "Über das Elektrenkephalogramm des Menschen." Archiv für Psychiatrie und Nervenkrankheiten **87**: 527-570.

Berkovic, S. F., F. Andermann, et al. (1987). "Concepts of absence epilepsies: discrete syndromes or biological continuum?" Neurology **37**(6): 993-1000.

Berman, R., M. Negishi, et al. (2010). "Simultaneous EEG, fMRI, and behavior in typical childhood absence seizures." Epilepsia **51**(10): 2011-2022.

Binder, J. R., J. A. Frost, et al. (1999). "Conceptual processing during the conscious resting state. A functional MRI study." J Cogn Neurosci **11**(1): 80-95.

Binnie, C. D. (2003). "Cognitive impairment during epileptiform discharges: is it ever justifiable to treat the EEG?" Lancet Neurol **2**(12): 725-730.

Biraben, A., F. Semah, et al. (2004). "PET evidence for a role of the basal ganglia in patients with ring chromosome 20 epilepsy." Neurology **63**(1): 73-77.

Birn, R. M., J. B. Diamond, et al. (2006). "Separating respiratory-variation-related fluctuations from neuronal-activity-related fluctuations in fMRI." Neuroimage **31**(4): 1536-1548.

Birn, R. M., M. A. Smith, et al. (2008). "The respiration response function: The temporal dynamics of fMRI signal fluctuations related to changes in respiration." Neuroimage **40**(2): 644-654.

Biswal, B., F. Z. Yetkin, et al. (1995). "Functional connectivity in the motor cortex of resting human brain using echo-planar MRI." Magn Reson Med **34**(4): 537-541.

Bloom, A. S., R. G. Hoffmann, et al. (1999). "Determination of drug-induced changes in functional MRI signal using a pharmacokinetic model." Hum Brain Mapp **8**(4): 235-244.

Blume, W. T., D. Ociepa, et al. (2001). "Frontal lobe seizure propagation: scalp and subdural EEG studies." Epilepsia **42**(4): 491-503.

Blumenfeld, H. (2011). "New strategies for preventing epileptogenesis: perspective and overview." Neurosci Lett **497**(3): 153-154.

Blumenfeld, H., K. A. McNally, et al. (2004). "Positive and negative network correlations in temporal lobe epilepsy." Cereb Cortex **14**(8): 892-902.

Blumenfeld, H., M. Rivera, et al. (2004). "Ictal neocortical slowing in temporal lobe epilepsy." Neurology **63**(6): 1015-1021.

Bode, H. (1992). "Intracranial blood flow velocities during seizures and generalized epileptic discharges." Eur J Pediatr **151**(9): 706-709.

Boly, M., C. Phillips, et al. (2008). "Intrinsic brain activity in altered states of consciousness: how conscious is the default mode of brain function?" Ann N Y Acad Sci **1129**: 119-129.

Bonelli, S. B., R. H. Powell, et al. (2010). "Imaging memory in temporal lobe epilepsy: predicting the effects of temporal lobe resection." Brain : a journal of neurology **133**(Pt 4): 1186-1199.

Bonmassar, G., N. Hadjikhani, et al. (2001). "Influence of EEG electrodes on the BOLD fMRI signal." Hum Brain Mapp **14**(2): 108-115.

Bonmassar, G., P. L. Purdon, et al. (2002). "Motion and ballistocardiogram artifact removal for interleaved recording of EEG and EPs during MRI." Neuroimage **16**(4): 1127-1141.

Born, A. P., I. Law, et al. (2002). "Cortical deactivation induced by visual stimulation in human slow-wave sleep." Neuroimage **17**(3): 1325-1335.

Bouilleret, V., F. Semah, et al. (2005). "Involvement of the basal ganglia in refractory epilepsy: an 18F-fluoro-L-DOPA PET study using 2 methods of analysis." J Nucl Med **46**(3): 540-547.

Bouvard, S., N. Costes, et al. (2005). "Seizure-related short-term plasticity of benzodiazepine receptors in partial epilepsy: a [11C]flumazenil-PET study." Brain : a journal of neurology **128**(Pt 6): 1330-1343.

Brazdil, M., M. Mikl, et al. (2007). "Effective connectivity in target stimulus processing: a dynamic causal modeling study of visual oddball task." Neuroimage **35**(2): 827-835.

Brodbeck, V., A. Kuhn, et al. (2012). "EEG microstates of wakefulness and NREM sleep." Neuroimage **62**(3): 2129-2139.

Bronstein, J. M., M. Tagliati, et al. (2011). "Deep brain stimulation for Parkinson disease: an expert consensus and review of key issues." Arch Neurol **68**(2): 165.

Brooks-Kayal, A. R., M. D. Shumate, et al. (1998). "Selective changes in single cell GABA(A) receptor subunit expression and function in temporal lobe epilepsy." Nat Med **4**(10): 1166-1172.

Buchheim, K., H. Obrig, et al. (2004). "Decrease in haemoglobin oxygenation during absence seizures in adult humans." Neurosci Lett **354**(2): 119-122.

Buckner, R. L., J. R. Andrews-Hanna, et al. (2008). "The brain's default network: anatomy, function, and relevance to disease." Annals of the New York Academy of Sciences **1124**: 1-38.

Burton, H., A. Z. Snyder, et al. (2004). "Default brain functionality in blind people." Proc Natl Acad Sci U S A **101**(43): 15500-15505.

Caporro, M., Z. Haneef, et al. (2011). "Functional MRI of sleep spindles and K-complexes." Clinical neurophysiology : official journal of the International Federation of Clinical Neurophysiology.

Carmichael, D., S. Vulliemoz, et al. (2011). Simultaneous Intracranial EEG-fMRI in Humans Suggests that High Gamma Frequencies are the Closest

Neurophysiological Correlate of BOLD fMRI. 19th Scientific Meeting of the ISMRM. Montréal, Book of Abstracts**:** 107.

Carmichael, D. W., J. S. Thornton, et al. (2008). "Safety of localizing epilepsy monitoring intracranial electroencephalograph electrodes using MRI: radiofrequency-induced heating." J Magn Reson Imaging **28**(5): 1233-1244.

Carmichael, D. W., J. S. Thornton, et al. (2010). "Feasibility of simultaneous intracranial EEG-fMRI in humans: a safety study." Neuroimage **49**(1): 379-390.

Cavanna, A. E. (2007). "The precuneus and consciousness." CNS Spectr **12**(7): 545-552.

Cavanna, A. E. and M. R. Trimble (2006). "The precuneus: a review of its functional anatomy and behavioural correlates." Brain **129**(Pt 3): 564-583.

Chan, S., T. Baldeweg, et al. (2011). "A role for sleep disruption in cognitive impairment in children with epilepsy." Epilepsy Behav **20**(3): 435-440.

Chaudhary, U. J., J. S. Duncan, et al. (2011). "Mapping hemodynamic correlates of seizures using fMRI: A review." Human Brain Mapping.

Clemens, B., M. Bessenyei, et al. (2007). "Characteristic distribution of interictal brain electrical activity in idiopathic generalized epilepsy." Epilepsia **48**(5): 941-949.

Commission on Classification and Terminology of the International League Against Epilepsy (1989). "Proposal for revised classification of epilepsies and epileptic syndromes." Epilepsia **30**(4): 389-399.

Craiu, D., S. Magureanu, et al. (2006). "Are absences truly generalized seizures or partial seizures originating from or predominantly involving the pre-motor areas? Some clinical and theoretical observations and their implications for seizure classification." Epilepsy research **70 Suppl 1**: S141-155.

Cunningham, V. J. and T. Jones (1993). "Spectral analysis of dynamic PET studies." J Cereb Blood Flow Metab **13**(1): 15-23.

Czisch, M., R. Wehrle, et al. (2004). "Functional MRI during sleep: BOLD signal decreases and their electrophysiological correlates." Eur J Neurosci **20**(2): 566-574.

Czisch, M., R. Wehrle, et al. (2009). "Acoustic oddball during NREM sleep: a combined EEG/fMRI study." PLoS One **4**(8): e6749.

Czisch, M., T. C. Wetter, et al. (2002). "Altered processing of acoustic stimuli during sleep: reduced auditory activation and visual deactivation detected by a combined fMRI/EEG study." Neuroimage **16**(1): 251-258.

Daunizeau, J., C. Grova, et al. (2007). "Symmetrical event-related EEG/fMRI information fusion in a variational Bayesian framework." Neuroimage **36**(1): 69-87.

Daunizeau, J., A. E. Vaudano, et al. (2010). "Bayesian multi-modal model comparison: a case study on the generators of the spike and the wave in generalized spike-wave complexes." Neuroimage **49**(1): 656-667.

David, O., I. Guillemain, et al. (2008). "Identifying neural drivers with functional MRI: an electrophysiological validation." PLoS Biol **6**(12): 2683-2697.

Davis, H., P. A. Davis, et al. (1937). "Changes in Human Brain Potentials during the Onset of Sleep." Science **86**(2237): 448-450.

De Luca, M., C. F. Beckmann, et al. (2006). "fMRI resting state networks define distinct modes of long-distance interactions in the human brain." Neuroimage **29**(4): 1359-1367.

De Martino, F., F. Gentile, et al. (2007). "Classification of fMRI independent components using IC-fingerprints and support vector machine classifiers." Neuroimage **34**(1): 177-194.

de Munck, J. C., S. I. Goncalves, et al. (2008). "A study of the brain's resting state based on alpha band power, heart rate and fMRI." Neuroimage **42**(1): 112-121.

De Simone, R., M. Silvestrini, et al. (1998). "Changes in cerebral blood flow velocities during childhood absence seizures." Pediatr Neurol **18**(2): 132-135.

De Tiege, X., S. Goldman, et al. (2011). "Neuronal networks in children with continuous spikes and waves during slow sleep." Brain : a journal of neurology **134**(Pt 5): e177.

De Tiege, X., S. Harrison, et al. (2007). "Impact of interictal epileptic activity on normal brain function in epileptic encephalopathy: an electroencephalography-functional magnetic resonance imaging study." Epilepsy Behav **11**(3): 460-465.

Debener, S., K. J. Mullinger, et al. (2007). "Properties of the ballistocardiogram artefact as revealed by EEG recordings at 1.5, 3 and 7 T static magnetic field strength." Int J Psychophysiol **2007 Jul 12 [Epub ahead of print]**: doi: 10.1016/j.ijpsycho.2007.1005.1010.

Debener, S., A. Strobel, et al. (2007). "Improved quality of auditory event-related potentials recorded simultaneously with 3-T fMRI: removal of the ballistocardiogram artefact." Neuroimage **34**(2): 587-597.

Dempsey, M. F., B. Condon, et al. (2001). "Investigation of the factors responsible for burns during MRI." J Magn Reson Imaging **13**(4): 627-631.

Depaulis, A., M. Vergnes, et al. (1994). "Endogenous control of epilepsy: the nigral inhibitory system." Prog Neurobiol **42**(1): 33-52.

Deransart, C., L. Vercueil, et al. (1998). "The role of basal ganglia in the control of generalized absence seizures." Epilepsy Res **32**(1-2): 213-223.

Desmond, J. E. and G. H. Glover (2002). "Estimating sample size in functional MRI (fMRI) neuroimaging studies: statistical power analyses." J Neurosci Methods **118**(2): 115-128.

Diehl, B. and J. S. Duncan (2011). Temporal lobe epilepsy. From Science to Society. Oxford, http://www.epilepsysociety.org.uk.

Diehl, B., S. Knecht, et al. (1998). "Cerebral hemodynamic response to generalized spike-wave discharges." Epilepsia **39**(12): 1284-1289.

Diehl, B., A. Salek-Haddadi, et al. (2003). "Mapping of spikes, slow waves, and motor tasks in a patient with malformation of cortical development using simultaneous EEG and fMRI." Magn Reson Imaging **21**(10): 1167-1173.

Duffy, F. H. and J. L. Burchfiel (1975). "Eye movement-related inhibition of primate visual neurons." Brain Res **89**(1): 121-132.

Duncan, J. S. (1997). "Idiopathic generalized epilepsies with typical absences." J Neurol **244**(7): 403-411.

Duncan, J. S. (2011). "Epilepsy in 2010: Refinement of optimal medical and surgical treatments." Nature reviews. Neurology **7**(2): 72-74.

Duncan, J. S. (2011). "Selecting patients for epilepsy surgery: synthesis of data." Epilepsy Behav **20**(2): 230-232.

Duncan, J. S. and M. J. Koepp (2000). "PET: central benzodiazepine neuroreceptor mapping in localization-related epilepsies." Advances in neurology **83**: 131-136.

Duncan, J. S. and H. J. Sagar (1987). "Seizure characteristics, pathology, and outcome after temporal lobectomy." Neurology **37**(3): 405-409.

Duncan, J. S., J. W. Sander, et al. (2006). "Adult epilepsy." Lancet **367**(9516): 1087-1100.

Ekstrand, J. J., M. E. Domroese, et al. (2001). "A new subdivision of anterior piriform cortex and associated deep nucleus with novel features of interest for olfaction and epilepsy." J Comp Neurol **434**(3): 289-307.

Ellingson, M. L., E. Liebenthal, et al. (2004). "Ballistocardiogram artifact reduction in the simultaneous acquisition of auditory ERPS and fMRI." Neuroimage **22**(4): 1534-1542.

Engel, J., Jr., P. Lubens, et al. (1985). "Local cerebral metabolic rate for glucose during petit mal absences." Ann Neurol **17**(2): 121-128.

Eriksson, S. H. (2011). "Epilepsy and sleep." Current opinion in neurology **24**(2): 171-176.

Faymonville, M. E., M. Boly, et al. (2006). "Functional neuroanatomy of the hypnotic state." J Physiol Paris **99**(4-6): 463-469.

Federico, P., D. F. Abbott, et al. (2005). "Functional MRI of the pre-ictal state." Brain **128**(Pt 8): 1811-1817.

Fink, A., R. H. Grabner, et al. (2005). "EEG alpha band dissociation with increasing task demands." Brain Res Cogn Brain Res **24**(2): 252-259.

Fisher, R. S., W. van Emde Boas, et al. (2005). "Epileptic seizures and epilepsy: definitions proposed by the International League Against Epilepsy (ILAE) and the International Bureau for Epilepsy (IBE)." Epilepsia **46**(4): 470-472.

Ford, M. R., S. Sands, et al. (2004). "Overview of artifact reduction and removal in evoked potential and event-related potential recordings." Phys Med Rehabil Clin N Am **15**(1): 1-17.

Fornai, F., C. L. Busceti, et al. (2005). "AMPA receptor desensitization as a determinant of vulnerability to focally evoked status epilepticus." Eur J Neurosci **21**(2): 455-463.

Forsgren, L., E. Beghi, et al. (2005). "The epidemiology of epilepsy in Europe - a systematic review." Eur J Neurol **12**(4): 245-253.

Fox, M. D. and M. E. Raichle (2007). "Spontaneous fluctuations in brain activity observed with functional magnetic resonance imaging." Nat Rev Neurosci **8**(9): 700-711.

Fox, M. D., A. Z. Snyder, et al. (2005). "From The Cover: The human brain is intrinsically organized into dynamic, anticorrelated functional networks." Proc Natl Acad Sci U S A **102**(27): 9673-9678.

Fox, M. D., A. Z. Snyder, et al. (2005). "The human brain is intrinsically organized into dynamic, anticorrelated functional networks." Proc Natl Acad Sci U S A **102**(27): 9673-9678.

Frackowiak, R. S. J. (1997). Human brain function. San Diego, Academic Press.

Fransson, P. (2005). "Spontaneous low-frequency BOLD signal fluctuations: An fMRI investigation of the resting-state default mode of brain function hypothesis." Hum Brain Mapp.

Fransson, P. (2005). "Spontaneous low-frequency BOLD signal fluctuations: an fMRI investigation of the resting-state default mode of brain function hypothesis." Hum Brain Mapp **26**(1): 15-29.

Fransson, P. (2006). "How default is the default mode of brain function? Further evidence from intrinsic BOLD signal fluctuations." Neuropsychologia **44**(14): 2836-2845.

Fransson, P. and G. Marrelec (2008). "The precuneus/posterior cingulate cortex plays a pivotal role in the default mode network: Evidence from a partial correlation network analysis." Neuroimage **42**(3): 1178-1184.

Freeman, W. J. (2004). "Origin, structure, and role of background EEG activity. Part 1. Analytic amplitude." Clinical neurophysiology : official journal of the International Federation of Clinical Neurophysiology **115**(9): 2077-2088.

Friston, K. (2009). "Causal modelling and brain connectivity in functional magnetic resonance imaging." PLoS Biol **7**(2): e33.

Friston, K. J., C. D. Frith, et al. (1990). "The relationship between global and local changes in PET scans." J Cereb Blood Flow Metab **10**(4): 458-466.

Friston, K. J., C. D. Frith, et al. (1991). "Comparing functional (PET) images: the assessment of significant change." J Cereb Blood Flow Metab **11**(4): 690-699.

Friston, K. J., L. Harrison, et al. (2003). "Dynamic causal modelling." Neuroimage **19**(4): 1273-1302.

Friston, K. J., A. P. Holmes, et al. (1999). "Multisubject fMRI studies and conjunction analyses." Neuroimage **10**(4): 385-396.

Friston, K. J., A. P. Holmes, et al. (1999). "How many subjects constitute a study?" Neuroimage **10**(1): 1-5.

Friston, K. J., O. Josephs, et al. (2000). "To smooth or not to smooth? Bias and efficiency in fMRI time-series analysis." Neuroimage **12**(2): 196-208.

Friston, K. J., K. E. Stephan, et al. (2005). "Mixed-effects and fMRI studies." Neuroimage **24**(1): 244-252.

Friston, K. J., S. Williams, et al. (1996). "Movement-related effects in fMRI time-series." Magn Reson Med **35**(3): 346-355.

Friston, K. J., K. J. Worsley, et al. (1994). "Assessing the significance of focal activations using their spatial extent." Human Brain Mapping **1**(3): 210-220.

Gale, K. (1995). "Chemoconvulsant seizures: advantages of focally-evoked seizure models." Ital J Neurol Sci **16**(1-2): 17-25.

Gale, K., P. Zhong, et al. (1992). "Amino acid neurotransmitter interactions in 'area tempestas': an epileptogenic trigger zone in the deep prepiriform cortex." Epilepsy research. Supplement **8**: 229-234.

Gallen, C. C., E. Tecoma, et al. (1997). "Magnetic source imaging of abnormal low-frequency magnetic activity in presurgical evaluations of epilepsy." Epilepsia **38**(4): 452-460.

Gambardella, A., J. Gotman, et al. (1995). "Focal intermittent delta activity in patients with mesiotemporal atrophy: a reliable marker of the epileptogenic focus." Epilepsia **36**(2): 122-129.

Garreffa, G., M. Carni, et al. (2003). "Real-time MR artifacts filtering during continuous EEG/fMRI acquisition." Magn Reson Imaging **21**(10): 1175-1189.

Garrido, M. I., J. M. Kilner, et al. (2007). "Dynamic causal modelling of evoked potentials: a reproducibility study." Neuroimage **36**(3): 571-580.

Geyer, J. D., E. Bilir, et al. (1999). "Significance of interictal temporal lobe delta activity for localization of the primary epileptogenic region." Neurology **52**(1): 202-205.

Gloor, P. (1968). "Generalized cortico-reticular epilepsies. Some considerations on the pathophysiology of generalized bilaterally synchronous spike and wave discharge." Epilepsia **9**(3): 249-263.

Gloor, P. (1978). "Generalized epilepsy with bilateral synchronous spike and wave discharge. New findings concerning its physiological mechanisms." Electroencephalogr Clin Neurophysiol Suppl(34): 245-249.

Gloor, P. (1986). "Consciousness as a neurological concept in epileptology: a critical review." Epilepsia **27 Suppl 2**: S14-26.

Gloor, P., M. Avoli, et al. (1990). Thalamo-cortical relationships in generalized epilepsy with bilaterally synchronous spike-and-wave discharge. Generalized epilepsy : neurobiological approaches

M. Avoli. Boston, Birkhäuser**:** xv, 481 p.

Gloor, P., J. Metrakos, et al. (1982). Neurophysiological, genetic and biochemical nature of the epileptic diathesis. Henry Gastaut and the Marseilles School's contribution to the neurosciences. R. J. Broughton. Amsterdam, Elsevier Biomedical Press**:** pp. 45–56.

Glover, G. H., T. Q. Li, et al. (2000). "Image-based method for retrospective correction of physiological motion effects in fMRI: RETROICOR." Magn Reson Med **44**(1): 162-167.

Goldman-Rakic, P. S. (1988). "Topography of cognition: parallel distributed networks in primate association cortex." Annu Rev Neurosci **11**: 137-156.

Goldman, R. I., J. M. Stern, et al. (2000). "Acquiring simultaneous EEG and functional MRI." Clin Neurophysiol **111**(11): 1974-1980.

Goldman, R. I., J. M. Stern, et al. (2002). "Simultaneous EEG and fMRI of the alpha rhythm." Neuroreport **13**(18): 2487-2492.

Goldman, R. I., J. M. Stern, et al. (2002). "Simultaneous EEG and fMRI of the alpha rhythm." Neuroreport **13**(18): 2487-2492.

Goncalves, S. I., P. J. Pouwels, et al. (2007). "Correction for desynchronization of EEG and fMRI clocks through data interpolation optimizes artifact reduction." Conf Proc IEEE Eng Med Biol Soc **2007**: 1590-1594.

Gotman, J., C. G. Benar, et al. (2004). "Combining EEG and FMRI in epilepsy: methodological challenges and clinical results." J Clin Neurophysiol **21**(4): 229-240.

Gotman, J., C. Grova, et al. (2005). "Generalized epileptic discharges show thalamocortical activation and suspension of the default state of the brain." Proc Natl Acad Sci U S A.

Gotman, J., C. Grova, et al. (2005). "Generalized epileptic discharges show thalamocortical activation and suspension of the default state of the brain." Proc Natl Acad Sci U S A **102**(42): 15236-15240.

Gotman, J., E. Kobayashi, et al. (2006). "Combining EEG and fMRI: a multimodal tool for epilepsy research." J Magn Reson Imaging **23**(6): 906-920.

Gottfried, J. A. and D. H. Zald (2005). "On the scent of human olfactory orbitofrontal cortex: meta-analysis and comparison to non-human primates." Brain research. Brain research reviews **50**(2): 287-304.

Greicius, M. D., B. Krasnow, et al. (2003). "Functional connectivity in the resting brain: a network analysis of the default mode hypothesis." Proc Natl Acad Sci U S A **100**(1): 253-258.

Greicius, M. D. and V. Menon (2004). "Default-mode activity during a passive sensory task: uncoupled from deactivation but impacting activation." J Cogn Neurosci **16**(9): 1484-1492.

Greicius, M. D., G. Srivastava, et al. (2004). "Default-mode network activity distinguishes Alzheimer's disease from healthy aging: evidence from functional MRI." Proc Natl Acad Sci U S A **101**(13): 4637-4642.

Grouiller, F., R. C. Thornton, et al. (2011). "With or without spikes: localization of focal epileptic activity by simultaneous electroencephalography and functional magnetic resonance imaging." Brain : a journal of neurology **134**(Pt 10): 2867-2886.

Grouiller, F., L. Vercueil, et al. (2007). "A comparative study of different artefact removal algorithms for EEG signals acquired during functional MRI." Neuroimage **38**(1): 124-137.

Grova, C., E. Kobayashi, et al. (2006). "BOLD responses in Temporal Lobe Epilepsy using Group Analysis (156-T PM)." NeuroImage

Twelfth Annual Meeting of the Organization for Human Brain Mapping **31**(Supplement 1): 29-185.

Guey, J., M. Bureau, et al. (1969). "A study of the rhythm of petit mal absences in children in relation to prevailing situations. The use of EEG telemetry during psychological examinations, school exercises and periods of inactivity." Epilepsia **10**(4): 441-451.

Gupte, A. A., D. Shrivastava, et al. (2011). "MRI-related heating near deep brain stimulation electrodes: more data are needed." Stereotactic and functional neurosurgery **89**(3): 131-140.

Gusnard, D. A., E. Akbudak, et al. (2001). "Medial prefrontal cortex and self-referential mental activity: relation to a default mode of brain function." Proc Natl Acad Sci U S A **98**(7): 4259-4264.

Gusnard, D. A. and M. E. Raichle (2001). "Searching for a baseline: functional imaging and the resting human brain." Nat Rev Neurosci **2**(10): 685-694.

Haberly, L. B. (2001). "Parallel-distributed processing in olfactory cortex: new insights from morphological and physiological analysis of neuronal circuitry." Chemical senses **26**(5): 551-576.

Haginoya, K., M. Munakata, et al. (2002). "Ictal cerebral haemodynamics of childhood epilepsy measured with near-infrared spectrophotometry." Brain **125**(Pt 9): 1960-1971.

Halasz, P. (2010). "The concept of epileptic networks. Part 1." Ideggyogy Sz **63**(9-10): 293-303.

Halasz, P. (2010). "The concept of epileptic networks. Part 2." Ideggyogy Sz **63**(11-12): 377-384.

Hamandi, K., H. Laufs, et al. (2007). "BOLD and perfusion changes during epileptic generalized spike wave activity." Neuroimage: doi:10.1016/j.neuroimage.2007.1007.1009.

Hamandi, K., H. Laufs, et al. (2008). "BOLD and perfusion changes during epileptic generalised spike wave activity." Neuroimage **39**(2): 608-618.

Hamandi, K., H. W. Powell, et al. (2008). "Combined EEG-fMRI and tractography to visualise propagation of epileptic activity." J Neurol Neurosurg Psychiatry **79**(5): 594-597.

Hamandi, K., A. Salek-Haddadi, et al. (2004). "EEG/functional MRI in epilepsy: The Queen Square Experience." J Clin Neurophysiol **21**(4): 241-248.

Hamandi, K., A. Salek-Haddadi, et al. (2004). "EEG/Functional MRI in Epilepsy: The Queen Square Experience." J Clin Neurophysiol **21**(4): 241-248.

Hamandi, K., A. Salek-Haddadi, et al. (2006). "EEG-fMRI of idiopathic and secondarily generalized epilepsies." Neuroimage **31**(4): 1700-1710.

Hamandi, K., A. Salek-Haddadi, et al. (2006). "EEG-fMRI of Generalised Spike-Wave Activity." Neuroimage **31**(4): 1700-1710.

Hamandi, K., A. Salek Haddadi, et al. (2005). "fMRI temporal clustering analysis in patients with frequent interictal epileptiform discharges: comparison with EEG-driven analysis." Neuroimage **26**(1): 309-316.

Hammers, A. (2004). "Flumazenil positron emission tomography and other ligands for functional imaging." Neuroimaging clinics of North America **14**(3): 537-551.

Hammers, A., M. J. Koepp, et al. (2005). "Periventricular white matter flumazenil binding and postoperative outcome in hippocampal sclerosis." Epilepsia **46**(6): 944-948.

Hammers, A., M. J. Koepp, et al. (2003). "Grey and white matter flumazenil binding in neocortical epilepsy with normal MRI. A PET study of 44 patients." Brain : a journal of neurology **126**(Pt 6): 1300-1318.

Handwerker, D. A., J. M. Ollinger, et al. (2004). "Variation of BOLD hemodynamic responses across subjects and brain regions and their effects on statistical analyses." Neuroimage **21**(4): 1639-1651.

Hanson, L. G., A. Skimminge, et al. (2006). "Encoding of EEG in MR images." Neuroimage (HBM abstract) **31**(S1): S131.

Henson, R. N., C. J. Price, et al. (2002). "Detecting latency differences in event-related BOLD responses: application to words versus nonwords and initial versus repeated face presentations." Neuroimage **15**(1): 83-97.

Herrmann, C. S. and S. Debener (2007). "Simultaneous recording of EEG and BOLD responses: A historical perspective." Int J Psychophysiol.

Hershey, T., F. J. Revilla, et al. (2003). "Cortical and subcortical blood flow effects of subthalamic nucleus stimulation in PD." Neurology **61**(6): 816-821.

Hill, R. A., K. H. Chiappa, et al. (1995). "EEG during MR imaging: differentiation of movement artifact from paroxysmal cortical activity." Neurology **45**(10): 1942-1943.

Hill, R. A., K. H. Chiappa, et al. (1999). "Hemodynamic and metabolic aspects of photosensitive epilepsy revealed by functional magnetic resonance imaging and magnetic resonance spectroscopy." Epilepsia **40**(7): 912-920.

Himanen, S. L. and J. Hasan (2000). "Limitations of Rechtschaffen and Kales." Sleep Med Rev **4**(2): 149-167.

Hoffmann, A., L. Jager, et al. (2000). "Electroencephalography during functional echo-planar imaging: detection of epileptic spikes using post-processing methods." Magn Reson Med **44**(5): 791-798.

Holmes, G. L., M. McKeever, et al. (1987). "Absence seizures in children: clinical and electroencephalographic features." Ann Neurol **21**(3): 268-273.

Holmes, M. D., M. Brown, et al. (2004). "Are "generalized" seizures truly generalized? Evidence of localized mesial frontal and frontopolar discharges in absence." Epilepsia **45**(12): 1568-1579.

Holtzheimer, P. E. and H. S. Mayberg (2011). "Deep brain stimulation for psychiatric disorders." Annu Rev Neurosci **34**: 289-307.

Howard, J. D., J. Plailly, et al. (2009). "Odor quality coding and categorization in human posterior piriform cortex." Nature neuroscience **12**(7): 932-938.

Huiskamp, G. J. (2005). "Reduction of the Ballistocardiogram Artifact in Simultaneous EEG-fMRI using ICA." Conf Proc IEEE Eng Med Biol Soc **4**: 3691-3694.

Iannetti, G. D., C. Di Bonaventura, et al. (2002). "fMRI/EEG in paroxysmal activity elicited by elimination of central vision and fixation." Neurology **58**(6): 976-979.

Iannetti, G. D. and R. G. Wise (2007). "BOLD functional MRI in disease and pharmacological studies: room for improvement?" Magn Reson Imaging **25**(6): 978-988.

Ives, J. R., S. Warach, et al. (1993). "Monitoring the patient's EEG during echo planar MRI." Electroencephalogr Clin Neurophysiol **87**(6): 417-420.

Jack, S., G. J. Kemp, et al. (2010). "Patterns of brain activity in response to respiratory stimulation in patients with idiopathic hyperventilation (IHV)." Advances in experimental medicine and biology **669**: 341-345.

Jacobs, J., E. Kobayashi, et al. (2007). "Hemodynamic Responses to Interictal Epileptiform Discharges in Children with Symptomatic Epilepsy." Epilepsia: doi:10.1111/j.1528-1167.2007.01192.x.

Jäger, L., K. J. Werhahn, et al. (2002). "Focal epileptiform activity in the brain: detection with spike-related functional MR imaging--preliminary results." Radiology **223**(3): 860-869.

Jahnke, K., F. von Wegner, et al. (2011). "To wake or not to wake? The two-sided nature of the human K-complex." Neuroimage.

Jahnke, K., F. von Wegner, et al. (2012). "To wake or not to wake? The two-sided nature of the human K-complex." Neuroimage **59**(2): 1631-1638.

Jasper, H. and J. Drooglever-Fortuyn (1947). "Experimental studies on the functional anatomy of petit mal epilepsy." Res Publ Assoc Nerv Ment Dis **26**(1): 272-298.

Jensen, F. E. (2011). "Epilepsy as a spectrum disorder: Implications from novel clinical and basic neuroscience." Epilepsia **52 Suppl 1**: 1-6.

Jensen, O. and A. Mazaheri (2010). "Shaping functional architecture by oscillatory alpha activity: gating by inhibition." Frontiers in human neuroscience **4**: 186.

Johnson, S. C., L. C. Baxter, et al. (2002). "Neural correlates of self-reflection." Brain **125**(Pt 8): 1808-1814.

Kemna, L. J. and S. Posse (2001). "Effect of respiratory CO(2) changes on the temporal dynamics of the hemodynamic response in functional MR imaging." Neuroimage **14**(3): 642-649.

Kherif, F., J. B. Poline, et al. (2002). "Multivariate model specification for fMRI data." Neuroimage **16**(4): 1068-1083.

Kiebel, S. J., M. I. Garrido, et al. (2009). "Dynamic causal modeling for EEG and MEG." Hum Brain Mapp **30**(6): 1866-1876.

Kiebel, S. J., M. I. Garrido, et al. (2008). "Dynamic causal modelling for EEG and MEG." Cogn Neurodyn **2**(2): 121-136.

Kilner, J. M., J. Mattout, et al. (2005). "Hemodynamic correlates of EEG: A heuristic." Neuroimage.

Kim, K. H., H. W. Yoon, et al. (2004). "Improved ballistocardiac artifact removal from the electroencephalogram recorded in fMRI." J Neurosci Methods **135**(1-2): 193-203.

Kinnari, K., J. H. Peter, et al. (2000). "Vigilance stages and performance in OSAS patients in a monotonous reaction time task." Clin Neurophysiol **111**(6): 1130-1136.

Kleinschmidt, A., H. Bruhn, et al. (1999). "Effects of sedation, stimulation, and placebo on cerebral blood oxygenation: a magnetic resonance neuroimaging study of psychotropic drug action." NMR Biomed **12**(5): 286-292.

Klingelhofer, J., C. Bischoff, et al. (1991). "Do brief bursts of spike and wave activity cause a cerebral hyper- or hypoperfusion in man?" Neurosci Lett **127**(1): 77-81.

Kobayashi, E., A. P. Bagshaw, et al. (2005). "Negative BOLD responses to epileptic spikes." Hum Brain Mapp.

Kochen, S., B. Giagante, et al. (2002). "Spike-and-wave complexes and seizure exacerbation caused by carbamazepine." Eur J Neurol **9**(1): 41-47.

Koepp, M. J., M. P. Richardson, et al. (1996). "Cerebral benzodiazepine receptors in hippocampal sclerosis. An objective in vivo analysis." Brain **119 (Pt 5)**: 1677-1687.

Koskinen, M. and N. Vartiainen (2009). "Removal of imaging artifacts in EEG during simultaneous EEG/fMRI recording: reconstruction of a high-precision artifact template." Neuroimage **46**(1): 160-167.

Kostopoulos, G. K. (2000). "Spike-and-wave discharges of absence seizures as a transformation of sleep spindles: the continuing development of a hypothesis." Clin Neurophysiol **111 Suppl 2**: S27-38.

Koutroumanidis, M., C. D. Binnie, et al. (1998). "Interictal regional slow activity in temporal lobe epilepsy correlates with lateral temporal hypometabolism as imaged with 18FDG PET: neurophysiological and metabolic implications." J Neurol Neurosurg Psychiatry **65**(2): 170-176.

Koutroumanidis, M., C. Martin-Miguel, et al. (2004). "Interictal temporal delta activity in temporal lobe epilepsy: correlations with pathology and outcome." Epilepsia **45**(11): 1351-1367.

Koutroumanidis, M., C. Martin-Miguel, et al. (1999). "Significance of interictal temporal lobe delta activity for localization of the primary epileptogenic region." Neurology **53**(8): 1892.

Krakow, K., P. J. Allen, et al. (2000). "Methodology: EEG-correlated fMRI." Adv Neurol **83**: 187-201.

Krakow, K., P. J. Allen, et al. (2000). "EEG recording during fMRI experiments: image quality." Hum Brain Mapp **10**(1): 10-15.

Krakow, K., F. G. Woermann, et al. (1999). "EEG-triggered functional MRI of interictal epileptiform activity in patients with partial seizures." Brain **122 (Pt 9)**: 1679-1688.

Kuzniecky, R. (1999). "Magnetic resonance spectroscopy in focal epilepsy: 31P and 1H spectroscopy." Revue neurologique **155**(6-7): 495-498.

Kuzniecky, R. (2004). "Clinical applications of MR spectroscopy in epilepsy." Neuroimaging clinics of North America **14**(3): 507-516.

Kwan, P., A. Arzimanoglou, et al. (2010). "Definition of drug resistant epilepsy: consensus proposal by the ad hoc Task Force of the ILAE Commission on Therapeutic Strategies." Epilepsia **51**(6): 1069-1077.

Labate, A., R. S. Briellmann, et al. (2005). "Typical childhood absence seizures are associated with thalamic activation." Epileptic Disord **7**(4): 373-377.

Laufs, H. (2008). "Endogenous brain oscillations and related networks detected by surface EEG-combined fMRI." Hum Brain Mapp **29**(7): 762-769.

Laufs, H. (2012). "Functional imaging of seizures and epilepsy: evolution from zones to networks." Curr Opin Neurol **25**(2): 194-200.

Laufs, H. (2012). "A personalized history of EEG-fMRI integration." Neuroimage **62**(2): 1056-1067.

Laufs, H., J. Daunizeau, et al. (2008). "Recent advances in recording electrophysiological data simultaneously with magnetic resonance imaging." Neuroimage **40**(2): 515-528.

Laufs, H. and J. S. Duncan (2007). "Electroencephalography/functional MRI in human epilepsy: what it currently can and cannot do." Curr Opin Neurol **20**(4): 417-423.

Laufs, H., K. Hamandi, et al. (2006). "Temporal lobe interictal epileptic discharges affect cerebral activity in "default mode" brain regions." Hum Brain Mapp **28**(10): 1923-1932.

Laufs, H., K. Hamandi, et al. (2007). "Temporal lobe interictal epileptic discharges affect cerebral activity in "default mode" brain regions." Human Brain Mapping **28**(10): 1023-1032.

Laufs, H., K. Hamandi, et al. (2006). "EEG-fMRI mapping of asymmetrical delta activity in a patient with refractory epilepsy is concordant with the epileptogenic region determined by intracranial EEG." Magn Reson Imaging **24**(4): 367-371.

Laufs, H., J. L. Holt, et al. (2006). "Where the BOLD signal goes when alpha EEG leaves." Neuroimage **31**(4): 1408-1418.

Laufs, H., A. Kleinschmidt, et al. (2003). "EEG-correlated fMRI of human alpha activity." Neuroimage **19**(4): 1463-1476.

Laufs, H., K. Krakow, et al. (2003). "Electroencephalographic signatures of attentional and cognitive default modes in spontaneous brain activity fluctuations at rest." Proc Natl Acad Sci U S A **100**(19): 11053-11058.

Laufs, H., U. Lengler, et al. (2005). "Linking generalized spike and wave discharges and resting state brain activity using EEG/fMRI in a patient with absence seizures." Epilepsia **in press**.

Laufs, H., U. Lengler, et al. (2006). "Linking Generalized Spike-and-Wave Discharges and Resting State Brain Activity by Using EEG/fMRI in a Patient with Absence Seizures." Epilepsia **47**(2): 444-448.

Laufs, H., M. P. Richardson, et al. (2011). "Converging PET and fMRI evidence for a common area involved in human focal epilepsies." Neurology **77**(9): 904-910.

Laufs, H., M. C. Walker, et al. (2007). "'Brain activation and hypothalamic functional connectivity during human non-rapid eye movement sleep: an EEG/fMRI study'--its limitations and an alternative approach." Brain **130**(Pt 7): e75; author reply e76.

Laufs, H., M. C. Walker, et al. (2007). ""Brain activation and hypothalamic functional connectivity during human non-rapid eye movement sleep: an EEG/fMRI study" - its limitations and an alternative approach." Brain **130**(Pt 7): e75.

Laureys, S., A. M. Owen, et al. (2004). "Brain function in coma, vegetative state, and related disorders." Lancet Neurol **3**(9): 537-546.

Laureys, S., F. Perrin, et al. (2004). "Cerebral processing in the minimally conscious state." Neurology **63**(5): 916-918.

Lazeyras, F., I. Zimine, et al. (2001). "Functional MRI with simultaneous EEG recording: feasibility and application to motor and visual activation." J Magn Reson Imaging **13**(6): 943-948.

Leclercq, Y., J. Schrouff, et al. (2011). "FMRI artefact rejection and sleep scoring toolbox." Comput Intell Neurosci **2011**: 598206.

Lehmann, D. and T. Koenig (1997). "Spatio-temporal dynamics of alpha brain electric fields, and cognitive modes." Int J Psychophysiol **26**(1-3): 99-112.

Leichnetz, G. R. (2001). "Connections of the medial posterior parietal cortex (area 7m) in the monkey." Anat Rec **263**(2): 215-236.

Lemieux, L., P. J. Allen, et al. (1997). "Recording of EEG during fMRI experiments: patient safety." Magn Reson Med **38**(6): 943-952.

Lemieux, L., H. Laufs, et al. (2008). "Noncanonical spike-related BOLD responses in focal epilepsy." Hum Brain Mapp **29**(3): 329-345.

Lemieux, L., A. Salek-Haddadi, et al. (2001). "Event-related fMRI with simultaneous and continuous EEG: description of the method and initial case report." Neuroimage **14**(3): 780-787.

Lemieux, L., A. Salek-Haddadi, et al. (2007). "Modelling large motion events in fMRI studies of patients with epilepsy." Magn Reson Imaging **25**(6): 894-901.

Lin, J. J., M. Mula, et al. (2012). "Uncovering the neurobehavioural comorbidities of epilepsy over the lifespan." Lancet **380**(9848): 1180-1192.

Liston, A. D., J. C. De Munck, et al. (2006). "Analysis of EEG-fMRI data in focal epilepsy based on automated spike classification and Signal Space Projection." Neuroimage **31**(3): 1015-1024.

Liston, A. D., T. E. Lund, et al. (2006). "Modelling cardiac signal as a confound in EEG-fMRI and its application in focal epilepsy studies." Neuroimage **30**(3): 827-834.

Loeb, J. A. (2011). "Identifying targets for preventing epilepsy using systems biology." Neuroscience letters **497**(3): 205-212.

Logothetis, N. K., J. Pauls, et al. (2001). "Neurophysiological investigation of the basis of the fMRI signal." Nature **412**(6843): 150-157.

Loomis, A. L., E. N. Harvey, et al. (1935). "Potential Rhythms of the Cerebral Cortex during Sleep." Science **81**(2111): 597-598.

Loomis, A. L., E. N. Harvey, et al. (1935). "Further observations on the potential rhythms of the cerebral cortex during sleep." Science(82): 198-200.

Loomis, A. L., E. N. Harvey, et al. (1937). "Cerebral states during sleep, as studied by human brain potentials." J Exp Psychol(21): 127-144.

Löscher, W. and U. Ebert (1996). "The role of the piriform cortex in kindling." Progress in neurobiology **50**(5-6): 427-481.

Luessi, M., S. D. Babacan, et al. (2011). "Bayesian symmetrical EEG/fMRI fusion with spatially adaptive priors." Neuroimage **55**(1): 113-132.

Lund, T. E., M. D. Norgaard, et al. (2005). "Motion or activity: their role in intra- and inter-subject variation in fMRI." Neuroimage **26**(3): 960-964.

Lytton, W. W. (2008). "Computer modelling of epilepsy." Nature reviews. Neuroscience **9**(8): 626-637.

Mahadevan, A., D. H. Mugler, et al. (2008). "Adaptive filtering of ballistocardiogram artifact from EEG signals using the dilated discrete Hermite transform." Conf Proc IEEE Eng Med Biol Soc **2008**: 2630-2633.

Mandelkow, H., D. Brandeis, et al. (2010). "Good practices in EEG-MRI: the utility of retrospective synchronization and PCA for the removal of MRI gradient artefacts." Neuroimage **49**(3): 2287-2303.

Mandelkow, H., P. Halder, et al. (2006). "Synchronization facilitates removal of MRI artefacts from concurrent EEG recordings and increases usable bandwidth." Neuroimage **32**(3): 1120-1126.

Mantini, D., M. G. Perrucci, et al. (2007). "Complete artifact removal for EEG recorded during continuous fMRI using independent component analysis." Neuroimage **34**(2): 598-607.

Maquet, P. (2000). "Functional neuroimaging of normal human sleep by positron emission tomography." J Sleep Res **9**(3): 207-231.

Marcus, E. M. and C. W. Watson (1968). "Symmetrical epileptogenic foci in monkey cerebral cortex. Mechanisms of interaction and regional variations in capacity for synchronous discharges." Arch Neurol **19**(1): 99-116.

Marcus, E. M., C. W. Watson, et al. (1968). "An experimental model of some varieties of petit mal epilepsy. Electrical-behavioral correlations of acute bilateral epileptogenic foci in cerebral cortex." Epilepsia **9**(3): 233-248.

Margineanu, D. G. (2011). "Systems biology impact on antiepileptic drug discovery." Epilepsy Res.

Masterton, R. A., D. F. Abbott, et al. (2007). "Measurement and reduction of motion and ballistocardiogram artefacts from simultaneous EEG and fMRI recordings." Neuroimage **37**(1): 202-211.

Mazoyer, B., L. Zago, et al. (2001). "Cortical networks for working memory and executive functions sustain the conscious resting state in man." Brain Res Bull **54**(3): 287-298.

McGuire, P. K., E. Paulesu, et al. (1996). "Brain activity during stimulus independent thought." Neuroreport **7**(13): 2095-2099.

McIntyre, D. C. and K. L. Gilby (2006). "Parahippocampal networks, intractability, and the chronic epilepsy of kindling." Advances in neurology **97**: 77-83.

McLean, M. A. and J. J. Cross (2009). "Magnetic resonance spectroscopy: principles and applications in neurosurgery." British journal of neurosurgery **23**(1): 5-13.

Meeren, H., G. van Luijtelaar, et al. (2005). "Evolving concepts on the pathophysiology of absence seizures: the cortical focus theory." Arch Neurol **62**(3): 371-376.

Meeren, H. K., J. P. Pijn, et al. (2002). "Cortical focus drives widespread corticothalamic networks during spontaneous absence seizures in rats." J Neurosci **22**(4): 1480-1495.

Meyer, C., J. Fernandez Gavela, et al. (2006). "Combining algorithms in automatic detection of QRS complexes in ECG signals." IEEE Trans Inf Technol Biomed **10**(3): 468-475.

Michal, M., C. Roder, et al. (2007). "Spontaneous dissociation during functional MRI experiments." J Psychiatr Res **41**(1-2): 69-73.

Millan, M. H., S. Patel, et al. (1986). "Focal injection of 2-amino-7-phosphonoheptanoic acid into prepiriform cortex protects against pilocarpine-induced limbic seizures in rats." Neurosci Lett **70**(1): 69-74.

Mizobuchi, M., N. Ito, et al. (1999). "Unidirectional olfactory hallucination associated with ipsilateral unruptured intracranial aneurysm." Epilepsia **40**(4): 516-519.

Moeller, F., H. R. Siebner, et al. (2009). "fMRI activation during spike and wave discharges evoked by photic stimulation." Neuroimage **48**(4): 682-695.

Moeller, F., H. R. Siebner, et al. (2008). "Changes in activity of striato-thalamo-cortical network precede generalized spike wave discharges." Neuroimage **39**(4): 1839-1849.

Moeller, F., H. R. Siebner, et al. (2009). "Mapping brain activity on the verge of a photically induced generalized tonic-clonic seizure." Epilepsia **50**(6): 1632-1637.

Moosmann, M., P. Ritter, et al. (2003). "Correlates of alpha rhythm in functional magnetic resonance imaging and near infrared spectroscopy." Neuroimage **20**(1): 145-158.

Moosmann, M., V. H. Schonfelder, et al. (2009). "Realignment parameter-informed artefact correction for simultaneous EEG-fMRI recordings." Neuroimage **45**(4): 1144-1150.

Morgan, V. L., R. R. Price, et al. (2004). "Resting functional MRI with temporal clustering analysis for localization of epileptic activity without EEG." Neuroimage **21**(1): 473-481.

Morillon, B., K. Lehongre, et al. (2010). "Neurophysiological origin of human brain asymmetry for speech and language." Proc Natl Acad Sci U S A **107**(43): 18688-18693.

Morrell, M. (2006). "Brain stimulation for epilepsy: can scheduled or responsive neurostimulation stop seizures?" Curr Opin Neurol **19**(2): 164-168.

Mullinger, K., S. Debener, et al. (2007). "Effects of simultaneous EEG recording on MRI data quality at 1.5, 3 and 7 tesla." Int J Psychophysiol **2007 Aug 7 [Epub ahead of print]**: doi:10.1016/j.ijpsycho.2007.1006.1008.

Mullinger, K. J., W. X. Yan, et al. (2011). "Reducing the gradient artefact in simultaneous EEG-fMRI by adjusting the subject's axial position." Neuroimage **54**(3): 1942-1950.

Nagai, Y., H. D. Critchley, et al. (2004). "Brain activity relating to the contingent negative variation: an fMRI investigation." Neuroimage **21**(4): 1232-1241.

Nagai, Y., H. D. Critchley, et al. (2004). "Activity in ventromedial prefrontal cortex covaries with sympathetic skin conductance level: a physiological account of a "default mode" of brain function." Neuroimage **22**(1): 243-251.

Nakamura, W., K. Anami, et al. (2006). "Removal of ballistocardiogram artifacts from simultaneously recorded EEG and fMRI data using independent component analysis." IEEE Trans Biomed Eng **53**(7): 1294-1308.

Negishi, M., M. Abildgaard, et al. (2004). "Removal of time-varying gradient artifacts from EEG data acquired during continuous fMRI." Clin Neurophysiol **115**(9): 2181-2192.

Negishi, M., B. I. Pinus, et al. (2007). "Origin of the radio frequency pulse artifact in simultaneous EEG-fMRI recording: rectification at the carbon-metal interface." IEEE Trans Biomed Eng **54**(9): 1725-1727.

Neuner, I., T. Warbrick, et al. (2011). EEG Acquisition in Ultra-High Static Magnetic Field Up to 9.4T. 19th Scientific Meeting of the ISMRM. Montréal, Book of Abstracts**:** 1557.

Neuper, C. and G. Pfurtscheller (2001). "Event-related dynamics of cortical rhythms: frequency-specific features and functional correlates." Int J Psychophysiol **43**(1): 41-58.

Niazy, R. K., C. F. Beckmann, et al. (2005). "Removal of FMRI environment artifacts from EEG data using optimal basis sets." Neuroimage **28**(3): 720-737.

Niedermeyer, E. (1966). "Generalized seizure discharges and possible precipitating mechanisms." Epilepsia **7**(1): 23-29.

Niedermeyer, E. (1997). "Alpha rhythms as physiological and abnormal phenomena." Int J Psychophysiol **26**(1-3): 31-49.

Niedermeyer, E., E. R. Laws, Jr., et al. (1969). "Depth EEG findings in epileptics with generalized spike-wave complexes." Arch Neurol **21**(1): 51-58.

Nöth, U., H. Laufs, et al. (2010). Safety in EEG-MRI: Heating Beneath EEG Scalp Electrodes for Different RF Transmit Coils. 18th Scientific Meeting of the ISMRM. Stockholm, Book of Abstracts**:** 3889.

Nöth, U., H. Laufs, et al. (2012). "Simultaneous electroencephalography-functional MRI at 3 T: an analysis of safety risks imposed by performing anatomical reference scans with the EEG equipment in place." Journal of magnetic resonance imaging : JMRI **35**(3): 561-571.

Nunez, P. L. and R. B. Silberstein (2000). "On the relationship of synaptic activity to macroscopic measurements: does co-registration of EEG with fMRI make sense?" Brain Topogr **13**(2): 79-96.

Nusser, Z., N. Hajos, et al. (1998). "Increased number of synaptic GABA(A) receptors underlies potentiation at hippocampal inhibitory synapses." Nature **395**(6698): 172-177.

Ochs, R. F., P. Gloor, et al. (1987). "Effect of generalized spike-and-wave discharge on glucose metabolism measured by positron emission tomography." Ann Neurol **21**(5): 458-464.

Ogawa, S., T. M. Lee, et al. (1990). "Brain magnetic resonance imaging with contrast dependent on blood oxygenation." Proc Natl Acad Sci U S A **87**(24): 9868-9872.

Ota, T., R. Toyoshima, et al. (1996). "Measurements by biphasic changes of the alpha band amplitude as indicators of arousal level." Int J Psychophysiol **24**(1-2): 25-37.

Ota, T., R. Toyoshima, et al. (1996). "Measurements by biphasic changes of the alpha band amplitude as indicators of arousal level." International journal of psychophysiology : official journal of the International Organization of Psychophysiology **24**(1-2): 25-37.

Otzenberger, H., D. Gounot, et al. (2007). "Optimisation of a post-processing method to remove the pulse artifact from EEG data recorded during fMRI: an application to P300 recordings during e-fMRI." Neurosci Res **57**(2): 230-239.

Pacia, S. V. and J. S. Ebersole (1997). "Intracranial EEG substrates of scalp ictal patterns from temporal lobe foci." Epilepsia **38**(6): 642-654.

Parkes, L. M., P. Fries, et al. (2004). "Reduced BOLD response to periodic visual stimulation." Neuroimage **21**(1): 236-243.

Penny, W. and A. Holmes (2006). Random Effects Analysis. Human brain function. J. A. K. Friston, S. Kiebel, T. Nichols, W. Penny. San Diego, Academic Press.

Penny, W. D., K. E. Stephan, et al. (2004). "Comparing dynamic causal models." Neuroimage **22**(3): 1157-1172.

Petrides, M. and D. N. Pandya (1984). "Projections to the frontal cortex from the posterior parietal region in the rhesus monkey." J Comp Neurol **228**(1): 105-116.

Petsche, H., S. Kaplan, et al. (1997). "The possible meaning of the upper and lower alpha frequency ranges for cognitive and creative tasks." Int J Psychophysiol **26**(1-3): 77-97.

Pfurtscheller, G., A. Stancak, Jr., et al. (1996). "Event-related synchronization (ERS) in the alpha band--an electrophysiological correlate of cortical idling: a review." International journal of psychophysiology : official journal of the International Organization of Psychophysiology **24**(1-2): 39-46.

Pfurtscheller, G., A. Stancak, Jr., et al. (1996). "Event-related synchronization (ERS) in the alpha band--an electrophysiological correlate of cortical idling: a review." Int J Psychophysiol **24**(1-2): 39-46.

Pictet, J., R. Meuli, et al. (2002). "Radiofrequency heating effects around resonant lengths of wire in MRI." Phys Med Biol **47**(16): 2973-2985.

Piredda, S. and K. Gale (1985). "A crucial epileptogenic site in the deep prepiriform cortex." Nature **317**(6038): 623-625.

Piredda, S. and K. Gale (1986). "Anticonvulsant action of 2-amino-7-phosphonoheptanoic acid and muscimol in the deep prepiriform cortex." Eur J Pharmacol **120**(1): 115-118.

Polack, P. O., I. Guillemain, et al. (2007). "Deep layer somatosensory cortical neurons initiate spike-and-wave discharges in a genetic model of absence seizures." J Neurosci **27**(24): 6590-6599.

Post, M., H. van Duinen, et al. (2007). "Reduced cortical activity during maximal bilateral contractions of the index finger." Neuroimage **35**(1): 16-27.

Powell, H. W. and J. S. Duncan (2005). "Functional magnetic resonance imaging for assessment of language and memory in clinical practice." Current opinion in neurology **18**(2): 161-166.

Power, J. D., A. L. Cohen, et al. (2011). "Functional network organization of the human brain." Neuron **72**(4): 665-678.

Prevett, M. C., J. S. Duncan, et al. (1995). "Demonstration of thalamic activation during typical absence seizures using H2(15)O and PET." Neurology **45**(7): 1396-1402.

Raichle, M. E., A. M. MacLeod, et al. (2001). "A default mode of brain function." Proc Natl Acad Sci U S A **98**(2): 676-682.

Raichle, M. E. and A. Z. Snyder (2007). "A default mode of brain function: a brief history of an evolving idea." Neuroimage **37**(4): 1083-1090; discussion 1097-1089.

Rasche, D., P. C. Rinaldi, et al. (2006). "Deep brain stimulation for the treatment of various chronic pain syndromes." Neurosurg Focus **21**(6): E8.

Ray, W. J. and H. W. Cole (1985). "EEG alpha activity reflects attentional demands, and beta activity reflects emotional and cognitive processes." Science **228**(4700): 750-752.

Rechtschaffen, A. and A. A. Kales (1968). A manual of standardized terminology, techniques and scoring system for sleep stages of human subjects. Washington, D.C.

Rechtschaffen, A. and A. A. Kales (1968). A manual of standardized terminology, techniques and scoring system for sleep stages of human subjects. Washington, D.C., Government Printing Office.

Ricci, G. B., D. De Carli, et al. (2004). "Hemodynamic response (BOLD/fMRI) in focal epilepsy with reference to benzodiazepine effect." Magn Reson Imaging **22**(10): 1487-1492.

Richardson, M. P., P. Grosse, et al. (2006). "BOLD correlates of EMG spectral density in cortical myoclonus: description of method and case report." Neuroimage **32**(2): 558-565.

Ritter, P., R. Becker, et al. (2007). "Evaluating gradient artifact correction of EEG data acquired simultaneously with fMRI." Magn Reson Imaging **25**(6): 923-932.

Ritter, P. and A. Villringer (2006). "Simultaneous EEG-fMRI." Neurosci Biobehav Rev **30**(6): 823-838.

Rodionov, R., F. De Martino, et al. (2007). "Independent component analysis of interictal fMRI in focal epilepsy: comparison with general linear model-based EEG-correlated fMRI." Neuroimage **38**(3): 488-500.

Rosa, M. J., J. Daunizeau, et al. (2010). "EEG-fMRI integration: a critical review of biophysical modeling and data analysis approaches." Journal of integrative neuroscience **9**(4): 453-476.

Rosenkranz, K. and L. Lemieux (2010). "Present and future of simultaneous EEG-fMRI." MAGMA.

Rosenow, F. and H. Luders (2001). "Presurgical evaluation of epilepsy." Brain **124**(Pt 9): 1683-1700.

Rosenow, F. and H. Lüders (2001). "Presurgical evaluation of epilepsy." Brain **124**(Pt 9): 1683-1700.

Roth, B. (1961). "The clinical and theoretical importance of EEG rhythms corresponding to states of lowered vigilance." Electroencephalography and clinical neurophysiology **13**: 395-399.

Rowan, A., F. Liegeois, et al. (2004). "Cortical lateralization during verb generation: a combined ERP and fMRI study." Neuroimage **22**(2): 665-675.

Ryali, S., G. H. Glover, et al. (2009). "Development, validation, and comparison of ICA-based gradient artifact reduction algorithms for simultaneous EEG-spiral in/out and echo-planar fMRI recordings." Neuroimage **48**(2): 348-361.

Salanova, V. and R. Worth (2007). "Neurostimulators in epilepsy." Curr Neurol Neurosci Rep **7**(4): 315-319.

Salek-Haddadi, A., B. Diehl, et al. (2006). "Hemodynamic correlates of epileptiform discharges: an EEG-fMRI study of 63 patients with focal epilepsy." Brain Res **1088**(1): 148-166.

Salek-Haddadi, A., K. J. Friston, et al. (2003). "Studying spontaneous EEG activity with fMRI." Brain Res Brain Res Rev **43**(1): 110-133.

Salek-Haddadi, A., L. Lemieux, et al. (2003). "Functional magnetic resonance imaging of human absence seizures." Ann Neurol **53**(5): 663-667.

Salmenpera, T. M. and J. S. Duncan (2005). "Imaging in epilepsy." J Neurol Neurosurg Psychiatry **76 Suppl 3**: iii2-iii10.

Sanada, S., N. Murakami, et al. (1988). "Changes in blood flow of the middle cerebral artery during absence seizures." Pediatr Neurol **4**(3): 158-161.

Scarff, C. J., A. Reynolds, et al. (2004). "Simultaneous 3-T fMRI and high-density recording of human auditory evoked potentials." Neuroimage **23**(3): 1129-1142.

Schmahmann, J. D. and D. N. Pandya (1990). "Anatomical investigation of projections from thalamus to posterior parietal cortex in the rhesus monkey: a WGA-HRP and fluorescent tracer study." J Comp Neurol **295**(2): 299-326.

Schmid, M. C., A. Oeltermann, et al. (2006). "Simultaneous EEG and fMRI in the macaque monkey at 4.7 Tesla." Magn Reson Imaging **24**(4): 335-342.

Seeck, M., F. Lazeyras, et al. (1998). "Non-invasive epileptic focus localization using EEG-triggered functional MRI and electromagnetic tomography." Electroencephalogr Clin Neurophysiol **106**(6): 508-512.

Shewmon, D. A. and R. J. Erwin (1988). "Focal spike-induced cerebral dysfunction is related to the after-coming slow wave." Ann Neurol **23**(2): 131-137.

Shmuel, A., M. Augath, et al. (2006). "Negative functional MRI response correlates with decreases in neuronal activity in monkey visual area V1." Nat Neurosci **9**(4): 569-577.

Shulman, G. L., J. A. Fiez, et al. (1997). "Common Blood Flow Changes across Visual Tasks: II. Decreases in Cerebral Cortex." J. Cogn. Neurosci. **9**(5): 648-663.

Sijbers, J., I. Michiels, et al. (1999). "Restoration of MR-induced artifacts in simultaneously recorded MR/EEG data." Magn Reson Imaging **17**(9): 1383-1391.

Sijbersa, J., J. Van Audekerke, et al. (2000). "Reduction of ECG and gradient related artifacts in simultaneously recorded human EEG/MRI data." Magn Reson Imaging **18**(7): 881-886.

Sinha, S. R. (2011). "Basic mechanisms of sleep and epilepsy." Journal of clinical neurophysiology : official publication of the American Electroencephalographic Society **28**(2): 103-110.

Siniatchkin, M., K. Groening, et al. (2010). "Neuronal networks in children with continuous spikes and waves during slow sleep." Brain : a journal of neurology **133**(9): 2798-2813.

Siniatchkin, M., F. Möller, et al. (2007). "Spatial filters and automated spike detection based on brain topographies improve sensitivity of EEG-fMRI studies in focal epilepsy." Neuroimage **37**(3): 834-843.

Skrandies, W. (1990). "Global field power and topographic similarity." Brain Topogr **3**(1): 137-141.

Snisarenko, A. A. (1978). "The cardiac rhythm during waking and the various periods of sleep." Hum Physiol **4**(1): 79-83.

Spencer, S. S. (2002). "Neural networks in human epilepsy: evidence of and implications for treatment." Epilepsia **43**(3): 219-227.

Srivastava, G., S. Crottaz-Herbette, et al. (2005). "ICA-based procedures for removing ballistocardiogram artifacts from EEG data acquired in the MRI scanner." Neuroimage **24**(1): 50-60.

Stefan, H., S. Rampp, et al. (2011). "Magnetoencephalography adds to the surgical evaluation process." Epilepsy & behavior : E&B **20**(2): 172-177.

Stephan, K. E., L. M. Harrison, et al. (2007). "Dynamic causal models of neural system dynamics:current state and future extensions." J Biosci **32**(1): 129-144.

Stephen, L. J. and M. J. Brodie (2012). "Antiepileptic drug monotherapy versus polytherapy: pursuing seizure freedom and tolerability in adults." Current opinion in neurology **25**(2): 164-172.

Steriade, M. (2005). "Sleep, epilepsy and thalamic reticular inhibitory neurons." Trends Neurosci **28**(6): 317-324.

Steriade, M. and D. Contreras (1998). "Spike-wave complexes and fast components of cortically generated seizures. I. Role of neocortex and thalamus." J Neurophysiol **80**(3): 1439-1455.

Tagliazucchi, E., F. von Wegner, et al. (2012). "Automatic sleep staging using fMRI functional connectivity data." Neuroimage **63**(1): 63-71.

Tagliazucchi, E., F. von Wegner, et al. (2012). "Dynamic BOLD functional connectivity in humans and its electrophysiological correlates." Frontiers in human neuroscience **6**: 339.

Thees, S., F. Blankenburg, et al. (2003). "Dipole source localization and fMRI of simultaneously recorded data applied to somatosensory categorization." Neuroimage **18**(3): 707-719.

Theodore, W. H. (2002). "When is positron emission tomography really necessary in epilepsy diagnosis?" Current opinion in neurology **15**(2): 191-195.

Theodore, W. H., R. Brooks, et al. (1985). "Positron emission tomography in generalized seizures." Neurology **35**(5): 684-690.

Thom, M., J. Zhou, et al. (2005). "Quantitative post-mortem study of the hippocampus in chronic epilepsy: seizures do not inevitably cause neuronal loss." Brain **128**(Pt 6r): 1344-1357.

Thornton, R., H. Laufs, et al. (2010). "EEG correlated functional MRI and postoperative outcome in focal epilepsy." Journal of neurology, neurosurgery, and psychiatry **81**(8): 922-927.

Thornton, R., H. Laufs, et al. (2010). "EEG-correlated fMRI and Post-Operative Outcome in Focal Epilepsy." JNNP **in press**.

Thornton, R., H. Laufs, et al. (2007). "Correlation of pre-surgical EEG fMRI and postsurgical imaging and outcome in patients with focal epilepsy." Epilepsia **48**(s6): 397.

Thornton, R., S. Vulliemoz, et al. (2011). "Epileptic networks in focal cortical dysplasia revealed using electroencephalography-functional magnetic resonance imaging." Annals of Neurology **70**(5): 822-837.

Thornton, R. C., R. Rodionov, et al. (2010). "Imaging haemodynamic changes related to seizures: comparison of EEG-based general linear model, independent component analysis of fMRI and intracranial EEG." Neuroimage **53**(1): 196-205.

Timofeev, I. and M. Steriade (2004). "Neocortical seizures: initiation, development and cessation." Neuroscience **123**(2): 299-336.

Touboul, J., F. Wendling, et al. (2011). "Neural mass activity, bifurcations, and epilepsy." Neural computation **23**(12): 3232-3286.

Tucker, D. M., M. Brown, et al. (2007). "Discharges in ventromedial frontal cortex during absence spells." Epilepsy Behav **11**(4): 546-557.

Uddin, L. Q., A. M. Clare Kelly, et al. (2008). "Functional connectivity of default mode network components: Correlation, anticorrelation, and causality." Hum Brain Mapp.

Valdes-Sosa, P. A., J. M. Sanchez-Bornot, et al. (2009). "Model driven EEG/fMRI fusion of brain oscillations." Hum Brain Mapp **30**(9): 2701-2721.

Van Audekerkea, J., R. Peeters, et al. (2000). "Special designed RF-antenna with integrated non-invasive carbon electrodes for simultaneous magnetic resonance imaging and electroencephalography acquisition at 7T." Magn Reson Imaging **18**(7): 887-891.

van den Heuvel, M. P. and H. E. Hulshoff Pol (2010). "Exploring the brain network: a review on resting-state fMRI functional connectivity." European neuropsychopharmacology : the journal of the European College of Neuropsychopharmacology **20**(8): 519-534.

van Duinen, H., I. Zijdewind, et al. (2005). "Surface EMG measurements during fMRI at 3T: accurate EMG recordings after artifact correction." Neuroimage **27**(1): 240-246.

van Gelder, N. M., I. Siatitsas, et al. (1983). "Feline generalized penicillin epilepsy: changes of glutamic acid and taurine parallel the progressive increase in excitability of the cortex." Epilepsia **24**(2): 200-213.

Van Hoesen, G., R. Maddock, et al. (1993). Connections of the monkey cingulate cortex. Neurobiology of cingulate cortex and limbic thalamus : a comprehensive handbook. B. A. Vogt and M. Gabriel. Boston, Birkhäuser**:** xiii, 639 p.

Van Paesschen, W., P. Dupont, et al. (2007). "The use of SPECT and PET in routine clinical practice in epilepsy." Current opinion in neurology **20**(2): 194-202.

Van Paesschen, W., P. Dupont, et al. (2003). "SPECT perfusion changes during complex partial seizures in patients with hippocampal sclerosis." Brain **126**(Pt 5): 1103-1111.

van Rootselaar, A. F., R. Renken, et al. (2007). "fMRI analysis for motor paradigms using EMG-based designs: a validation study." Human Brain Mapping **28**(11): 1117-1127.

Vasios, C. E., L. M. Angelone, et al. (2006). "EEG/(f)MRI measurements at 7 Tesla using a new EEG cap ("InkCap")." Neuroimage **33**(4): 1082-1092.

Vaudano, A. E., H. Laufs, et al. (2009). "Causal hierarchy within the thalamo-cortical network in spike and wave discharges." PLoS One **4**(8): e6475.

Velasco, M., F. Velasco, et al. (1989). "Epileptiform EEG activities of the centromedian thalamic nuclei in patients with intractable partial motor, complex partial, and generalized seizures." Epilepsia **30**(3): 295-306.

Vijayaraghavan, L., S. Natarajan, et al. (2011). "Peri-ictal and ictal cognitive dysfunction in epilepsy." Behav Neurol **24**(1): 27-34.

Vincent, J. L., L. J. Larson-Prior, et al. (2007). "Moving GLM ballistocardiogram artifact reduction for EEG acquired simultaneously with fMRI." Clin Neurophysiol **118**(5): 981-998.

Vogt, B. A. and S. Laureys (2005). "Posterior cingulate, precuneal and retrosplenial cortices: cytology and components of the neural network correlates of consciousness." Prog Brain Res **150**: 205-217.

Vogt, K. M., J. W. Ibinson, et al. (2011). "Comparison between end-tidal CO and respiration volume per time for detecting BOLD signal fluctuations during paced hyperventilation." Magnetic resonance imaging **29**(9): 1186-1194.

Vulliemoz, S., D. W. Carmichael, et al. (2011). "Simultaneous intracranial EEG and fMRI of interictal epileptic discharges in humans." Neuroimage **54**(1): 182-190.

Waites, A. B., R. S. Briellmann, et al. (2006). "Functional connectivity networks are disrupted in left temporal lobe epilepsy." Ann Neurol **59**(2): 335-343.

Wan, X., K. Iwata, et al. (2006). "Artifact reduction for simultaneous EEG/fMRI recording: adaptive FIR reduction of imaging artifacts." Clin Neurophysiol **117**(3): 681-692.

Wan, X., K. Iwata, et al. (2006). "Artifact reduction for EEG/fMRI recording: nonlinear reduction of ballistocardiogram artifacts." Clin Neurophysiol **117**(3): 668-680.

Wang, L., Y. Zang, et al. (2006). "Changes in hippocampal connectivity in the early stages of Alzheimer's disease: Evidence from resting state fMRI." Neuroimage.

Warach, S., J. R. Ives, et al. (1996). "EEG-triggered echo-planar functional MRI in epilepsy." Neurology **47**(1): 89-93.

Warach, S., J. R. Ives, et al. (1996). "EEG-triggered echo-planar functional MRI in epilepsy." Neurology **47**(1): 89-93.

Wenzel, R., P. Wobst, et al. (2000). "Saccadic suppression induces focal hypooxygenation in the occipital cortex." J Cereb Blood Flow Metab **20**(7): 1103-1110.

Wiebe, S., W. T. Blume, et al. (2001). "A randomized, controlled trial of surgery for temporal-lobe epilepsy." N Engl J Med **345**(5): 311-318.

Wiebe, S. and N. Jette (2012). "Epilepsy surgery utilization: who, when, where, and why?" Current opinion in neurology **25**(2): 187-193.

Williams, D. (1953). "A study of thalamic and cortical rhythms in petit mal." Brain **76**(1): 50-69.

Wilson, D. A. and R. J. Stevenson (2003). "Olfactory perceptual learning: the critical role of memory in odor discrimination." Neuroscience and biobehavioral reviews **27**(4): 307-328.

Winden, K. D., S. L. Karsten, et al. (2011). "A systems level, functional genomics analysis of chronic epilepsy." PLoS One **6**(6): e20763.

Wyler, A. R., B. P. Hermann, et al. (1989). "Results of reoperation for failed epilepsy surgery." J Neurosurg **71**(6): 815-819.

Yeni, S. N., L. Kabasakal, et al. (2000). "Ictal and interictal SPECT findings in childhood absence epilepsy." Seizure **9**(4): 265-269.

Yeterian, E. H. and D. N. Pandya (1985). "Corticothalamic connections of the posterior parietal cortex in the rhesus monkey." J Comp Neurol **237**(3): 408-426.

Zahneisen, B., T. Hugger, et al. (2012). "Single shot concentric shells trajectories for ultra fast fMRI." Magnetic resonance in medicine : official journal of the Society of Magnetic Resonance in Medicine / Society of Magnetic Resonance in Medicine **68**(2): 484-494.

Zijlmans, M., G. Huiskamp, et al. (2007). "EEG-fMRI in the preoperative work-up for epilepsy surgery." Brain **130**(Pt 9): 2343-2353.

Zschocke, S. (1995). Klinische Elektroenzephalographie. Berlin Heidelberg New York, Springer-Verlag.

Dänischenhagen, February 2013 Helmut Laufs